



SCUOLA DI DOTTORATO  
UNIVERSITÀ DEGLI STUDI DI MILANO-BICOCCA

School of Medicine and Surgery

PhD program in Translational and Molecular Medicine (DIMET)

*XXXVI Cycle*

**Inhibition of FGF23 is a therapeutic strategy to  
target hematopoietic stem cell niche defects in  
 $\beta$ -thalassemia**

Dr. Laura Raggi

Matr. No. 875313

Tutor: Prof. Marta Serafini

Co-Tutor: Prof. Giuliana Ferrari

Coordinator: Prof. Francesco Mantegazza

Academic year 2022/2023

# TABLE OF CONTENTS

CHAPTER I.....	5
INTRODUCTION .....	5
1. $\beta$ -Thalassemia .....	5
1.1 BThal pathophysiology.....	5
1.1.1 Ineffective erythropoiesis and enhanced EPO signaling .....	6
1.1.2 Iron overload.....	8
1.1.3 Bone disease.....	8
1.1.4 Multi-organ complications.....	10
1.2 Murine model of BThal.....	12
1.3 Therapeutic options for BThal .....	12
1.3.1 Strategies to improve anemia and IO .....	13
1.3.2 Strategies to improve bone defects .....	14
1.3.3 Allogeneic hematopoietic stem cell transplantation and gene therapy .....	16
2 Hematopoiesis .....	18
2.1 HSC regulation in the BM niche .....	20
2.2 HSC regulation by BM niche populations.....	20
2.2.1 Stromal BM cells.....	21
2.2.2 Hematopoietic BM cells .....	23
2.3 HSC niche in homeostasis and stress conditions.....	24
3 Function of HSC and BM niche in BThal .....	25
3.1 HSC defect in BThal.....	25
3.2 Stromal niche defect in BThal.....	26
3.3 Hematopoietic and soluble niche factors .....	27
4 Fibroblast growth factor 23 (FGF23).....	28
4.1 The impact of systemic and local factors on FGF23 regulation.....	29
4.2 Molecular mechanism regulating FGF23 .....	31
4.3 Key factors that induced FGF23 production .....	32
4.3.1 Erythropoietin .....	33
4.3.2 Iron deficiency .....	33
4.3.3 Inflammation.....	34
4.4 Inhibition strategies of FGF23 signaling.....	35
4.4.1 FGF23 effect on the BM niche.....	37
AIMS OF THE PROJECT: .....	41
CHAPTER II (Published Papers).....	43
CHAPTER III.....	44
NEW RESULTS .....	44
1. High EPO downregulates GALNT3 through Erk1/2 and Stat5 signaling in bone and BM erythroid cells .....	44
2. Increased BMD and HSC cell cycle was maintained after the discontinuation of cFGF23 treatment.....	45
DISCUSSION OF NEW RESULTS:.....	47
OVERALL DISCUSSION: .....	49
REFERENCES .....	53

## ACRONYMS AND ABBREVIATIONS

ADHR = Autosomal dominant hypophosphatemic rickets  
AECs = arteriolar endothelial cells  
ANGPT1= angiopoietin 1  
BFU-E = burst-forming unit erythroid  
BM = bone marrow  
BMD = bone mineral density  
BMP = bone morphogenetic protein  
BMT = bone marrow transplantation  
BPs = bisphosphonate  
BThal =  $\beta$ -thalassemia  
CAR = CXCL12-abundant reticular  
cFGF23 = cleaved C-terminal fragment  
CFU-E = colony-forming unit erythroid  
CFU-Fs = colony-forming unit fibroblasts  
CLPs = common lymphoid progenitors  
CKD = chronic kidney disease  
CMPs = common myeloid progenitors  
CRISPR = clustered regularly interspaced short palindromic repeat  
CXCL12 = C-X-C motif chemokine ligand 12  
DMP1 = dentin matrix protein 1  
DNM = denosumab  
ECs = endothelial cells  
EMA = European Medicines Agency  
EPO = erythropoietin  
EPO-R = erythropoietin-receptor  
ERFE = erythroferrone  
FDA = Food and Drug Administration  
FGFs = fibroblast growth factors  
FGFRs = fibroblast growth factor receptors  
FGF23 = fibroblast growth factor 23  
GALNT3 = N-acetylglucosaminyltransferase 3  
G-CSF = granulocyte-colony-stimulating factor  
GE = gene editing  
GH = growth hormone  
GT = gene therapy  
Hb = hemoglobin  
HbF = fetal hemoglobin  
HIF1 $\alpha$  = hypoxia-inducible factor 1 alpha  
HSCs = hematopoietic stem cells  
HSCT = hematopoietic stem cell transplantation  
HSPCs = hematopoietic stem and progenitor cells  
IDA = iron deficiency anemia

IE = ineffective erythropoiesis  
iFGF23 = intact fibroblast growth factor 23  
IL-7 = interleukin-7  
IO = iron overload  
ko = knock-out  
LCR = locus control region  
LEPR = leptin receptor  
Lin<sup>-</sup> = lineage negative cells  
MAPK = mitogen-activated protein kinase  
MDS = myelodysplastic syndrome  
MFI = mean fluorescent intensity  
MKs = megakaryocytes  
MPPs = multipotent progenitors  
MSCs = mesenchymal stromal cells  
Mφs = macrophages  
NTDT = non-transfusion dependent thalassemia  
OBs = osteoblasts  
OCs = osteoclast  
OPN = osteopontin  
OPG = osteoprotegerin  
OTs = osteocytes  
PB = peripheral blood  
PCSK5 = proprotein convertase enzyme 5  
PHEX = phosphate-regulating gene with homologies to endopeptidases on the X chromosome  
PTH = parathyroid hormone  
PαS = PDGFRα<sup>+</sup> Sca1<sup>+</sup>  
RANKL = receptor activator of nuclear factor kappa-β ligand  
RBC = red blood cells  
ROS = reactive oxygen species  
SCD = sickle cell disease  
SCF = stem cell factor  
SECs = sinusoidal endothelial cells  
SOST = sclerostin  
SPC1 = subtilisin-like proprotein convertases  
TDT = transfusion-dependent thalassemia  
TGF-β = transforming growth factor-beta  
Th3 = Hbb<sup>th3/+</sup> thalassemic mice  
TIO = tumor-induced osteomalacia  
TM = thalassemia major  
TPO = thrombopoietin  
Tregs = regulatory T cells  
wt = wild type  
XLH = X-linked hypophosphatemic rickets  
ZFNs = zinc finger nucleases

# CHAPTER I

## INTRODUCTION

### 1. $\beta$ -Thalassemia

$\beta$ -Thalassemia (BThal) was described for the first time by Thomas Cooley and Peral Lee in 1925 as a form of severe anemia. BThal is one of the most widespread monogenic disorders, affecting the adult  $\beta$ -globin gene (*HBB*), with a consequent reduced or absent synthesis of  $\beta$ -globin chains. Hemoglobin (Hb) is a tetramer made of four polypeptide chains containing a heme prosthetic group, and different combinations of globin chains are assembled during embryonic, fetal, and adult life. The human globin locus is located on chromosome 11 and contains five  $\beta$ -like globin genes ( $\epsilon$ ,  $G\gamma$ ,  $A\gamma$ ,  $\delta$ ,  $\beta$ )<sup>1</sup>. Adult human Hb is characterized by two pairs of bound globin chains ( $\alpha_2\beta_2$  tetramer), tightly regulated to ensure balanced synthesis. Defects in  $\alpha$ -globin chains give rise to  $\alpha$ -thalassemia, whereas alterations in  $\beta$ -globin chains cause BThal<sup>2</sup>. The highest prevalence of BThal has been recorded in the Mediterranean countries, the Middle East, the Indian subcontinent, Southeast Asia, and Africa. However, because of the mass migration of populations, BThal is present in the United States, Canada, Australia, South America, and North Europe<sup>3</sup>. It has been estimated that 1-5% of the world population are carriers of thalassemia mutations<sup>4</sup>. Hence, BThal has become an important worldwide health problem<sup>5</sup>.

The diagnosis of BThal relies on the evaluation of several parameters, such as red blood cell (RBC) indices, Hb levels and reticulocyte count. Molecular genetic tests are becoming important to obtain an accurate diagnosis for BThal severity, indeed, over 300 different types of causative mutations have been described affecting the  $\alpha$ -/ $\beta$ -chains ratio<sup>6</sup>, giving rise to a clinically heterogeneous spectrum of the disease from asymptomatic expression (Thalassemia minor), mild clinical anemia (Thalassemia intermedia) and severe one (Thalassemia major)<sup>7</sup>. However, at present, BThal patients have been classified based on transfusion therapy requirements into transfusion-dependent thalassemia (TDT) or non-transfusion-dependent thalassemia (NTDT). TDT patients are unable to produce an adequate amount of Hb and require lifelong transfusion treatments for survival. NTDT patients can still require occasional transfusions but not throughout their entire lifespan<sup>8</sup>.

#### 1.1 BThal pathophysiology

### 1.1.1 Ineffective erythropoiesis and enhanced EPO signaling

At the molecular level, BThal mutations impair the production of  $\beta$ -globin chains, leading to an imbalance between  $\alpha/\beta$ -globin chains. This results in the formation and accumulation of the free  $\alpha$ -globin tetramers in RBCs. The presence of free Hb and heme promotes the generation of reactive oxygen species (ROS), resulting in oxidative damage, hemolysis of RBCs in peripheral blood (PB), and premature death of erythroid precursors in the bone marrow (BM). The clinical manifestations of BThal include chronic severe anemia, which stimulates the production of erythropoietin (EPO). Consequently, there is an intense but ineffective expansion of the erythroid compartment in the BM, leading to ineffective erythropoiesis (IE), alteration of BM homeostasis, and the release of stress signals<sup>4</sup>. BThal BM is characterized by an expansion of erythroid progenitors, with a blockade in maturation occurring at the polychromatic stage<sup>9</sup>. The increased production of RBCs in the BM is accompanied by expansion of BM and subsequent development of bone defects<sup>4</sup>.

In adult, erythropoiesis occurs in the BM and is characterized by the differentiation of hematopoietic stem cells (HSCs) into mature enucleate erythrocytes<sup>10</sup>. Erythropoiesis is characterized by three different phases: the first step is the commitment towards erythroid progenitor cells consisting of a burst-forming unit erythroid (BFU-E) and colony-forming unit erythroid (CFU-E) cells<sup>11</sup>. The second step consists of precursor expansion and maturation, from pro-erythroblasts to basophilic, polychromatophilic, and orthochromatic erythroblasts. During this stage the Hb synthesis gradually increases. Finally, the cells terminally differentiate into mature RBCs that have no nuclei or RNA<sup>12</sup>. Several growth factors are associated with erythropoiesis including EPO, which is a glycoprotein cytokine that plays a crucial role in regulating the final phases of erythroid maturation. EPO is primarily produced by adult human kidneys and secreted into the bloodstream, where it binds to its receptor (EPO-R), mainly expressed by erythroid progenitor cells in the BM<sup>13</sup> (Fig. 1). Only the initial phase, from CFU-E to the basophilic stage, is EPO-dependent, whereas in later stages the cells lose EPO-R and become EPO-independent<sup>13</sup>. While EPO is constantly secreted at low levels in the blood, its production can also be triggered in the liver and BM osteoblasts during stress conditions, such as IE and hypoxia<sup>14,15</sup>.

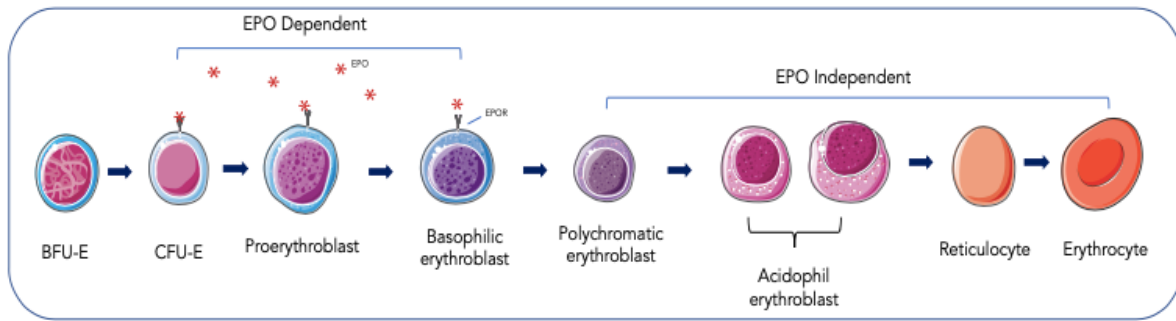


**Figure 1. Overview of erythropoiesis**, a stepwise process from HSC, BFU-E, CFU-E, Pro-E, Baso-E, Poli-E, Ortho-E and RBCs. During the process of progenitor differentiation, significant changes occur, including a decrease in cell size, chromatin condensation, and hemoglobinization. EPOR is expressed from CFU-E to polychromatophilic erythroblast (adapted from <sup>13</sup>).

In response to hypoxia, IE leads to increased production of EPO, which activates a downstream signaling cascade. Upon EPO binding, the EPO-R receptors undergo homodimerization, leading to the activation of Janus kinase 2. This, in turn, leads to the phosphorylation of various signaling molecules, including signal transducer and activator of transcription as STAT5, PI3K/AKT, NFκB and ERK2-MAPK pathway. This signaling cascade plays a significant role not only in promoting proliferation and differentiation of RBCs but also in exerting anti-inflammatory and anti-apoptotic effects<sup>13</sup>. The specific outcomes of these pathways depend on the specific players involved in the process (Fig 2).

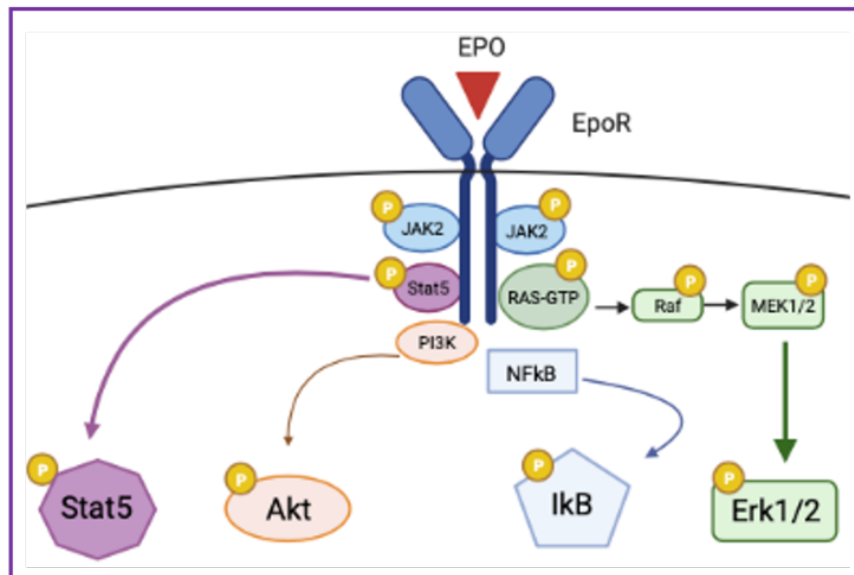


**Figure 2. EPO-EPOR signaling pathway.** Signaling cascades observed in erythroid progenitor cells upon activation of the EPO-R by EPO (adapted from <sup>13</sup>).

### 1.1.2 Iron overload

Hemolytic anemia triggers a cascade of events, including increased levels of iron and heme in the circulation <sup>4</sup>. IE in BThal results in increased iron absorption and primary iron overload (IO) due to decreased levels of the hepatic hormone hepcidin. Indeed, EPO prompts the production of a hormone called erythroferrone (ERFE) by the erythroid precursors acting as a potent inhibitor of hepcidin production, which in turn triggers an excessive absorption of dietary iron and promotes the release of iron from macrophages and hepatocytes into the bloodstream (Fig 3). Additionally, transfusional iron intake can saturate the capacity of transferrin receptors, leading to secondary IO. This excess of iron can cause damage to various organs, including liver, heart, endocrine organs and bones <sup>8</sup>. Despite advancements in iron chelation therapies, IO remains one of the most significant clinical complications in BThal patients.

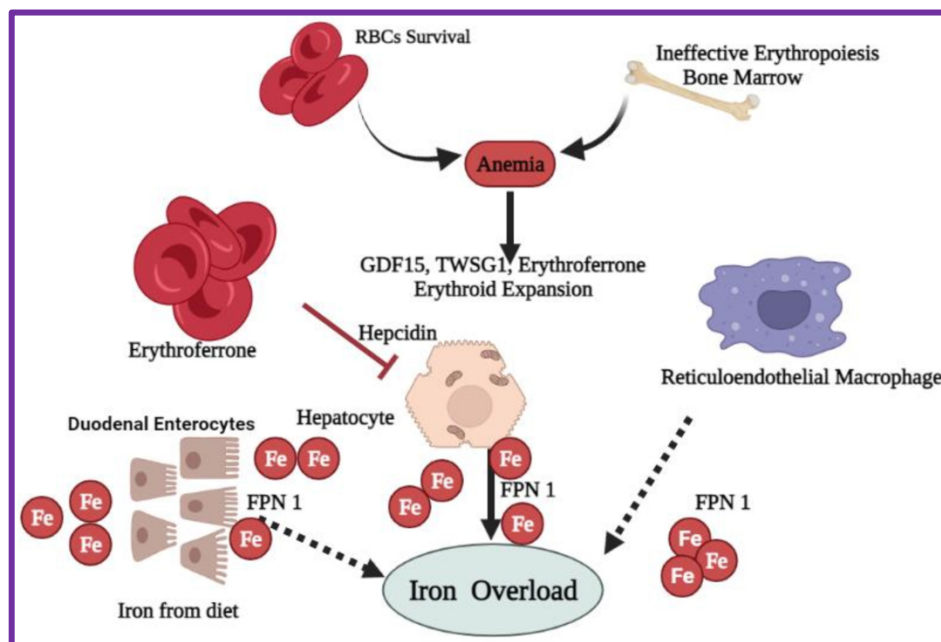


**Figure 3. Causes of IO in BThal.** IE and peripheral hemolysis of RBCs, lead to excessive erythroid factors, which suppress hepcidin expression in liver cells, this generates IO due to increased iron absorption from duodenal enterocytes, an increase in iron from hepatocytes and the reticuloendothelial macrophages <sup>16</sup>.

### 1.1.3 Bone disease

Emerging clinical data highlights the connection between changes in EPO and altered bone homeostasis, suggesting a functional interplay between erythropoiesis regulation and bone dynamics within hereditary anemias <sup>17</sup>. BThal bone disease includes a diverse range of conditions, such as bone deformities, pain, marrow expansion, decreased bone density,



and susceptibility to fractures. Among patients with BThal, common bone disorders like osteopenia and osteoporosis have been frequently observed, which are characterized by a significant decrease in bone mineral density (BMD) and an increased risk of fractures<sup>18,19</sup>. TDT patients exhibit distinctive features such as bone deformities (i.g. frontal bossing, maxillary hyperplasia, limb deformities) along with pain. While still debated, the actual causes of bone loss are attributed to a range of risk factors including hormonal deficiencies, marrow expansion, iron toxicity and increased bone turnover<sup>20,21</sup>.

One possible molecular mechanism suggests a decrease in the ratio of osteoprotegerin (OPG) to receptor activator of nuclear factor kappa- $\beta$  ligand (RANKL), leading to enhanced expression of RANKL by stromal cells or osteoblasts (OBs). This, in turn, contributes to increased bone resorption by osteoclasts (OCs)<sup>22</sup>. The imbalance in RANKL to OPG expression is evident in TDT patients, inducing elevated bone turnover primarily driven by enhanced OCs<sup>23</sup>. Another study revealed a negative correlation between RANKL and free testosterone in males, as well as with 17- $\beta$  estradiol in females with BThal<sup>22</sup>. This infers the potential involvement of the RANKL/OPG pathway in mediating the influence of sex steroids on bone. Additionally, delayed sexual maturation, primarily due to endocrinopathies caused by IO, significantly influences bone remodeling<sup>23</sup>. Reduced levels of estrogen and progesterone impair the inhibition of OC activity and bone formation, while diminished levels of testosterone result in reduced stimulation of OB proliferation and differentiation. Furthermore, excessive accumulation of free iron in the pituitary gland can result in a deficiency of growth hormone (GH) or insulin-like growth factor I (IGF-1), diminishing OB proliferation and the formation of bone matrix and promoting bone loss through the activation of OCs<sup>23,24</sup>. Sclerostin (SOST), another molecule implicated in bone defects, was found elevated in BThal patients. SOST, an inhibitor of Wnt signaling produced by osteocytes (OTs), acts to inhibit OB activity (Fig. 4). A significant correlation was identified between SOST levels and BMD at different skeletal locations including the lumbar spine, femoral neck, and radius<sup>18</sup>. These findings suggest that increased SOST levels may serve as an indicator of enhanced OT activity in BThal patients.

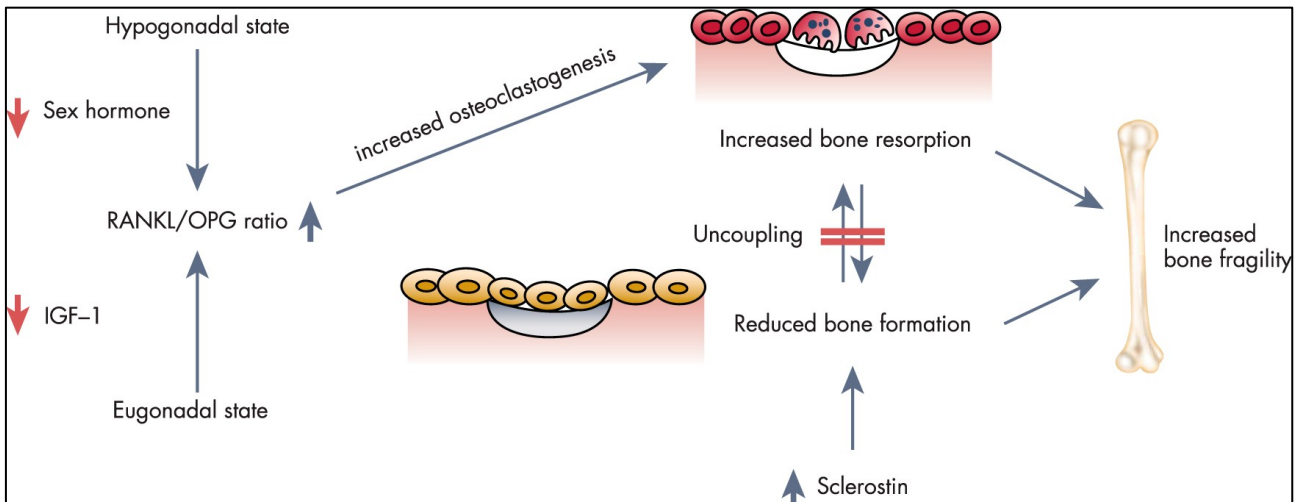


**Figure 4. The role of RANKL/OPG and WNT/ $\beta$ -catenin signaling involved in BThal bone defects.** Enhanced OC activity can be influenced by deficiencies in sex hormones and GH, leading to increased bone resorption by elevating the RANKL/OPG ratio. Elevated levels of SOST contribute to reduced bone formation. The impact of increased RANKL/OPG ratio or elevated SOST levels results in low bone mass and increased bone fragility (Adapted from <sup>25</sup>).

However, the pathophysiology of bone loss is controversial in BThal, and bone disease correlates with high morbidity despite available therapies. Understanding the underlying pathophysiology of BThal is crucial for developing effective diagnostic and therapeutic approaches to manage this condition and its comorbidities.

### 1.1.4 Multi-organ complications

Secondary multi-organ complications due to the primary genetic defects are present in BTHAL patients <sup>5</sup> (Fig. 5). To counteract the increased loss of blood cells, multiple sites of hematopoiesis are activated outside the BM resulting in increased erythroid activity, in extramedullary hematopoietic sites, splenomegaly and hepatomegaly. Other complications include endocrinopathies such as hypogonadism, hypothyroidism, hypoparathyroidism, as well as impaired bone metabolism <sup>8</sup>. The bone defect is associated with low circulating parathyroid hormone (PTH), a condition of hypoparathyroidism observed in a fraction of BThal patients, thought to be an endocrine secondary defect by IO<sup>26</sup>. Moreover, the peripheral hemolysis characteristic of BThal can lead to thrombosis and vascular events by causing prothrombotic markers to be exposed on the surface of RBCs. The endothelial damage led to platelet activation and increased aggregation. As medical care continues to advance, patient survival rates improve, leading to a new array of challenges, including heart

disease, diabetes, renal dysfunction, and cancers, influenced by risk factors analogous to those prevalent in the wider non-thalassemia population.

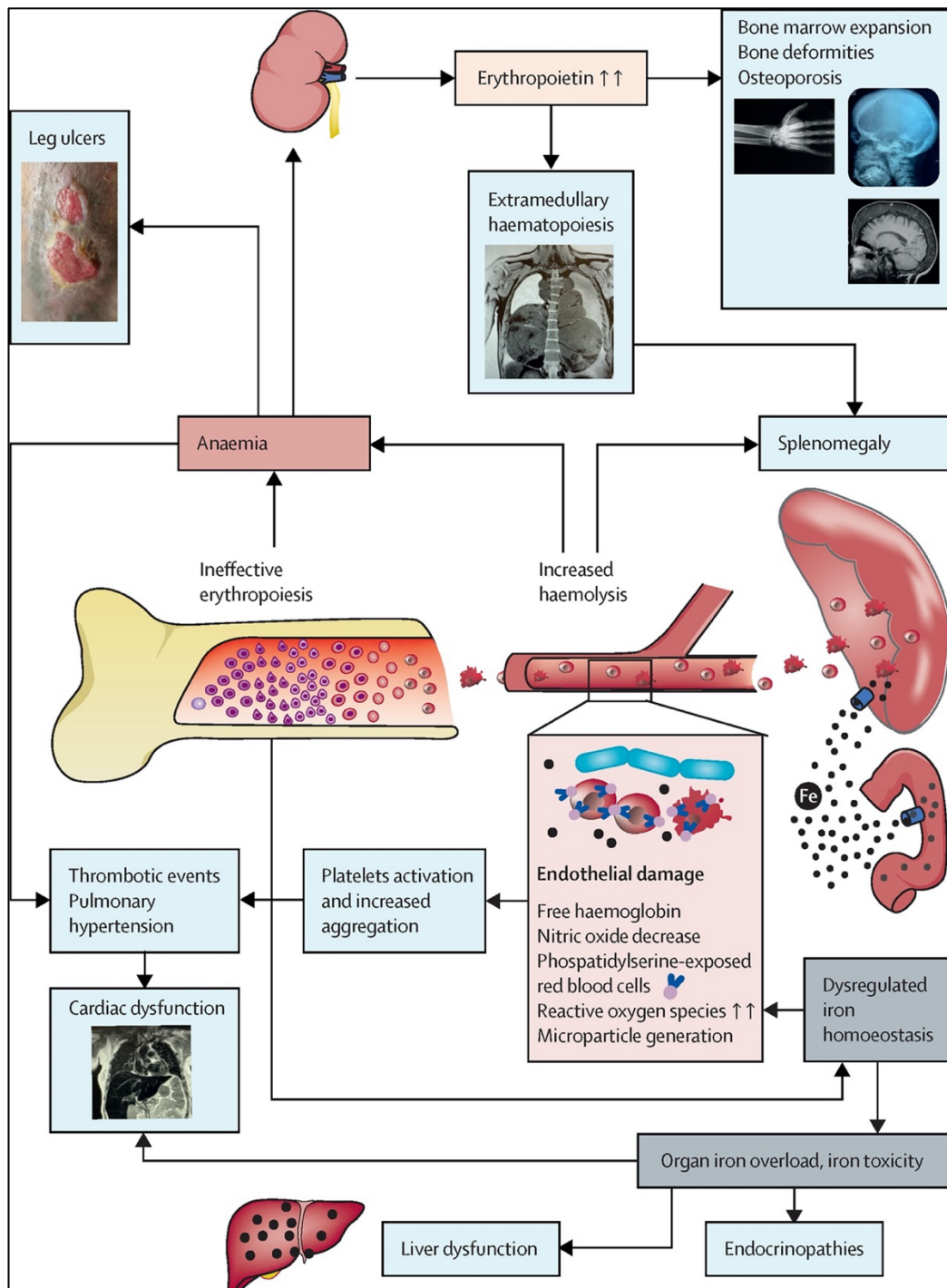


**Figure 5. Pathophysiology of BThal.** The unbalanced synthesis of  $\alpha/\beta$  chain results in IE, with compensative erythropoietic expansion in the BM and extramedullary hematopoiesis, chronic hemolytic anemia, and IO, leading to many secondary multi-organ alterations <sup>5</sup>.

## 1.2 Murine model of BThal

Several mouse models have been developed to replicate different forms of BThal <sup>27-29</sup>. Among them, Hbbth3/+ (*th3*) model lacks both  $\beta^{\text{major}}$  and  $\beta^{\text{minor}}$  genes and shows a severe phenotype. Homozygous *th3* mice experience perinatal mortality, resembling the most severe form of Cooley's anemia in humans <sup>30</sup>. Heterozygotes of *th3* mice exhibit characteristics of BThal intermedia, including IE, anemia, reduced RBC counts, increased reticulocytes, and extramedullary hematopoiesis but do not require RBC transfusion for survival, similarly to NTDT patients <sup>30</sup>. Additionally, *th3* mice display bone abnormalities with reduced BMD <sup>31</sup>. Furthermore, *th3* mice show high production of ERFE and subsequent reduced expression of hepcidin, leading to IO in the spleen, kidneys, and liver <sup>32,33</sup>. For these reasons, *th3* animals have been widely used for studying the complex pathophysiology of BThal.

## 1.3 Therapeutic options for BThal

In severe BThal cases, the mainstay treatment involves the combination of regular blood transfusions and iron chelation therapies. TDT patients require regular blood transfusions to suppress IE, increase Hb concentration and reduce the severity of bone fragility and deformity. Iron chelation therapy plays a crucial role in reducing systemic and hepatic iron burden, both in TDT and NTDT, thereby decreasing the risk of IO-related complications. Chelation agents, such as deferoxamine, deferiprone, and deferasirox, are crucial to prevent iron toxicity and related organ damage <sup>34</sup>. However, the effectiveness of current therapies is often limited to the need for repeated transfusions and challenges with patient compliance. The development of new therapies is necessary to further reduce the burden of the disease and remains an unmet need <sup>35</sup> (Fig. 6).

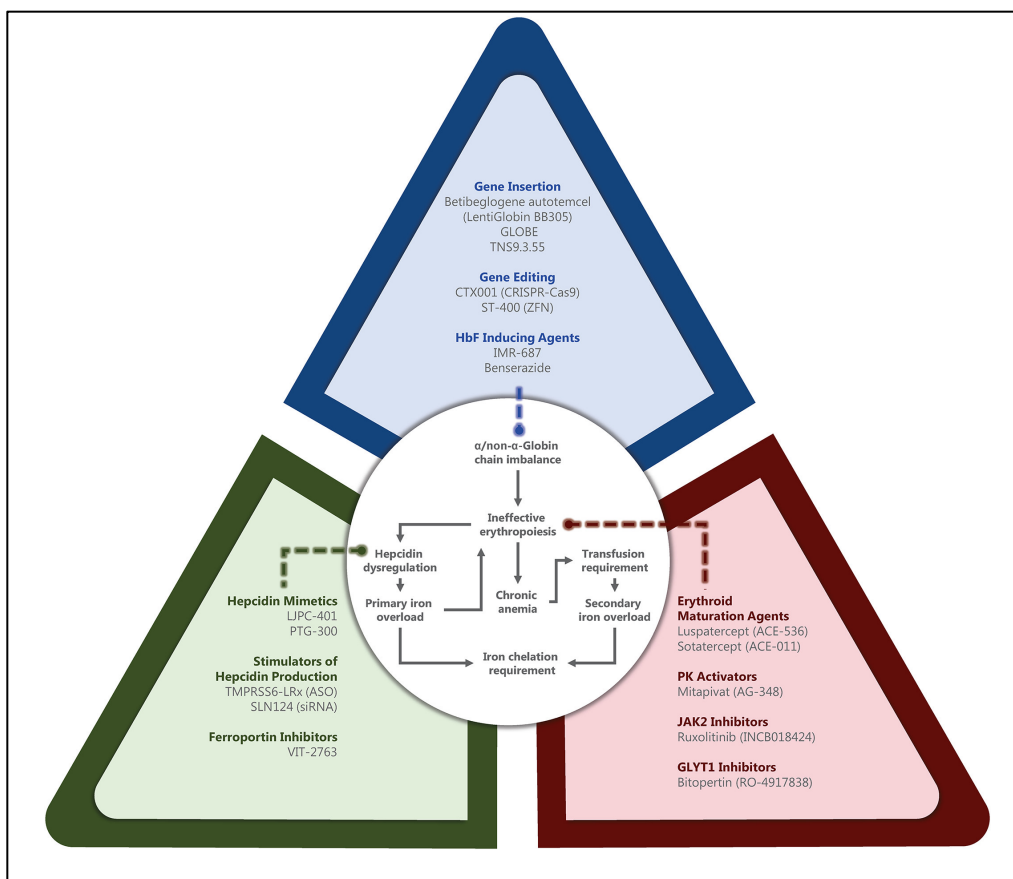


**Figure 6. New treatment options for BThal patients at various stages of clinical development. Emerging therapies include the treatment for improving IE, iron metabolism and to correct genetic defect<sup>35</sup>.**

### 1.3.1 Strategies to improve anemia and IO

Emerging therapies are explored to target IE. One significant advancement in the field is the approval of Luspatercept in 2019 by the Food and Drug Administration (FDA) and in 2020 by the European Medicines Agency (EMA) for the treatment of anemia in TDT adult patients. Although the precise mechanism of action is not yet fully understood, Luspatercept is an activin receptors IIA ligand traps, which binds to transforming growth factor-beta (TGF- $\beta$ ) superfamily ligands and inhibits SMAD2/3 signaling pathway, thereby acting on the late stages of RBCs and promoting erythroid maturation<sup>36</sup>.

The efficacy and safety of Luspatercept were evaluated in the multicenter Phase 3 BELIEVE clinical study, demonstrating a significant reduction of at least 33% in transfusion requirements among TDT patients. Moreover, some patients even achieved transfusion independence<sup>34</sup>. However, due to the complexity of the disease, limitations in the study include patients' selection, age limit (>18 years), genotype, IO and the heterogeneous response to Luspatercept, highlighting the importance of a personalized approach<sup>37</sup>.

Similar results were observed with another ligand trap for activin A receptor, called Sotatercept (ACE-011) <sup>38</sup>. Originally developed to address bone loss disorders, clinical studies of Sotatercept unexpectedly showed increased Hb levels in BThal treated patients <sup>39,40</sup>. However, Sotatercept was not selected for phase 3 development, due to its minimal binding to activin A, which could potentially result in off-target effects.

Mitapivat, an oral small molecule classified as pyruvate kinase activator, has demonstrated positive effects in reducing markers of IE and anemia by enhancing RBCs the metabolism in mouse model of BThal <sup>41</sup>. The safety and efficacy of Mitapivat were recently assessed in phase 2 study conducted by Kuo et al. in NTDT adults' patients <sup>42</sup>.

In BThal IE and hypoxia lead to decreased production of the hepatic hormone hepcidin. In both preclinical and clinical studies, interventions targeting hepcidin levels, such as minihepcidins that mimic the endogenous hepcidin <sup>43</sup>, and TMPRSS6 inhibitors <sup>44</sup> have shown significant improvements in IE, anemia, and IO in a mouse model. Clinical trials are currently ongoing, evaluating the use of these agents in NTDT patients <sup>35</sup>.

Furthermore, molecules targeting iron metabolism are being studied in BThal patients. Vamifeport (VIT-2763), the first oral ferroportin inhibitor, has demonstrated promising results improving anemia and erythropoiesis in *th3* mouse model <sup>45</sup>. A Phase IIa study was conducted to evaluate the safety and tolerability of Vamifeport compared to placebo in NTDT patients, publication of the results from this trial is pending <sup>46</sup>.

### **1.3.2 Strategies to improve bone defects**

Optimal transfusion and chelation therapy effectively reduce bone fragility and deformity in BThal <sup>47</sup>. While calcium and vitamin D supplementation is prevalent, evidence for improved BMD and fracture prevention remains limited, like in the general population.

Osteoporotic drugs can be categorized into two groups based on their mechanism of action: 1) Antiresorptive drugs which slow down the bone loss, which include bisphosphonates (BPs), Denosumab (DMAB) and estrogens and anabolic drugs, which increase bone formation and bone density. Examples are Teriparatide and Romosozumab.

BPs, potent inhibitors of bone resorption, are the main pharmacological treatment for BThal-related osteoporosis <sup>25</sup>. They act by interfering with the mevalonate pathway and blocking GTP-binding proteins <sup>48</sup>. This leads to decreased OC recruitment, differentiation, activity, and survival, increasing OC apoptosis and resulting in diminished bone resorption <sup>49</sup>. While BPs demonstrated a reduction in bone turnover markers and an increase in BMD, clinical data regarding fracture prevention in BThal patients are still lacking. Future research

should focus on determining the most effective timing and duration of BP therapy. Even the concept of BPs breaks has been explored in postmenopausal osteoporosis, its applicability to TDT patients remains unclear and necessitates further in-depth investigation <sup>50</sup>.

DMAB, a human monoclonal antibody targeting RANKL, is a potent antiresorptive for osteoporosis showing efficacy in both men and postmenopausal women with osteoporosis <sup>51,52</sup>. Studies using the same DMAB dosing schedule in TDT-induced osteoporosis showed significant increase of lumbar spine BMD accompanied by common side effects including back/extremity pain, nausea, and hypocalcemia <sup>53,54</sup>. It's important to note that DMAB's mechanism of action involves blocking RANKL, which can lead to the accumulation of osteomorphs, a specific cell stage in the OC development process <sup>55</sup>. Osteomorphs are highly mobile daughter cells of OCs that remain in the nearby BM and retain the ability to fuse back together to form functional OCs <sup>56</sup>. When RANKL signaling is restored, typically upon discontinuing DMAB treatment, it can lead to a rapid and extensive breakdown of bone tissue, resulting in a sudden increase in bone resorption. This phenomenon may potentially lead to rebound fractures occurring in a very short period <sup>57</sup>.

Currently, no research explores the impact of hormone replacement therapy on fracture outcomes in BThal. While existing literature highlights the positive effects of sex hormone replacement on skeletal health, unanswered questions persist regarding dosing, administration methods, and treatment's influence on fracture prevention in BThal.

Teriparatide has demonstrated increased BMD and reduced fractures in men <sup>58</sup> and postmenopausal women <sup>59</sup>. A recent study published by Gagliardi I. et al showed teriparatide as a promising treatment for thalassemia major (TM)-related osteoporosis by enhancing BMD, particularly in the lumbar spine, and reducing fragility fractures. However, five out of eleven patients developed side effects, such as muscle and bone pain, compared to the non-TM population. This divergence in side effects might arise from the complex and diverse pathogenesis of osteoporosis and bone pain in TM. Further investigations are necessary to validate the long-term efficacy, safety, and dosing regimen of teriparatide therapy for TM patients, as well as to elucidate the underlying physiological mechanisms, especially related to bone pain <sup>60</sup>. Teriparatide has an anabolic window that typically lasts for approximately two years. During this period, bone formation exceeds bone resorption, resulting in a net increase in bone mass. However, after this two-year anabolic window, the balance shifts, no further net increase in bone mass can be achieved <sup>61,62</sup>.

Romsozumab is an anti-SOST monoclonal antibody, and it has received recent FDA approval for the treatment of osteoporosis. Clinical studies have demonstrated that

Romozosumab has the potential to increase BMD in various skeletal regions, including the lumbar spine, total hip, and femoral neck, particularly in postmenopausal individuals with osteoporosis<sup>63</sup>. Romozosumab could be a promising strategy also for the treatment of TDT-related osteoporosis since SOST has been discovered to be elevated in BThal patients. Thalassemia-related bone disease has emerged as a significant challenge in managing the increasing burden of morbidity associated with TDT, highlighting an existing medical gap despite available treatments.

### **1.3.3 Allogeneic hematopoietic stem cell transplantation and gene therapy**

For many years, the primary curative treatment option for patients with BThal has been allogeneic hematopoietic stem cell transplantation (HSCT). However, this approach has several limitations. Firstly, it is challenging to find suitable donors, making it available to less than 20% of patients. Additionally, there is a risk of graft rejection associated with allogeneic HSCT<sup>64</sup>. More recently, autologous transplantation of genetically corrected cells through gene therapy (GT) has been developed<sup>65</sup>. GT is a promising therapeutic strategy for the treatment of BThal that aims to correct the underlying genetic defects in hematopoietic progenitor cells (HSPCs) and restore normal production of Hb through gene addition and gene editing (GE) approaches<sup>66</sup>. Autologous transplantation consists of multi-step process starting with the harvest of autologous HSPCs from the patient through leukapheresis or BM aspirates followed by their *ex vivo* culture and genetic modification, achieved by either gene transfer or GE. Finally, the engineered HSPCs are reinfused into pre-conditioned patient, where they can reconstitute the BM and differentiate into healthy RBCs<sup>67</sup> (Fig. 7).



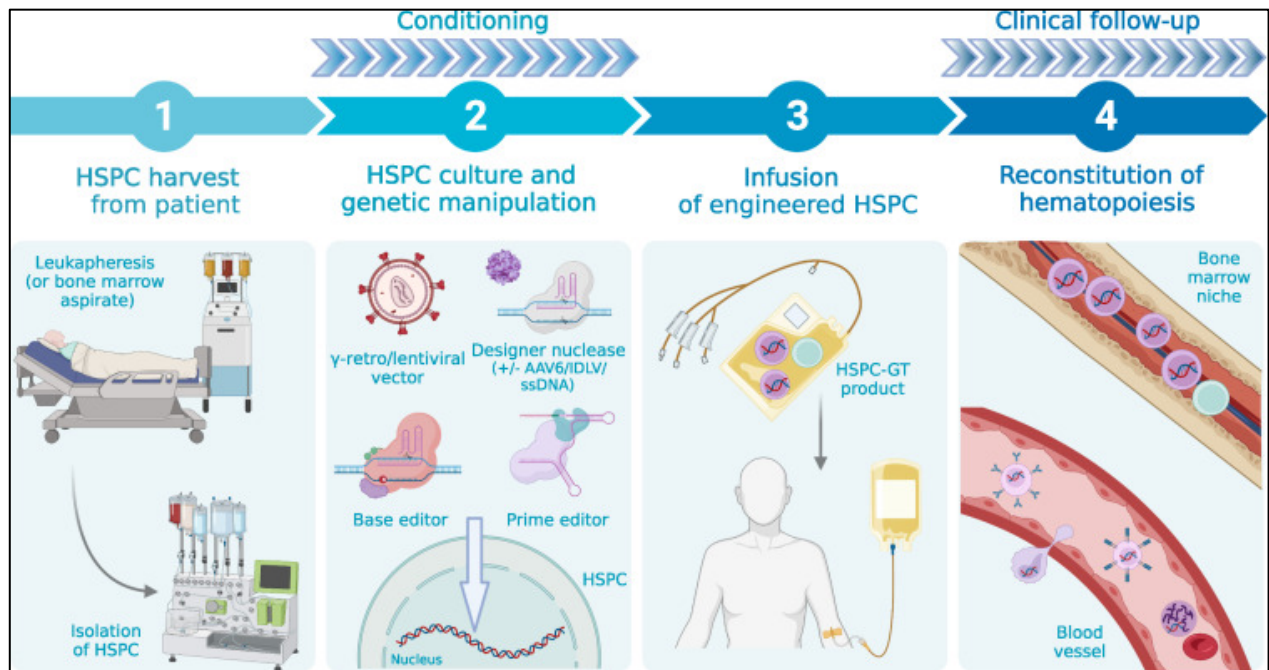


**Figure 7. Representation of the HSPC-GT process.** Autologous HSPCs are harvested from the patient and undergo *ex vivo* genetic manipulation consisting in viral vectors or genome editing tools like CRISPR-Cas9. Prior to transplantation, the patient undergoes a conditioning regimen to create space within its BM and suppress the immune system. The genetically modified HSPCs are then infused back into the patient's bloodstream, where they can reconstitute the BM and correct hematopoiesis<sup>67</sup>.

In the first clinical trial for BThal, TDT patients were infused with autologous CD34<sup>+</sup> HSPCs transduced with the lentiviral vector BB305 (Zynteglo). This vector encodes for a  $\beta$ -globin transgene with anti-sickling properties (HbAT87Q). The trial showed safety and efficacy in both sickle cell disease (SCD) and BThal patients, indeed 80% of non- $\beta$ 0 $\beta$ 0 patients and 38% of  $\beta$ 0 $\beta$ 0 patients achieved transfusion independence, while the remaining patients decreased the number of transfusions<sup>68,69</sup>. On August 17, 2022, the US FDA announced the approval of Zynteglo (betibeglogene autotemcel), which is the first cell-based gene therapy for the treatment of adult and pediatric patients with BThal who require regular RBC transfusions (<https://www.fda.gov/news-events/press-announcements/fda-approves-first-cell-based-gene-therapy-treat-adult-and-pediatric-patients-beta-thalassemia-who>).

Moreover, in the TIGET-BTHAL clinical trial, nine TDT patients, including three adults and six children, were treated by directly administering autologous HSPCs intrabone. These cells were genetically modified using the lentiviral vector GLOBE, which carries the  $\beta$ -globin gene under the control of a minimal locus control region (LCR). The trial achieved the primary endpoints of safety and efficacy since adult patients showed transfusion reduction and three out of four evaluated children reached complete transfusion independence<sup>70</sup>.

GE strategies aim to directly correct the genetic mutations or disrupt specific DNA sequences in the patient's genome using nucleases, such as CRISPR-Cas9 or zinc finger nucleases (ZFNs), exploiting the cellular DNA repair machinery. Clinical trials using gene editing approaches, such as CTX001 (CRISPR-Cas9) and ST-400 (ZFNs), aim to reactivate fetal hemoglobin (HbF) production by inhibiting the BCL11A gene. These trials are currently ongoing and have shown promising initial results for both TDT and SCD <sup>71</sup>.

In GT, various factors including HSC source, transduction efficiency, and BM microenvironment status can impact clinical outcomes. Since cases of graft rejection in allotransplants and poor HSC harvest or low levels of engrafted genetically modified HSC after gene therapy are common complications, a comprehensive understanding of HSPCs and the BM microenvironment is crucial for achieving successful outcomes in both allogeneic and autologous transplantation approaches in the context of BThal. Moreover, potential risks associated with GT or GE for BThal include off target effects, immunogenic response, and the long-term consequences of genetic interventions.

## **2 Hematopoiesis**

The blood system is a highly regenerative tissue in mammals, constantly producing billions of cells daily in adults in a continuous and dynamic process called hematopoiesis. Hematopoiesis orchestrates self-renewal, proliferation, and differentiation of a limited pool of HSCs in the BM. HSCs give rise to progenitor cells, which further proliferate and differentiate into mature blood cells <sup>72</sup>.

At steady state, adult HSCs remain in a quiescent state within the BM to maintain blood homeostasis and prevent exhaustion of the stem cell pool. However, in response to stressors like oxidative stress and inflammatory cues, HSCs can become activated and enter a proliferative state to replenish the hematopoietic system. HSCs are defined by their capacity to fully reconstitute all functional blood cells of a lethally irradiated recipient mice, whereas progenitor cells have limited self-renewal ability and fail to engraft long-term after transplantation <sup>73</sup>. To explain the diversity of blood cell population, the conventional hierarchical model of hematopoiesis suggests that HSCs positioned at the top of a hierarchy, lose their self-renewal capacity, and acquire lineage-specific potential, giving rise to multipotent progenitors (MPPs), common myeloid progenitors (CMPs), and common lymphoid progenitors (CLPs) <sup>74</sup>. However, this model oversimplifies the complexity of the process and has some limitations. Recent advancements in single-cell RNA sequencing and *in vivo* cell tracking have challenged this traditional hierarchical model, revealing the

heterogeneity of HSCs and early lineage segregation <sup>75</sup> (Fig. 8). In this model, there is heterogeneity within the HSC population with respect to lineage potential, including megakaryocyte (Mks)-biased HSCs that directly give rise to Mk-Er progenitors and bypass the classical intermediate commitment stages, including the MPPs and CMPs stages <sup>76-80</sup>. These findings suggest that the lineage commitment of HSCs may occur earlier than previously supposed <sup>72</sup>.

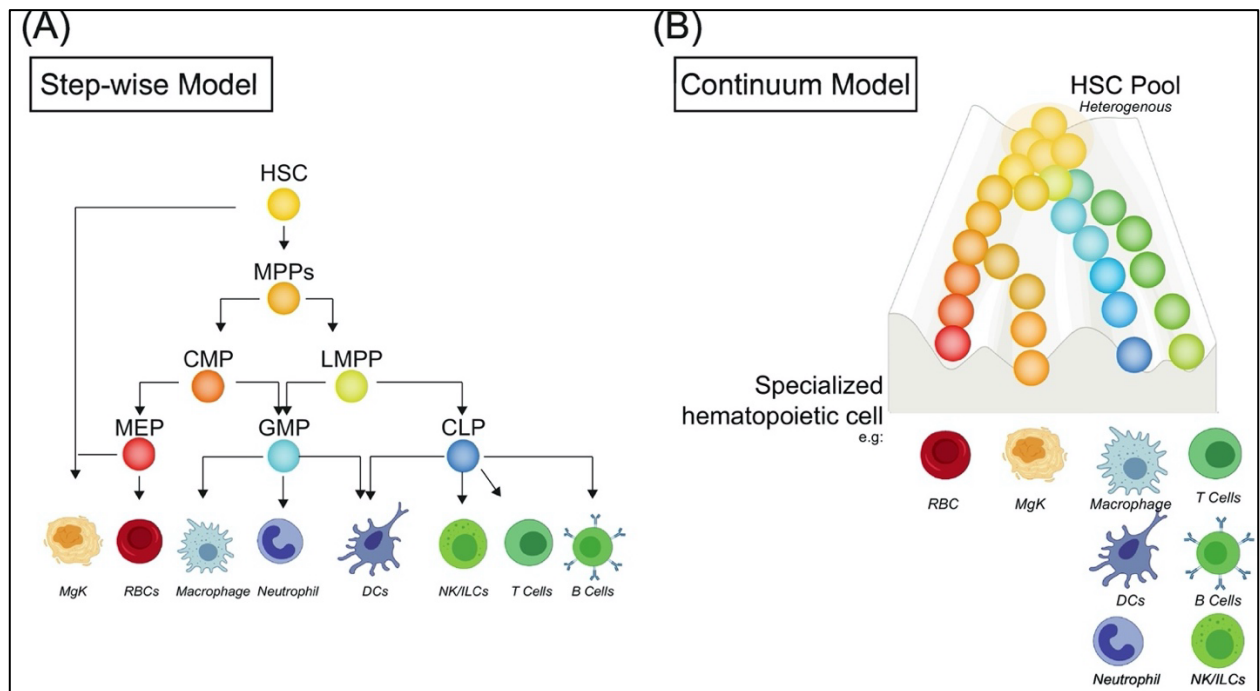


**Figure 8. Schematic HSC lineage commitment. A)** The classical hierarchical model where HSCs contribute equally to each blood lineage. **B)** The new revised model showing hematopoiesis as a continuum process where only a small fraction of HSCs produces an equal outcome for all mature blood cells, while most HSCs exhibit a bias towards differentiating into a specific lineage <sup>75</sup>.

In the mouse, long term HSCs are classified based on their phenotypic characteristics as Lin<sup>-</sup> ckit<sup>+</sup> Sca1<sup>+</sup> CD48<sup>-</sup> CD150<sup>+</sup>, while MPPs are Lin<sup>-</sup> ckit<sup>+</sup> Sca1<sup>+</sup> CD48<sup>-</sup> CD150<sup>-</sup> <sup>81</sup>. In humans, HSCs are phenotypically defined as Lin<sup>-</sup> CD34<sup>+</sup> CD38<sup>-</sup> CD45RA<sup>-</sup> Thy1<sup>+</sup> Rho10 CD49f<sup>+</sup>, while human MPPs are Lin<sup>-</sup> CD34<sup>+</sup> CD38<sup>-</sup> CD45RA<sup>-</sup> Thy1<sup>-</sup> Rho10 CD49f<sup>-</sup> <sup>73</sup>.

Adult HSCs reside in a specialized microenvironment in the BM called “niche”. The BM niche plays a crucial role in regulating HSC self-renewal, proliferation, and differentiation by both extrinsic and intrinsic factors and through interactions with various cellular components <sup>82</sup>. The BM niche comprises distinct regions, including endosteal niches near the bone surface and perivascular niches close to arterioles or sinusoids within the BM <sup>83</sup>. Recently,

high-resolution imaging studies have shown that the most quiescent HSCs are located close to both sinusoids and endosteum, while activated HSCs become more motile and move away from the endosteum. The localization of HSCs within the niche undergoes changes during lineage commitment, and stress signals can influence their spatial distribution <sup>84</sup>. Moreover, studies reported that aged HSCs localize further away from the endosteum as compared to young HSCs <sup>85</sup>.

## **2.1 HSC regulation in the BM niche**

HSC regulation in the BM niche is a critical aspect of hematopoiesis. Understanding the intricate regulatory mechanisms within the BM niche is essential for deciphering the balance between HSC quiescence and activation, as well as the control of HSC fate decisions. The regulation of HSCs within the niche involves interactions with various cell types, including non-hematopoietic stem cells as well as mature hematopoietic cells which contribute to HSC behavior by releasing a range of molecules including cytokine, chemokine, growth factors and physical cues. In addition to the extrinsic signals from the HSC niche, intrinsic factors also contribute to HSC heterogeneity, such as metabolic state, epigenetic alterations, and DNA mutations <sup>82</sup>.

HSCs are susceptible to various insults that can directly alter their function. These insults can occur through the accumulation of toxic molecules or a decrease in nutrient availability. Additionally, HSC function can be indirectly affected by altering the crosstalk between HSCs and other BM niche components. A deeper understanding of the relative contributions of cellular and molecular components in regulating HSC activity will pave the way for novel therapeutic approaches <sup>86</sup>.

## **2.2 HSC regulation by BM niche populations**

Extensive research involving conditional deletion of different cell types, depletion of niche factors, and advanced imaging techniques in mouse models has provided valuable insights into the cellular players within the HSC niche. The BM populations are closely interconnected, playing a crucial role in regulating HSC behavior and function within the BM microenvironment. Among them, stromal BM cells, including OBs, adipocytes, Schwann cells, mesenchymal stromal cells (MSCs) and endothelial cells (ECs), provide structural support and secrete various factors that influence HSC maintenance, proliferation, and differentiation. Hematopoietic BM cells, such as macrophages, OCs, lymphocytes,

neutrophils, and MKs, contribute to HSC regulation through direct cell-to-cell interactions and the release of soluble factors<sup>87</sup> (Fig. 9).

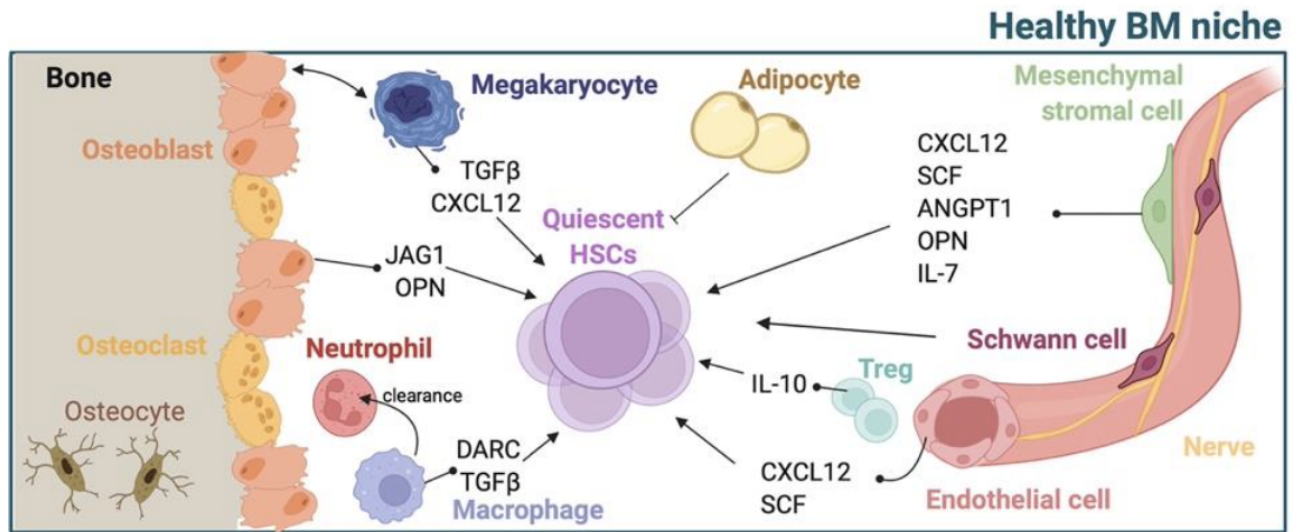


**Figure 9. The BM niche at steady state.** Several stromal (OBs, MSCs, ECs, adipocytes, sympathetic nerves and Schwann cells) and hematopoietic (OCs, Mφs, MKs, neutrophils and regulatory T cells) cell types and niche factors regulate HSC activity<sup>87</sup>.

### 2.2.1 Stromal BM cells

Stromal BM cells are a key component of the HSC niche, playing a crucial role in the regulation of HSC behavior. BM stromal cells, including osteolineage cells, MSCs, and ECs provide physical support to HSC.

Osteolineage cells, found on the bone surface, are a heterogeneous pool of bone-forming cell, including pre-osteoblasts, OBs, and terminally differentiated OTs<sup>88</sup>. Osteolineage cells were the first cell population associated with HSC regulation<sup>89-91</sup>. Studies have demonstrated that human OBs induce HSC differentiation towards myeloid lineages *in vitro*<sup>92</sup>, while murine OBs were found to enhance HSC engraftment in co-transplantation settings *in vivo*<sup>93</sup>. The activation of OBs by PTH and PTH-stimulated OBs contribute to HSC expansion through the activation of Notch signaling<sup>89</sup>. OBs also produce various growth factors and cytokines, including osteopontin (OPN), C-X-C motif chemokine ligand 12 (CXCL12), stem cell factor (SCF), thrombopoietin (TPO), and angiopoietin1 (ANGPT1). Recent studies using transgenic mice with specific deletion of CXCL12 and SCF from mature OBs have shown that this primarily affects early lymphoid progenitors but not HSCs or MEP, and it does not lead to the mobilization of these cells into the circulation<sup>94,95</sup>. OB-derived OPN has been reported to play a crucial role in controlling HSC homing and engraftment, as well as exerting an inhibitory effect on HSC proliferation<sup>96</sup>. However, recent

evidence suggests that osteolineage cells do not directly regulate HSCs, since other cell populations are considered the main functional sources of CXCL12, SCF, TPO, and ANGPT1. Studies have shown that hepatocytes are the primary functional source of TPO for the maintenance of HSCs <sup>97</sup>, while hematopoietic and stromal cells are considered the main sources of ANGPT1 <sup>98</sup>. Although, the essential role of osteolineage cells is controversial, *in vivo* live imaging studies suggest that the localization and function of HSCs are closely linked to bone turnover, as HSC expansion is observed in bone cavities exhibiting both OB and OC activity <sup>84</sup>.

MSCs are a rare population found near blood vessels in the BM which possess the ability to differentiate into bone, fat, and cartilage. Human MSCs marked by CD146 can generate colony-forming unit fibroblasts (CFU-Fs) *in vitro* and form heterotopic ossicles *in vivo*, demonstrating their regenerative potential <sup>99,100</sup>.

Different subpopulations of MSCs have been characterized using transgenic mice models, by distinct surface markers including Nestin+ perivascular cells, CXCL12-abundant reticular (CAR) cells, leptin receptor (LEPR)+ cells and PDGFR $\alpha$ + Sca1+ (PaS) cells <sup>94,101,102</sup>. However, it is now widely recognized that there is overlap between these stromal populations. MSCs exert their influence on HSC activity through both direct interactions and the secretion of soluble factors. N-cadherin-mediated physical interaction between MSCs and HSCs has been shown to modulate HSC activity <sup>103</sup>. However, the main control of HSCs by MSCs is indirect, mediated by the secretion of factors such as SCF, CXCL12, ANGPT1, OPN, and interleukin 7 (IL-7). MSCs also play a protective role in maintaining HSC function under stress conditions such as oxidative stress and infections. By neutralizing excessive ROS, MSCs help preserve HSC quiescence and function <sup>104</sup>.

Adipocytes, which arise from MSCs, have been shown to have both beneficial and detrimental effects on HSC regulation and their role remains controversial. Adipocyte progenitors have been found to support HSC regeneration by increasing the secretion of SCF in response to radiation-induced stress <sup>98</sup>. Adiponectin has been demonstrated to maintain HSC self-renewal and protect HSCs from inflammatory cytokines, particularly in HSCs and to a lesser extent in differentiated cells <sup>105</sup>. In contrast, the number of BM adipocytes is inversely correlated with HSC content, and inhibiting adipogenesis accelerates HSC engraftment after transplantation or chemotherapy <sup>106</sup>.

ECs that line the blood vessels in the BM are essential in controlling vascular integrity, and in regulating HSC trafficking and function. The BM contains two distinct types of ECs which can be identified based on their localization and surface marker expression: Arteriolar

endothelial cells (AECs) and sinusoidal endothelial cells (SECs). Approximately 10% of HSCs are closely associated with arterioles, while the majority are in proximity to sinusoids. The permeability of blood vessels in the BM microenvironment is important for regulating the levels of ROS in adjacent HSCs and niche populations. Arterioles, which are less permeable, help maintain HSCs in a quiescent state with low ROS levels. On the other hand, leaky sinusoids increase ROS levels, promoting HSC activation and mobilization <sup>107</sup>. *In vivo* studies using genetic modifications to specifically delete niche factors in ECs have provided insights into the importance of endothelial-derived factors in HSC regulation. These studies have demonstrated the essential role of CXCL12 and SCF produced by ECs in HSC self-renewal and hematopoietic regeneration after injury. Furthermore, ECs regulate HSC quiescence through the expression of surface marker E-selectin <sup>108,109</sup>.

The sympathetic nervous system (SNS) extensively innervates the BM and plays a crucial role in modulating HSC mobilization and protecting against genotoxic stress. Nerve fibers of SNS target Nestin<sup>+</sup> MSCs, stimulating the production of CXCL12 via  $\beta$ 3-adrenergic receptors and regulating the release of HSCs into the bloodstream under the circadian rhythm <sup>110</sup>. Furthermore, the SNS is involved in facilitating hematopoietic recovery following genotoxic stress <sup>111</sup>. Non-myelinating Schwann cells, which surround sympathetic nerves, not only support the formation of new blood vessels (angiogenesis) and bone tissue (osteogenesis), but also directly interact with HSCs, promoting their quiescent state through the activation of TGF $\beta$  and SMAD signaling pathways <sup>112</sup>.

### **2.2.2 Hematopoietic BM cells**

BM niche is orchestrated by various terminally differentiated cells, including macrophages (M $\phi$ s), neutrophils, regulatory T (Tregs) cells, OCs and MKs which contribute to the regulation of HSC behavior. These cells interact with HSCs directly and through the secretion of soluble factors, influencing HSC quiescence, activation, and differentiation.

M $\phi$ s are a heterogeneous population with phagocytic activity, that directly modulates HSC quiescence and self-renewal through physical interaction and the release of cytokines <sup>113,114</sup>. M2 M $\phi$ s promote HSC self-renewal, while M1 M $\phi$ s have the opposite effect, preserving HSC repopulating potential <sup>115</sup>. Additionally, BM M $\phi$ s indirectly control HSC location by inducing the expression of HSC retention factors by MSCs and promoting HSC mobilization via neutrophil clearance <sup>116,117</sup>. M $\phi$ s also play a crucial role in erythrophagocytosis, contributing to iron homeostasis and providing iron to HSCs during hematopoietic stress.

Neutrophils and Tregs have been implicated in the control of HSC retention through their interactions with osteolineage cells although the precise mechanisms of their direct regulation of HSC function are not yet fully understood <sup>118-120</sup>.

OCs play a key role in bone resorption and remodeling, which is regulated by systemic endocrine factors such as PTH and estrogen under normal physiological conditions. PTH signaling leads to a reduction in TGF- $\beta$  levels in OTs and activates PTH-PTH receptor signaling cascades in osteoblasts. These events stimulate the formation of OCs, initiating the process of bone resorption <sup>121</sup>. The interaction between OCs and HSPCs is bidirectional. OCs can regulate HSPC retention within the BM niche by creating a physical barrier that keeps HSPCs near the endosteal surface, thereby preventing their mobilization into the bloodstream. The absence of OCs can disrupt this retention mechanism, potentially resulting in increased HSPC mobilization <sup>122</sup>. Moreover, OCs secrete the coupling factor sphingosine 1-phosphate (S1P), which acts on HSC through S1P1 receptors to regulate cell trafficking, particularly in the context of cell egress after treatment with mobilizing agents like granulocyte-colony-stimulating factor (G-CSF) <sup>123</sup>.

MKs exhibit a non-random spatial association with HSCs in the BM, and their depletion leads to an expansion of the HSC pool. Under steady-state conditions, MKs maintain HSC quiescence by secreting specific factors like CXCL4 and TGF $\beta$  <sup>124,125</sup>. However, in response to chemotherapeutic stress, MKs promote HSC expansion through fibroblast growth factor 1 signaling (FGF1) <sup>125</sup>. MKs also indirectly regulate HSC function by interacting with bone cells, and they support OBs survival and HSC engraftment after myeloablative irradiation <sup>126</sup>.

### **2.3 HSC niche in homeostasis and stress conditions**

The BM niche is a dynamic environment responding to both normal and stress conditions, such as oxidative stress, iron, variation of oxygen level and inflammatory signals. Under physiological circumstances, the niche supports HSC maintenance, self-renewal, and balanced hematopoiesis. However, during stress conditions, such as infection, inflammation, or hematological disorders, the niche undergoes alterations and HSCs adapt their metabolic state and cell cycle <sup>127</sup>. Understanding the adaptive changes of the BM niche in response to different stressors is crucial for comprehending the impact of pathological conditions on hematopoiesis and developing therapeutic strategies to restore niche homeostasis.



### 3 Function of HSC and BM niche in BThal

HSCT is a crucial treatment for hematological inherited disease. However, HSC- niche interactions in improving HSCT outcomes are still underexplored in the context of BThal. In allogeneic HSCT, the engraftment of normal donor HSCs can be compromised by the host BThal niche, while both the donor HSCs and the BM niche are altered in autologous HSCT, potentially impacting the clinical outcome. Recent studies have demonstrated that HSC function in BThal is negatively affected by their prolonged exposure to an impaired BM niche<sup>128</sup>, with detrimental effects caused by the accumulation of toxic molecules like iron and ROS and changes in BM cell populations<sup>129</sup>. The *th3* mouse model, which mimics the features of BThal intermedia, has been used to study the HSC niche, providing valuable insights that validate findings observed in patient-derived samples. Overall, a more comprehensive understanding of the HSC compartment and BM niche is necessary to develop targeted strategies that improve the outcomes of HSCT in BThal.

#### 3.1 HSC defect in BThal

A recent study conducted by Aprile A. et al. shed light on hematopoiesis in the context of BThal. The authors found impaired HSC function using the *th3* mouse model, recapitulating severe BThal intermedia<sup>128</sup>. They focused on the most primitive HSCs defined by SLAMF family markers as Lin<sup>-</sup>, cKit<sup>+</sup>, Sca1<sup>+</sup> CD48<sup>-</sup> CD150<sup>+</sup><sup>81</sup> and observed a reduced number of HSCs in the *th3* mice compared to wild-type (wt) mice. Additionally, the BThal HSCs displayed decreased quiescence and increased cycling, with a higher proportion of cells in the S and G2/M phases and a lower proportion in the G0 phase. RNA sequencing analysis of sorted BThal HSCs confirmed these findings, showing enrichment of cell cycle G1/S phase transition genes and reduced expression of stemness genes like *Cdkn1c*, *Runx1l1*, *Fgd5*, and *Hes1*. The increased cell proliferation in BThal HSCs was associated with the accumulation of DNA damage.

To evaluate HSC function, the authors conducted transplant experiments. Primary transplantation of equal numbers of wt and BThal HSCs into *th3* mice demonstrated a competitive disadvantage of BThal HSCs, and this disadvantage was further exacerbated upon secondary transplantation. However, when BThal HSCs were transplanted into wt recipients, their defects were restored. These findings indicate that the dysfunction of BThal HSCs is not intrinsic but is caused by an altered BM niche. Consistently, Gene Set Enrichment Analysis (GSEA) on the RNA sequencing data confirmed significant enrichment

of genes associated with cellular responses to stress in the BThal HSC transcriptome, suggesting that stress signals in the BThal BM niche impact HSC function. Interestingly, the defects in HSC frequency and cell cycle were not observed in newborn animals but appeared around 4 weeks of age and worsened in adult mice, indicating that prolonged exposure to the impaired BM niche contributes to HSC dysfunction. Notably, no differences were found in the frequency of more committed progenitors, suggesting a distinct behavior between HSCs and progenitors in BThal that requires further investigation.

Interestingly, similar findings were observed in patients with TDT which exhibited an increased frequency of CD34+CD38- primitive HSPCs in active cell cycle phase compared to healthy donors. Moreover, RNA-seq analysis of TDT CD34+ cells also displayed heightened responses to stress stimuli and reduced expression of key stemness genes <sup>128</sup>, suggesting that TDT HSPCs are exposed to an altered BM niche.

Overall, these findings highlight the impact of the BM niche on HSC function in BThal and suggest the importance of addressing the altered niche to improve HSC-based therapies for BThal patients.

### **3.2 Stromal niche defect in BThal**

To further investigate the transplantation outcomes of *th3* HSCs in a BThal BM niche, Aprile et al. focused on the interactions between HSCs and stromal cells, including osteolineage cells and MSCs. Bone abnormalities such as osteoporosis and osteopenia are common complications in BThal patients, resulting from hormonal deficiency, BM expansion, and iron toxicity <sup>18</sup>. The study also observed reduced BMD in *th3* mice due to decreased activity of OBs and low levels of circulating PTH <sup>128</sup>, which aligns with bone fragility and low PTH levels observed in BThal patients <sup>26</sup>. PTH plays a crucial role in regulating bone metabolism and maintaining HSC function through Notch signaling <sup>89</sup>. Additionally, PTH directly influences MSCs by promoting their differentiation into OBs <sup>130</sup>. In *th3* mice, low PTH levels result in reduced OB activity and inhibit their secretion of OPN, which suppresses HSC proliferation and retention, as well as JAG1, a Notch-ligand implicated in HSC self-renewal capacity.

*In vivo* treatment of *th3* mice with PTH rescues bone defects by increasing BMD and enhancing the expression of JAG1 and OPN by stromal cells, thereby restoring HSC frequency and normalizing their cycling activity. However, the incomplete restoration of *th3* HSC repopulating ability after PTH treatment suggests the involvement of additional cellular and molecular factors within the complex BThal BM niche in regulating HSCs. Furthermore,

*th3* MSCs display reduced frequency and decreased JAG1 secretion due to low PTH levels<sup>128</sup>. Importantly, these findings were confirmed in BThal patients' samples. Crippa et al. demonstrated that IO generates oxidative stress, thus reducing the frequency and the proliferation of BThal MSCs and impairing their differentiation. BThal MSCs exhibit reduced expression of key hematopoietic supportive factors and fail to support HSC expansion and engraftment *in vitro* and *in vivo* experiments. However, treatment with iron chelation restores the HSC-MSc niche crosstalk by reducing iron transporters' expression. These findings indicate that IO impairs BThal MSCs, thereby negatively impacting HSC function<sup>129</sup>.

### **3.3 Hematopoietic and soluble niche factors**

Data obtained from studies on BThal mice indicate that multiple alterations in the BM niche contribute to the impaired self-renewal and repopulating capacity of HSCs. Analysis of the BM microenvironment revealed elevated levels of FGF23, a negative regulator of bone metabolism and PTH secretion, which negatively affects the interaction between HSCs and the stromal niche<sup>131</sup>. Additionally, altered levels of factors such as SCF, ANGPT1, CXCL12, and reduced serum TPO were observed, impacting HSC-niche interactions<sup>128</sup>.

Moreover, focusing on hematopoietic populations of the BM microenvironment, resident Mφs have been found to indirectly regulate HSC retention within the BM niche by interacting with stromal cells<sup>132</sup>. Recent studies have shown that in SCD, free-iron and heme overloads can induce the M1 phenotype in bone marrow-derived macrophages (BMDM), which was reported to reduce HSC self-renewal<sup>133</sup>. However, evidence of M1-polarized macrophages in β-Thal is still lacking.

Overall, the BThal BM niche is influenced by various factors including hormonal factors, such as PTH and FGF23, cytokines and stress signals as iron, ROS and inflammatory molecules. These factors can have direct or indirect effects on HSCs as well as other cell populations in the BM niche<sup>87</sup> (Fig. 10).

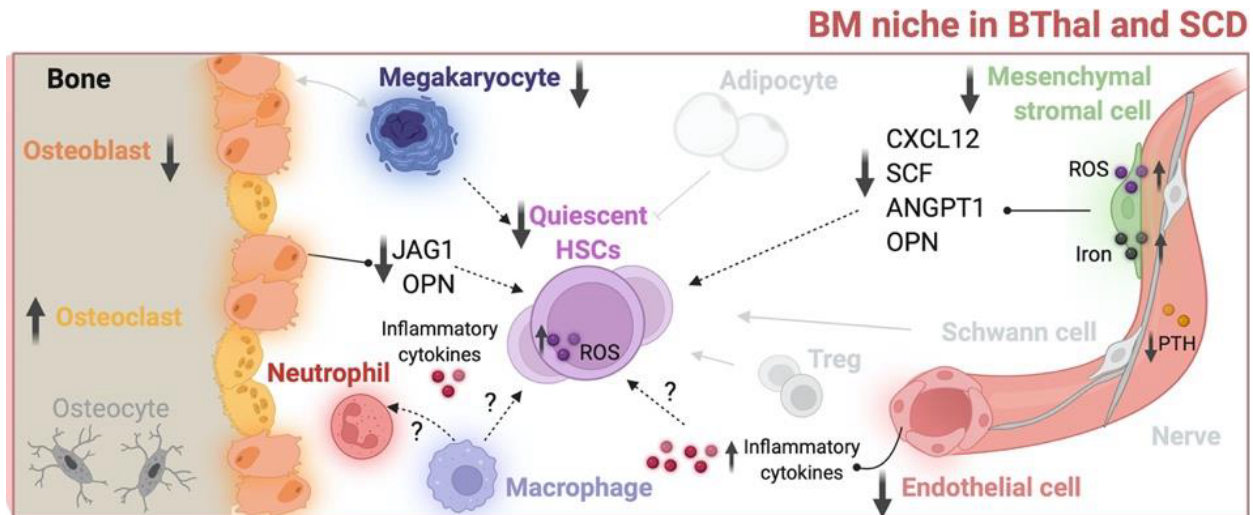


**Figure 10. BThal BM niche.** BThal HSC function is impaired due to prolonged exposure to an altered BM niche. Several BM niche populations, such as OBs, MSCs, MKs and M $\phi$ s, are impaired and accumulation of toxic molecules, such as iron, ROS and inflammatory cytokines potentially contributing to the decline in HSC function<sup>87</sup>.

#### 4 Fibroblast growth factor 23 (FGF23)

FGFs are a group of small, secreted proteins that belong to the larger family of growth factors<sup>134</sup>. The FGF family is classified into subfamilies based on sequence similarity, including canonical FGFs (FGF1-10), the hormone-like FGFs (FGF19, FGF21, FGF23), and the unconventional FGFs (FGF11-14)<sup>135</sup>. FGFs bind to and activate a family of transmembrane receptor tyrosine kinases known as FGF receptors (FGFRs). There are four FGFR isoforms (FGFR1-4), and the binding specificity between FGFs and FGFRs is primarily determined by the heparan sulfate proteoglycans present on the cell surface, which act as co-receptors<sup>136</sup>. FGFs mediate autocrine and paracrine signaling, regulating several cellular processes such as cell proliferation, differentiation, survival, and migration. Upon binding to FGFRs, FGFs induce receptor dimerization and activation of downstream signaling pathways, such as the MAPK/ERK, PI3K/Akt, and PLC $\gamma$  pathways<sup>137</sup>. Paracrine FGFs act locally and mediate signaling between adjacent cells, influencing tissue development and homeostasis. Endocrine FGFs, on the other hand, act as hormones and are secreted into the bloodstream to regulate systemic metabolic processes. They depend on the presence of  $\alpha$ -klotho in their respective target tissues.  $\alpha$ -klotho enhances the binding affinity between endocrine FGFs and their specific FGFRs, leading to a more efficient and effective signaling response<sup>138,139</sup>. FGF23 has emerged as a significant player in the regulation of mineral metabolism and the pathogenesis of renal and cardiovascular diseases. FGF23 gene was identified as mutated in patients with Autosomal dominant

hypophosphatemic rickets (ADHR) <sup>140</sup>. ADHR patients show elevated FGF23 in the bloodstream, which leads to an altered phosphate homeostasis and results in rickets, a condition which affects bone development. Since then, several studies have revealed FGF23 a key phosphaturic hormone mainly secreted by OTs, that primarily acts on the kidneys and plays a crucial role in maintaining phosphate, calcium and bone homeostasis <sup>141</sup>.

#### 4.1 The impact of systemic and local factors on FGF23 regulation

FGF23 production and secretion are tightly regulated by various factors. High levels of phosphate, active vitamin D, and PTH stimulate FGF23 synthesis and release from OTs. On the other side, FGF23 inhibits bone mineralization and PTH, this negative feedback mechanism ensures that phosphate remains within the physiological range <sup>142</sup>. Additionally, other factors, including anemia, iron status and inflammation can modulate FGF23 production <sup>143</sup> (Fig. 11).

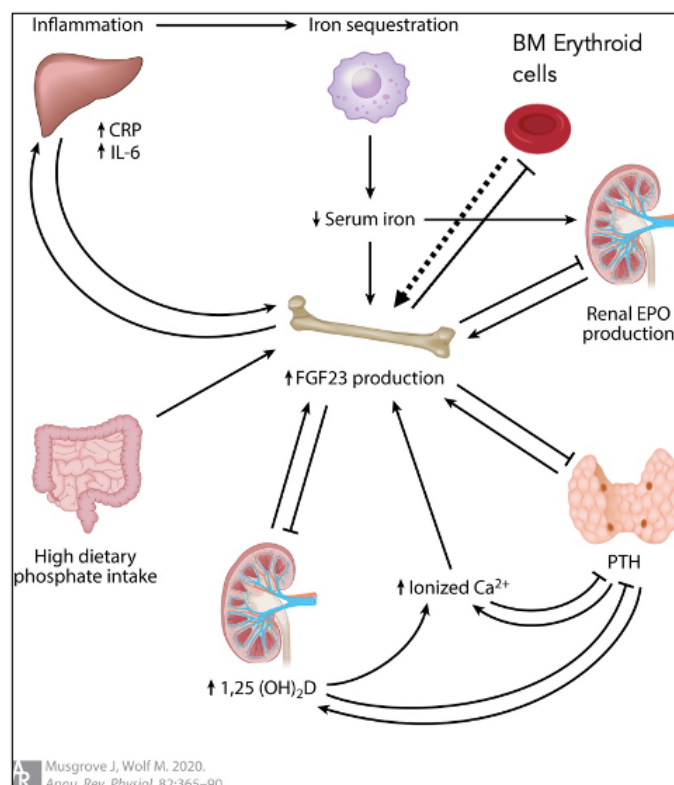


**Figure 11. Inducers of FGF23 production.** FGF23 production is regulated by several systemic factors including phosphates, Vitamin D, PTH, EPO, iron deficiency and inflammation (Adapted from <sup>143</sup>).

Phosphate is an essential mineral that plays crucial roles in energy production, DNA synthesis, and bone mineralization. FGF23, a principal regulator of phosphate homeostasis, responds to changes in dietary phosphate intake. It has been shown that an increase in dietary phosphate intake increased FGF23<sup>144</sup>. On the contrary, restricting phosphate intake reduces FGF23. A recent study revealed the molecular mechanism by which phosphate modulates FGF23 levels. Phosphate itself can bind to this receptor, leading to the upregulation of the N-acetylglucosaminyltransferase 3 (*Galnt3*) gene, which increases the proportion of biologically active iFGF23<sup>145</sup>.

Vitamin D plays a crucial role in maintaining calcium and phosphate homeostasis in the body. It promotes calcium absorption from the intestine and enhances phosphate reabsorption in the kidneys, ensuring sufficient levels of these minerals for various physiological functions. The active form of vitamin D directly stimulates the transcription of the *Fgf23* gene. Mice injected with the 1,25-dihydroxy-vitamin D increased *Fgf23* transcription, specifically in bone, resulting in elevated serum FGF23 protein<sup>146</sup>. Furthermore, another study in murine models has revealed that calcium can directly increase *Fgf23* transcription by acting on the promoter of the *Fgf23* gene<sup>147</sup>.

PTH has been identified as a regulator of FGF23 by directly increasing its expression in bone cells in an experimental model of chronic kidney disease (CKD)<sup>148</sup>. Moreover, PTH action on bone cells includes the suppression of the gene encoding *Sost*. SOST acts as a local inhibitor of the Wnt signaling pathway, indirectly suppressing FGF23 production<sup>149,150</sup>. Therefore, when PTH suppresses SOST, it allows FGF23 to be released, resulting in elevated FGF23 production.

FGF23 is regulated at the local level within bone cells by several regulators. One factor is dentin matrix protein 1 (DMP1), a member of the SIBLING family, which is produced by OTs<sup>151</sup>. DMP1 acts as a suppressor of FGF23, leading to a decrease in FGF23 production and secretion and enhancing bone mineralization. Another regulator is the phosphate-regulating gene with homologies to endopeptidases on the X chromosome (PHEX), predominantly expressed by OBs. PHEX is also supposed to suppress the transcription of *Fgf23* rather than its degradation<sup>152</sup>. Inherited mutations in either PHEX or DMP1 lead to genetic disorders associated with renal phosphate wasting and elevated FGF23 levels. Inactivating mutation in PHEX causes X-linked hypophosphatemic rickets (XLH), a condition characterized by elevated FGF23, hypophosphatemia, rickets and osteomalacia<sup>153</sup>. While inactivating mutations in *DMP1* result in autosomal recessive hypophosphatemic rickets (ARHR) (*ADHR Consortium 2000*).

FGF23 function is mainly studied in CKD. CKD manifests with anemia due to reduced EPO production by kidney and iron deficiency and bone abnormalities<sup>154</sup>. Several studies demonstrated that FGF23 levels increase in children and adults with CKD before the increase in PTH and phosphate and the decrease in vitamin D and calcium concentrations<sup>155,156</sup>. Once CKD with secondary hyperparathyroidism is established, FGF23 antibody neutralization fully normalized vitamin D and precipitated severe hyperphosphatemia. With the progression of CKD, FGF23 expression increases within OTs, a process dependent on bone-related Klotho expression and its concentration is associated with cardiovascular disease<sup>157</sup>. The primary driver of increased FGF23 levels in CKD is the retention of phosphate due to reduced urinary excretion. Additionally, various CKD-associated factors, including anemia-induced tissue hypoxia and iron deficiency, contribute to the increase of FGF23. FGF23 is considered a potential biomarker for CKD-related bone disease but also a novel cardiovascular risk factor<sup>158</sup>.

#### **4.2 Molecular mechanism regulating FGF23**

FGF23, primarily expressed by bone cells, including OBs and OTs<sup>159</sup> and BM<sup>160</sup> cells, plays a crucial role in maintaining phosphate and bone homeostasis<sup>141</sup>. The regulation of FGF23 production involves three steps: transcription, translation and post-translational modification of nascent peptide and cleavage of mature FGF23.

Human FGF23 is a 32-kDa glycoprotein encoded by three exons on chromosome 12p. FGF23 consists of 251 amino acids with a hydrophobic secretory signal sequence and a conserved FGF core region, along with a unique 72-amino acid COOH-terminus<sup>161</sup>. FGF23 can be cleaved intracellularly at arginine residues (176 and 179) by subtilisin-like proprotein convertases (SPC1 or FURIN) or proprotein convertase enzyme 5 (PCSK5), resulting in three circulating molecular species: the full-length biologically active FGF23 (iFGF23), a shorter N-terminal fragment lacking the C-terminal portion and the cleaved C-terminal fragment (cFGF23). Alternatively, FGF23 can be O-glycosylated at Threonine 178 by the GALNT3 enzyme, which preserves the intact form of FGF23. However, phosphorylation of FGF23 at serine180 by kinase family with sequence similarity 20-member C (FAM20C) prevents O-glycosylation and promotes FURIN-mediated cleavage<sup>162</sup>. The cFGF23 fragment specifically blocks FGF23 signaling by competing with iFGF23 for binding to FGFR<sup>161</sup>. However, other functions of this peptide are still being explored. The balance between these processes determines the ratio of iFGF23 to cFGF23 in circulation<sup>141</sup> (Fig.12).

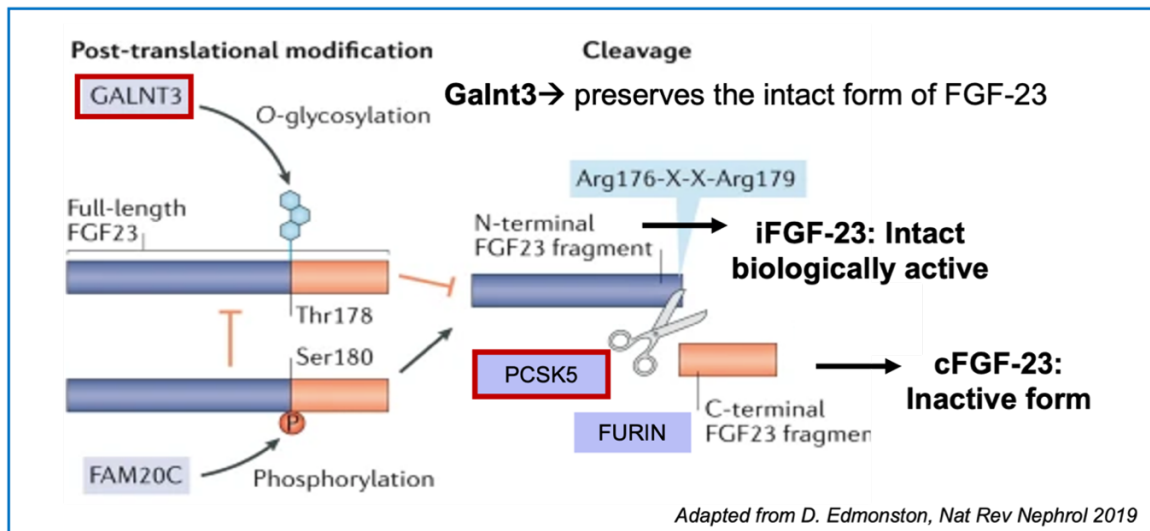


**Figure 12. FGF23 post-translational modifications.** GALNT3 O-glycosylation stabilizes the FGF23 nascent peptide and protects it from cleavage. Conversely, phosphorylation by protein kinase FAM20C inhibits O-glycosylation and marks FGF23 for proteolytic cleavage by *FURIN* or *PCSK5*. Adapted from <sup>141</sup>.

### 4.3 Key factors that induced FGF23 production

The production and cleavage of FGF23 can be influenced by several factors including EPO, iron and inflammation which are hallmarks of hereditary anemias, as BThal and SCD, as well as secondary anemias like CKD (Fig 13).

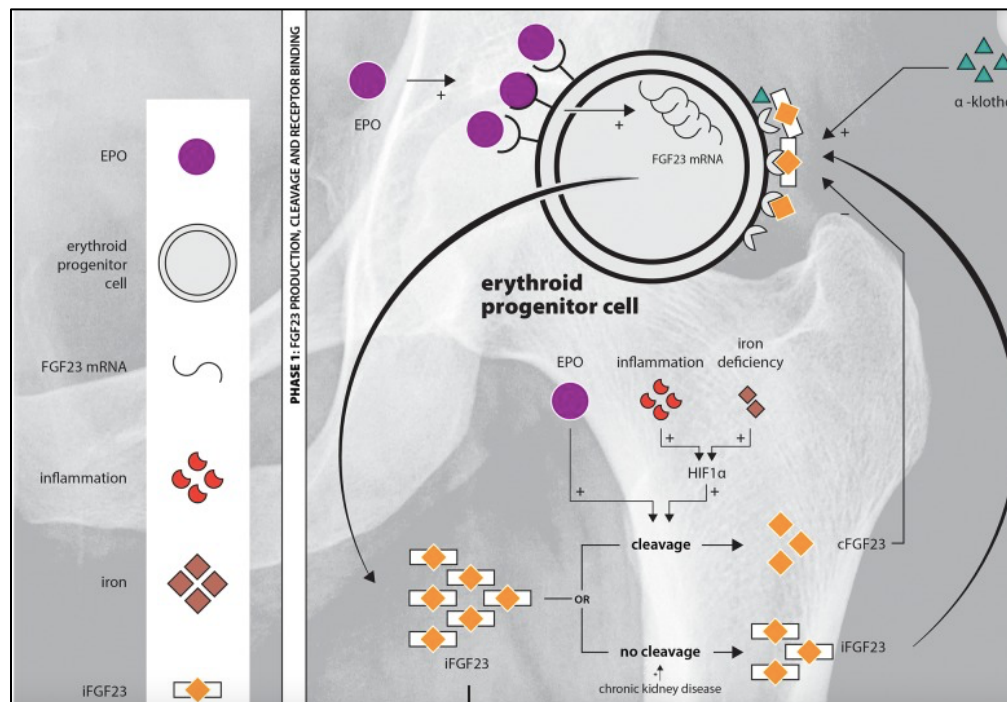


**Figure 13. Overview of EPO-FGF23 signaling pathway.** FGF23 production and cleavage by erythroid BM cells, adapted from <sup>163</sup>.



### 4.3.1 Erythropoietin

EPO is an important regulator of FGF23 production and cleavage<sup>163</sup>. Recent correlative studies have shown that EPO administration induces FGF23 production in OBs and in murine hematopoietic progenitors<sup>164</sup>. Additionally, acute blood loss leads to an increase in circulating EPO and in cFGF23 peptide, suggesting that FGF23 contributes to maintaining erythropoietic homeostasis<sup>165</sup>. Loss of FGF23 through FGF23-knockout or blocking iFGF23 signaling in mice results in increased erythropoiesis, reduced erythroid cell apoptosis and elevated BM *Epo* mRNA expression, leading to higher circulating EPO<sup>160</sup>. *In vivo* administration of FGF23 has been shown to cause a rapid decrease in erythropoiesis<sup>160</sup>. Consistently, in conditions of severe anemia, especially those associated with CKD, levels of circulating FGF23 are increased. Inhibition of FGF23 signaling has been demonstrated to stimulate erythropoiesis by significantly reducing erythroid cell apoptosis and influencing HSC commitment towards the erythroid fate and this rescued anemia in a model of CKD<sup>166</sup>. Overall, these data show that EPO increases the total amount of circulating FGF23 (iFGF23 and cFGF23) and influences the balance between iFGF23/cFGF23 by promoting cFGF23 production. This effect is achieved through EPO-mediated inhibition of *Galnt3* expression in bone BM cells<sup>167</sup>. While previous studies have established only a positive correlation between EPO and FGF23, the underlying mechanisms remained elusive. Our recent work demonstrated for the first time EPO is the causal factor inducing *Fgf23* transcription, this was achieved by blocking the EPO pathway through monoclonal anti-EPO antibody. Moreover, we identified the molecular mechanism by which EPO modulates *Fgf23* expression by acting on bone and erythroid cells through the activation of Erk1/2 and Stat5 pathways, respectively<sup>131</sup>.

### 4.3.2 Iron deficiency

The first evidence linking iron deficiency and FGF23 regulation came from studies on ADHR, a disorder characterized by elevated FGF23 due to defective FGF23 proteolytic cleavage. In individuals with ADHR, serum iron was found to negatively correlate with circulating FGF23<sup>168</sup>. Further investigation in a cohort of pre-menopausal women revealed that serum iron levels inversely correlate with the increased cFGF23, but not with iFGF23<sup>169</sup>. Similarly, in a cohort of elderly individuals, low iron parameters were associated with higher concentrations of both cFGF23 and iFGF23, with a more pronounced increase observed in cFGF23<sup>170</sup>. Moreover, wt mice studies showed that iron deficiency leads to an

increase in the FGF23 cleaved form<sup>164,167</sup>. This effect is associated with the stabilization of pre-existing hypoxia-inducible factor 1-alpha (HIF1 $\alpha$ ) which upregulates intracellular iFGF23 cleavage<sup>171</sup>. One key player in iron regulation is hepcidin, a peptide hormone that controls iron absorption and distribution. Elevated production of hepcidin in response to inflammatory cytokines is a significant contributor to functional iron deficiency and anemia<sup>172</sup> (Fig.13). cFGF23 has been found to downregulate hepcidin expression, thereby enhancing iron availability in the context of acute inflammation<sup>173</sup>. In this study conducted by Courbon and colleagues, wt mice co-injected with bone morphogenetic protein (BMP) 2-9 and cFGF23 exhibited a decrease in serum hepcidin and an increase in serum iron levels, thus indicating that c-terminal peptide directly regulates iron metabolism by reducing hepcidin secretion by acting as a BMP antagonist<sup>173</sup>. Further investigations are needed to explore if a modest increase of cFGF23 during chronic inflammation is sufficient to reduce hepcidin and increase iron bioavailability. Recently, Li X. et al. elucidated the cellular sources of FGF23 upregulation during iron deficiency anemia (IDA), using mice lacking transmembrane serine protease 6 (Tmprss6), a model for Iron-Refractory Iron Deficiency Anemia, an autosomal recessive disorder<sup>174</sup>. Tmprss6<sup>-/-</sup> exhibited elevated hepcidin without signs of inflammation and showed increased circulating FGF23 levels. Using an Fgf23<sup>eGFP</sup> reporter allele in vascular regions of BM they identified *Fgf23* mRNA upregulation by BM SEC in chronic genetically-induced IDA, in acute phlebotomy-induced anemia, and after injection of EPO in wt mice. Genetically induced IDA is characterized by elevated levels of EPO, which probably directly influences BM-SEC to enhance FGF23 production. Intriguingly, analysis of single-cell RNA sequencing data of BM stroma from wt mice revealed the presence of both *Fgf23* and *Epor* expression within BM-SEC<sup>175</sup>.

### 4.3.3 Inflammation

In two murine models of acute inflammation, there was a significant increase in bone *Fgf23* mRNA expression and cFGF23 serum concentrations, without changes in iFGF23<sup>171</sup>. Acute inflammation drives FGF23 production and its cleavage in OTs. Pro-inflammatory cytokines such as TNF- $\alpha$ , IL-1 $\beta$  and IL-6 are potent inducers of FGF23 secretion<sup>176</sup>. A recent study has shed light on another important aspect of cFGF23's role in inflammation. Bone-produced cFGF23 peptide directly regulates iron metabolism by antagonizing BMP-induced hepcidin production<sup>173</sup>. In summary, inflammation appears to augment both FGF23 expression and its cleavage by increasing HIF1 $\alpha$  expression and stabilization and enhanced Furin activity, but also via hepcidin-induced functional iron deficiency and subsequent non-

hypoxic HIF1 $\alpha$  stabilization (Fig. 14). In the context of chronic inflammation, increased amounts of total FGF23 with increased amounts of iFGF23, and the FGF23 cleavage system seems to be downregulated <sup>171</sup>.

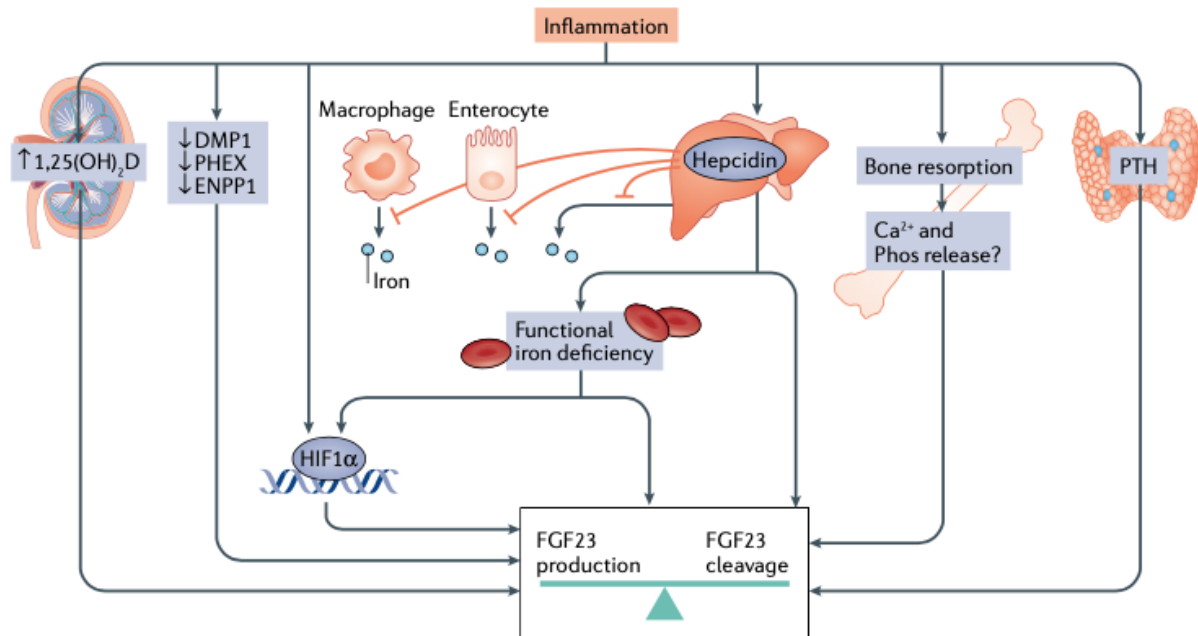


**Figure 14. Pathways linking inflammation, iron deficiency and FGF23 regulation.** Inflammation stimulates FGF23 production and cleavage through various mechanisms, including elevating active vitamin D and PTH levels, boosting the expression of HIF1 $\alpha$ , and reducing the expression of inhibitors of FGF23 transcription. Inflammation also promotes the production of hepcidin in the liver, which, by inhibiting the export of iron from cells, induces functional iron deficiency and subsequently increases both FGF23 production and cleavage. Moreover, increased bone resorption during inflammatory conditions releases calcium, phosphate, and potentially FGF23 from bone, further contributing to elevated FGF23 levels <sup>141</sup>.

#### 4.4 Inhibition strategies of FGF23 signaling

Given the role of excessive FGF23 production in the development of human diseases, several studies have explored targeting FGF23 as a potential treatment for disorders associated with its dysregulation. One approach relies on the use of neutralizing antibodies that specifically bind to FGF23, which has been shown to restore normal phosphate, vitamin D levels and increase BMD in *Hyp* mice, which recapitulate hypophosphatemia <sup>177</sup>. Based on these results, a humanized anti-FGF23 antibody, Burosumab, was developed and tested in clinical trials. Burosumab increases serum phosphate levels and improves skeletal health in XLH by preventing FGF23 from binding to FGFRs <sup>178</sup>. The anti-FGF23 neutralizing

antibody partially improved bone mineralization in XLH mice <sup>179</sup>. Long-term treatment with anti-FGF23 antibody improves bone microarchitecture and ameliorates anemia in a mouse model of Myelodysplastic syndrome (MDS) <sup>180</sup>. Burosumab is currently approved by the FDA for the treatment of XLH and tumor-induced osteomalacia (TIO). However, addressing XLH remains a challenge, as not all patients exhibit a complete response to the treatment <sup>181</sup>. Therefore, it may be necessary to explore alternative treatment options. In a recent study, Fuente et al. investigated the efficacy of three short C-terminal FGF23 peptides with an improved half-life as a treatment for XLH mice injected for seven consecutive days. To enhance the stability and half-life of the 72-amino acid fragment, a fusion molecule containing the FGF23 c-tail was generated through C-amidation and N-acetylation <sup>182</sup>. The study revealed positive outcomes, including enhanced growth rate and normalized growth plate by improving mineralization and the structure of primary spongiosa. Additionally, the mineralization of cortical bone and the number of OCs were improved after treatment. However, longer treatments are necessary to fully address bone deformities and restore hormonal balance in the bloodstream <sup>183</sup>.

c-terminal fragments of FGF23 have recently emerged to inhibit FGF23 binding to the Klotho-FGF receptor complex. The purified cFGF23 protein has been shown to compete with iFGF23 for binding to the FGFR complex <sup>161</sup>. Administration of the cFGF23 peptide has been reported to temporarily increase serum phosphate in *Hyp* mice <sup>161</sup> and rescue anemia by decreasing erythroid cell apoptosis in CKD mice <sup>166</sup>.

In addition, targeting FGFR has been demonstrated to inhibit FGF23 activities <sup>184</sup>. NVP-BGJ398, a pan FGFR inhibitor, increased serum phosphate, enhanced bone growth and improved mineralization in *Hyp* mice <sup>185</sup>.

#### **4.5 Effects of FGF23 signaling**

FGF23 plays a crucial role as a major regulator of phosphate and calcium homeostasis, along with vitamin D and PTH <sup>186,187</sup>. FGF23 exerts its actions primarily in the kidney, parathyroid gland, and bone by binding to the Klotho-FGF23 receptor complex <sup>138,139,188</sup>. FGF23 reduces serum phosphate by inhibiting intestinal phosphate absorption through the downregulation of the sodium-phosphate cotransport NaPi2a and NaPi2c in the proximal tubule, thus increasing urinary phosphate excretion <sup>188,189</sup>. Additionally, FGF23 downregulates enzymes that metabolize vitamin D, as 1 $\alpha$ -hydroxylase, leading to reduced levels of available active 1,25-dihydroxy-vitamin D and suppressing intestinal phosphate absorption <sup>190</sup>. FGF23 also directly inhibits the secretion of PTH, which increases the uptake

of phosphate from bone and upregulates  $1\alpha$ -hydroxylase, leading to increased vitamin D activation and enhanced phosphate reabsorption in the intestine <sup>142,191</sup> (Fig.15).

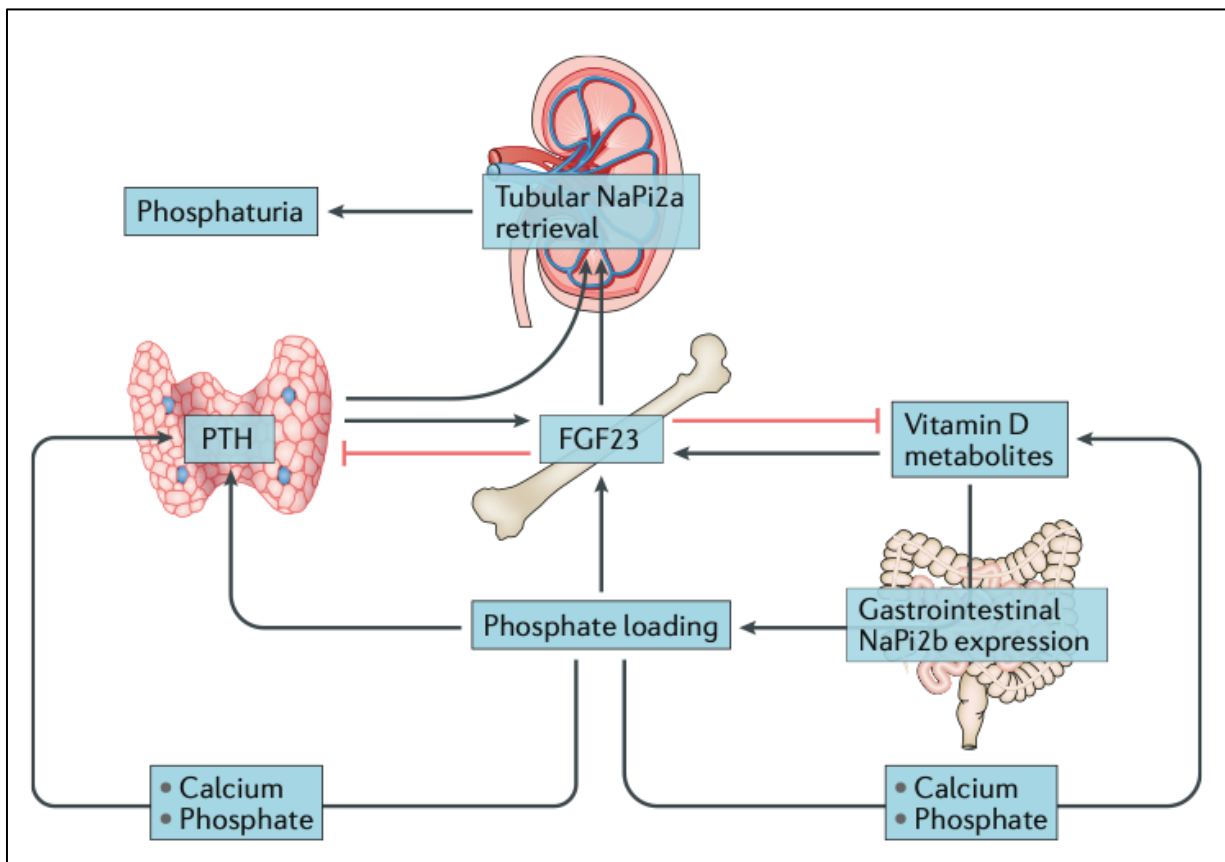


**Figure 15. The action of FGF23 in phosphate regulation.** FGF23 acts to counteract positive phosphate balance and hyperphosphatemia by modulating phosphate reabsorption in the kidney, by directly inhibiting PTH secretion from the parathyroid glands and indirectly reducing 1,25-dihydroxy vitamin D production, adapted from <sup>191</sup>.

Mice with overexpression of FGF23 exhibit low BMD. FGF23 can affect bone matrix mineralization by suppressing tissue non-specific alkaline phosphatase (TNAP), with subsequent pyrophosphate accumulation and indirect downregulation of OPN <sup>152</sup>.

#### 4.4.1 FGF23 effect on the BM niche

The role of FGF23 in the BM niche has become a topic of increasing interest due to its involvement in the regulation of HSC mobilization. A potential role of FGF23 in hematopoiesis was initially suggested by Coe and colleagues, which showed that loss of FGF23 leads to increased HSC frequency and differentiation toward the erythroid lineage. The enhanced erythropoiesis observed in PB and BM in FGF23 deficient mice could be attributed to FGF23's direct regulation of EPO or by increasing the expression of HIF in the

BM, liver, and kidney. Ongoing investigations aim to explore whether FGF23 also acts directly on erythroid cells, as well as elucidate the mechanisms through which FGF23 affects fetal liver erythropoiesis <sup>160</sup>.

A study conducted by Ishii and colleagues showed that FGF23 plays a role in G-CSF-mediated HSPC mobilization. The authors demonstrated that hypoxia, induced in the BM microenvironment by G-CSF, leads to an increased production of FGF23 by BM erythroblasts within the first 24 hours. Additionally, G-CSF activates signals from the sympathetic nervous system, influencing the HSPC mobilization. The increase of FGF23 acts as an intrinsic inhibitor of cell attraction, facilitating the G-CSF-induced mobilization of HSPCs <sup>192</sup>. Importantly, chimeric mice lacking FGF23 in the BM that were transplanted in wt recipients also had inhibition of G-CSF-dependent stem cell mobilization, suggesting that hematopoietic cells, likely erythroblastic cells, are a critical source of FGF23 that respond to G-CSF-induced mobilization. The authors explored the impact of FGF23 on CXCL12, a cytokine that regulates HSC retention in the BM. However, this inhibition appears to result from FGF23-dependent signaling rather than the alteration of CXCL12 binding to its receptor. Essentially, FGF23 can counteract the function of CXCR4 and mobilize HSCs <sup>192</sup> (Fig 16). Additional research focusing on targeting the deletion of FGF23 in erythroid populations, may provide further insights into the physiological role of FGF23 in HSPC retention in the BM. Despite these findings, the specific mechanisms by which FGF23 regulates HSPC mobilization remain unclear. Lastly, it remains to be determined whether high circulating levels of FGF23 in CKD and other congenital anemia including BThal and SCD may impair HSPC retention in the BM.

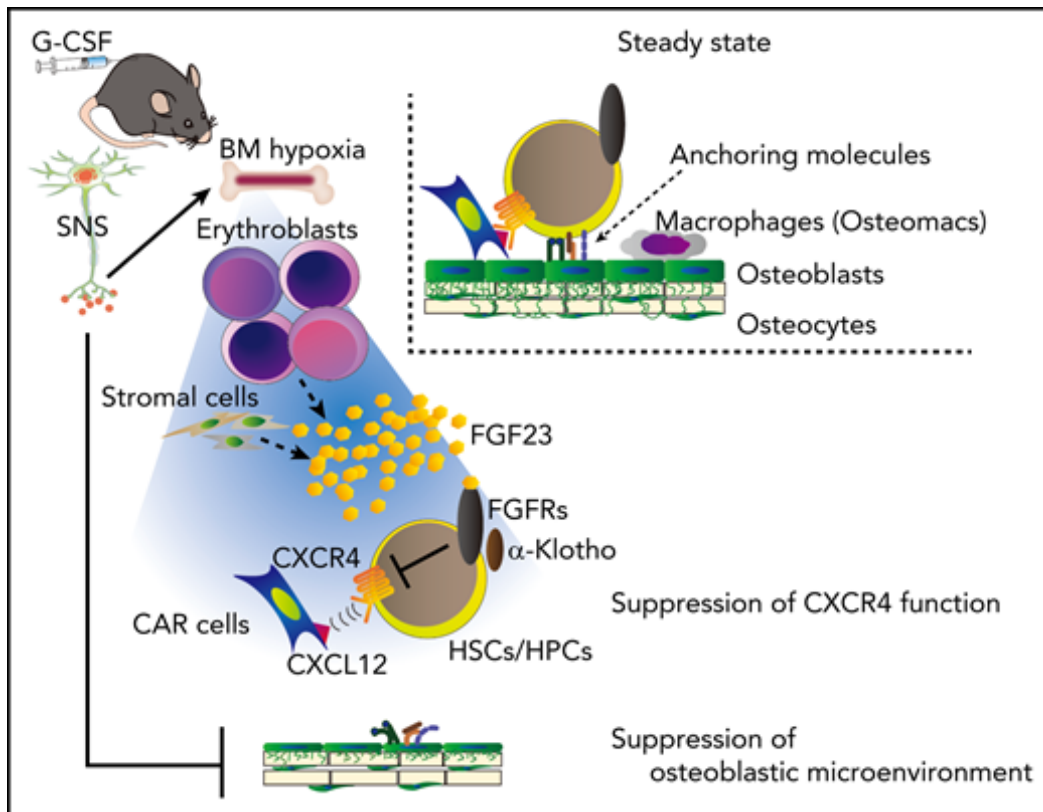


**Figure 16. A model for G-CSF–induced mobilization by FGF23 from erythroblasts.** G-CSF administration or activation of the sympathetic nervous system, inducing hypoxia, lead to increased expression and release of FGF23, primarily from erythroblasts and to some extent from stromal cells. These events disrupt the homeostatic mechanisms that normally anchor HSPCs to the BM microenvironment. Chemoattraction toward CXCL12 is inhibited by the high concentration of BM FGF23, which counteracts the CXCR4 function via FGFRs <sup>192</sup>.

In wt mice, the induction of *Fgf23* expression was observed in both CD45-Ter-119+CD71+ and CD45-Ter-119- cell populations. The latter population is expected to include BM-SEC, which suggests the possibility that FGF23 produced by BM-SEC may influence the mobilization of HSPCs <sup>192</sup>. Moreover, the BM microvasculature plays a crucial role in supporting HSCs <sup>82,193</sup>, regulating HSC self-renewal and differentiation through direct contact and endothelial cell-derived paracrine factors <sup>194</sup>. It has been shown that FGF23 is involved in the BM sinusoidal endothelial niche regulation <sup>195</sup>. The study by Heil J. and colleagues focused on the consequences of  $\beta$ -catenin overactivation in BM-SEC (Ctnnb1<sup>OE-SEC</sup>), which are expressed in the SEC of the BM, liver, spleen, and lymph nodes. Their research revealed abnormal sinusoidal differentiation and increased levels of both iFGF23 and cFGF23 in the serum of Ctnnb1<sup>OE-SEC</sup> mice.

Additionally, fluorescence in situ hybridization analysis of BM tissue indicated an upregulation of *Fgf23* expression specifically in BM-SEC. The study demonstrated that BM-

SEC actively regulates erythropoiesis. These findings were further supported by a recent study conducted by Li X. et al. demonstrating that BM-SEC is a site of FGF23 upregulation in iron deficiency anemia (IDA) <sup>175</sup> and indicating its broad impact on various components of the BM microenvironment. The authors used a mouse model lacking *Tmprss6* (*Tmprss6*<sup>-/-</sup>), which is known to develop chronic IDA. They observed a significant increase in circulating cFGF23 in these mice. Importantly, single-cell RNA sequencing data of BM stroma from wt mice revealed the presence of both *Fgf23* and *Epor* expression in BM-SEC. Additionally, in non-anemic *Fgf23*<sup>+eGFP</sup> mice, direct injection of EPO led to an increased expression of the *Fgf23*<sup>eGFP</sup> reporter in BM-SEC compared to vehicle-treated controls. These findings suggest a model in which elevated circulating levels of EPO, observed in both chronic genetically induced IDA and acute injection of EPO, directly stimulate BM-SEC to produce FGF23. Future studies will be needed to elucidate the mechanisms underlying *Fgf23* upregulation in BM-SEC and the local consequences of FGF23 elevation in BM-SEC during anemic states <sup>175</sup>.

Moreover, FGF23 has been observed to impact other populations within the BM niche, including MSCs. FGF23 seems to influence the differentiation of MSCs into OBs *in vivo*, such as in CKD patients, potentially affecting bone metabolism <sup>196</sup>. Although mouse cell lines were initially used in the experiments, the inclusion of data from human primary cells and a human cell line provided support for these findings. In previous research, a study reported that high doses of FGF23 in pre-OB MC3T3-E1 cell lines stimulated the proliferation of MSCs while inhibiting their mineralization <sup>197</sup>. Conversely, other authors found that significantly lower concentrations of FGF23 directed MSCs toward OB differentiation <sup>198</sup>. These contradictory results may be attributed, at least in part, to variations in FGF23 concentrations and the stages of cell differentiation. Furthermore, MSCs express FGF23, and its expression levels increase during the osteo-differentiation process. However, in experiments involving M2-10B4 cells, no release of FGF23 was observed <sup>196</sup>.

In summary, the role of FGF23 in the BM niche is complex and interconnected with various cellular and molecular components. Further research is required to fully elucidate the mechanisms underlying FGF23's actions within the BM and its implications for hematopoiesis, especially in the context of anemia and other hematological disorders.



## AIMS OF THE PROJECT:

We will exploit the *Hbb<sup>th3/+</sup>* (*th3*) murine model of BThal to achieve the following aims:

1. To investigate the molecular mechanisms regulating *Fgf23* expression in BThal mice:
  - 1.1 To evaluate gene expression of *Fgf23* and correlated enzymes (e.g., *Galnt3*, *Fam20c*, *Furin*, *Pcsk5*) that regulate its post-translational modifications and cleavage in bone cells and BM erythroid precursors.
  - 1.2 To demonstrate the EPO-mediated stimulation of *Fgf23* expression by blocking EPO pathway through monoclonal anti-EPO antibody.
  - 1.3 To identify the molecular mechanism by which EPO modulates *Fgf23* expression through *in vitro* EPO stimulation and inhibition experiments.
2. To rescue bone and HSC-BM niche crosstalk by *in vivo* FGF23 inhibition:
  - 2.1 To evaluate the rescue of defective bone mineralization and deposition by analyzing bone mineral density (BMD) and mineral apposition rate (MAR) and gene expression analysis of mineralization-related genes in bone cells.
  - 2.2 To investigate the rescue of the altered BM niche-HSC crosstalk and the restoration of HSC function.
  - 2.3 To investigate the effect of FGF23 inhibition on ameliorating anemia, acting through EPO and its potential anti-apoptotic effect on expanded erythroblasts in BThal BM.
3. To validate our results on BThal patients' samples
  - 3.1 To dose circulating levels of FGF23 in patients affected by transfusion-dependent versus transfusion-independent BThal.
  - 3.2 To evaluate if high FGF23 levels in BThal patients correlate with EPO, bone and erythropoietic parameters.

In our recent publication, we demonstrated the molecular mechanisms responsible for EPO-mediated FGF23 upregulation in BThal, focusing on the impact of high FGF23 levels on bone and HSC-BM niche crosstalk in *th3* mice. We developed a targeting strategy to improve bone and HSC niche by inhibiting FGF23 signaling using cFGF23 as a blocking peptide. Notably, *in vivo* FGF23 inhibition by cFGF23 peptide in *th3* mice fully rescued bone defects, BM niche and HSC function<sup>131</sup>, with potential translational relevance in improving HSC transplantation and gene therapy for BThal.

In the section on new results, we deeply investigated the molecular mechanism by which EPO regulates *Galnt3* expression. Since we revealed differences in the balance between intact and C-terminal cleaved forms of FGF23 in *th3* mice, we analyzed the molecules involved in post-translational modification of FGF23. Our analysis revealed reduced GALNT3 enzyme, which preserves the intact form of FGF23, suggesting an increasing FGF23 cleavage, both in bone and BM erythroid cells. Indeed, our *in vitro* experiments revealed that EPO activated the Erk1/2 and Stat5 pathways in bone and BM erythroid cells, leading to a decrease in Galnt3 transcription. This reduction in GALNT3 enzyme levels explained the increased cleavage of FGF23 found in the serum.

On the other hand, we focused on the FGF23 targeting strategy in improving HSC engraftment. We demonstrated that when we transplanted wt and *th3* cells in a competitive setting into untreated *th3* or *th3*+cFGF23 recipients, we observed partially enhanced engraftment in the cFGF23-treated mice indicating that FGF23 inhibition improves the supportive capacity of the damaged niche. We hypothesized that prolonged cFGF23 administration to recipient mice after transplantation could further restore the BM niche and boost the graft, thus achieving therapeutic outcomes. We set up several experiments to establish the proper dose regimen with withdrawal periods for prolonged cFGF23 treatment and we analyzed the BMD and HSC cell cycle at 1 and 2 weeks after discontinuing cFGF23 administration. Our results showed that rescued BMD and the restoration of defective quiescence in *th3* HSCs were sustained after the discontinuation of treatment for 1 and 2 weeks.

To strengthen the translational relevance of our approach, we will combine *in vivo* autologous GT transplantation with FGF23 inhibition, thus potentially improving the outcome since cFGF23 treatment pre- and post-transplantation will refurbish bone and HSC niche before HSC harvest and promote early engraftment and terminal erythroid maturation after GT.

Moreover, the use of the FGF23 inhibition strategy could potentially represent a new therapeutic approach for the treatment of osteoporosis in BThal patients.

**CHAPTER II (Published Papers)**



## THALASSEMIA

# Inhibition of FGF23 is a therapeutic strategy to target hematopoietic stem cell niche defects in $\beta$ -thalassemia

Annamaria Aprile<sup>1\*†</sup>, Laura Raggi<sup>1,2†</sup>, Simona Bolamperti<sup>3,4</sup>, Isabella Villa<sup>3,4</sup>, Mariangela Storto<sup>1</sup>, Gaia Morello<sup>5</sup>, Sarah Marktel<sup>6</sup>, Claudio Tripodo<sup>5,7</sup>, Maria Domenica Cappellini<sup>8,9</sup>, Irene Motta<sup>8,9</sup>, Alessandro Rubinacci<sup>3</sup>, Giuliana Ferrari<sup>1,10\*</sup>

Copyright © 2023 The Authors, some rights reserved; exclusive licensee American Association for the Advancement of Science. No claim to original U.S. Government Works

Clinical evidence highlights a relationship between the blood and the bone, but the underlying mechanism linking these two tissues is not fully elucidated. Here, we used  $\beta$ -thalassemia as a model of congenital anemia with bone and bone marrow (BM) niche defects. We demonstrate that fibroblast growth factor 23 (FGF23) is increased in patients and mice with  $\beta$ -thalassemia because erythropoietin induces FGF23 overproduction in bone and BM erythroid cells via ERK1/2 and STAT5 pathways. We show that *in vivo* inhibition of FGF23 signaling by carboxyl-terminal FGF23 peptide is a safe and efficacious therapeutic strategy to rescue bone mineralization and deposition in mice with  $\beta$ -thalassemia, normalizing the expression of niche factors and restoring hematopoietic stem cell (HSC) function. FGF23 may thus represent a molecular link connecting anemia, bone, and the HSC niche. This study provides a translational approach to targeting bone defects and rescuing HSC niche interactions, with potential clinical relevance for improving HSC transplantation and gene therapy for hematopoietic disorders.

## INTRODUCTION

The bone marrow (BM) is the primary hematopoietic organ giving rise to adult blood lineages because of the complex interaction between hematopoietic stem cells (HSCs) and the BM microenvironment, termed “niche” (1, 2). Osteolineage cells were the first cell population to be associated with HSC regulation (3–5). Although their essential role is controversial, recent literature suggests that HSC maintenance is tightly dependent on bone turnover (6). Moreover, decades of studies demonstrated a close relationship between hematopoiesis and bone in disease (7), including clinical evidence that congenital hemolytic anemias have a deleterious impact on bone health and are often associated with osteoporosis and bone defects (8–10). However, the molecular link connecting anemia, bone, and the HSC niche is still missing.

In this view,  $\beta$ -thalassemia may represent a paradigm to study this relationship.  $\beta$ -Thalassemia is caused by mutations in the hemoglobin (Hb)  $\beta$  chain gene and results in ineffective erythropoiesis, severe anemia, extramedullary hematopoiesis, hepatosplenomegaly, iron accumulation, and multiorgan involvement, including endocrinopathies and bone defects (11). Results on the mechanisms of bone loss are controversial, and bone disease

retains high morbidity despite current therapies. Correction of  $\beta$ -thalassemia is achieved by transplantation of HSC from healthy donors (HDs) (12) or more recently by autologous gene therapy and experimental gene editing approaches (13–17). The success of engraftment of transplanted cells in both procedures depends on the quality of HSC and BM microenvironment; thus, the cross-talk between HSCs and the niche plays a crucial role in transplant outcome.

We recently demonstrated impaired HSC function in the *Hbb<sup>th3/+</sup>* (*th3*) mouse model of  $\beta$ -thalassemia due to the altered cross-talk with the BM stromal niche. Osteolineage cells and mesenchymal stromal cells (MSCs) affect *th3* HSC number, quiescence, and self-renewal capacity (18). In addition, MSCs from patients with  $\beta$ -thalassemia showed a defective hematopoietic supportive capacity (19). *th3* mice have reduced bone density associated with low circulating parathyroid hormone (PTH), and PTH treatment is sufficient to recover the BM niche and HSC function (18).

To develop targeting strategies to improve bone complications and the HSC niche in transplantation settings, we focused our attention on the role of fibroblast growth factor 23 (FGF23), an inhibitor of bone mineralization and PTH production (20). FGF23 is a phosphaturic hormone mainly secreted by bone cells, and its primary role is to contribute to phosphate, calcium, and bone homeostasis (21). In the past decade, its function has been extensively studied as a negative regulator of phosphate tubular resorption and vitamin D activation in the kidney. FGF23 is produced as a biologically active intact protein (iFGF23), inactivated by proteolytic cleavage in the C-terminal fragment (cFGF23). The 72-amino acid-long cFGF23 peptide specifically blocks FGF23 signaling competing with iFGF23 for binding to FGF receptor (FGFR) (22), although additional functions of this fragment are still underexplored. FGF23 action is mediated by binding to FGFR and Klotho co-receptor and expressed by the kidney, parathyroid glands, and bone (21). Inherited defects in *Fgf23* and *Fgf23* processing genes cause rickets, osteomalacia, fractures, and hypo/hyperphosphatemic disorders.

<sup>1</sup>San Raffaele-Telethon Institute for Gene Therapy (SR-TIGET), IRCCS San Raffaele Scientific Institute, 20132 Milan, Italy. <sup>2</sup>University of Milano Bicocca, 20126 Milan, Italy. <sup>3</sup>Bone Metabolism Unit, Division of Genetics and Cell Biology, IRCCS San Raffaele Scientific Institute, 20132 Milan, Italy. <sup>4</sup>Endocrine and Osteometabolic Laboratory, Institute of Endocrine and Metabolic Sciences, IRCCS San Raffaele Scientific Institute, 20132 Milan, Italy. <sup>5</sup>Tumor Immunology Unit, Human Pathology Section, Department of Health Sciences, University of Palermo, 90134 Palermo, Italy. <sup>6</sup>Hematology and Bone Marrow Transplantation Unit, IRCCS San Raffaele Scientific Institute, 20132 Milan, Italy. <sup>7</sup>IFOM ETS, AIRC Institute of Molecular Oncology, 20139 Milan, Italy. <sup>8</sup>General Medicine Unit, Fondazione IRCCS Ca' Granda Ospedale Maggiore Policlinico, 20122 Milan, Italy. <sup>9</sup>Department of Clinical Sciences and Community Health, University of Milan, 20122 Milan, Italy. <sup>10</sup>Vita-Salute San Raffaele University, 20132 Milan, Italy.

\*Corresponding author. Email: ferrari.giuliana@hsr.it (G.F.); aprile.annamaria@hsr.it (A.A.)

†These authors contributed equally to this work.

Recent literature based on descriptive and correlative studies placed FGF23 at the crossroads of bone and erythropoiesis. Erythropoietin (EPO) administration was associated with FGF23 expression (23), and loss of FGF23 resulted in increased erythropoiesis, whereas in vivo administration of FGF23 caused a rapid decrease in erythropoiesis (24). Consistently, in secondary anemia associated with chronic kidney disease (CKD), inhibition of FGF23 signaling rescues anemia (25). Among the inhibition strategies effective in rescuing bone defects, the anti-FGF23 antibody partially improved bone mineralization (26, 27), with amelioration of anemia in a mouse model of myelodysplastic syndrome (MDS) (28).

Thus, in the past few years, FGF23 regulation and involvement in bone disease and erythropoiesis are being increasingly investigated. However, the molecular mechanisms linking anemia to bone defects are still unsolved, and the essential role of FGF23 in regulating the BM niche remains poorly understood. Here, we provide the first evidence of a significant correlation between increased FGF23, EPO, and bone disease in patients affected by  $\beta$ -thalassemia, as a condition of chronic EPO stimulation. These results were confirmed in the murine model, which allowed us to mechanistically prove the causative role of EPO and to propose the inhibition of FGF23 signaling by cFGF23 peptide as a therapeutic strategy to restore the impaired BM niche and HSC function.

## RESULTS

### Patients with $\beta$ -thalassemia who have marked bone defects showed increased circulating FGF23

To unravel the molecular mechanisms underlying the relationship between anemia and bone, we used  $\beta$ -thalassemia as a disease model of severe anemia with bone defects (8, 29, 30). Our analysis included a large cohort of 40 patients with  $\beta$ -thalassemia, both transfusion-dependent (TDT) and nontransfusion-dependent (NTDT), and HD controls (tables S1 and S2). We measured a significantly higher concentration of total FGF23 in the plasma of patients compared with HDs ( $P = 0.0008$ ; Fig. 1A) and no changes in iFGF23 (table S3). This cohort of patients displayed bone defects in bone density and quality. The reduction in areal bone mineral density (BMD<sub>a</sub>) revealed at least osteopenia ( $T$  score  $< -1$ ) in 78.6% and osteoporosis ( $T$  score  $< -2.5$ ) in 50% of cases (Fig. 1B). The trabecular bone score (TBS) showed partially degraded bone microarchitecture (TBS  $< 1.35$ ) in the 85.7% of patients and degraded bone (TBS  $< 1.2$ ) in the 60.7% of patients (Fig. 1C). The  $T$  scores, both at vertebral and femoral levels, negatively correlated with the concentration of FGF23 (Fig. 1D) and the osteoblast-derived factor osteocalcin (Fig. 1E). We observed a negative correlation between iFGF23 and  $T$  score, suggesting that iFGF23 in thalassaemic patients, even within normal range, is associated with bone dysfunction (Fig. 1F). Among hematological parameters, FGF23 negatively correlated with Hb (Fig. 1G) and positively correlated with the absolute count of circulating reticulocytes (Fig. 1H). PTH, vitamin D, calcium, and phosphate serum concentrations were in the normal range (table S3). Overall, these results provide evidence of an association among FGF23, anemia, and bone defects in a human condition associated with chronic EPO stimulation.

### High EPO induces FGF23 through Erk1/2 and Stat5 signaling in bone and BM erythroid cells

Elevated EPO is a hallmark of  $\beta$ -thalassemia. Our cohort of patients showed increased plasma EPO (Fig. 2A), which positively correlated with an enhanced concentration of FGF23 (Fig. 2B). To provide mechanistic insight into this relationship, we used the  $\beta$ -thalassemia murine model *th3* (31), which recapitulates the major features of NTDT, including ineffective erythropoiesis, anemia, and bone defects (18, 32). Increased circulating EPO and total FGF23 were confirmed in *th3* mice as compared with wild-type (WT) controls (Fig. 2, C and D), along with a positive correlation with EPO and anemia parameters (Fig. 2E and fig. S1, A and B). In vivo neutralization of EPO signaling by injection of anti-EPO antibodies was sufficient to down-regulate FGF23 (Fig. 2F), affecting both iFGF23 and cFGF23 (fig. S2, A and B), indicating a potential causative role of EPO in inducing high FGF23 in  $\beta$ -thalassemia. We excluded the contribution of other factors associated with ineffective erythropoiesis, such as erythroferrone (ERFE), because anti-EPO treatment was able to suppress FGF23 production without affecting circulating ERFE (fig. S2C).

Bone cells (mainly osteocytes) and erythroid Ter119<sup>+</sup> cells accounted for much of the enhanced FGF23 production in *th3* BM fluids (Fig. 2, G and H), although other less-abundant populations, such as endothelial cells, may also contribute to *Fgf23* expression (fig. S3A). Both bioactive iFGF23 and cleaved cFGF23 were higher in *th3* sera than in WT (fig. S3, B and C). The analysis of molecules involved in FGF23 regulation revealed reduced expression of the *Galnt3* enzyme, which stabilizes by glycosylation of the FGF23 peptide and protects it from cleavage, and down-regulation of the *Pcsk5* protease in both bone and BM erythroid cells (fig. S3, D and E). Conversely, *Fam20c* protein kinase marking FGF23 for proteolytic cleavage and *Furin* protease were unchanged (fig. S3, F and G). These data explain the enhanced production of FGF23 due to its increased expression and cleavage.

To unravel the signaling pathways involved in EPO induction of FGF23, we modeled in vitro EPO stimulation of WT bone-derived and BM Ter119<sup>+</sup> erythroid cells (Fig. 2I), both expressing the EPO receptor (*Epor*) (fig. S4A). Upon in vitro exposure of bone cells to recombinant human EPO (rhEPO), we found a 3.8-fold activation of extracellular signal-regulated kinase 1/2 (ERK1/2) (Fig. 2J) with up-regulation of *Fgf23* expression (fig. S4B). Subsequent inhibition of ERK1/2 signaling by U0126 (fig. S4C) was sufficient to suppress *Fgf23* expression in EPO-stimulated bone cells (Fig. 2K). On the other hand, in erythroid cells, where the signal transducers and activators of transcription 5 (STAT5) signaling is the most activated cascade, we observed a 2.1-fold increase in Stat5 activation upon in vitro rhEPO stimulation (Fig. 2L) and induced expression of *Fgf23* (fig. S4D). Inhibition of STAT5 signaling by pimozide (fig. S4E) decreased *Fgf23* expression (Fig. 2M). Preliminary in silico bioinformatic analysis identified consensus sequences for transcription factors associated with ERK1/2 and STAT5 signaling within the promoter region of the *Fgf23* gene (fig. S4F), suggesting a transcriptional regulation mechanism. Western blot analysis confirmed the preferential activation of ERK1/2 in bone cells and of STAT5 in erythroid cells (fig. S4, G and H). Overall, in vitro EPO stimulation and signaling inhibition strategies showed that ERK1/2 and STAT5 pathways enhance *Fgf23* transcription in bone and BM erythroid cells, respectively.

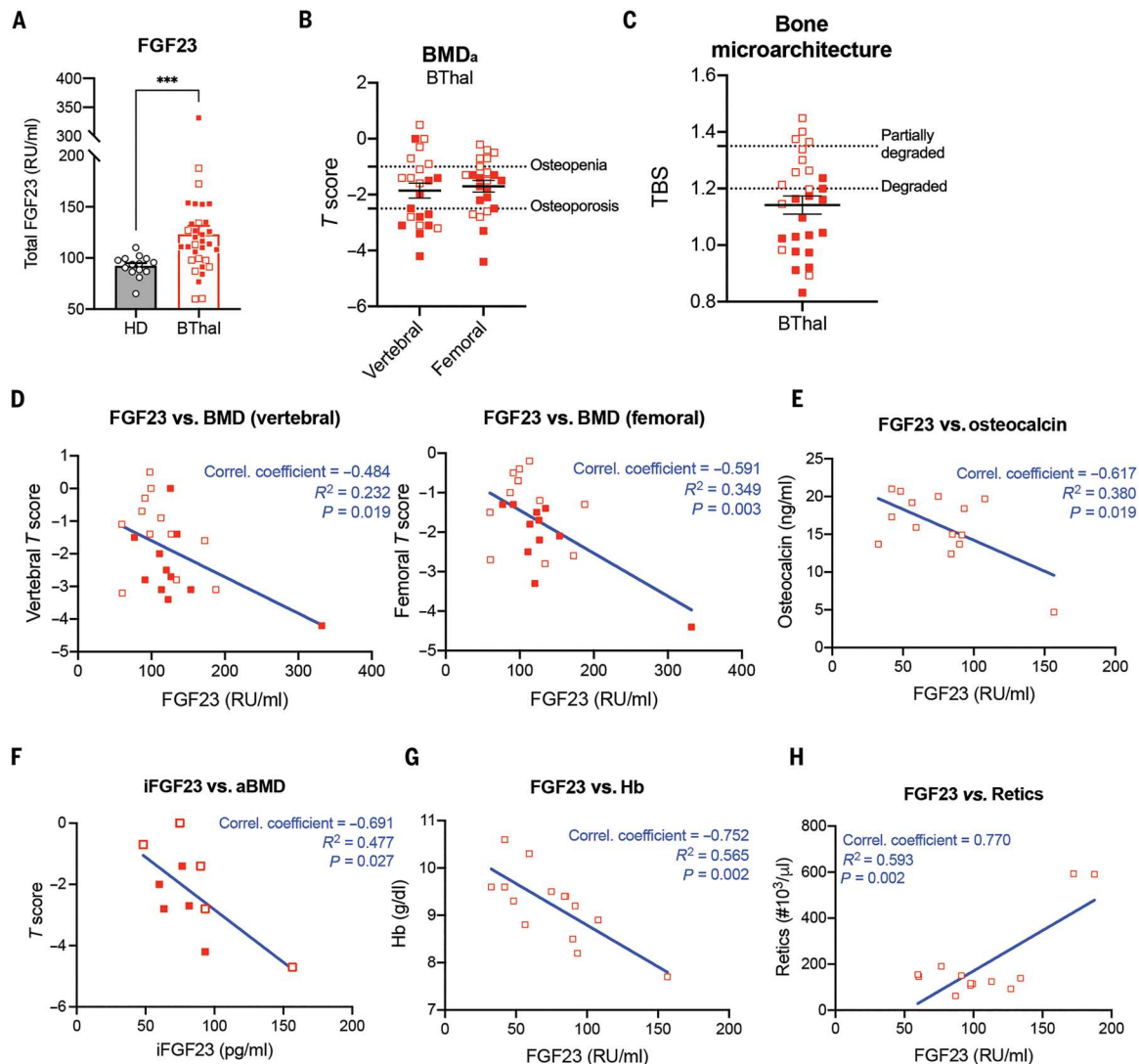


**Fig. 1. Patients with  $\beta$ -thalassemia with marked bone defects showed increased circulating FGF23.** (A) Total FGF23 in plasma from HDs ( $n = 14$ ) and patients with  $\beta$ -thalassemia (BThal;  $n = 33$ ) by enzyme-linked immunosorbent assay (ELISA). RU, relative unit. (B) Areal bone mineral density (BMD<sub>a</sub>) at lumbar spine (vertebral) and femoral level in patients, reported as T score by DXA ( $n = 23$ ). (C) Quality of bone microarchitecture of patients, reported as trabecular bone score (TBS;  $n = 28$ ). (D) Correlation between FGF23 and BMD at vertebral and femoral levels ( $n = 23$ ). (E) Correlation between FGF23 and the bone marker osteocalcin dosed in the blood ( $n = 14$ ). (F) Correlation between iFGF23 and T score ( $n = 10$ ). (G) Correlation between FGF23 and Hb concentration ( $n = 14$ ). (H) Correlation between FGF23 and reticulocyte count (Retics;  $n = 13$ ). Red squares indicate patients with transfusion-dependent thalassemia (TDT); white squares indicate patients with nontransfusion-dependent thalassemia (NTDT). Values are means  $\pm$  SEM. Two-tailed Mann-Whitney test (A) and Pearson correlation coefficient test (D to H) were used to evaluate statistical significance (\*\*\* $P < 0.001$ ).

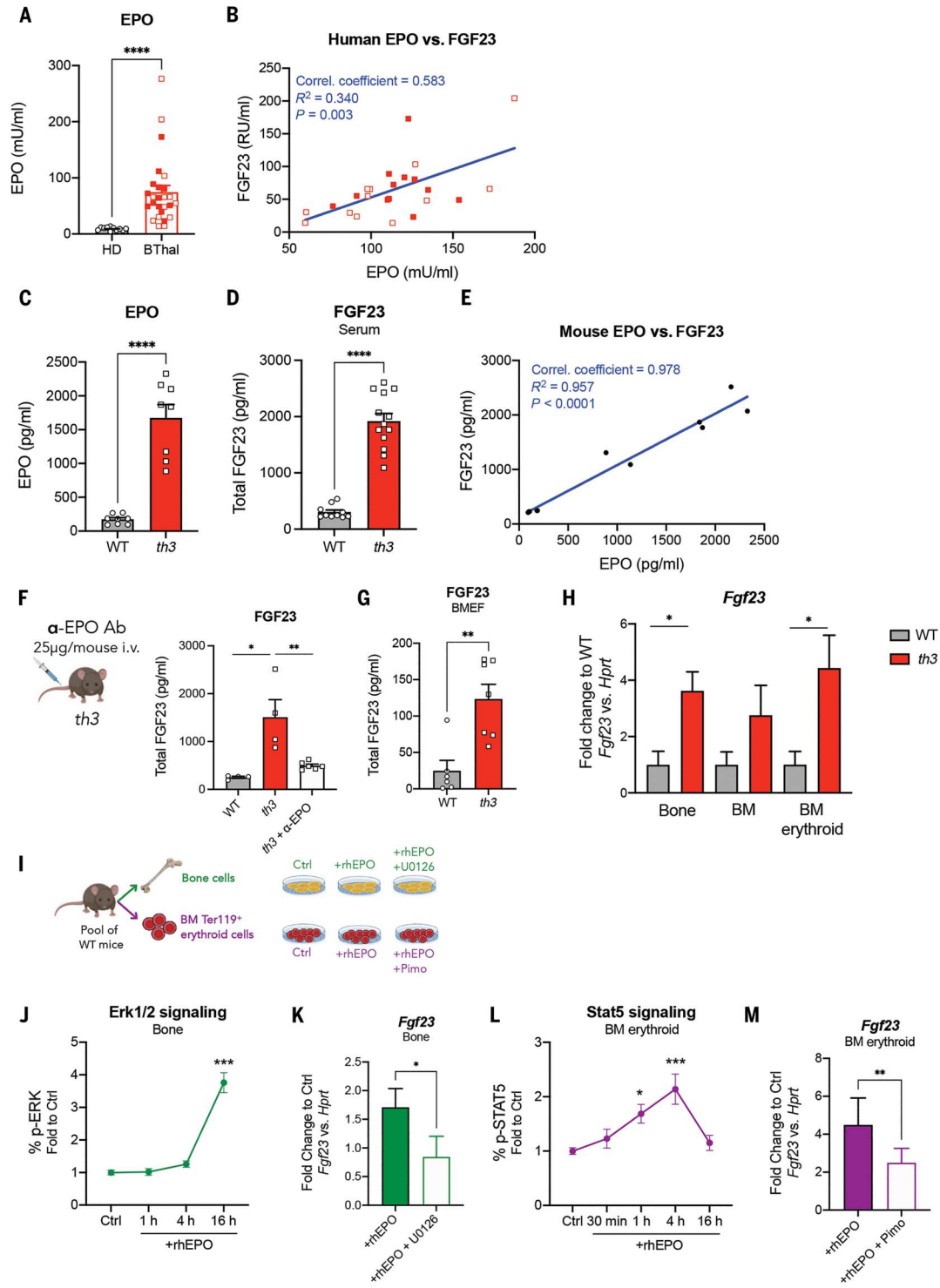
### High FGF23 causes bone loss, and its inhibition by cFGF23 rescues bone defects

Consistent with our results in patients, we found that FGF23 negatively associated with volumetric trabecular bone mineral density (Tb.BMD) and bone parameters in  $\beta$ -thalassemia mice (fig. S5, A and B). To investigate the causative role of high FGF23 on bone defects in a condition of chronic EPO stimulation, we inhibited FGF23 signaling by administering cFGF23 in vivo (FGF23inh). cFGF23 was reported to be an endogenous competitor to the biologically active iFGF23 in kidney and erythroid cells (22, 25), but the effects of this inhibition strategy on the bone are unclear.

*th3* mice were treated with two consecutive doses of cFGF23 and terminated after 38 hours, a time point at which both serum phosphate and calcium normalized (table S4), indicating the acute action of the blocking peptide on the phosphaturic function of FGF23. Treatment efficacy was confirmed by the transitory increase in serum phosphate. A concomitant acute effect on bone parameters was also evaluated. Peripheral quantitative computed tomography (pQCT) analysis showed that treatment rescued the reduced Tb.BMD (Fig. 3A) in *th3* mice (18). Histomorphometric analyses did not show any increase in the mineral apposition rate (MAR) compared with untreated animals (Fig. 3B), suggesting that the rescue of BMD is independent of osteoblastic activity and

**Fig. 2. High EPO induces FGF23 through Erk1/2 and Stat5 signaling in bone and BM erythroid cells.**

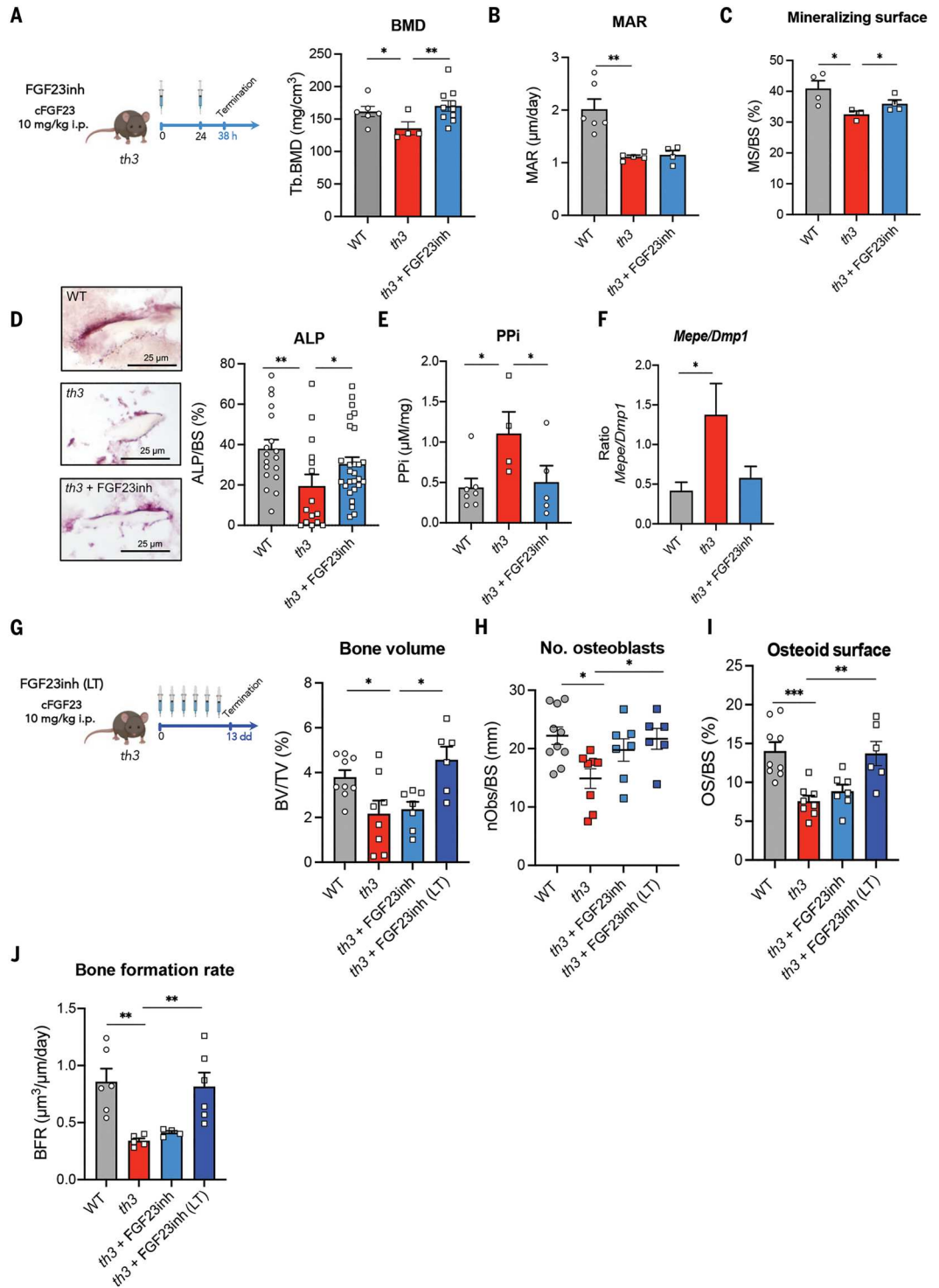
(A) Erythropoietin (EPO) in plasma from HDs ( $n = 11$ ) and patients with  $\beta$ -thalassemia (BThal;  $n = 26$ ) by ELISA. (B) Correlation between EPO and FGF23 in  $\beta$ -thalassemia samples ( $n = 24$ ). (C) EPO in sera from WT ( $n = 8$ ) and  $th3$  ( $n = 8$ ) mice. (D) Total FGF23 in sera from WT ( $n = 10$ ) and  $th3$  ( $n = 13$ ) mice. (E) Correlation between EPO and FGF23 ( $n = 11$ ). (F) Experimental design of in vivo administration of anti-EPO ( $\alpha$ -EPO) antibody to  $th3$  mice. Mice were euthanized 4 hours after the injection. Total FGF23 in sera from WT ( $n = 4$ ),  $th3$  ( $n = 4$ ), and  $th3 + \alpha$ -EPO ( $n = 6$ ) mice by ELISA. i.v., intravenously; Ab, antibody. (G) Total FGF23 in BM extracellular fluid (BMEF) from WT ( $n = 6$ ) and  $th3$  ( $n = 7$ ) mice. (H) *Fgf23* expression relative to *Hprt* in total bone, BM, and BM erythroid cells from WT (gray bar,  $n \geq 6$ ) and  $th3$  (red bar,  $n \geq 4$ ) mice by droplet digital polymerase chain reaction (ddPCR), reported as fold to WT. (I) Experimental design of WT bone-derived and BM Ter119<sup>+</sup> erythroid cells stimulated by recombinant human EPO (rhEPO; 100 U/ml) and pretreated for 2 hours with ERK1/2 and STAT5 inhibitors, respectively. (J) Analysis of ERK1/2 signaling in bone cells after 1, 4, and 16 hours of rhEPO stimulation, assessed as frequency of cells expressing phosphorylated ERK (p-ERK) by flow cytometry and expressed as fold to unstimulated control (Ctrl) ( $n \geq 5$ ). (K) *Fgf23* expression in bone cells upon rhEPO stimulation and ERK1/2 inhibition by U0126, reported as fold to WT relative to *Hprt* ( $n = 5$ ). (L) Analysis of STAT5 signaling in BM erythroid cells upon 30 min and 1, 4, and 16 hours of rhEPO stimulation, assessed as frequency of cells expressing phosphorylated STAT5 (p-STAT5) by flow cytometry and expressed as fold to unstimulated control (Ctrl) ( $n \geq 5$ ). (M) *Fgf23* expression in BM erythroid cells upon rhEPO stimulation and Stat5 inhibition by pimoziide (Pimo), reported as fold to WT relative to *Hprt* ( $n = 7$ ). Red squares indicate patients with transfusion-dependent thalassemia (TDT); white squares indicate patients with nontransfusion-dependent thalassemia (NTDT). Values are means  $\pm$  SEM. One- or two-tailed Mann-Whitney test (A, C, D, F, G, H, J, and L), Pearson correlation coefficient test (B and E), and Wilcoxon test (K and M) were used to evaluate statistical significance (\* $P < 0.05$ , \*\* $P < 0.01$ , \*\*\* $P < 0.001$ , and \*\*\*\* $P < 0.0001$ ). Bonferroni correction was applied for comparison among more than two groups.



Downloaded from https://www.science.org at Universita Vita Salute - Hospital s. Raffaele on October 30, 2023

**Fig. 3. High FGF23 causes bone loss, and its inhibition by cFGF23 rescues bone defects.**

**(A)** In vivo FGF23 inhibition in 8- to 9-week-old female *th3* mice by injection of two doses of C-terminal FGF23 (cFGF23) (10 mg/kg, i.p.); analyses were performed at termination upon 38 hours. Volumetric trabecular bone mineral density (Tb.BMD) of the proximal tibiae by pQCT of WT ( $n = 6$ ), *th3* ( $n = 4$ ), and *th3* + FGF23inh ( $n = 10$ ) mice is shown. **(B)** To quantify mineral apposition rate (MAR), mineralizing surface, and bone formation rate (BFR), WT, *th3*, and *th3*-treated mice received intraperitoneal injection of calcein (40 mg/kg of body weight) and xylenol orange (90 mg/kg of body weight) at 7 and 2 days before euthanasia, respectively. MAR of WT ( $n = 6$ ), *th3* ( $n = 5$ ) and *th3* + FGF23inh ( $n = 4$ ) mice. **(C)** Percentage of mineralizing surface on bone surface (MS/BS) in WT ( $n = 4$ ), *th3* ( $n = 3$ ), and *th3* + FGF23inh ( $n = 4$ ) mice. **(D)** Representative images of ALP<sup>+</sup> cells and percentage of ALP<sup>+</sup> area on bone surface (ALP/BS) in WT ( $n = 18$ ), *th3* ( $n = 15$ ), and *th3* + FGF23inh ( $n = 27$ ) mice. **(E)** PPI concentration in micromolar per milligram of bone tissue of WT ( $n = 7$ ), *th3* ( $n = 4$ ), and *th3* + FGF23inh ( $n = 5$ ) mice. **(F)** *Mepe:Dmp1* gene expression ratio in total bone cells relative to *Hprt* from WT ( $n = 4$ ), *th3* ( $n = 3$ ), and *th3* + FGF23inh ( $n = 4$ ) by ddPCR. **(G)** In vivo long-term FGF23 inhibition [FGF23inh (LT)] in *th3* mice by injection of six doses of cFGF23 (10 mg/kg, i.p.); analyses were performed at termination upon 13 days. Percentage of bone volume on trabecular volume (BV/TV) of WT ( $n = 9$ ), *th3* ( $n = 8$ ), *th3* + FGF23inh ( $n = 7$ ), and *th3* + FGF23inh (LT) ( $n = 6$ ) mice. **(H)** Number of osteoblasts per millimeter of bone surface (nObs/BS) in WT ( $n = 10$ ), *th3* ( $n = 8$ ), *th3* + FGF23inh ( $n = 7$ ), and *th3* + FGF23inh (LT) ( $n = 6$ ) mice. **(I)** Percentage of osteoid surface on bone surface (OS/BS) in WT ( $n = 9$ ), *th3* ( $n = 8$ ), *th3* + FGF23inh ( $n = 7$ ), and *th3* + FGF23inh (LT) ( $n = 6$ ) mice. **(J)** Bone formation rate (BFR/BS) of WT ( $n = 6$ ), *th3* ( $n = 5$ ), *th3* + FGF23inh ( $n = 4$ ), and *th3* + FGF23inh (LT) ( $n = 6$ ) mice. Values are means  $\pm$  SEM. One or two-tailed Mann-Whitney test was used to evaluate statistical significance (\* $P < 0.05$ , \*\* $P < 0.01$ , and \*\*\* $P < 0.001$ ), followed by Bonferroni correction for comparison among more than two groups.







deposition of new matrix. Nevertheless, we detected a significant increase in the mineralizing surface in treated mice ( $P = 0.0286$ ; Fig. 3C), suggesting that Tb.BMD increased because of restored mineralization of the existing matrix. Thus, we analyzed the activity of alkaline phosphatase (ALP), which promotes bone mineralization, and the amount of inorganic pyrophosphate (PPi), an inhibitor of bone mineralization that accumulates when ALP activity is reduced. We found that reduced activity of ALP and high PPi in *th3* mice were normalized upon FGF23inh treatment (Fig. 3, D and E). Moreover, FGF23inh reversed the high expression of *Mepe*, an inhibitor of bone mineralization, and the low expression of *Dmp1*, a promoter of bone mineralization (Fig. 3F) by *th3* total bone cells. Together, these data support that FGF23inh is sufficient to rescue bone matrix mineralization.

To test the efficacy and safety of prolonged treatment [FGF23inh (LT)], we injected *th3* mice with cFGF23 every 2 days for 13 days (Fig. 3G). The extended regimen did not alter systemic phosphate and calcium concentrations (table S4). FGF23inh (LT) administration maintained the increase in Tb.BMD and the positive effect on bone mineralization observed after short-term treatment (fig. S6, A to E). Treated *th3* mice also showed an ameliorated bone parameters related to bone formation, including restored bone mass, osteoblast abundance, osteoid surface, and MAR and bone formation rates (BFRs) (Fig. 3, G to J, and fig. S6F), without an effect on osteocyte or osteoclast numbers or osteoclast resorbing activity (fig. S7). Consistent with the negative role of FGF23 on PTH production, our inhibition strategy increased the PTH observed in *th3* mice (table S4)

(18). A prolonged treatment of 4 weeks confirmed the normalization of BMD and MAR parameters (fig. S8), demonstrating the longer-term efficacy of this strategy.

### FGF23 inhibition restores BM niche defects and in vivo HSC function

We recently demonstrated that defective cross-talk with osteolineage cells due to bone defects impairs HSC function in  $\beta$ -thalassemia (18). Thus, FGF23 inhibition treatment may potentially restore the altered BM niche and HSCs in  $\beta$ -thalassemia. Immunohistochemistry analysis on femurs of FGF23inh-treated animals revealed the rescue of the key niche factors osteopontin (OPN), Jagged-1 (JAG1), and C-X-C motif chemokine ligand 12 (CXCL12) in situ expression, especially after prolonged administration (Fig. 4, A to C, and fig. S9A). Transcriptional analysis in total bone cells confirmed these results (fig. S9, B to D). Moreover, immunofluorescence of OPN, JAG1, and CXCL12 costained with anti-bone-specific Runt-related transcription factor 2 (RUNX2) antibody assessed the restored production of these niche factors specifically in the osteolineage population (fig. S10, A to C).

In addition, FGF23inh fully restored the quiescent state of *th3* HSCs, measured as an increased proportion of HSCs in the  $G_0$  phase and a decreased frequency of cycling cells in the  $G_1$  or S phase (Fig. 4D and fig. S11). To assess the rescue of in vivo HSC function, we transplanted CD45.1 lethally irradiated recipients with CD45.2 donor cells from *th3* mice treated with FGF23inh (fig. S12A). Analysis at 16 weeks from transplantation showed

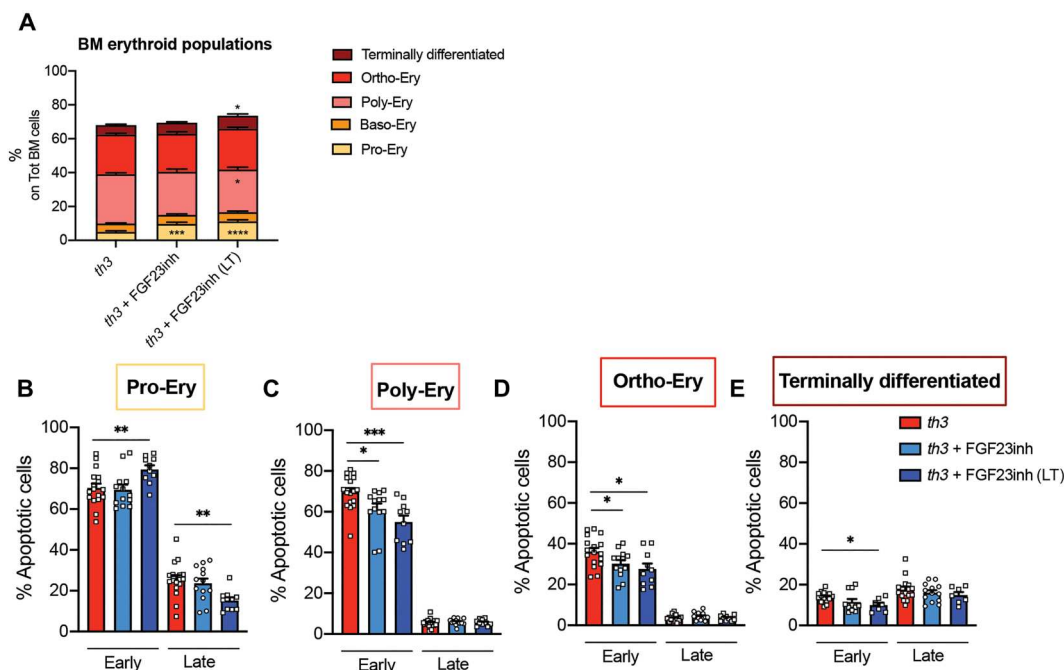


**Fig. 5. FGF23 inhibition ameliorates the maturation of BM erythroblasts in a congenital anemia.** (A) Frequencies of BM erythroid cells at different stages of maturation (Pro-Ery, proerythroblasts; Baso-Ery, basophilic erythroblasts; Poly-Ery, polychromatic erythroblasts; Ortho-Ery, orthochromatic erythroblasts; terminally differentiated reticulocytes and RBCs) were analyzed by labeling total BM cells of *th3* ( $n = 12$ ), *th3* + FGF23inh ( $n = 11$ ), and *th3* + FGF23inh (LT) ( $n = 7$ ) mice with antibodies against Ter119, CD44, and CD71 expressed on total BM cells by flow cytometry. (B to E) Percentages of early and late apoptotic cells on BM erythroblasts at different stages of maturation in the BM stained with anti-annexin V antibody and propidium iodide of *th3* ( $n = 17$ ), *th3* + FGF23inh ( $n = 13$ ), and *th3* + FGF23inh (LT) ( $n = 10$ ) mice by flow cytometry. Values are means  $\pm$  SEM. Two-tailed Mann-Whitney test was used to evaluate statistical significance (\* $P < 0.05$ , \*\* $P < 0.01$ , \*\*\* $P < 0.001$ , and \*\*\*\* $P < 0.0001$ ), followed by Bonferroni correction for comparison among more than two groups.

that HSCs gained a normal quiescent state (Fig. 4E) and were able to reconstitute hematopoiesis in peripheral blood (PB) and BM, as assessed by restored chimerism (fig. S12, B and C) and balanced frequencies of B lymphocytes, T lymphocytes, and myeloid cells (fig. S12, D to F), overcoming the impaired repopulation potential of HSC from untreated donors. Transplantation of *th3* cells into untreated *th3* or *th3* + FGF23inh (LT) recipients partially ameliorated the engraftment in the cFGF23-treated niche (fig. S12, G to I), suggesting a rescued supportive capacity. Overall, these results showed that our FGF23inh strategy achieved correction of BM niche and HSC defects.

### FGF23 inhibition ameliorates the maturation of BM erythroblasts in congenital anemia

FGF23 has been recently identified as a negative regulator of erythropoiesis (24). In secondary anemias, high FGF23 increases the apoptosis of erythroid precursors, whereas FGF23 inhibition ameliorates erythropoiesis (25, 28). However, the outcome of in vivo inhibition of FGF23 in congenital anemias is unclear. In  $\beta$ -thalassemia, ineffective erythropoiesis is characterized by the expansion of erythroid precursors compensating for anemia and prematurely dying in the marrow by apoptosis (33), resulting in a low number of circulating red blood cells (RBCs) and reduced Hb. After FGF23inh treatment, the frequency of early-stage proerythroblasts (Pro-Ery) and terminally differentiated cells, mostly reticulocytes, increased, with no change in the proportion of total BM Ter119<sup>+</sup> erythroid component and intermediate precursors (Fig. 5, A to E, and fig. S13, A and B). The observed amelioration of erythropoiesis was ascribed to an antiapoptotic effect on the erythroid populations, evaluated as a reduction in the frequency of early and late apoptotic cells. In particular, the increase in Pro-Ery population is due to the decrease of the late apoptotic cells and to a higher frequency of proliferating ones (Fig. 5B and fig. S13C). We ruled out the contribution of the antiapoptotic effect of EPO or ERFE, because the FGF23inh treatment did not affect EPO or ERFE concentrations (fig. S13, D and E). Although erythroid maturation was improved, Hb concentration and RBC number were unaffected because of the genetic defect (fig. S13, F and G). These results suggest a positive effect of FGF23inh strategy on erythroid differentiation that could be of potential therapeutic value in combination with the genetic correction of the  $\beta$ -globin defect.

### DISCUSSION

Bone hosts the primary site of adult hematopoiesis, and osteolineage cells are a component of the HSC niche within the BM. Reciprocally, clinical evidence highlighted the association of hematological disorders with bone defects, and, especially, congenital hemolytic anemias are often paired with bone disease. However, the molecular link connecting anemia, bone, and the BM niche was undefined. As the ideal model to study these interactions, we turned to  $\beta$ -thalassemia, a severe congenital anemia with ineffective erythropoiesis and multiorgan secondary complications, including bone alterations. We recently demonstrated an impaired function of HSC due to the altered cross-talk with the stromal BM niche in  $\beta$ -thalassemia *th3* mice (18) and a defective supporting capacity of BM stroma in patients (19). This work demonstrates that FGF23 is increased in  $\beta$ -thalassemia in serum and BM because of up-regulated FGF23 production in bone and erythroid cells after chronic high

EPO. Thus, FGF23 is a key molecule responsible for bone and BM niche homeostasis in a congenital hemolytic anemia. We proved the efficacy of the FGF23 inhibition strategy, exploiting its naturally produced blocking peptide cFGF23, to correct bone mineralization and deposition, and rescue of the impaired cross-talk between HSCs and the niche.

A recent association study in hereditary hemolytic anemias described positive correlation of EPO with FGF23 (34), but no mechanistic clue was investigated. The negative correlation of increased FGF23 with bone quality, BMD, and osteocalcin and its positive correlation with EPO, anemia, and ineffective erythropoiesis set FGF23 as the molecule at the crossroads of erythropoiesis and bone metabolism in the context of both TDT and NTDT human disease. Consistent with previous reports (34), iFGF23 in our cohort of patients with thalassemia was not different from healthy controls. Notably, osteopenia and osteoporosis were evident in most of the patients, highlighting an unmet medical need for efficacious therapies to correct bone defects in  $\beta$ -thalassemia. Further analysis on larger cohorts of patients will allow extending our conclusions to other conditions associated with anemia. Moreover, because EPO is clinically used to stimulate erythropoiesis in anemia resulting from CKD, MDS, or cancer (35), understanding the increase in FGF23 and the impact on the bone in EPO-treated patients is relevant. Our findings provide interesting insights into the extrahematopoietic effect of erythropoietic stress, with a broader impact in basic research and clinics.

In vivo neutralization of EPO axis was sufficient to normalize FGF23, thus demonstrating a causative role of EPO in up-regulating FGF23 production. ERK1/2 and STAT5 pathways were triggered by EPO in activating *Fgf23* transcription by bone and BM erythroid cells, respectively, suggesting transcriptional regulation. The proposed mechanisms do not exclude a direct effect of EPO on bone cells. EPO was reported to directly act on bone osteoclasts and osteoprogenitors via EPOR controlling bone mass maintenance and contributing to EPO-induced bone loss (36, 37). The inhibition of bone formation was hypothesized to occur via an unknown intermediary (36), and we cannot exclude that the missing molecule acting as a negative regulator on bone osteoblasts is FGF23. In addition, other BM stromal populations, such as sinusoidal endothelial cells that express *Epor*, might also have a role in producing FGF23 in response to EPO (38).

Conversely, we excluded the contribution of other anemia-related factors, such as ERFE, in enhancing FGF23. Our results are in line with an ERFE-independent induction of FGF23, as suggested by other groups. Decrease in ERFE after marrow myeloablation was shown to be ineffective on FGF23 production (23), and no correlation was found between ERFE and FGF23 in patients suffering from hemolytic anemias (34). Consistently, a recent study revealed an osteoprotective effect of ERFE by inhibiting bone resorption (39).

To develop targeting strategies to improve bone complications and the HSC niche condition in transplantation settings, we inhibited FGF23 signaling by cFGF23, which was reported to be active in the kidney to reduce the phosphaturic function (22) and in erythroid cells to exert an antiapoptotic effect (25). This work provides evidence of the efficacy of cFGF23 blocking peptide in correcting bone mineralization and deposition. In vivo FGF23inh rescued the defective trabecular bone density in *th3* mice. A short treatment of 38 hours was sufficient to enhance matrix mineralization by

acting on ALP and the expression of the main regulators of mineralization, *Dmp1* and *Mepx*, and long-term administration additionally restored bone formation. Given the inhibitory function of FGF23 on PTH secretion (20), we cannot exclude a positive effect on bone by the restored PTH upon FGF23inh (LT) treatment.

Our rationale of overdosing cFGF23, which is present at a higher basal concentration in  $\beta$ -thalassemia, relied on the hypothesis of boosting a physiological feedback response. In  $\beta$ -thalassemia mice, the molar excess of cFGF23 is 16.7-fold, whereas a 76-fold excess is necessary to completely block the binding of bioactive iFGF23 to the FGFR-Klotho complex (22). Thus, the administration of exogenous peptide enforced the endogenous mechanism leading to FGF23 signaling inhibition. To date, other strategies of FGF23 inhibition have been preferred to target bone defects. In particular, anti-FGF23 neutralizing antibody partially improved bone mineralization (26, 27) and has been recently approved by the U.S. Food and Drug Administration for the treatment of X-linked hypophosphatemia and tumor-induced osteomalacia. The kinetics of cFGF23 action is faster than that of anti-FGF23 antibody, which was effective at partially improving bone mineralization defects after at least 6 weeks of in vivo treatment (26). Thus, the advantage of our cFGF23 inhibition strategy relies on boosting a physiological feedback response that might be relevant for amplifying a potentially self-limiting mechanism.

Inhibition of FGF23 signaling normalized the expression of key niche molecules, such as OPN, JAG1, and CXCL12, involved in the functional cross-talk between HSC and the stromal niche (40, 41), thus acting as a therapeutic niche “booster” for an altered BM microenvironment (18, 42). Consistently, FGF23inh treatments restored the frequency of quiescent  $\beta$ -thalassemia HSCs and rescued their in vivo function. These results might explain the reported action of FGF23 on expanding the HSC population, suggesting that this effect was not only due to a reduced HSC apoptosis (24) but was possibly also mediated by the BM niche. In this view, FGF23 would represent the molecule connecting EPO to hematopoiesis, bone remodeling, and the BM microenvironment. The study of the role of FGF23 on the BM niche has recently gained increasing interest because of its function in promoting HSC mobilization (43) and contributing to the regulation of the BM sinusoidal endothelial niche (44).

The inhibition of FGF23 also had an antiapoptotic effect on the expanded BM erythroid compartment, promoting the maturation of erythroid precursors, as previously shown in secondary anemias (25). As expected, this is not sufficient to recover the defective Hb production and RBC count caused by the genetic defect in a congenital anemia. Nevertheless, in a translational approach, the combination of autologous gene therapy with FGF23 inhibition has the potential to improve the outcome because cFGF23 treatment before and after transplantation could potentially refurbish the bone and the HSC niche before HSC harvest and promote early engraftment and terminal erythroid maturation after gene therapy. The translation of our finding to clinical application might include the use of cFGF23 as an antiosteoporotic therapy to preserve a healthy bone in thalassemia, because, despite available treatments, bone defects are still an unmet medical need for patients. Although a role of FGF23 in granulocyte colony-stimulating factor–mediated HSC mobilization has been described (41), the efficacy of combining FGF23 inhibition and mobilization strategies will need further investigation. This study reports the evidence for

the use of cFGF23 as an efficacious inhibitory strategy to restore bone and BM microenvironment defects and provides mechanistic insight on the role of FGF23 in the HSC niche, adding a contribution to osteohematology and BM niche biology. We propose FGF23 as the molecule connecting erythroid cells to the bone because these populations are both producers and target cells of FGF23, thus capable of responding to FGF23 signaling as well as to its inhibition (fig. S14).

This study presents some limitations. First, the comparison of circulating FGF23 in patients with thalassemia and healthy controls should be interpreted with some caution because the two cohorts were not fully matched for age or sex because of constraints in sample collection. Second, although this research was focused on the most abundant bone-derived cells and on erythroid cells as the main contributors to FGF23 production within the BM, the role of other less-abundant populations, such as endothelial cells, cannot be excluded. Further studies will unravel this aspect. Last, because the results of competitive transplantation in animals treated by cFGF23 showed only a nonsignificant trend of superior engraftment, we hypothesize that a prolonged administration of cFGF23 after transplantation might be needed to achieve a supportive therapeutic effect.

Overall, we provide three main findings: FGF23 inhibition by cFGF23 is efficacious in correcting bone mineralization and deposition in a condition of increased FGF23; FGF23 inhibition is a therapeutic strategy to rescue BM niche and HSC defect; and, last, EPO is the causal factor inducing *Fgf23* transcription by bone and erythroid cells acting on ERK1/2 and STAT5 pathways, respectively. Therefore, the inhibition of FGF23 signaling provides a strategy to ameliorate bone disease and restore HSC-BM niche interactions by a “two birds with one stone” approach, with potential translational relevance for improving HSC transplantation and gene therapy for  $\beta$ -thalassemia.

## MATERIALS AND METHODS

### Study design

The objective of this study was to investigate the cause of increased FGF23 production in  $\beta$ -thalassemia and to demonstrate the restoration of bone and BM niche defects upon inhibition of FGF23 signaling. Our goal was to provide proof-of-concept data for potential translational application. We developed an in vivo protocol to treat a mouse model of  $\beta$ -thalassemia by administration of cFGF23 peptide. Efficacy was evaluated in terms of rescue of bone density, bone deposition, and expression of BM niche molecules by osteolineage cells. The impact of the corrected BM niche on restoring HSC quiescence and in vivo cycling activity after transplantation was assessed. Plasma samples were obtained from patients with TDT or NTDT from San Raffaele Hospital and Maggiore Policlinico Hospital, Milan, Italy. For control purposes, normal plasma samples were collected. All samples were obtained after informed consent and with the approval of Institutional Ethical Committees (TIGET09 and BETANICHE protocols). All animal experiments were performed in accordance with approved protocols of the Institutional Animal Care and Use Committees of San Raffaele Institute (IACUC #1135). In all experiments, mice of similar ages and sex were used across all groups and were randomly assigned to each group. Sample sizes were determined according to previous publications and experimental experience. The investigators were blinded from the

group allocation until the treatment and data collection were done. Experimental data were repeated in two to five independent experiments to obtain an adequate number of biological replicates. All data presented are biological replicates. No data were excluded from analysis. Sample sizes, experimental replicates, and statistics are given in the corresponding figures, figure legends, and data files. Raw data are reported in data files S1 and S2.

### Human samples

Plasma samples were obtained from patients with  $\beta$ -thalassemia during periodic routine checks, including endocrinological, hematological, and bone densitometry evaluation. Blood cell counts were performed by the Coulter counter (Sysmex XN 9000). Automated routine procedures were used for assays of PTH, vitamin D, calcium, phosphate, and osteocalcin. Bone density was measured by dual x-ray photon absorptiometry (DXA; Hologic Bone Densitometer, QDR DiscoveryA, version 12.7.3.1), and BMD values were expressed as *T* score calculated as SDs from a normal reference population database (30). Data were classified as normal (*T* score > -1), osteopenia (-1 > *T* score > -2.5), or osteoporosis (*T* score < -2.5), in accordance with the definition of the World Health Organization. TBS is a gray-level textural measure that estimates the spatial distribution of bone trabeculae (three-dimensional), providing information about bone quality. TBS can be extracted from the two-dimensional DXA image of lumbar spine based on experimental variograms of this image (29).

### Mouse model

Female C57BL/6 and C57BL/6-CD45.1 (B/6.SJLCD45a-Pep3b) WT mice were purchased from Charles River Laboratories. *th3* mice were purchased from the Jackson Laboratory (B6.129P2-*Hbb-b1<sup>tm1Unc</sup>* *Hbb-b2<sup>tm1Unc</sup>*], JAX:003253) and bred to maintain the colony in heterozygosity. All analyses were performed on adult 8- to 10-week-old female mice. Mouse blood counts, including Hb and RBC measurements, were performed by the hemocytometer IDEXX ProCyte (IDEXX Laboratories) on whole PB.

### In vivo treatments

Monoclonal rat anti-mouse EPO antibody (R&D Systems) was administered via intravenous injection at 25  $\mu$ g per mouse, and mice were euthanized 4 hours later. To inhibit FGF23, 8- to 9-week-old female *th3* mice were injected intraperitoneally (i.p.) with two doses of cFGF23 (10 mg/kg; custom-made production by ProteoGenix). For long-term treatment [FGF23inh (LT)], 6- to 7-week-old female *th3* mice were treated three times per week for 2 weeks with cFGF23 (10 mg/kg, i.p.), and for even longer treatment (FGF23inh-4 weeks), 6- to 7-week-old female *th3* mice were treated three times per week for 4 weeks with cFGF23 (10 mg/kg, i.p.) and euthanized 14 hours after the last injection. On the day of euthanasia, retroorbital blood, serum, long bones, and BM were collected for histomorphometric, histological, flow cytometry, and molecular analyses. To analyze biochemical parameters, *th3* mice were treated with a single injection of cFGF23 (10 mg/kg) and euthanized after 24 hours.

### Statistical analysis

All statistical analyses were performed using GraphPad Prism software, version 9. The specific statistical analysis used in individual experiments is reported in the corresponding figure legend. Data are expressed as single values or means  $\pm$  SEM. The Mann-

Whitney test was used for comparisons between two independent groups, whereas the Wilcoxon test was performed for comparisons between dependent groups. Bonferroni correction was applied for comparisons among more than two groups. Correlation analysis was performed by Pearson correlation coefficient test.

### Supplementary Materials

#### This PDF file includes:

Materials and Methods

Figs. S1 to S14

Tables S1 to S4

Reference (45)

#### Other Supplementary Material for this

#### manuscript includes the following:

Data files S1 to S3

MDAR Reproducibility Checklist

[View/request a protocol for this paper from Bio-protocol.](#)

### REFERENCES AND NOTES

1. S. J. Morrison, D. T. Scadden, The bone marrow niche for haematopoietic stem cells. *Nature* **505**, 327–334 (2014).
2. S. Pinho, P. S. Frenette, Haematopoietic stem cell activity and interactions with the niche. *Nat. Rev. Mol. Cell Biol.* **20**, 303–320 (2019).
3. L. M. Calvi, G. B. Adams, K. W. Weibrecht, J. M. Weber, D. P. Olson, M. C. Knight, R. P. Martin, E. Schipani, P. Divieti, F. R. Bringhurst, L. A. Milner, H. M. Kronenberg, D. T. Scadden, Osteoblastic cells regulate the haematopoietic stem cell niche. *Nature* **425**, 841–846 (2003).
4. C. Lo Celso, H. E. Fleming, J. W. Wu, C. X. Zhao, S. Miake-Lye, J. Fujisaki, D. Cote, D. W. Rowe, C. P. Lin, D. T. Scadden, Live-animal tracking of individual haematopoietic stem/progenitor cells in their niche. *Nature* **457**, 92–96 (2009).
5. M. Bowers, B. Zhang, Y. Ho, P. Agarwal, C. C. Chen, R. Bhatia, Osteoblast ablation reduces normal long-term hematopoietic stem cell self-renewal but accelerates leukemia development. *Blood* **125**, 2678–2688 (2015).
6. C. Christodoulou, J. A. Spencer, S. A. Yeh, R. Turcotte, K. D. Kokkalis, R. Panero, A. Ramos, G. Guo, N. Seyedhassantehrani, T. V. Esipova, S. A. Vinogradov, S. Rudzinskas, Y. Zhang, A. S. Perkins, S. H. Orkin, R. A. Calogero, T. Schroeder, C. P. Lin, F. D. Camargo, Live-animal imaging of native haematopoietic stem and progenitor cells. *Nature* **578**, 278–283 (2020).
7. A. Teti, S. L. Teitelbaum, Congenital disorders of bone and blood. *Bone* **119**, 71–81 (2019).
8. M. G. Vogiatzi, E. A. Macklin, E. B. Fung, A. M. Cheung, E. Vichinsky, N. Olivieri, M. Kirby, J. L. Kwiatkowski, M. Cunningham, I. A. Holm, J. Lane, R. Schneider, M. Fleisher, R. W. Grady, C. C. Peterson, P. J. Giardina, N., Bone disease in thalassemia: A frequent and still unresolved problem. *J. Bone Miner. Res.* **24**, 543–557 (2009).
9. A. Almeida, I. Roberts, Bone involvement in sickle cell disease. *Br. J. Haematol.* **129**, 482–490 (2005).
10. H. Al-Samkari, R. F. Grace, A. Glenthoej, O. Andres, W. Barcellini, F. Galacteros, K. H. M. Kuo, D. M. Layton, M. Morado, V. Viprakasit, Y. Dong, F. Tai, P. Hawkins, S. Gheuens, C. Bowden, J. B. Porter, E. Van Beers, Early-onset osteopenia and osteoporosis in patients with pyruvate kinase deficiency. *Blood* **136**, 30–32 (2020).
11. A. T. Taher, K. M. Musallam, M. D. Cappellini,  $\beta$ -Thalassemias. *N. Engl. J. Med.* **384**, 727–743 (2021).
12. D. Baronciani, E. Angelucci, U. Potschger, J. Gaziev, A. Yesilipek, M. Zecca, M. G. Orofino, C. Giardini, A. Al-Ahmar, S. Markt, J. de la Fuente, A. Ghavamzadeh, A. A. Hussein, C. Targhetta, F. Pilo, F. Locatelli, G. Dini, P. Bader, C. Peters, Hemopoietic stem cell transplantation in thalassemia: A report from the European Society for Blood and Bone Marrow Transplantation Hemoglobinopathy Registry, 2000–2010. *Bone Marrow Transplant.* **51**, 536–541 (2016).
13. G. Ferrari, A. J. Thrasher, A. Aiuti, Gene therapy using haematopoietic stem and progenitor cells. *Nat. Rev. Genet.* **22**, 216–234 (2021).
14. S. Markt, S. Scaramuzza, M. P. Cicalese, F. Galglio, S. Galimberti, M. R. Lidonnici, V. Calbi, A. Assanelli, M. E. Bernardo, C. Rossi, A. Calabria, R. Milani, S. Gattillo, F. Benedicenti, G. Spinuzzi, A. Aprile, A. Bergami, M. Casiraghi, G. Consiglieri, N. Masera, E. D'Angelo, N. Mirra, R. Origa, I. Tartaglione, S. Perrotta, R. Winter, M. Coppola, G. Viarengo, L. Santoleri, G. Graziadei, M. Gabaldo, M. G. Valsecchi, E. Montini, L. Naldini, M. D. Cappellini, F. Ciceri,

- A. Aiuti, G. Ferrari, Intrabone hematopoietic stem cell gene therapy for adult and pediatric patients affected by transfusion-dependent  $\beta$ -thalassemia. *Nat. Med.* **25**, 234–241 (2019).
15. F. Locatelli, A. A. Thompson, J. L. Kwiatkowski, J. B. Porter, A. J. Thrasher, S. Hongeng, M. G. Sauer, I. Thuret, A. Lal, M. Algeri, J. Schneiderman, T. S. Olson, B. Carpenter, P. J. Amrolia, U. Anurathapan, A. Schambach, C. Chabannon, M. Schmidt, I. Labik, H. Elliot, R. Guo, M. Asmal, R. A. Colvin, M. C. Walters, Betibeglogene autotemcel gene therapy for non- $\beta^0/\beta^0$  genotype  $\beta$ -thalassemia. *N. Engl. J. Med.* **386**, 415–427 (2022).
  16. E. Magrin, M. Semeraro, N. Hebert, L. Joseph, A. Magnani, A. Chalumeau, A. Gabrion, C. Roudaut, J. Marouene, F. Lefrere, J. S. Diana, A. Denis, B. Neven, I. Funck-Brentano, O. Negre, S. Renolleau, V. Brousse, L. Kiger, F. Touzot, C. Poirot, P. Bourget, W. El Nemer, S. Blanche, J. M. Treluyer, M. Asmal, C. Walls, Y. Beuzard, M. Schmidt, S. Hacein-Bey-Abina, V. Asnafi, I. Guichard, M. Poiree, F. Monpoux, P. Touraine, C. Brouzes, M. de Montalembert, E. Payen, E. Six, J. A. Ribeil, A. Miccio, P. Bartolucci, P. Leboulch, M. Cavazzana, Long-term outcomes of lentiviral gene therapy for the  $\beta$ -hemoglobinopathies: The HGB-205 trial. *Nat. Med.* **28**, 81–88 (2022).
  17. H. Frangoul, D. Altschuler, M. D. Cappellini, Y. S. Chen, J. Domm, B. K. Eustace, J. Foell, J. de la Fuente, S. Grupp, R. Handgretinger, T. W. Ho, A. Kattamis, A. Kernysky, J. Lekstrom-Himes, A. M. Li, F. Locatelli, M. Y. Mapara, M. de Montalembert, D. Rondelli, A. Sharma, S. Sheth, S. Soni, M. H. Steinberg, D. Wall, A. Yen, S. Corbacioglu, CRISPR-Cas9 gene editing for sickle cell disease and  $\beta$ -thalassemia. *N. Engl. J. Med.* **384**, 252–260 (2021).
  18. A. Aprile, A. Gulino, M. Storto, I. Villa, S. Beretta, I. Merelli, A. Rubinacci, M. Ponzoni, S. Markt, C. Tripodo, M. R. Lidonnici, G. Ferrari, Hematopoietic stem cell function in  $\beta$ -thalassemia is impaired and is rescued by targeting the bone marrow niche. *Blood* **136**, 610–622 (2020).
  19. S. Crippa, V. Rossella, A. Aprile, L. Silvestri, S. Rivas, S. Scaramuzza, S. Pirroni, M. A. Avanzini, L. Basso-Ricci, R. J. Hernandez, M. Zecca, S. Markt, F. Ciceri, A. Aiuti, G. Ferrari, M. E. Bernardo, Bone marrow stromal cells from  $\beta$ -thalassemia patients have impaired hematopoietic supportive capacity. *J. Clin. Investig.* **129**, 1566–1580 (2019).
  20. I. Z. Ben-Dov, H. Galitzer, V. Lavi-Moshayoff, R. Goetz, M. Kuro-o, M. Mohammadi, R. Sirkis, T. Naveh-Many, J. Silver, The parathyroid is a target organ for FGF23 in rats. *J. Clin. Invest.* **117**, 4003–4008 (2007).
  21. D. Edmonston, M. Wolf, FGF23 at the crossroads of phosphate, iron economy and erythropoiesis. *Nat. Rev. Nephrol.* **16**, 7–19 (2020).
  22. R. Goetz, Y. Nakada, M. C. Hu, H. Kurosu, L. Wang, T. Nakatani, M. Shi, A. V. Eliseenkova, M. S. Razaque, O. W. Moe, M. Kuro-o, M. Mohammadi, Isolated C-terminal tail of FGF23 alleviates hypophosphatemia by inhibiting FGF23-FGFR-Klotho complex formation. *Proc. Natl. Acad. Sci. U.S.A.* **107**, 407–412 (2010).
  23. E. L. Clinkenbeard, M. R. Hanudel, K. R. Stayrook, H. N. Appaiah, E. G. Farrow, T. A. Cass, L. J. Summers, C. S. Ip, J. M. Hum, J. C. Thomas, M. Ivan, B. M. Richine, R. J. Chan, T. L. Clemens, E. Schipani, Y. Sabbagh, L. Xu, E. F. Srour, M. B. Alvarez, M. A. Kacena, I. B. Salusky, T. Ganz, E. Nemeth, K. E. White, Erythropoietin stimulates murine and human fibroblast growth factor-23, revealing novel roles for bone and bone marrow. *Haematologica* **102**, e427–e430 (2017).
  24. L. M. Coe, S. V. Madathil, C. Casu, B. Lanske, S. Rivella, D. Sitara, FGF-23 is a negative regulator of prenatal and postnatal erythropoiesis. *J. Biol. Chem.* **289**, 9795–9810 (2014).
  25. R. Agoro, A. Montagna, R. Goetz, O. Aligbe, G. Singh, L. M. Coe, M. Mohammadi, S. Rivella, D. Sitara, Inhibition of fibroblast growth factor 23 (FGF23) signaling rescues renal anemia. *FASEB J.* **32**, 3752–3764 (2018).
  26. L. Xiao, C. Homer-Bouthiette, M. M. Hurley, FGF23 neutralizing antibody partially improves bone mineralization defect of HMWFGF23 isoforms in transgenic female mice. *J. Bone Miner. Res.* **33**, 1347–1361 (2018).
  27. K. L. Insogna, K. Briot, E. A. Imel, P. Kamenicky, M. D. Ruppe, A. A. Portale, T. Weber, P. Pitukcheewanont, H. I. Cheong, S. Jan de Beur, Y. Imanishi, N. Ito, R. H. Lachmann, H. Tanaka, F. Perwad, L. Zhang, C. Y. Chen, C. Theodore-Oklota, M. Mealiffe, J. San Martin, T. O. Carpenter, AXLES 1 Investigators, A randomized, double-blind, placebo-controlled, phase 3 trial evaluating the efficacy of burosumab, an anti-FGF23 antibody, in adults with X-linked hypophosphatemia: Week 24 primary analysis. *J. Bone Miner. Res.* **33**, 1383–1393 (2018).
  28. H. Weidner, U. Baschant, F. Lademann, M. G. Ledesma Colunga, E. Balaian, C. Hofbauer, B. M. Misof, P. Roschger, S. Blouin, W. G. Richards, U. Platzbecker, L. C. Hofbauer, M. Rauner, Increased FGF-23 levels are linked to ineffective erythropoiesis and impaired bone mineralization in myelodysplastic syndromes. *JCI Insight* **5**, e137062 (2020).
  29. M. Baldini, F. M. Olivieri, S. Forti, S. Serafino, S. Seghezzi, A. Marcon, F. Giarda, C. Messina, E. Cassinero, B. Aubry-Rozier, D. Hans, M. D. Cappellini, Spine bone texture assessed by trabecular bone score (TBS) to evaluate bone health in thalassemia major. *Calcif. Tissue Int.* **95**, 540–546 (2014).
  30. M. Baldini, A. Marcon, F. M. Olivieri, S. Seghezzi, R. Cassin, C. Messina, M. D. Cappellini, G. Graziadei, Bone quality in beta-thalassemia intermedia: Relationships with bone quantity and endocrine and hematologic variables. *Ann. Hematol.* **96**, 995–1003 (2017).
  31. B. Yang, S. Kirby, J. Lewis, P. J. Detloff, N. Maeda, O. Smithies, A mouse model for beta 0-thalassemia. *Proc. Natl. Acad. Sci. U.S.A.* **92**, 11608–11612 (1995).
  32. M. G. Vogiatzi, J. Tsay, K. Verdelis, S. Rivella, R. W. Grady, S. Doty, P. J. Giardina, A. L. Boskey, Changes in bone microarchitecture and biomechanical properties in the th3 thalassemia mouse are associated with decreased bone turnover and occur during the period of bone accrual. *Calcif. Tissue Int.* **86**, 484–494 (2010).
  33. L. A. Mathias, T. C. Fisher, L. Zeng, H. J. Meiselman, K. I. Weinberg, A. L. Hiti, P. Malik, Ineffective erythropoiesis in beta-thalassemia major is due to apoptosis at the polychromatophilic normoblast stage. *Exp. Hematol.* **28**, 1343–1353 (2000).
  34. A. J. van Vuren, M. F. Eisenga, S. van Straaten, A. Glenthoj, C. Gaillard, S. J. L. Bakker, M. H. de Borst, R. van Wijk, E. J. van Beers, Interplay of erythropoietin, fibroblast growth factor 23, and erythroferone in patients with hereditary hemolytic anemia. *Blood Adv.* **4**, 1678–1682 (2020).
  35. J. Bohlius, K. Bohlke, R. Castelli, B. Djulbegovic, M. B. Lustberg, M. Martino, G. Mountzios, N. Peswani, L. Porter, T. N. Tanaka, G. Trifiro, H. Yang, A. Lazo-Langner, Management of cancer-associated anemia with erythropoiesis-stimulating agents: ASCO/ASH clinical practice guideline update. *Blood Adv.* **3**, 1197–1210 (2019).
  36. S. Hiram-Bab, T. Liron, N. Deshet-Unger, M. Mittelman, M. Gassmann, M. Rauner, K. Franke, B. Wielockx, D. Neumann, Y. Gabet, Erythropoietin directly stimulates osteoclast precursors and induces bone loss. *FASEB J.* **29**, 1890–1900 (2015).
  37. M. Rauner, M. Murray, S. Thiele, D. Watts, D. Neumann, Y. Gabet, L. C. Hofbauer, B. Wielockx, Epo/EpoR signaling in osteoprogenitor cells is essential for bone homeostasis and Epo-induced bone loss. *Bone Res.* **9**, 42 (2021).
  38. X. Li, L. Lozovatsky, J. A. Fretz, K. E. Finberg, Bone marrow sinusoidal endothelial cells are a site of *Fgf23* upregulation in iron deficiency anemia. *Blood* **138**, 759 (2021).
  39. M. Castro-Mollo, S. Gera, M. Ruiz-Martinez, M. Feola, A. Gumerova, M. Planoutene, C. Clementelli, V. Sangkhae, C. Casu, S. M. Kim, V. Ostland, H. Han, E. Nemeth, R. Fleming, S. Rivella, D. Lizneva, T. Yuen, M. Zaidi, Y. Ginzburg, The hepcidin regulator erythroferone is a new member of the erythropoiesis-iron-bone circuitry. *eLife* **10**, e68217 (2021).
  40. S. Stier, Y. Ko, R. Forkert, C. Lutz, T. Neuhaus, E. Grunewald, T. Cheng, D. Dombkowski, L. M. Calvi, S. R. Rittling, D. T. Scadden, Osteopontin is a hematopoietic stem cell niche component that negatively regulates stem cell pool size. *J. Exp. Med.* **201**, 1781–1791 (2005).
  41. T. Sugiyama, H. Kohara, M. Noda, T. Nagasawa, Maintenance of the hematopoietic stem cell pool by CXCL12-CXCR4 chemokine signaling in bone marrow stromal cell niches. *Immunity* **25**, 977–988 (2006).
  42. N. Carlesso, Targeting the bone marrow niche in hemoglobinopathies. *Blood* **136**, 529–531 (2020).
  43. S. Ishii, T. Suzuki, K. Wakahashi, N. Asada, Y. Kawano, H. Kawano, A. Sada, K. Minagawa, Y. Nakamura, S. Mizuno, S. Takahashi, T. Matsui, Y. Katayama, FGF-23 from erythroblasts promotes hematopoietic progenitor mobilization. *Blood* **137**, 1457–1467 (2021).
  44. J. Heil, V. Olsavszky, K. Busch, K. Klapproth, C. de la Torre, C. Sticht, K. Sandorski, J. Hoffmann, H. Schonhaber, J. Zierow, M. Winkler, C. D. Schmidt, T. Staniczek, D. E. Daniels, J. Frayne, G. Metzgeroth, D. Nowak, S. Schneider, M. Neumaier, V. Weyer, C. Groden, H. J. Grone, K. Richter, C. Mogler, M. M. Taketo, K. Schledzewski, C. Geraud, S. Goerd, P. S. Koch, Bone marrow sinusoidal endothelium controls terminal erythroid differentiation and reticulocyte maturation. *Nat. Commun.* **12**, 6963 (2021).
  45. S. K. Murali, P. Roschger, U. Zeitz, K. Klaushofer, O. Andrukhova, R. G. Erben, FGF23 regulates bone mineralization in a 1,25(OH)<sub>2</sub>D<sub>3</sub> and Klotho-independent manner. *J. Bone Miner. Res.* **31**, 129–142 (2016).

**Acknowledgments:** We thank S. Beretta and I. Merelli from SR-Tiget Bioinformatic core for support with in silico analysis of transcription factor binding sites. We thank V. Bancaloni from IRCCS Ca' Granda Foundation Maggiore Policlinico Hospital for managing patient samples. We thank the Flow Cytometry Resource, Advanced Cytometry Technical Applications Laboratory (FRACTAL) at Ospedale San Raffaele for flow cytometry analysis and F. Cugnata from the University Centre of Statistics in the Biomedical Sciences (CUSSB) at Vita-Salute San Raffaele University for help with statistical analysis. We thank the patients enrolled in the approved protocols. **Funding:** This work was supported by Telethon Foundation SR-TIGET Core grants A3 2016 and 2022 (to G.F.), AABF's National Blood Foundation Early-Career Research grant 2020 (to A.A.), European Hematology Association Junior Research Grant 2019 (to A.A.), American Society of Hematology Global Research Award 2021 (to A.A.), Italian Foundation for Cancer Research 5x1000 AIRC grant 2019 22759 (to C.T.), and Italian Ministry of Education, University and Research PRIN grant 2017 2017K7FSYB (to C.T.). **Author contributions:** A.A. conceived the experimental work, performed research, analyzed, interpreted and discussed data, provided project coordination, contributed to financial support, and wrote the paper. L.R. performed research, analyzed and discussed data, and contributed to design the experimental work and to write the paper. S.B. and I.V. performed histomorphology and pQCT analysis on the bone, discussed data, and contributed to write the paper. M.S. helped perform in vivo experimental work. G.M. performed histopathological analysis and contributed to write the paper. S.M.

provided samples from thalassemic patients. C.T. performed histopathological analysis, discussed data, and helped write and critically review the paper. M.D.C. and I.M. provided samples from thalassemic patients, discussed data, and critically reviewed the paper. A.R. conceptualized and discussed data and helped write and critically review the paper. G.F. supervised the project providing coordination and financial support, discussed data, and wrote and critically reviewed the paper. All authors approved the final version of the manuscript.

**Competing interests:** The authors declare that they have no competing interests. **Data and**

**materials availability:** All data associated with this study are in the paper or the Supplementary Materials.

Submitted 12 December 2022

Accepted 27 April 2023

Published 31 May 2023

10.1126/scitranslmed.abq3679

## Inhibition of FGF23 is a therapeutic strategy to target hematopoietic stem cell niche defects in $\beta$ -thalassemia

Annamaria Aprile, Laura Raggi, Simona Bolamperti, Isabella Villa, Mariangela Storto, Gaia Morello, Sarah Markt, Claudio Tripodo, Maria Domenica Cappellini, Irene Motta, Alessandro Rubinacci, and Giuliana Ferrari

*Sci. Transl. Med.* **15** (698), eabq3679. DOI: 10.1126/scitranslmed.abq3679

### View the article online

<https://www.science.org/doi/10.1126/scitranslmed.abq3679>

### Permissions

<https://www.science.org/help/reprints-and-permissions>

Use of this article is subject to the [Terms of service](#)

---

*Science Translational Medicine* (ISSN 1946-6242) is published by the American Association for the Advancement of Science. 1200 New York Avenue NW, Washington, DC 20005. The title *Science Translational Medicine* is a registered trademark of AAAS.

Copyright © 2023 The Authors, some rights reserved; exclusive licensee American Association for the Advancement of Science. No claim to original U.S. Government Works



Supplementary Materials for  
**Inhibition of FGF23 is a therapeutic strategy to target hematopoietic stem  
cell niche defects in  $\beta$ -thalassemia**

Annamaria Aprile *et al.*

Corresponding author: Giuliana Ferrari, ferrari.giuliana@hsr.it; Annamaria Aprile, aprile.annamaria@hsr.it

*Sci. Transl. Med.* **15**, eabq3679 (2023)  
DOI: 10.1126/scitranslmed.abq3679

**The PDF file includes:**

Materials and Methods  
Figs. S1 to S14  
Tables S1 to S4  
Legends for data files S1 to S3  
Reference (45)

**Other Supplementary Material for this manuscript includes the following:**

Data files S1 to S3  
MDAR Reproducibility Checklist

1 **SUPPLEMENTARY MATERIALS AND METHODS**

2 *Flow cytometry*

3 Murine total BM cells were obtained by flushing femurs and tibiae. To analyze primitive progenitor  
4 and stem cell populations lineage depletion was performed to enrich for lineage negative (Lin-) cells,  
5 using lineage-specific antibodies (GR1, CD11b, CD45R/B220, CD3, TER-119, Milteny Biotech).  
6 Staining was performed with commercially prepared antibodies in MACS Buffer supplemented with  
7 BSA and EDTA (Milteny Biotech). Fluorochrome-conjugated antibodies specific against mouse c-  
8 kit (clone 2B8), Sca-1 (D7), CD48 (HM48-1), CD150 (Q38- 480), CD44 (IM7), Ter119 (TER-119),  
9 CD71 (C2), CD45.1 (A20), CD45.2 (104) and Lineage cocktail were purchased from BioLegend, BD  
10 or eBioscience. Cell-cycle analysis on murine HSC was performed using 7-AAD (BD Biosciences)  
11 and anti-Ki67 antibody (B56, BD Pharmingen) after treatment with permeabilization with Cytotfix-  
12 permeabilization and Permeabilization-wash Buffers (BD Biosciences). Erythroid progenitors were  
13 analyzed by labeling total BM cells with antibodies against Ter119, CD44 and CD71. Cells were  
14 stained with anti-Annexin V antibody and Propidium Iodide (BD Pharmingen) for apoptosis assay.  
15 *In vitro* EPO-stimulated bone and BM Ter119<sup>+</sup> erythroid cells were harvested in fixation buffer  
16 (Invitrogen) containing paraformaldehyde for 20 minutes at room temperature, permeabilized in  
17 methanol for 30 minutes at -20°C and stained with anti-phosphoERK1/2 (eBioscience) and with anti-  
18 phosphoSTAT5 (eBioscience), respectively for 30 minutes at room temperature. Cells were acquired  
19 using a FACS Canto II (BD Biosciences) and analyzed with FCS Express Software (De Novo  
20 Software). Sorting of bone-derived populations was performed by using the antibodies against CD45  
21 (30-F11), Ter119, CD31 (MEC13.3), Sca-1 and CD51 (RMV-7). CD31<sup>+</sup> endothelial cells and  
22 CD51<sup>+</sup>Sca-1<sup>-</sup> osteoprogenitors were sorted using a FACS Aria Fusion (BD Biosciences). A complete  
23 list of the antibodies used is reported in Data file S3.

24

25

26 *In vitro EPO stimulation and signaling inhibition*

27 Bone-derived cells were obtained upon digestion of wt femurs and tibiae with collagenase type I  
28 (STEMCELL Technologies) for 1h at 37°C and incubated with IMDM supplemented with 10% FBS,  
29 and 1% Penicillin/Streptomycin at  $1 \times 10^5$  cells/well for 30 minutes. Bone cells were either stimulated  
30 with rhEPO (100U/ml, Janssen) or pre-treated for 2h with the ERK1/2 inhibitor U0126 (Cell  
31 Signaling) 500  $\mu$ M and incubated with rhEPO.

32 Total BM cells from femurs and tibiae of wt mice were labeled with anti-mouse Ter-119 MicroBeads  
33 (Milteny Biotech) and positively selected by QuadroMACS Separator (Milteny Biotech) to enrich in  
34 Ter119<sup>+</sup> erythroid cells. BM Ter119<sup>+</sup> cells were incubated with IMDM supplemented with 10% FBS,  
35 and 1% Penicillin/Streptomycin at  $1 \times 10^6$  cells/well for 30 minutes. Cells were either stimulated with  
36 rhEPO (100U/ml, Janssen) or pretreated for 2 h with STAT5 inhibitor Pimozide (Merk) 10  $\mu$ M and  
37 incubated with rhEPO.

38 Bone and erythroid cells were fixed, permeabilized, stained for intracellular p-ERK and p-STAT5,  
39 respectively, and analyzed by flow cytometry. Cells were also collected and RNA was extracted.

40

41 *pQCT and histomorphometric analysis*

42 Excised mouse tibiae were fixed 24h in 10% buffered formalin and kept in 70% ethanol. pQCT  
43 measurements were performed using a Stratec Research SA+ pQCT scanner (Stratec Medizintechnik  
44 GmbH) with a voxel size of 70  $\mu$ m and a scan speed of 3 mm/s. To orientate the long axes of the  
45 bones parallel to the image planes, the excised bone specimens were fixed with manufacturer-made  
46 plastic holders. The correct longitudinal positioning was determined by means of an initial “scout  
47 scan”. The scans were analyzed with pQCT software 6.00B using contour mode 2 and peel mode 2  
48 with a threshold of 500 mg/cm<sup>3</sup> for the calculation of trabecular and total bone parameters and with  
49 a threshold of 710 mg/cm<sup>3</sup> for cortical bone parameters. For histomorphometric analyses tibiae were  
50 incubated O.N. in 0.5M EDTA after fixation. Bones were embedded in 8% gelatin 20% sucrose 2%  
51 PVP 40 in PBS. Five  $\mu$ m sagittal sections were obtained at a Leica cryostat. To quantify nOBs, nOt,

52 BV/TV, osteoid surface in the secondary spongiosa Toluidine blue staining was performed and to  
53 quantify nOCs TRAP staining (Leukocyte Acid Phosphatase TRAP kit 387A, Sigma-Aldrich) was  
54 executed. ALP staining was performed using the Alkaline Phosphatase Staining Kit (Red) (ab242286)  
55 from Abcam (Cambridge, UK). To quantify MAR, MS, BFR wt, *th3* and *th3*-treated mice received  
56 i.p. injection of calcein (40 mg/kg body weight) and xylene orange (90 mg/kg body weight) at 7 and  
57 2 days prior to termination, respectively. Seven  $\mu\text{m}$  sagittal sections were mounted with Fluoromount  
58 G (Southern biotech). All images were acquired at a 20x magnification at a Nikon Eclipse 50i and  
59 quantified with Fiji software, following the standards provided by the ASBMR Histomorphometry  
60 Nomenclature Committee.

61

### 62 *Histological analysis*

63 Immunohistochemistry was carried out on FFPE murine femur tissue sections. Briefly, sections 2.5/3  
64  $\mu\text{m}$ -thick were cut from paraffin blocks, dried, de-waxed and rehydrated. The antigen unmasking  
65 technique was performed using Novocastra Epitope Retrieval Solutions pH6 and pH9 in a  
66 thermostatic bath at 98°C for 30 minutes. Subsequently, the sections were brought to room  
67 temperature and washed in PBS. After neutralization of the endogenous peroxidase with 3% H<sub>2</sub>O<sub>2</sub>  
68 and Fc blocking by 0.4% casein in PBS (Novocastra). Wt, *th3* and *th3*-treated samples were incubated  
69 over night with the following primary antibodies at 4 C°: monoclonal anti-mouse OPN (EPR3688,  
70 1:100 pH9, Abcam), monoclonal anti-mouse Jagged1 (E12, 1:100 pH9, Santa Cruz Biotechnology),  
71 monoclonal anti-mouse CXCL12/SDF-1 (79018, 1:50 pH9, R&D). The binding of the primary  
72 antibody was revealed by a polymer detection kit (Leica, Novocastra) and following specific  
73 secondary antibodies, donkey anti-rabbit IgG (H&L) 1:500 (Novex by Life Technologies), rabbit  
74 anti-mouse IgG 1:200 (Sigma Aldrich), and AEC (3-amino-9-ethylcarbazole) substrate-chromogen,  
75 following manufacturer's instructions. A complete list of the antibodies used is reported in Data file  
76 S3.

77 Microphotographs were collected using a Zeiss Axiocam 503 Color digital camera with the Zen 2.0  
78 Software (Zeiss). Slide digitalization was performed using an Aperio CS2 digital scanner (Leica  
79 Biosystems) with the ImageScope software (Aperio ImageScope version 12.3.2.8013, Leica  
80 Biosystems).

81 Quantitative analyses of IHC stainings were performed by calculating the average percentage of  
82 positive signals in five nonoverlapping fields at medium-power magnification (x200) using the  
83 Nuclear Hub (weak positivity: signal intensity threshold 210; moderate positivity: signal intensity  
84 threshold 188; strong positivity: signal intensity threshold 162), Positive Pixel Count v9 (1pweak  
85 positivity: signal intensity range 220–175; 2p moderate positivity: signal intensity range 175–100; 3p  
86 strong positivity: signal intensity range 100–0) ImageScope software and HALO image analysis  
87 segmentation software (v3.2.1851.229, Indica Labs).

88

#### 89 *Immunofluorescence analysis*

90 In double-marker immunofluorescence (IF) staining, tissue sections were incubated with the  
91 following primary antibodies: polyclonal anti- Runx-2 (HPA022040, 1:200 pH9 Sigma), monoclonal  
92 anti-JAG1 (E12, 1:100 pH9, Santa Cruz Biotechnology), monoclonal anti-OPN (EPR3688, 1:100  
93 pH9, Abcam), monoclonal anti-CXCL12/SDF-1 (79018, 1:50 pH9, R&D). Slides were analyzed  
94 under a Zeiss Axioscope A1 microscope equipped with four fluorescence channels widefield IF.  
95 Microphotographs were collected using a Zeiss Axiocam 503 Color digital camera with the Zen 2.0  
96 Software (Zeiss). A complete list of the antibodies used is reported in Data file S3.

97 Quantitative analyses of immunofluorescence staining were performed by calculating the average  
98 percentage of positive cells in five non-overlapping fields at medium-power magnification (x200)  
99 using the HALO image analysis software (v3.2.1851.229, Indica Labs).

100

101

102

103 *ELISA*

104 Human plasma samples were assayed for Total FGF23 (cFGF23; Immutopics/Quidel), intact FGF23  
105 (Immutopics/Quidel) and EPO (R&D Systems). ELISA for murine EPO (R&D Systems), PTH  
106 (RayBiotech), Total FGF23 (cFGF23, Immutopics /Quidel), intact FGF23 (Immutopics/Quidel),  
107 ERFE (DBA) and CTX-I (RatLaps) were assayed on sera from wt and *th3* and *th3*-treated mice. Total  
108 FGF23 was assayed also on BM extracellular fluid from wt and *th3* mice obtained by flushing femoral  
109 BM with 200  $\mu$ l of PBS, followed by centrifugation. All assays were performed according to  
110 manufacturer's protocols. Parameters were quantified by measuring the absorbance indicated in the  
111 protocol using Multiskan™ FC Microplate Photometer (Thermo Fisher) and evaluated with the  
112 associated analysis program.

113

114 *Western blots*

115 Bone cells were seeded at  $2 \times 10^5$  cells/well in triplicates in 48 well plates. After 30 minutes incubation,  
116 the cells were treated with the 100U/mL rhEPO and collected in 100ul of modified RIPA buffer  
117 (EDTA 0,5 M) with a protease and phosphatase inhibitor cocktail (1:50 and 1:100, Sigma-Aldrich)  
118 15 minutes after treatment. BM erythroid cells were seeded at  $2 \times 10^6$  cells/well in triplicates in 6 well  
119 plates. After 30 minutes incubation, the cells were treated with the 100U/mL rhEPO and collected in  
120 300ul of modified RIPA lysis buffer 15 minutes after treatment. 24ul of total protein were mixed with  
121 Laemmli sample loading buffer, heated at 95 °C for 10 min, and loaded onto 4–15% Tris-Gly precast  
122 polyacrylamide gels (Bio-Rad) Western blots were performed using specific antibodies for phospho-  
123 STAT5 (Tyr694, 1:200, Cell Signaling); total STAT5 (D2O6Y, 1:500, Cell Signaling); phospho-ERK  
124 (E-4, 1:500, St. Cruz); and total ERK1/2 (C-9, 1:500, St. Cruz ). Antibodies were diluted in 5% milk  
125 or BSA Tris-buffered saline with 0.1% Tween20 (Sigma-Aldrich,). After rinsing, membranes were  
126 treated with specific horseradish peroxidase-conjugated secondary antibodies (1:5000) (Cell  
127 Signaling). A complete list of the antibodies used is reported in Data file S3. Chemiluminescent

128 signals were collected with the UVITEC MiniHD9 (Cambridge, UK) and quantified by means of the  
129 manufacturer's Nine Alliance software v. 17.01. GAPDH or Calnexin were used as a loading controls.

130

131 *Gene expression analysis*

132 Tibias and femurs previously flushed out and snap frozen in liquid nitrogen were homogenized in  
133 Trizol reagent (Invitrogen, Life Technologies) and RNA was then isolated from total bone cells  
134 according to the manufacturer's protocol. Total RNA from BM Ter119<sup>+</sup> erythroid cells was isolated  
135 using the RNeasy Mini kit (Qiagen) and reverse transcribed. Gene expression analysis was performed  
136 on QX200 Droplet Digital PCR (ddPCR) System (Biorad).

137

138 *Transplantation of hematopoietic stem and progenitor cells*

139 For bone marrow transplantation (BMT) experiments, murine BM cells were harvested from wt, *th3*,  
140 *th3* +FGF23inh and *th3* +FGF23inh (LT) mice and purified as Lin<sup>-</sup> cells. 4 x 10<sup>5</sup> Lin<sup>-</sup> cells/mouse  
141 CD45.2 donor cells were injected i.v. into lethally irradiated (9 Gy) wt CD45.1 recipient animals.  
142 Percentage of donor-derived cells in PB was determined by FACS analysis at 16 weeks after BMT.  
143 At termination total BM cells were harvested and analyzed for chimerism and grafted HSC cell cycle  
144 profile.

145

146 *Competitive bone marrow transplantation*

147 For competitive BMT experiments, a limiting dose of 1x10<sup>5</sup> per mouse wt (CD45.1) and *th3* (CD45.2)  
148 cells are transplanted by i.v. injection into Busulfan-conditioned CD45.1 *th3* recipient mice. Recipient  
149 mice were either untreated or treated with cFGF23 peptide for 13days before BMT, resulting in two  
150 experimental groups. Percentage of donor-derived cells in PB and BM was determined by FACS  
151 analysis at 12 and 16 weeks after BMT, respectively.

152

153 *Quantification of PPi levels*

154 PPi was extracted as previously reported (45). Briefly, whole femurs were incubated in 300ul of 1.2  
155 M HCl at 4°C overnight. HCl was evaporated at 99°C for 1h, and samples were resuspended in 200μl  
156 of deionized water. The amount of PPi was quantified using the PhosphoWorks kit (AAT Bioquest)  
157 according to the manufacturer's protocol.

158

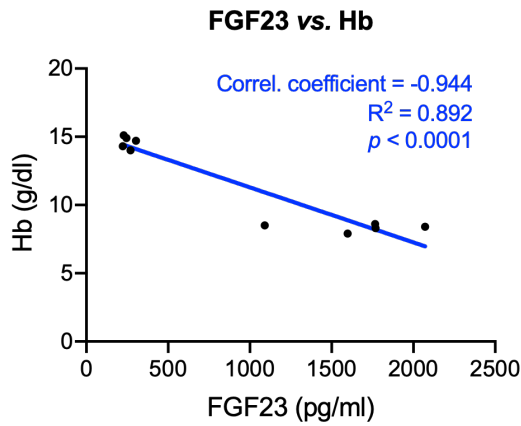
159 *In silico prediction of consensus sequences*

160 We selected the genomic region spanning 1000bp upstream of FGF23 promoter and we compared  
161 the enrichment of consensus motif for transcription factors associated to ERK1/2 and STAT5  
162 signaling provided by JASPAR and HOCOMOCO databases. This *in silico* analysis allowed us to  
163 identify the top-ranking transcription factors on *Fgf23* promoter with most significant *p* values.



Supplementary figures

**A**



**B**

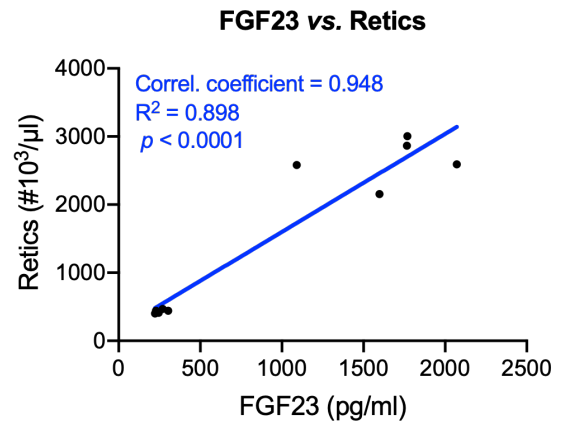


**Fig. S1. FGF23 correlates with anemia parameters.** (A) Correlation between FGF23 and hemoglobin concentration in wt and *th3* mice ( $n = 10$ ). (B) Correlation between FGF23 and reticulocyte count (Retics) in wt and *th3* mice ( $n = 10$ ). Pearson correlation coefficient test was used to evaluate statistical significance.

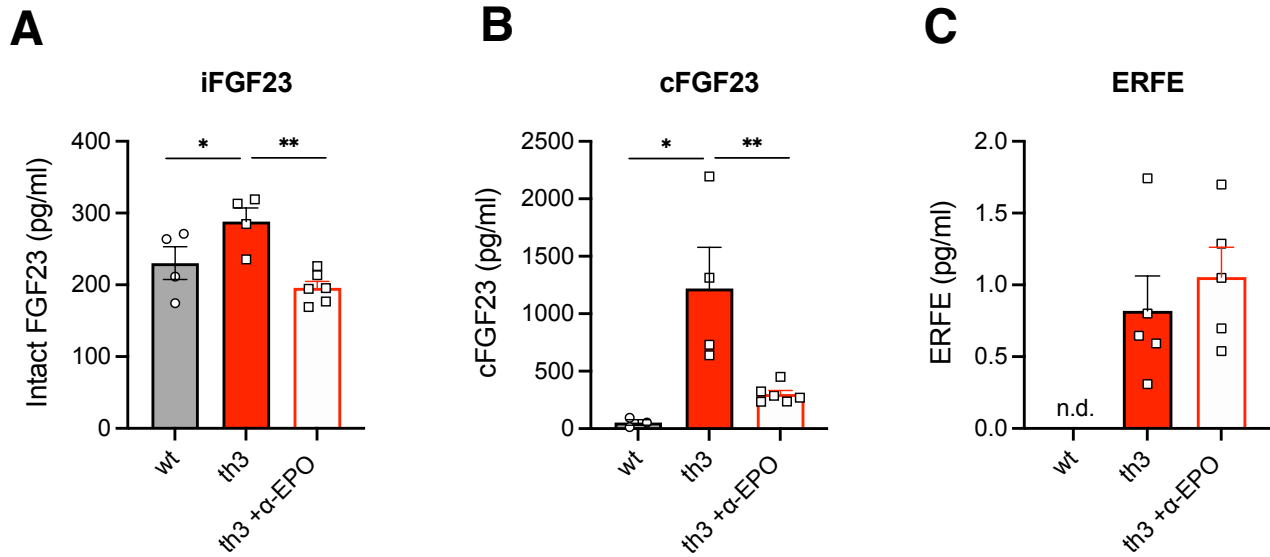


**Fig. S2. iFGF23, cFGF23, and ERFE upon EPO inhibition.** (A) iFGF23 in sera from wt ( $n = 4$ ), *th3* ( $n = 4$ ) and *th3*+anti-EPO antibody ( $\alpha$ -EPO) ( $n = 6$ ) animals by ELISA. (B) cFGF23 in sera from wt ( $n = 3$ ), *th3* ( $n = 4$ ) and *th3*+anti-EPO antibody ( $\alpha$ -EPO) ( $n = 6$ ) mice, calculated by subtracting the iFGF23 from the total FGF23 values obtained by ELISA. (C) ERFE in sera from wt (*not detectable, n.d.*), *th3* ( $n = 5$ ) and *th3*+anti-EPO antibody ( $\alpha$ -EPO) ( $n = 5$ ) mice by ELISA. Values represent means  $\pm$  SEM. One-tailed Mann-Whitney test was used to evaluate statistical significance (\*  $p < 0.05$ , \*\*  $p < 0.01$ ), followed by Bonferroni correction for comparison among more than 2 groups.

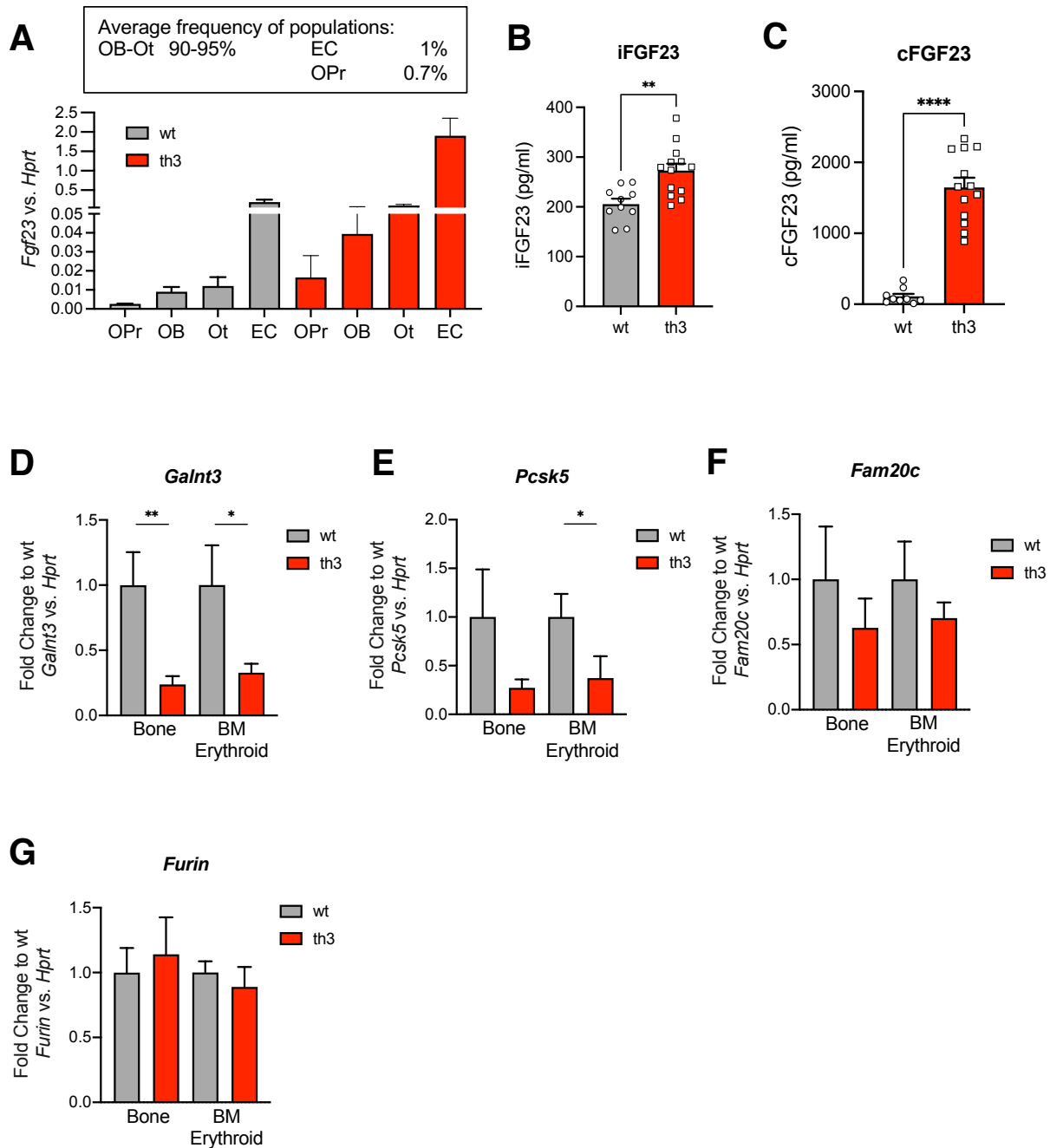


**Fig. S3. FGF23 production and processing by bone and BM erythroid cells.** (A) *Fgf23* expression relative to *Hprt* in bone-derived populations from wt (grey bar,  $n = 3$ ) and *th3* (red bar,  $n = 3$ ) mice by ddPCR: osteoprogenitors (OPr), osteoblasts (OB), osteocytes (Ot) and endothelial cells (EC). The average frequencies of each population were indicated as reported by literature or assessed by flow cytometry. (B) iFGF23 in sera from wt ( $n = 10$ ) and *th3* ( $n = 13$ ) animals by ELISA. (C) cFGF23 in sera from wt ( $n = 9$ ) and *th3* ( $n = 13$ ) mice calculated by subtracting the iFGF23 from the total FGF23 values obtained by ELISA. (D-G) *Galnt3* (D), *Pcsk5* (E), *Fam20c* (F), and *Furin* (G) gene expression relative to *Hprt* by total bone and BM erythroid cells from wt (grey bar,  $n \geq 4$ ) and *th3* (red bar,  $n \geq 4$ ) mice by ddPCR, reported as fold change relative to wt. Values represent means  $\pm$  SEM. Two-tailed Mann-Whitney test was used to evaluate statistical significance (\*  $p < 0.05$ , \*\*  $p < 0.01$ , \*\*\*\*  $p < 0.0001$ ).

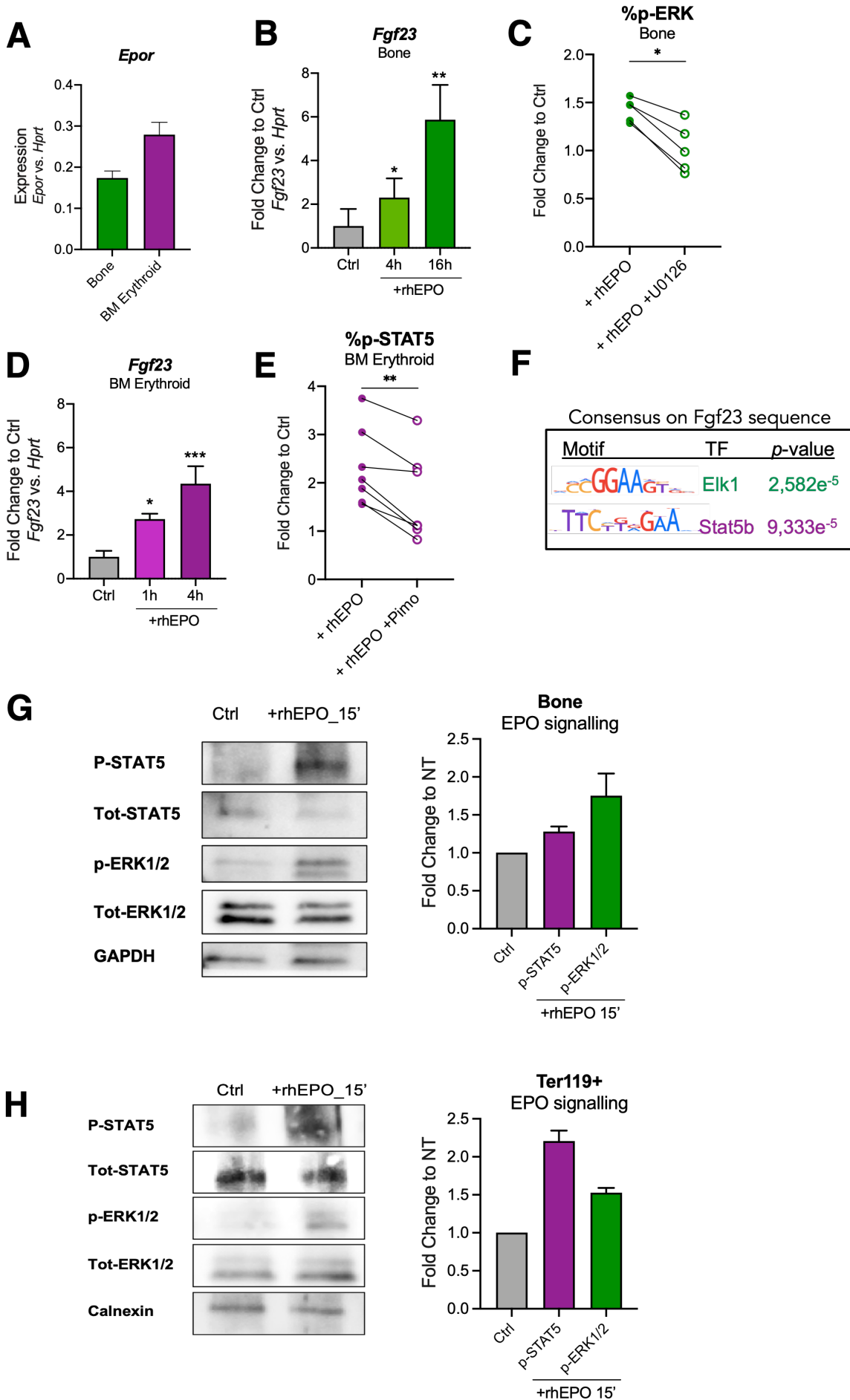


**Fig. S4. *In vitro* EPO stimulation in bone and Ter119<sup>+</sup> cells.** (A) *Epor* gene expression relative to *Hprt* by bone-derived ( $n = 4$ ) and BM erythroid cells ( $n = 7$ ) from wt mice by ddPCR. (B) *Fgf23* expression relative to *Hprt* by bone cells upon rhEPO treatment at 4 and 16 hours, reported as ratio to unstimulated control ( $n \geq 8$  mice/group). (C) Frequency of bone cells expressing phosphorylated ERK (p-ERK) upon rhEPO stimulation and inhibition by the ERK1/2 inhibitor U0126, by flow cytometry and expressed as fold to unstimulated control (Ctrl) ( $n = 5$  independent experiments, each dot represents a pool of 2-4 mice). (D) *Fgf23* expression relative to *Hprt* by BM erythroid cells upon rhEPO treatment at 1 and 4 hours, reported as ratio to unstimulated control ( $n \geq 4$  mice/group). (E) Frequency of BM erythroid cells expressing phosphorylated STAT5 (p-STAT5) upon rhEPO stimulation and inhibition by the STAT5 inhibitor pimozide, by flow cytometry and expressed as fold to unstimulated control (Ctrl) ( $n = 7$  independent experiments, each dot represents a pool of 2-4 mice). (F) Motif enrichment analysis showing top-ranking transcription factors (TF) identified on FGF23 promoter by JASPAR and HOCOMOCO databases. Putative TF and associated  $p$  values are shown. (G-H) Bone and BM erythroid cells were collected for protein analysis 15 minutes after EPO treatment which showed phosphorylation of STAT5 and ERK1/2 signaling protein by Western blot and expressed as fold to unstimulated control (Ctrl) ( $n = 3$  independent experiments, each dot represents a pool of 2-3 mice). Values represent means  $\pm$  SEM. One- or two-tailed Mann-Whitney test (B, D, G, H), and Wilcoxon test (C, E) were used to evaluate statistical significance (\*  $p < 0.05$ , \*\*  $p < 0.01$ , \*\*\*  $p < 0.001$ ). Bonferroni correction was applied for comparison among more than 2 groups.

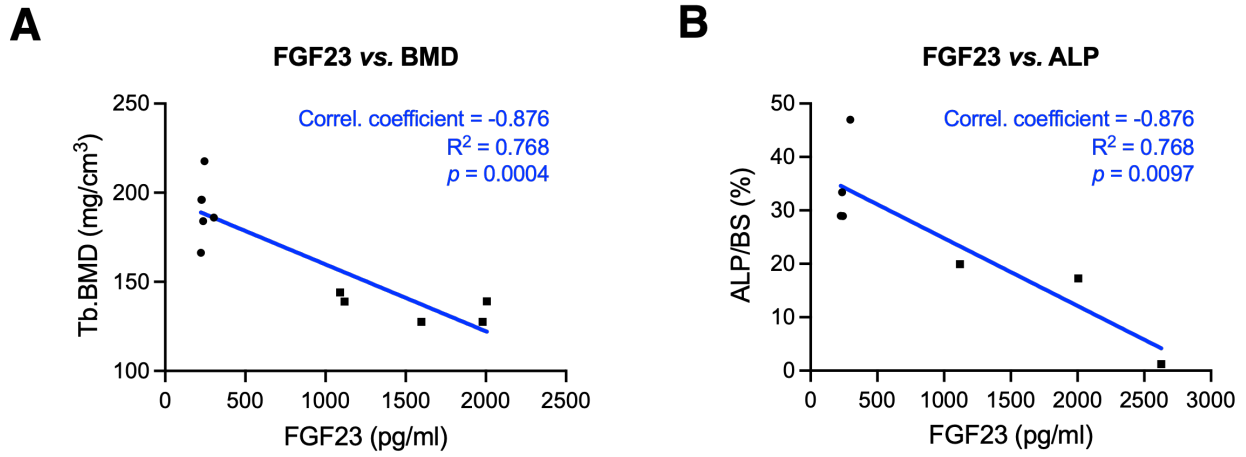


**Fig. S5. FGF23 correlates with trabecular bone mineral density.** (A) Correlation between FGF23 and Tb.BMD in wt and *th3* mice ( $n = 11$ ). (B) Correlation between FGF23 and ALP in wt and *th3* mice ( $n = 7$ ). Black rounds: wt mice; Black squares: *th3* mice. Pearson correlation coefficient test was used to evaluate statistical significance.

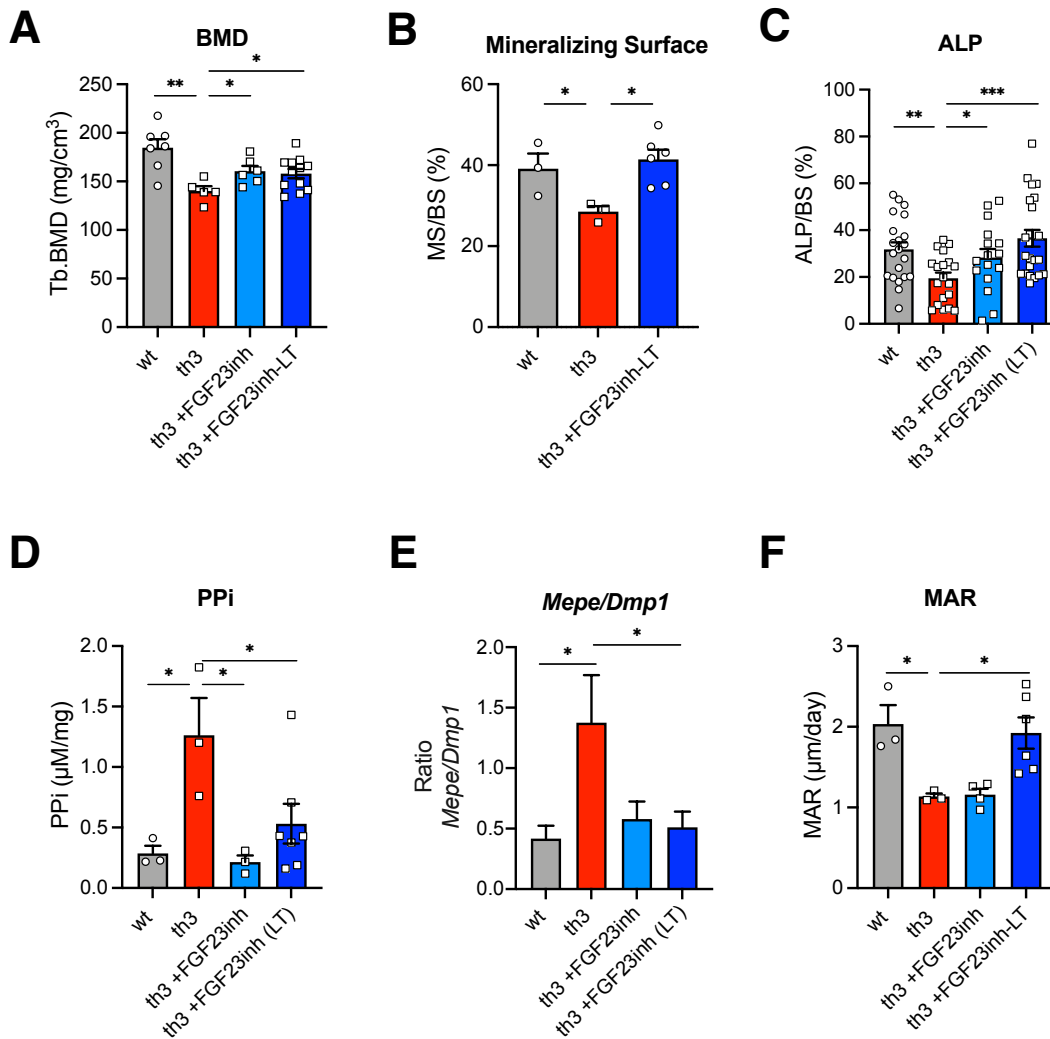


**Fig. S6. Bone features of wt, *th3* and *th3* upon FGF23 inhibition.** (A-C) Volumetric Tb.BMD by pQCT, percentage of mineralizing surface on bone surface (MS/BS) and percentage of ALP area on bone surface (ALP/BS) in wt ( $n \geq 3$ ), *th3* ( $n \geq 3$ ), *th3*+FGF23inh ( $n \geq 6$ ) and, *th3*+FGF23inh (LT) ( $n \geq 6$ ) mice. (D) PPI concentration  $\mu\text{M}/\text{mg}$  bone tissue of wt ( $n = 3$ ), *th3* ( $n = 3$ ), *th3*+FGF23inh ( $n = 3$ ) mice and *th3*+FGF23inh (LT) ( $n = 7$ ). (E) *Mepe* and *Dmp1* gene expression ratio relative to *Hprt* by wt ( $n = 5$ ), *th3* ( $n = 6$ ), *th3*+FGF23inh ( $n = 4$ ) and *th3*+FGF23inh (LT) ( $n = 5$ ) total bone cells by ddPCR, shown as fold to wt. (F) MAR of wt ( $n = 3$ ), *th3* ( $n = 3$ ), *th3*+FGF23inh ( $n = 4$ ) and *th3*+FGF23inh (LT) ( $n = 6$ ) mice. Values represent means  $\pm$  SEM. One-tailed Mann-Whitney test was used to evaluate statistical significance (\*  $p < 0.05$ , \*\*  $p < 0.01$ , \*\*\*  $p < 0.001$ ), followed by Bonferroni correction for comparison among more than 2 groups.

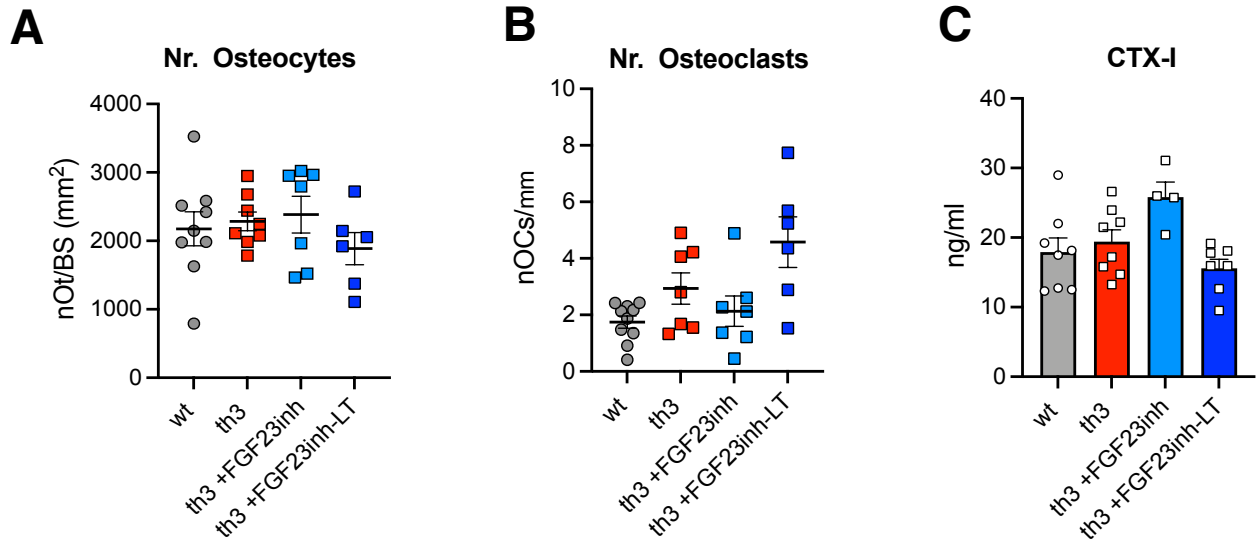


**Fig. S7. Osteocytes and osteoclasts in wt, *th3* and *th3* upon FGF23 inhibition.** (A) Number of osteocytes per mm<sup>2</sup> of bone surface (nOt/BS) by histomorphometric analysis of the proximal tibiae of wt (*n* = 9), *th3* (*n* = 8), *th3*+FGF23inh (*n* = 7) and *th3*+FGF23inh (LT) (*n* = 6). (B) Number of osteoclasts per mm of bone surface (nOCs/mm) by histomorphometric analysis of the proximal tibiae of wt (*n* = 10), *th3* (*n* = 7), *th3*+FGF23inh (*n* = 7) and *th3*+FGF23inh (LT) (*n* = 6). (C) CTX-I in sera from wt (*n* = 8), *th3* (*n* = 8), *th3*+FGF23inh (*n* = 4) and *th3*+FGF23inh (LT) (*n* = 7) mice by ELISA. Values represent means ± SEM.



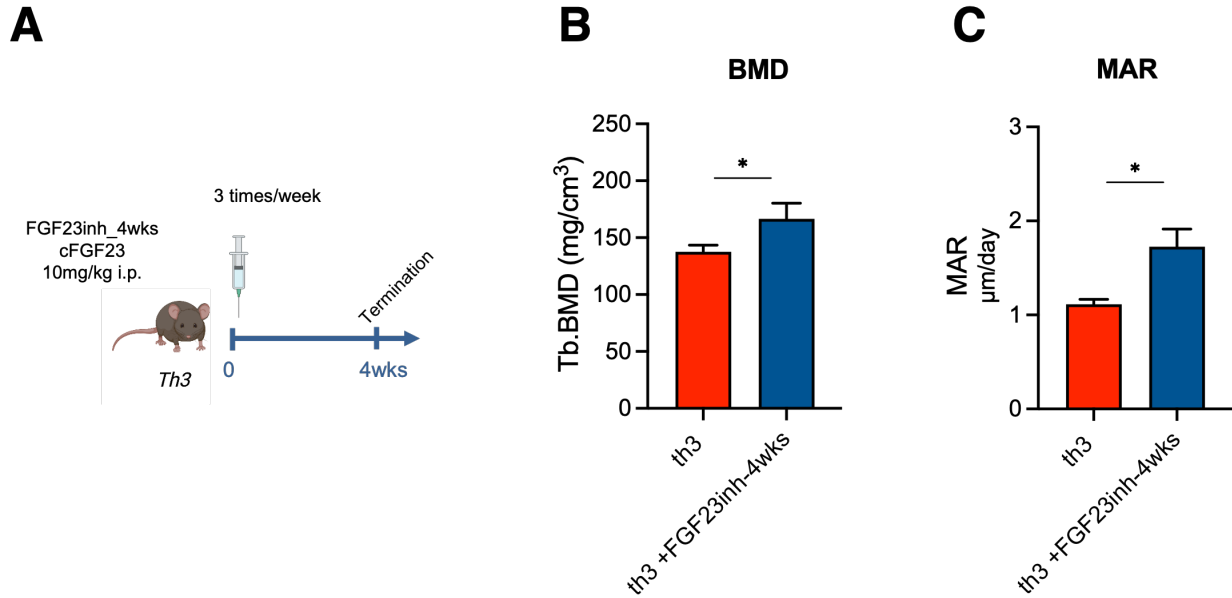


**Fig. S8. FGF23 inhibition restores bone features upon 4 weeks.** (A) *In vivo* FGF23 inhibition in *th3* mice by injection of three doses/week of cFGF23 (10 mg/kg i.p.); analyses were performed at termination upon 4 weeks. (B) Volumetric Tb.BMD by pQCT of *th3* ( $n = 5$ ) and *th3*+FGF23inh\_4wks ( $n = 5$ ). (C) MAR of *th3* ( $n = 5$ ) and *th3*+FGF23inh\_4wks ( $n = 5$ ) mice. Values represent means  $\pm$  SEM. One-tailed Mann-Whitney test was used to evaluate statistical significance (\*  $p < 0.05$ ).

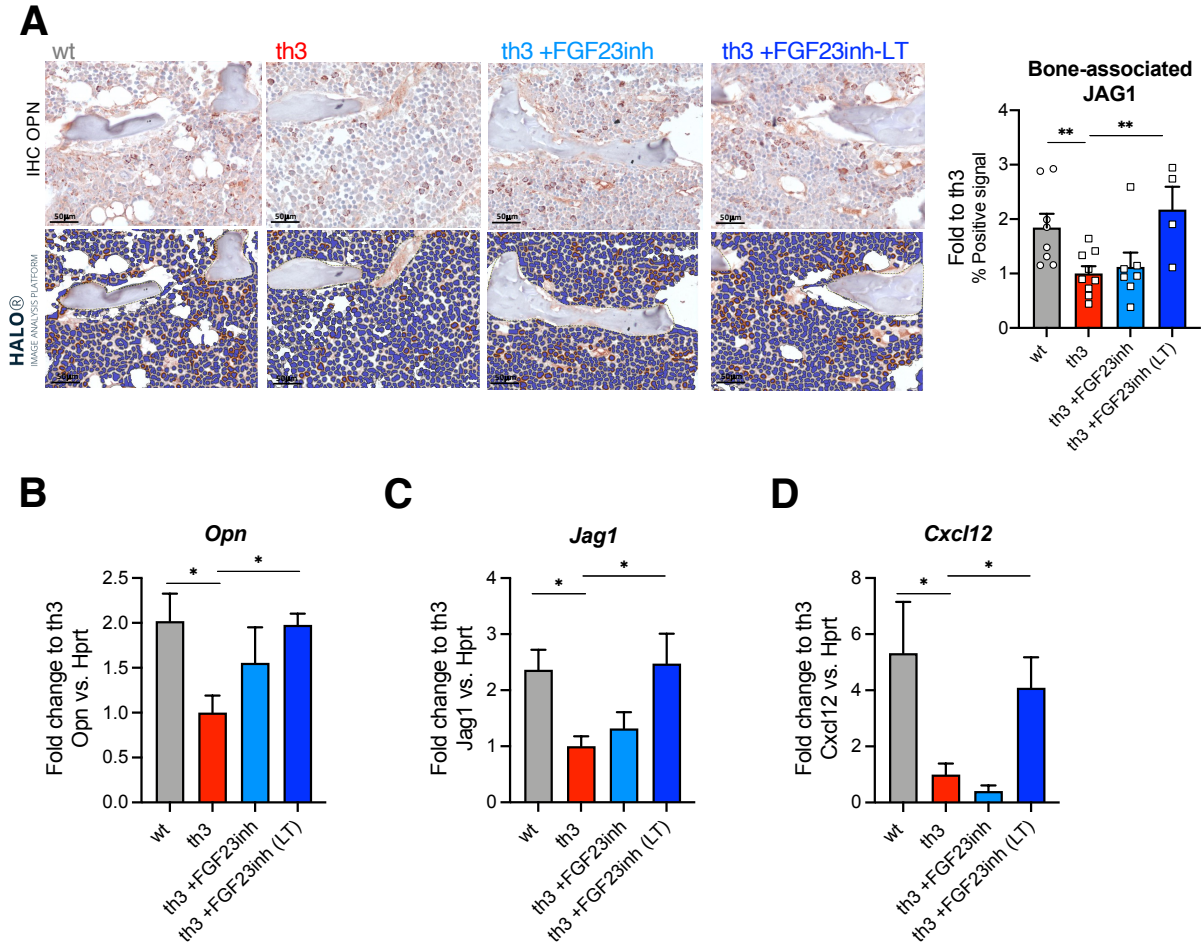
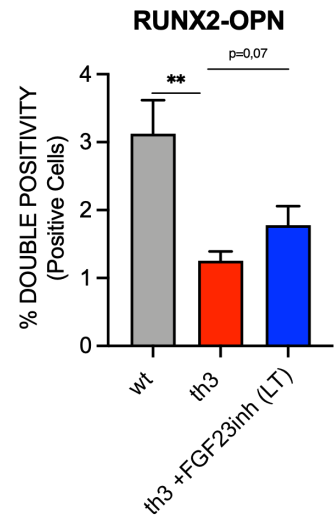
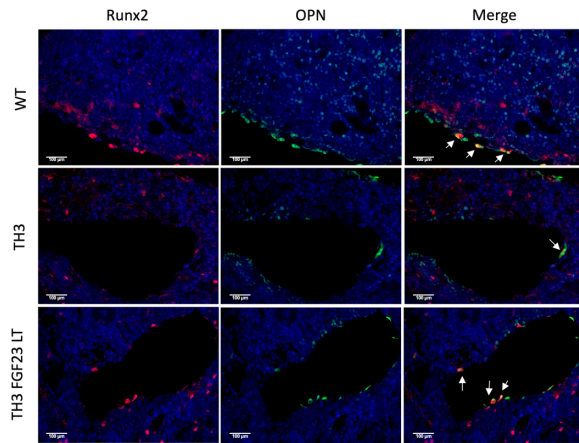
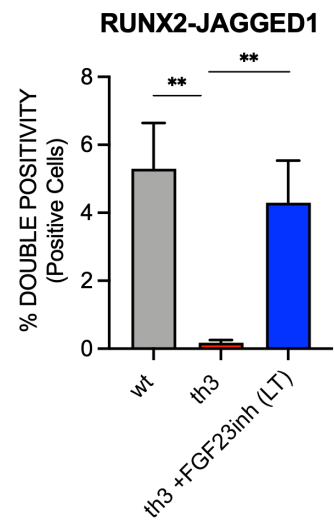
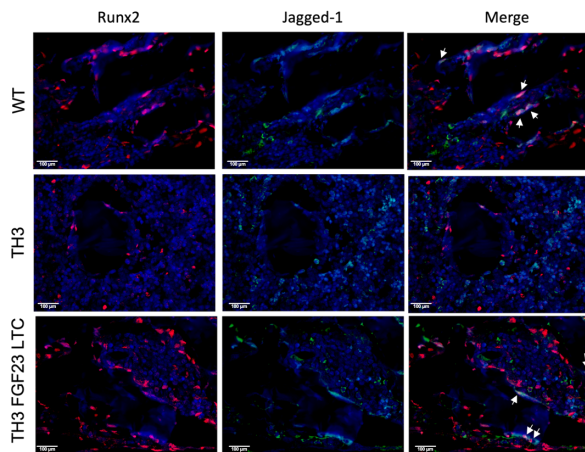


**Fig. S9. Long-term FGF23 inhibition restores expression of *Opn*, *Jag1*, and *Cxcl12* by osteolineage cells.** (A) IHC analysis of bone-associated JAG1 of wt ( $n = 8$ ), *th3* ( $n = 9$ ), *th3*+FGF23inh ( $n = 7$ ) and *th3*+FGF23inh (LT) ( $n = 4$ ) mice. Quantitative evaluation of stained area by HALO software analysis is expressed as fold expression relative to the *th3* on % of positive signal. (B-D) *Opn*, *Jag1*, *Cxcl12* expression relative to *Hprt* in total bone from wt ( $n = 4$ ), *th3* ( $n \geq 4$ ), *th3*+FGF23inh ( $n = 4$ ) and *th3*+FGF23inh\_LT ( $n = 4$ ) mice by ddPCR, shown as fold to *th3*. Values represent means  $\pm$  SEM. One-tailed Mann-Whitney test was used to evaluate statistical significance (\*  $p < 0.05$ , \*\*  $p < 0.01$ ), followed by Bonferroni correction for comparison among more than 2 groups.

**A**



**B**



**C**

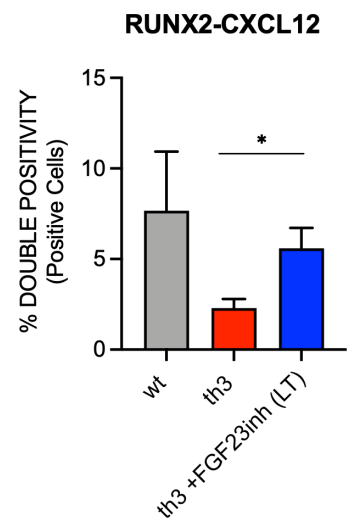
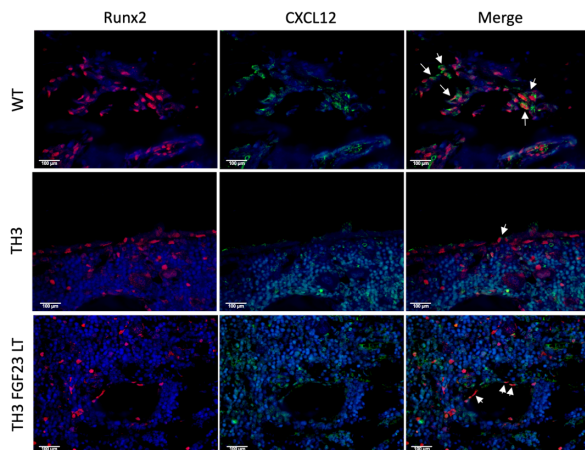


**Fig. S10. Evaluation of OPN, JAG1, and CXCL12 expression in osteolineage cells.**

Immunofluorescence analysis highlighted the expression of niche molecules in association with RUNX2<sup>+</sup> osteolineage cells (arrowheads). **(A)** Representative immunofluorescence images of RUNX2 (red signal) or OPN (green signal), in the BM of wt, *th3* and *th3*+FGF23inh (LT) mice. The percentage of RUNX2<sup>+</sup> and OPN<sup>+</sup> on total positive cells is reported ( $n = 5$ /group). **(B)** Representative immunofluorescence images of RUNX2 (red signal) or JAG1 (green signal), in the BM of wt, *th3* and *th3*+FGF23inh (LT) mice. The percentage of RUNX2<sup>+</sup> and JAG1<sup>+</sup> on total positive cells is reported ( $n = 5$ /group). **(C)** Representative immunofluorescence images of RUNX2 (red signal) or CXCL12 (green signal), in the BM of wt, *th3* and *th3*+FGF23inh (LT) mice. The percentage of RUNX2<sup>+</sup> and CXCL12<sup>+</sup> on total positive cells is reported ( $n = 5$ /group). DAPI is used as nuclear marker (blue signal). Original magnifications x200 and x400. Semi-quantitative evaluation is expressed as a percentage of double positive stained cells. Values represent means  $\pm$  SEM. One-tailed Mann-Whitney test was used to evaluate statistical significance (\*  $p < 0.05$ , \*\*  $p < 0.01$ ), followed by Bonferroni correction for comparison among more than 2 groups.

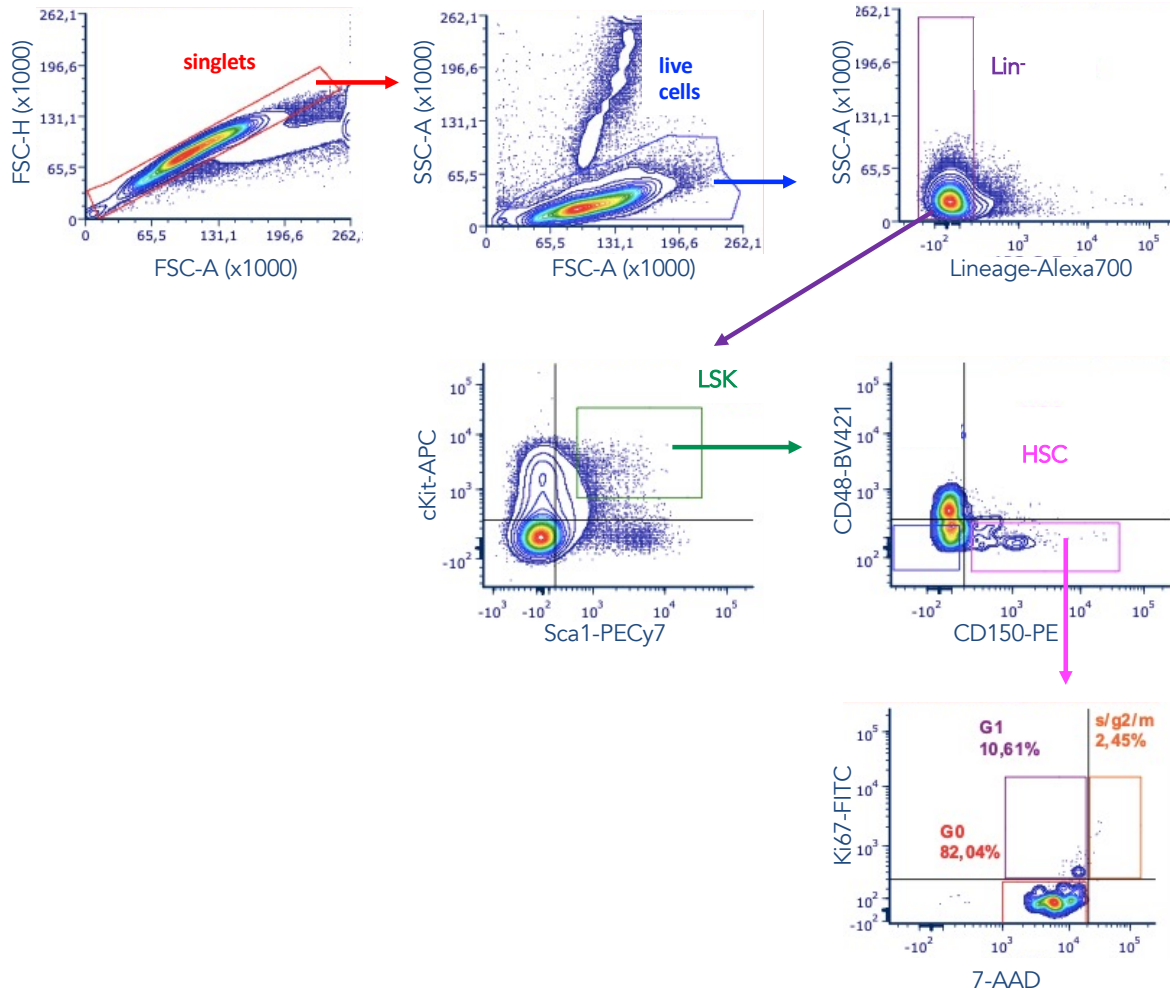


**Fig. S11. Gating strategy for analysis of BM HSC by flow cytometry.** Upon discrimination of doublets and dead cells by forward- (FSC) and side-scatter (SSC), cells were analyzed by excluding residual Lin<sup>+</sup> cells, identifying c-Kit<sup>+</sup> Sca1<sup>+</sup> on the Lin<sup>-</sup> gate (LSK) and HSC CD150<sup>+</sup> CD48<sup>-</sup> cells within the LSK population. Ki-67/7-AAD staining was performed to discriminate between G0, G1 phase and S-phase of cell cycle in the HSC population.

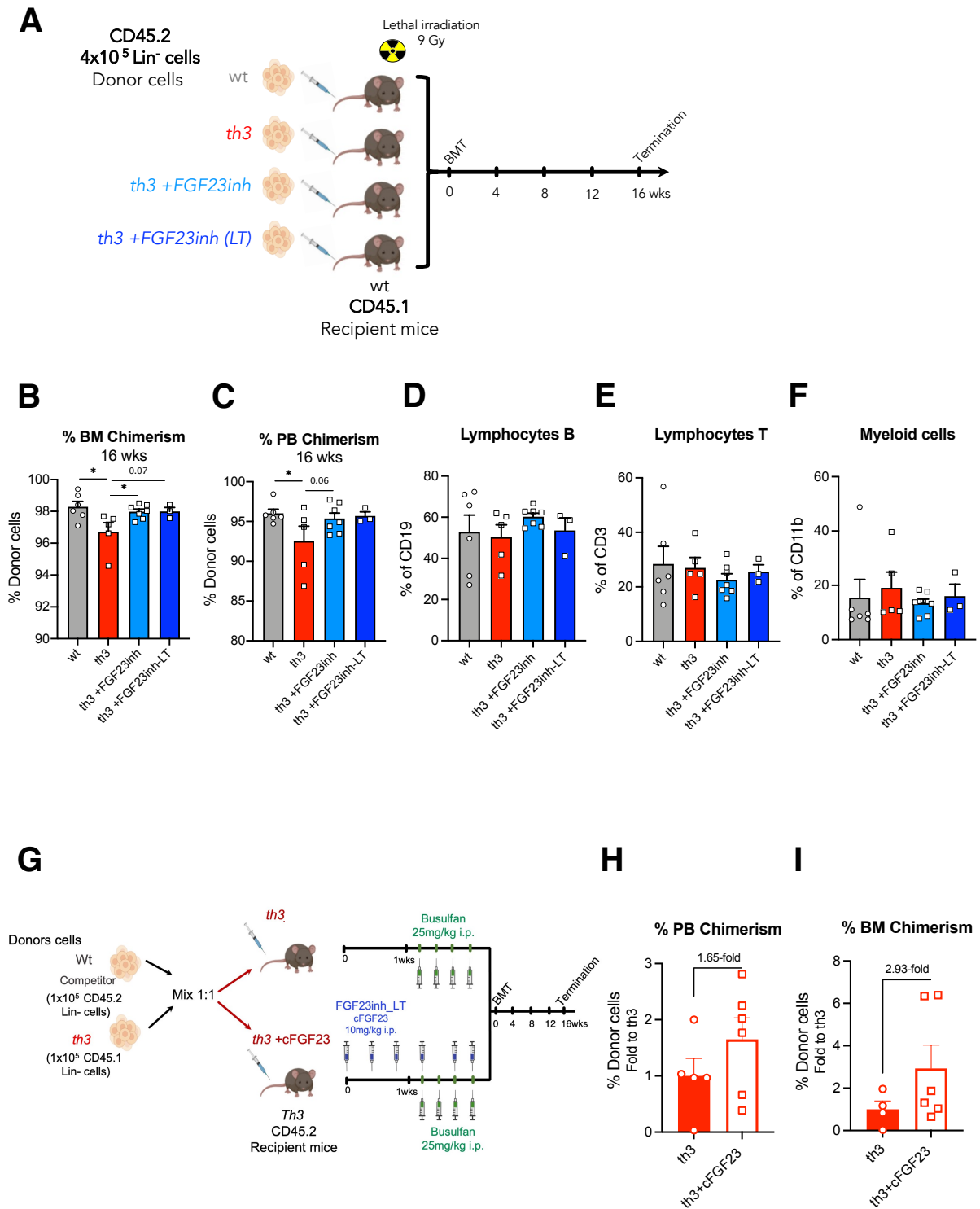


**Fig. S12. Transplantation of cells from wt, *th3*, and treated *th3* mice after FGF23 inhibition.** (A) Experimental design of BMT:  $4 \times 10^5$ /mouse BM Lin<sup>-</sup> cells from CD45.2 wt, *th3*, *th3*+FGF23inh and *th3*+FGF23inh (LT) mice are transplanted by i.v. injection into lethally irradiated CD45.1 wt recipients, resulting in four experimental groups. (B-C) Percentage of donor-derived cells in PB and BM was determined by FACS analysis at 16 weeks after BMT in wt ( $n = 6$ ), *th3* ( $n = 6$ ), *th3*+FGF23inh ( $n = 7$ ) and *th3*+FGF23inh (LT) ( $n = 3$ ). (D-F) Percentage of PB lineages (lymphocyte B, T and myeloid cells) was determined by FACS analysis at 16 weeks after BMT in wt ( $n = 6$ ), *th3* ( $n = 6$ ), *th3*+FGF23inh ( $n = 7$ ) and *th3*+FGF23inh (LT) ( $n = 3$ ). (G) Experimental design of

competitive BMT:  $1 \times 10^5$ /mouse BM Lin<sup>-</sup> cells from wt (competitive CD45.2 cells) and *th3* CD45.1 cells are transplanted by i.v. injection into Busulfan conditioned CD45.2 *th3* mice. Recipient mice were either untreated or treated with cFGF23 peptide for 13 days, resulting in two experimental groups. **(H)** Percentage of donor-derived cells in PB was determined by FACS analysis after BMT in *th3* ( $n = 5$ ) and *th3*+cFGF23 ( $n = 6$ ). **(I)** Percentage of donor-derived cells in BM was determined by FACS analysis at 16 weeks after BMT in *th3* ( $n = 4$ ) and *th3*+cFGF23 ( $n = 6$ ). Values represent means  $\pm$  SEM. One-tailed Mann-Whitney test was used to evaluate statistical significance (\*  $p < 0.05$ ), followed by Bonferroni correction for comparison among more than 2 groups.

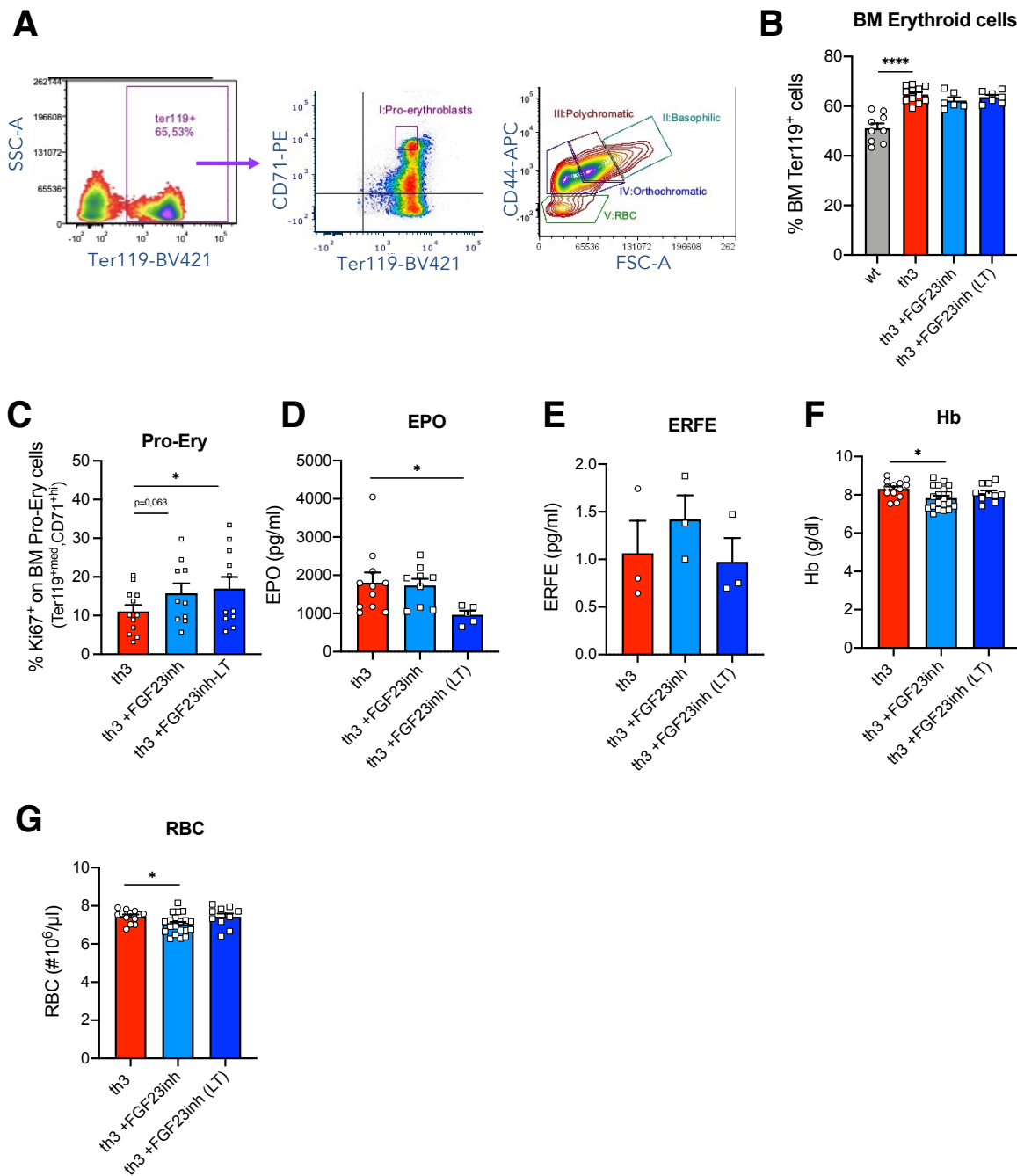


**Fig. S13. Erythroid parameters in *th3* mice upon FGF23 inhibition.** (A) Frequency of erythroid Ter119<sup>+</sup> cells in BM from wt ( $n = 9$ ), *th3* ( $n = 12$ ), *th3*+FGF23inh ( $n = 6$ ) and *th3*+FGF23inh (LT) ( $n = 7$ ). (B) Gating strategy for the analysis of BM erythroid populations by flow cytometry: Pro-erythroblasts are identified as Ter119<sup>dim</sup> CD71<sup>high</sup> cells; four distinct clusters can be identified by CD44 and FSC analysis on Ter119<sup>+</sup> cells (basophilic, polychromatic, orthochromatic erythroblasts, and terminally differentiated cells). (C) Percentage of positive pro-erythroblast stained for Ki-67 marker in the BM of *th3* ( $n = 12$ ), *th3*+FGF23inh ( $n = 10$ ) and *th3*+FGF23inh (LT) ( $n = 11$ ) mice by flow cytometry. (D) EPO in sera from *th3* ( $n = 11$ ), *th3*+FGF23inh ( $n = 9$ ) and *th3*+FGF23inh (LT) ( $n = 11$ ) mice.



( $n = 5$ ) mice by ELISA. **(E)** ERFE in sera from *th3* ( $n = 3$ ), *th3*+FGF23inh ( $n = 3$ ) and *th3*+FGF23inh (LT) ( $n = 3$ ) mice by ELISA. **(F,G)** Hb concentration (g/dL) and RBC ( $10^6/\mu\text{l}$ ) in PB of *th3* ( $n = 13$ ), *th3*+FGF23inh ( $n = 20$ ) and *th3*+FGF23inh (LT) ( $n = 10$ ). Values represent means  $\pm$  SEM. Two-tailed Mann-Whitney test was used to evaluate statistical significance (\*  $p < 0.05$ , \*\*\*\*  $p < 0.0001$ ), followed by Bonferroni correction for comparison among more than 2 groups.

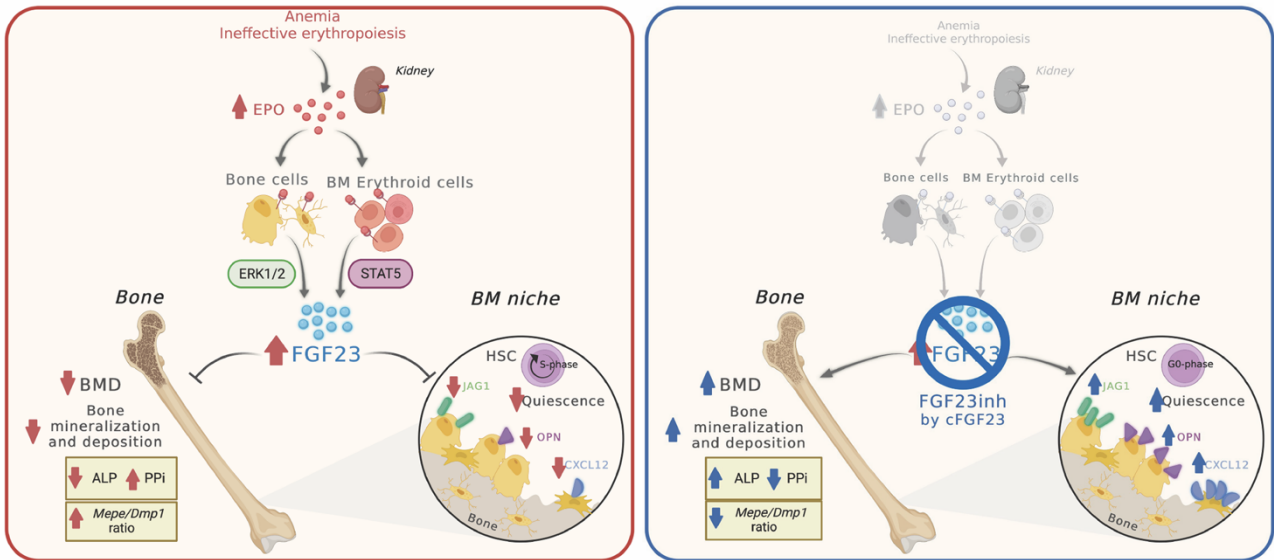


**Fig. S14. Working model of FGF23 regulation and action on bone and HSC niche.** Left panel, Chronic EPO stimulation, characteristic of  $\beta$ -thalassemia induces FGF23 overproduction by *th3* bone and BM erythroid cells, acting on ERK1/2 and STAT5 pathways, respectively. Increased FGF23 negatively affects bone mineralization and deposition, thus altering BM niche homeostasis and crosstalk with HSC. Right panel, *In vivo* inhibition of FGF23 signaling by cFGF23 restores  $\beta$ -thalassemia bone defects, BM niche and HSC function. Created with BioRender.com

**Table S1. Characteristics of the studied  $\beta$ -thalassemia cohort.**

Characteristic	Nr. of patients/total Nr. (%)	
Gender	Male	17/40 (42.5%)
	Female	23/40 (57.5%)
Age	$\leq 40$ yrs	13/40 (32.5%)
	41-50 yrs	18/40 (45.0%)
	$\geq 51$ yrs	9/40 (22.5%)
Disease	TDT	27/40 (67.5%)
	NTDT	13/40 (32.5%)
Transfusions	Regular	27/40 (67.5%)
	Occasional	7/40 (17.5%)
	No	6/40 (15.0%)
Chelation	Yes	28/40 (70.0%)
	No	12/40 (30.0%)

TDT, transfusion-dependent thalassemia; NTDT, non-transfusion-dependent thalassemia.

**Table S2. Characteristics of healthy donor controls.**

Characteristic	% of total	
Gender	Male	30%
	Female	70%
Age	$\leq 40$ yrs	60%
	41-50 yrs	30%
	$\geq 51$ yrs	10%

**Table S3. Serum parameters of patients with  $\beta$ -thalassemia.**

Parameter	BThal patients	Normal values
iFGF23 (pg/ml)	96.73 $\pm$ 8.10	39.2 – 137.3
PTH (pg/ml)	18.20 $\pm$ 1.90	6.5 – 36.8*
25OHVitD (ng/ml)	28.57 $\pm$ 1.99	21.0 – 40.0*
Serum Calcium (mg/dl)	9.22 $\pm$ 0.83	8.4 – 10.2*
Serum Phosphate (mg/dl)	3.54 $\pm$ 0.09	2.7 – 4.5*

\* Normal values are referred to the reference range on the laboratory test report

**Table S4. Biochemical analysis after cFGF23 treatment in  $\beta$ -thalassemia mice.**

Group	Serum Phosphate (mg/dl)	Statistics	Serum Calcium (mg/dl)	Statistics	Serum PTH (pg/ml)	Statistics
wt	7.47 $\pm$ 0.68	<i>n.s.</i> <i>p</i> = 0.079	8.24 $\pm$ 0.30	<i>n.s.</i> <i>p</i> = 0.909	21.98 $\pm$ 2.6	* <i>p</i> = 0.027
th3	9.01 $\pm$ 0.44	-	8.42 $\pm$ 0.34	-	14.32 $\pm$ 1.9	-
th3+FGF23inh (24h-1 dose)	11.03 $\pm$ 0.50	* <i>p</i> = 0.031	9.95 $\pm$ 0.25	* <i>p</i> = 0.013	N.D.	/
th3+FGF23inh (38h-2 doses)	7.61 $\pm$ 0.46	<i>n.s.</i> <i>p</i> = 0.078	9.03 $\pm$ 0.47	<i>n.s.</i> <i>p</i> = 0.163	18.77 $\pm$ 2.0	<i>n.s.</i> <i>p</i> = 0.077
th3+FGF23inh (LT) (13dd-6 doses)	8.87 $\pm$ 0.53	<i>n.s.</i> <i>p</i> = 0.906	8.40 $\pm$ 0.32	<i>n.s.</i> <i>p</i> = 0.616	23.11 $\pm$ 3.7	* <i>p</i> = 0.034

Statistics are referred to th3 group.  
N.D., not done.

### List of Data files



Data file S1. Raw data from main figures

Data file S2. Raw data from supplementary figures

Data file S3. List of antibodies

Review

# Targeting the Hematopoietic Stem Cell Niche in $\beta$ -Thalassemia and Sickle Cell Disease

Annamaria Aprile <sup>1,\*</sup>, Silvia Sighinolfi <sup>1,2,†</sup>, Laura Raggi <sup>1,3,†</sup> and Giuliana Ferrari <sup>1,2,\*</sup>

<sup>1</sup> San Raffaele-Telethon Institute for Gene Therapy (SR-TIGET), IRCCS San Raffaele Scientific Institute, 20132 Milan, Italy; sighinolfi.silvia@hsr.it (S.S.); raggi.laura@hsr.it (L.R.)

<sup>2</sup> Vita-Salute San Raffaele University, 20132 Milan, Italy

<sup>3</sup> University of Milano Bicocca, 20126 Milan, Italy

\* Correspondence: aprile.annamaria@hsr.it (A.A.); ferrari.giuliana@hsr.it (G.F.)

† These authors contributed equally to this work.

**Abstract:** In the last decade, research on pathophysiology and therapeutic solutions for  $\beta$ -thalassemia (BThal) and sickle cell disease (SCD) has been mostly focused on the primary erythroid defect, thus neglecting the study of hematopoietic stem cells (HSCs) and bone marrow (BM) microenvironment. The quality and engraftment of HSCs depend on the BM microenvironment, influencing the outcome of HSC transplantation (HSCT) both in allogeneic and in autologous gene therapy settings. In BThal and SCD, the consequences of severe anemia alter erythropoiesis and cause chronic stress in different organs, including the BM. Here, we discuss the recent findings that highlighted multiple alterations of the BM niche in BThal and SCD. We point out the importance of improving our understanding of HSC biology, the status of the BM niche, and their functional crosstalk in these disorders towards the novel concept of combined therapies by not only targeting the genetic defect, but also key players of the HSC–niche interaction in order to improve the clinical outcomes of transplantation.

**Keywords:**  $\beta$ -thalassemia; sickle cell disease; bone marrow niche; hematopoietic stem cells



**Citation:** Aprile, A.; Sighinolfi, S.; Raggi, L.; Ferrari, G. Targeting the Hematopoietic Stem Cell Niche in  $\beta$ -Thalassemia and Sickle Cell Disease. *Pharmaceuticals* **2022**, *15*, 592. <https://doi.org/10.3390/ph15050592>

Academic Editor:  
Massimiliano Tognolini

Received: 30 March 2022

Accepted: 5 May 2022

Published: 11 May 2022

**Publisher's Note:** MDPI stays neutral with regard to jurisdictional claims in published maps and institutional affiliations.



**Copyright:** © 2022 by the authors. Licensee MDPI, Basel, Switzerland. This article is an open access article distributed under the terms and conditions of the Creative Commons Attribution (CC BY) license (<https://creativecommons.org/licenses/by/4.0/>).

## 1. Introduction

Hemoglobinopathies are inherited disorders affecting hemoglobin (Hb) production, estimated to be the most common monogenic diseases worldwide [1]. They include deletions or point mutations in  $\alpha$ - or  $\beta$ -globin genes encoding for Hb chains, resulting in hemolytic anemia. Mutations can cause abnormalities in the amount of Hb, leading to thalassemia syndromes, such as  $\beta$ -thalassemia (BThal), or in the Hb structure, as in sickle cell disease (SCD). The highest prevalence of both diseases has initially been recorded in the Mediterranean area and Africa; however, because of migrations, they represent a global health problem nowadays. The severe form of BThal requires lifelong transfusions associated with iron chelation therapy [2]. As a major consequence of the disease and treatment, iron overload (IO) occurs in most cases, despite iron chelation, causing chronic organ damage. SCD is characterized by anemia and vaso-occlusive crises (VOCs), which can cause ischemic and oxidative organ damage [3]. Allogeneic hematopoietic stem cell transplantation (HSCT) from healthy donors is the only curative option for both BThal and SCD patients [4–7]. Gene therapy by gene addition or gene editing strategies in autologous hematopoietic stem cells (HSCs) are promising curative alternatives for patients lacking a suitable donor [8–13]. Cases of graft failure have been reported, but causes have not been deeply investigated and can include an impaired HSC function (autologous setting) and/or a defective supporting activity of the bone marrow (BM) niche (autologous and allogeneic settings), worsened by age and disease progression.

HSCs are regulated by signals from the BM microenvironment, termed niche, which tune hematopoiesis. Stromal and hematopoietic BM cells provide support to HSC activity and include mesenchymal stromal cells (MSCs), endothelial cells (ECs), megakary-

ocytes (MKs), and many other hematopoietic cells representing the differentiated progeny of HSCs [14,15]. Niche composition is dynamic and changes in response to perturbed hematopoiesis or regeneration following myeloablation and transplantation [16]. Many studies unraveled its regulation upon stress or in malignancies [17], but little is known about HSC–niche interactions in hematological-inherited disorders.

Over decades, research on hemoglobinopathies has been mostly focused on the primary erythroid defect, leaving the study of the HSC and the BM microenvironment almost completely unexplored. Since the quality and the engraftment of HSCs depend on the BM microenvironment, niche–HSC crosstalk is important for the outcome of allogeneic and especially autologous gene therapy HSCT, where both HSCs and BM niche are under stress.

Accumulating evidence highlights that, despite differences in etiology, in both BThal and SCD, the consequences of severe anemia alter BM erythropoiesis and cause chronic stress in different organs, including in the BM. In this view, recent findings challenged the paradigm of BThal and SCD, as disorders confined to erythropoiesis [18] and highlighted multiple alterations in the BM niche, paving the way towards potential combined therapies targeting not only the genetic defect, but also HSCs and the BM microenvironment, with the idea of “*Protecting the seed, fertilizing the soil*” [19].

In the present review, we summarize the state-of-the-art about HSCs and BM niche defects in BThal and SCD, and we discuss potential therapeutic solutions to ameliorate HSC and BM microenvironments in order to improve the clinical outcome of HSCT. We point out the importance of having a better understanding on HSC biology, the status of the BM niche, and their functional crosstalk towards the novel concept of targeting the BM niche.

## 2. Hemoglobinopathies

Hemoglobinopathies are a group of widespread inherited blood disorders primarily affecting red blood cells (RBCs), caused by mutations in the genes encoding for the chains of Hb. Hb is a tetramer composed of four polypeptide chains, each carrying a heme prosthetic group containing an iron molecule. During development, different combinations of globin chains are assembled. The first Hb switching event occurs with the transition of the site of erythropoiesis from the yolk sac to the fetal liver from the production of embryonic Hb to fetal Hb (HbF,  $\alpha_2\gamma_2$ ). The second switch in humans occurs perinatally with the decline in HbF synthesis, coupled with the increase in the adult form of Hb (HbA,  $\alpha_2\beta_2$ ).  $\alpha$ - and  $\beta$ -chains are tightly regulated to ensure balanced synthesis. Hemoglobinopathies are divided into two main groups: thalassemia syndromes with quantitative defects leading to reduced levels of one type of globin chain, and structural Hb variants, such as SCD, with qualitative defects causing a change in the structure of the Hb molecule. The highest prevalence of both diseases has been recorded in the Mediterranean countries, Middle East, Indian subcontinent, Southeast Asia, and Africa. The distribution of inherited Hb variants in specific regions is attributed to the natural selection of heterozygote carriers for resistance against *Plasmodium falciparum* malaria [20]. Through migration flows, hemoglobinopathies have spread in Northern Europe, North America, and Australia, evolving into a global health issue.

### 2.1. Thalassemia

Thalassemias are autosomal recessive diseases in which mutations occur in either  $\alpha$ - or  $\beta$ -globin genes, resulting in phenotypes with different severities of anemia due to the imbalanced production of globin chains of adult HbA [21]. It has been estimated that about 1.5% of the world population is a carrier of thalassemic mutations and more than 60,000 symptomatic individuals are born every year [22].

$\alpha$ -thalassemia is characterized by the deficient synthesis of  $\alpha$ -globin chains caused by deletions within the  $\alpha$ -globin gene cluster on human chromosome 16 [23].

BThal is caused by mutations in the  $\beta$ -globin gene on human chromosome 11, leading to reduced ( $\beta^+$ ) or absent ( $\beta^0$ ) synthesis of  $\beta$ -globin chains [24]. Based on the severity

of the clinical phenotype, patients with BThal have been traditionally classified as major ( $\beta^0\beta^0$  or  $\beta^0\beta^+$ ), intermedia ( $\beta+\beta+$ ), or minor (heterozygote carrier) [25]. However, more recently, BThal patients have been divided based on transfusion therapy requirements into transfusion-dependent thalassemia (TDT) or non-transfusion-dependent thalassemia (NTDT). TDT patients are not capable of producing sufficient Hb and undergo lifelong transfusion treatments for survival, while NTDT ones can still require transfusions occasionally and not for their entire lifetime [2].

More than 300 BThal alleles have been identified, most of which result in a single-nucleotide substitution in the  $\beta$ -globin gene or flanking regions, as well as small deletions or insertions within the gene or upstream regulatory elements may occur [25]. At the molecular level, BThal mutations lead to an imbalance of  $\alpha/\beta$ -globin chains, and an accumulation of the free  $\alpha$ -globins which form toxic aggregates. Free Hb and heme catalyze the formation of reactive oxygen species (ROS), leading to oxidative damage and hemolysis of circulating RBCs, as well as premature apoptosis of erythroid precursors in the BM. BThal disease manifestations result in chronic severe anemia which stimulates the production of erythropoietin (EPO) with a consequent intensive but ineffective expansion of the BM erythroid compartment, leading to ineffective erythropoiesis (IE), altered BM homeostasis, and stress signals [21]. In addition, erythroid activity increases in extramedullary hematopoietic sites, causing splenomegaly and hepatomegaly.

In BThal multi-organ complications secondary to the primary genetic defects occur, such as endocrinopathies, including hypogonadism, hypothyroidism, and hypoparathyroidism, as well as impaired bone metabolism. Indeed, bone disease, such as osteopenia and osteoporosis, is a common complication of BThal patients [26,27]. Osteoporosis is characterized by a significant decrease in bone mineral density (BMD), associated with a high prevalence of fractures. The causes of bone loss are controversial [28] and a possible molecular mechanism foresees the decrease in the osteoprotegerin (OPG)/receptor activator of nuclear factor kappa- $\beta$  ligand (RANKL) ratio, resulting in increased expression of RANKL by stromal cells or osteoblasts (OBs), which contributes to enhanced bone resorption by osteoclasts (OCs) [29]. However, the pathophysiology of bone loss is still under investigation in BThal patients since bone disease retains high morbidity despite therapies.

Finally, IE results in increased iron absorption and primary IO mediated by the decrease in hepatic hormone hepcidin levels. Moreover, transfusional iron intake saturates transferrin receptor capacity, leading to secondary IO, causing damage especially in the liver, heart, and endocrine organs [2]. Despite the improvement in iron chelation therapies, IO remains one of the most relevant clinical complications in BThal patients.

## 2.2. Sickle Cell Disease

SCD is an autosomal recessive inherited blood disorder that affects millions of people worldwide [1].

SCD is caused by a single-nucleotide mutation of the  $\beta$ -globin gene, resulting in the production of hemoglobin S (HbS), which induces RBCs to become rigid, sticky, and misshapen. HbS consists of an A to T transversion, leading to a substitution of a valine for glutamic acid at position 6 in the  $\beta$ -globin chain [30]. The most common type of SCD is the severe form, in which people inherit two sickle cell genes. Other forms of SCD include compound heterozygous conditions, such as HbC with HbS (HbSC) and HbS with BThal (HbS/ $\beta^0$ -thalassemia or HbS/ $\beta^+$ -thalassemia) [3].

HbS has a lower oxygen affinity compared to HbA and this condition increases HbS polymerization, promoting the formation of sickle-shaped RBCs (SS-RBCs) [31]. HbS polymerization induces cellular rigidity and changes the shape and physical properties of RBCs, impairing their rheology and survival [32]. Abnormal SS-RBCs cause hemolytic anemia, cell adhesion, vasoconstriction, and vaso-occlusion in small vessels.

Clinically, the major symptom of SCD is a pain crisis due to the vaso-occlusion of tiny blood vessels to the chest, abdomen and joints, resulting in VOCs. Several factors trigger VOCs, including the endothelium which becomes activated by SS-RBCs, recruitment

of adherent leukocytes, activation of neutrophils, interactions of RBCs with adherent neutrophils, and ischemia due to the obstruction, thus creating a feedback loop of worsening endothelial activation. Moreover, the damaged SS-RBCs and activated ECs can produce a proinflammatory environment that is exacerbated during episodes of crisis. They may lead to the production of ROS by the ECs and oxidant-dependent activation of the transcription factor NF- $\kappa$ B, causing inflammatory vasculopathy and vasospasm [33].

Skeletal abnormalities are often associated with SCD [34]. Sickle bone shows reduced BMD, widening of the marrow cavity, and thinning of the cortical bone due to erythroid hyperplasia associated with the disease. More than half of SCD patients have low BMD, closely resembling the features of osteoporotic bone and nearly 30% of adult patients reported multiple fractures due to low impact trauma. Due to vulnerability to infections, osteomyelitis occurs frequently in SCD patients and is caused by several types of germs that enter the bone, leading to osteonecrosis, impaired growth in children, and septic arthritis.

### 2.3. Therapeutic Options for Hemoglobinopathies

Chronic management for BThal and SCD includes blood transfusion, administration of hydroxyurea, and iron chelation therapy. A better understanding of the pathogenesis and improved treatments for hemoglobinopathies have dramatically ameliorated the life expectancy of patients.

The mainstay treatment for severe BThal patients is the association of regular blood transfusion and iron chelation therapies. Starting in the first few years of life, they suppress IE, thus limiting downstream pathophysiological complications, such as heart disease, bone and endocrine abnormalities, and increasing overall survival of TDT. Iron chelation can reduce systemic and hepatic iron burden, both in TDT and in NTDT, decreasing the risk of complications related to IO. However, these therapies are often ineffective due to repeated transfusions and inadequate patient compliance.

SCD patients need single acute transfusions by replacing SS-RBCs for immediate benefit, while chronic transfusions help in preventing long-term complications. Regularly transfused SCD patients require iron chelation treatments too. Hydroxyurea is a myelosuppressive agent which is used to prevent painful episodes in SCD. Current evidence suggests that it acts by inducing HbF, which in turn inhibits intracellular HbS polymerization [35].

The only definitive curative option for both BThal and SCD patients is represented by the replacement of diseased RBCs with those differentiating from transplanted normal HSCs [4,6,7,36]. Allogeneic HSCT from normal donors is available to less than 20% of patients and it is limited by the difficulty of finding suitably matched donors and the risk of graft rejection [5]. High mortality in patients who underwent transplants was observed with increased patient age; thus, current recommendations offer allogeneic HSCT to patients younger than 14 years old who have a suitable HLA-matched donor.

Over the last few decades, promising therapeutic approaches have been developed to achieve definitive correction of the erythroid defect by ex vivo gene therapy through both gene addition and gene editing strategies [37]. Gene therapy approach consists of autologous transplantation of genetically modified hematopoietic stem and progenitor cells (HSPCs) using lentiviral vectors expressing a globin gene ( $\beta$ -globin or fetal  $\gamma$ -globin) under the control of globin transcriptional regulatory elements. Recent gene therapy clinical trials for BThal and SCD have shown promising results. LentiGlobin<sup>TM</sup> BB305 medicinal product (commercial name Zyntheqlo) consists of autologous CD34<sup>+</sup> HSPCs transduced with BB305 lentiviral vector that encodes for anti-sickling hemoglobin (HbA<sup>T87Q</sup>) and showed safety and efficacy in severe SCD and TDT patients with a reduction in transfusion requirements up to transfusion independence in the vast majority of patients [9,11,12,38]. Furthermore, in the TIGET-BTHAL clinical trial, the primary endpoints of safety and efficacy were achieved. Decreased transfusion requirement in adult and pediatric TDT patients and complete independence from transfusions in three of four evaluated children were obtained by intrabone administration of autologous HSPCs transduced by the GLOBE lentiviral vector [10]. A different approach employed a lentiviral vector expressing a small



hairpin RNA targeting the  $\gamma$ -globin repressor BCL11A to increase HbF concentration with an anti-sickling effect. It was used in patients with severe SCD and showed promising initial results [39]. Regarding gene editing strategies, they are based on the direct correction of genetic mutation or disruption of specific DNA sequences in the genome using nucleases. Ongoing clinical trials in TDT and SCD patients are testing the safety and efficacy of HSPCs edited with CRISPR-Cas9 (CTX001 drug product) [13] or with ZFNs (ST-400 drug product). In both cases, targeted nuclease disruption of the repressor BCL11A gene led to  $\gamma$ -globin reactivation with HbF synthesis. Extended follow-up will define the long-term effects of gene therapy approaches.

Recently, other experimental therapeutic approaches are under investigation. A novel strategy aimed to ameliorate IE consists in Luspatercept administration, although the exact mechanism of action is not fully understood. Luspatercept binds to transforming growth factor (TGF)  $\beta$  superfamily ligands, enhances late-stage erythropoiesis by blocking SMAD2/3 signaling, and reduces RBC transfusion requirements in TDT with a proportion of patients achieving transfusion independence [40]. Mini-hepcidins (i.e., short peptides that mimic the activity of endogenous hepcidin) [41] and TMPRSS6 inhibitors [42] showed significant improvements in IE, anemia, and IO in mouse models. Moreover, phase I clinical studies of Vamifeport, the first oral ferroportin inhibitor, showed efficacy in reducing cellular iron efflux and in ameliorating IE [43].

Overall, HSCT remains the only definitive cure for hemoglobinopathies. Despite decades of allogeneic HSCT experience and promising results following gene therapy clinical trials for BThal and SCD, cases of graft failure have been reported. The causes need further investigation, but it can include a negative role of stressed BM microenvironment worsened by age and disease progression [10,37]. In gene therapy, the clinical outcome depends on different factors, such as the source of HSCs, the efficiency of transduction, and the status of the BM microenvironment [44]. Furthermore, a recent halt in SCD gene therapy trials, due to the development of myeloid neoplasms [45], raises the need for a better characterization of the BM microenvironment in genetic Hb disorders. Studies on the BM milieu in BThal and SCD suggest that the BM niche could have an impact on HSC function, thus potentially affecting the HSCT clinical outcome.

### 3. HSC and the BM Niche

The adult hematopoietic system is maintained by HSCs, which are able to self-renew and give rise to progenitor cells that proliferate and differentiate into all the mature blood cells. HSCs are essential to replenish the hematopoietic system after transplantation and upon exposure to stressors, such as oxidative stress and inflammatory signals [17].

HSCs reside in a specialized microenvironment within the BM, termed niche. At a steady state, HSCs are maintained quiescent to avoid the exhaustion of the stem cell pool, but they can rapidly exit from dormancy in response to stress conditions. HSC behaviour is governed by the complex interactions with different cellular components of the BM niche, soluble factors, and physical cues [15]. High-resolution imaging studies in mice revealed that HSC niche include endosteal niches, near the bone surface, and vascular niches, which can be further divided based on the proximity to arterioles or sinusoids.

#### 3.1. HSC Regulation by the BM Niche

Over the last two decades, the regulation of the BM niche at steady state has been extensively studied thanks to technical advances in mouse genetics and imaging technologies [46]. BM populations are intimately connected with each other; alterations of specific niche cells or depletions of specific factors could negatively impact other niche components, thus affecting HSC function. Several non-hematopoietic and hematopoietic cell types have been pointed out.

**Stromal BM cells.** BM stromal components, such as osteolineage cells, MSCs, and ECs, provide physical support and control HSC homeostasis.

Osteolineage cells, lining the endosteum, were the first population to be associated with HSC regulation [47,48]. OBs are activated by the parathyroid hormone (PTH), and PTH-stimulated OBs are increased in number and produce high levels of the Notch ligand Jagged-1 (JAG1), which in turn supports HSC expansion [49].

Osteolineage cells produce many cytokines, including osteopontin (OPN), C-X-C motif chemokine ligand 12 (CXCL12) (also known as stromal derived factor 1 (SDF1)), stem cell factor (SCF), thrombopoietin (TPO), and angiopoietin1 (ANGPT1). OB-derived OPN was reported to control HSC homing and engraftment, as well as suppress the proliferation of HSCs [50]. However, recent evidence suggests that osteolineage cells do not directly regulate HSCs, since other populations are the main functional sources of CXCL12, SCF, TPO, and ANGPT1 [51–54]. Although these studies raised doubts about the essential role of OBs for HSC maintenance, recent *in vivo* live imaging suggests that HSC localization and function are tightly dependent on bone turnover [55].

MSCs are a rare population in the BM located around the blood vessels, which can self-renew and differentiate into bone, fat, and cartilage. CD146 marks human MSCs that generate colony-forming unit fibroblasts (CFU-Fs) *in vitro* and heterotopic ossicles *in vivo* [56,57]. In mice, different MSC populations were identified using transgenic models, including Nestin<sup>+</sup> perivascular cells, CXCL12-abundant reticular (CAR) cells, leptin receptor (LEPR)<sup>+</sup> cells, and PDGFR $\alpha$ <sup>+</sup> Sca1<sup>+</sup> (P $\alpha$ S) cells [51,58–60]. However, it is now widely recognised that there is overlap among them. MSCs modulate HSC activity by direct interaction or through the secretion of soluble factors. Among these, N-cadherin mediates the adhesion of human CD34<sup>+</sup> HSPCs to MSCs, preserving their repopulating ability in a co-culture assay [61]. Of note, N-cadherin<sup>+</sup> stromal progenitors preserve HSCs upon chemotherapy insult [62]. MSCs mainly control HSCs through the release of SCF and CXCL12 along with other regulatory factors, such as ANGPT1, OPN, and interleukin 7 (IL-7). Moreover, MSCs protect HSCs from stress signals, such as oxidative stress and inflammation. High ROS levels affect HSC quiescence and function, and MSCs act as ROS scavengers, preventing myeloablation-induced oxidative damage in HSCs [63].

Adipocytes that arise from MSCs are negative regulators of HSC maintenance. The number of BM adipocytes inversely correlates with HSC content, and adipogenesis inhibition accelerates HSC engraftment after transplantation or chemotherapy [64]. By contrast, adipocyte progenitors were found to sustain HSC regeneration upon chemotherapy by secreting SCF [65]. Further investigation is required to clarify their regulatory activity.

BM ECs, lining the surface of blood vessels, control vascular integrity, which in turn affects HSC trafficking and function. Two different EC types can be distinguished based on their localization and the differential expression of surface markers, *i.e.*, arteriolar and sinusoidal ECs. The permeability of blood vessels regulates ROS levels in adjacent HSCs and niche populations, and less permeable arterioles maintain HSCs in a quiescent state with low ROS levels, whereas leaky sinusoids increase ROS levels in HSCs, thus leading to their activation and mobilization into the circulation [66]. ECs provide soluble factors that promote HSC self-renewal and hematopoietic regeneration after injury [67,68]. A loss of endothelial CXCL12 or SCF causes HSC depletion [51,69].

The sympathetic nervous system, which innervates both the bone and the BM, also regulates HSC function. Nerve fibers form a network with perivascular stromal cells, controlling HSC mobilization into the bloodstream and stimulating the hematopoietic recovery after genotoxic stress [70,71]. Non-myelinating Schwann cells that wrap sympathetic nerves contribute to HSC quiescence through activation of TGF $\beta$  and SMAD signaling [72].

**Hematopoietic BM cells.** Moreover, terminally differentiated cells, including MKs, macrophages (M $\phi$ s), neutrophils, and regulatory T cells (Tregs), play a key role in the BM niche.

Initial studies showed that HSCs are located close to MKs in the BM in a non-random fashion, and MK depletion increases the size of the HSC pool [73]. At a steady state, MKs directly maintain HSC quiescence by secreting specific factors, such as CXCL4 and TGF $\beta$  [73,74]. However, under chemotherapeutic stress conditions, MKs promote HSC ex-

pansion through fibroblast growth factor 1 (FGF1) signalling [74]. In addition, MKs regulate HSC function indirectly through the interaction with bone cells [75,76]. Furthermore, after myeloablative irradiation, MKs support OB survival by promoting HSC engraftment [77].

M $\phi$ s are a heterogeneous population with phagocytic activity present in various tissues. In response to different environmental signals, they can polarize to M1 (classically activated or pro-inflammatory) or M2 (alternatively activated or anti-inflammatory) phenotypes, protecting from infections and promoting tissue repair and regeneration, respectively. BM M $\phi$ s directly regulate HSC quiescence and self-renewal [78–80]. M2 M $\phi$ s induce HSC self-renewal, whereas M1 M $\phi$ s exert an opposite role in preserving HSC repopulating potential [81]. In addition, BM M $\phi$ s indirectly control HSC location by inducing the expression of HSC retention factors by MSCs, thus regulating the egress of HSCs into the circulation through neutrophil clearance [82].

Neutrophils control HSC retention by acting on osteolineage cells [83] and play a key role in the regeneration of the BM niche after transplantation [84]. Whether neutrophils can directly regulate HSC function remains poorly understood.

Tregs modulate HSCs by cytokine secretion and host immune regulation [85,86].

### 3.2. HSC Regulation by Stress Signals

Hematopoiesis can be challenged by different sources of stress, such as oxidative stress, variations in the partial pressure of oxygen, iron levels, and inflammatory signals. Quiescent HSCs reside in a hypoxic BM niche that promotes glycolytic metabolism over oxidative phosphorylation and protects HSCs from oxidative stress. Stress signals alter HSC function by impairing their self-renewal and regeneration capacity [16].

Oxidative stress is the result of intracellular ROS accumulation which causes oxidative damage of lipids, DNA, and proteins in stem cells [87]. ROS tightly regulates HSC function through direct modulation of redox-sensitive transcription factors [88] and HSCs maintain a low basal level of ROS, which preserves stem cell quiescence. In contrast, a physiological increase in ROS leads to cell proliferation and differentiation [89]. Moreover, the impairment of antioxidant defense mechanisms reduces HSC quiescence and repopulating ability [90].

Iron is an essential element required for many cellular functions; however, when in excess, it can cause uncontrolled production of ROS through the Fenton reaction. Moreover, heme, an iron-containing porphyrin, constitutes 95% of the total iron in humans and its degradation mediated by heme oxygenase 1 releases iron with further ROS production [91]. HSCs can uptake and store iron, and fluctuation of iron levels can regulate HSC function. Initial studies in an iron-overloaded mouse model revealed a ROS-mediated reduction in HSPC number and repopulating ability [92]. Moreover, intracellular IO in HSCs promotes oxidative stress, leading to their dysfunction and exhaustion [93]. Vice versa, treatments with iron chelators in vivo and in vitro restore HSPC quiescence and self-renewal [94]. Additionally, iron deficiency seems to negatively affect HSC function [95]. However, it remains to be explored how intracellular iron levels affect the metabolic and transcriptional programs underlying HSC function and fate.

Recent advances have highlighted the critical role of inflammation as a source of stress, affecting HSC fate. The expression of Toll-like receptors (TLRs) on HSC surfaces allows them to directly sense pathogen-derived products. HSCs proliferate, lose self-renewal capacity, and rapidly differentiate in response to many inflammatory signals, such as interferons (IFNs), tumor necrosis factors (TNFs), IL-1, granulocyte-colony stimulating factor (G-CSF), and damage-associated molecular patterns (DAMPs), in order to replenish myeloid cells [96]. However, chronic exposure to inflammatory cytokines can injure HSCs [97], and repeated activation of HSCs in response to inflammatory stimuli can cause DNA damage mediated by high ROS levels [98]. Furthermore, infections trigger hematopoiesis by acting on HSC cycling properties and long-term function [99] or on BM niche populations, such as ECs, MSCs, osteolineage, and immune cells [100–102].

Thus, given the complexity and heterogeneity of the BM niche, it is conceivable that stress signals exert their effect on HSCs, both directly and indirectly, by acting on niche populations.

### 3.3. The HSC Niche in Aging and Disease

Recently, the effects of stressed, aged, and malignant hematopoiesis on HSCs, as well as the BM microenvironment, have gained increasing attention [17].

During physiological aging, HSC function declines with alterations in immune responses, contributing to higher susceptibility to infections, autoimmunity, anemia, and myeloproliferative diseases. The absolute numbers of HSCs increase in aged mice, but their regenerative potential is reduced with myeloid-biased differentiation and enhanced mobilization into the circulation [103]. Aged HSCs localize far from the endosteum and close to sinusoidal ECs [104], suggesting that altered HSC distribution is a hallmark of aging. Aging leads to remodeling of the BM niche with a loss of innervation of BM arterioles [105], and also skews MSCs differentiation with reduced bone formation and increased adipogenesis.

The BM niches have been recognized as playing a key role in the pathogenesis and chemoresistance of hematological malignancies [106]. On the one hand, BM niche populations can facilitate the survival and the expansion of mutant hematopoietic cells, contributing to malignancy progression and providing protection of malignant cells from chemotherapy. On the other hand, malignant hematopoiesis can remodel the HSC niche [107–109].

Conversely, the composition and properties of the BM niche in non-malignant hematopoietic disorders affecting the differentiated progeny of HSCs is still under investigated. Few reports highlighted BM defects in severe combined immunodeficiencies (SCID), such as adenosine deaminase-SCID (ADA-SCID) with myeloid dysplasia, marrow hypocellularity, and a reduced frequency of HSCs [110,111]. In patients affected by chronic granulomatous disease (CGD), hematopoiesis was shown to be dysregulated, and a reduced proportion of HSCs was reported as a direct consequence of the inflammatory state associated with the disease [112]. In addition, HSPCs from patients affected by Wiskott–Aldrich syndrome displayed altered cytoskeleton function, impaired migratory, and homing capacity [113].

Thus, a better characterization of the features of the BM microenvironment and HSCs in hematological-inherited disorders, including BThal and SCD, is fundamental to assess potential defects and to improve therapeutic approaches based on allogeneic HSCT and autologous gene therapy [44].

## 4. The HSC Niche in BThal and SCD

The HSC BM niche is still poorly investigated in hemoglobinopathies. The status of HSCs and BM niche, indeed, should be considered in the context of allogeneic HSCT to ensure a sustained engraftment of donor cells and especially in recent autologous gene therapy settings, to develop optimized protocols for increasing the efficacy and safety of ex-vivo genetic manipulation [44]. The reduced number of HSCs available for collection and the impaired engraftment potential of HSCs in BThal and SCD mouse models [114,115] highlighted the need for a better characterization of the primitive HSC compartment and BM niche features to develop targeting strategies for improving the outcome of allogeneic and autologous HSCT.

To study HSC niche in BThal and SCD, mouse strains recapitulating the main features of the human diseases were exploited [116]. An investigation of BThal HSCs and BM niche was performed in the Hbb<sup>th3/+</sup> (th3) murine model. th3 mice lack both the adult  $\beta^{\text{maj}}$ - and  $\beta^{\text{min}}$ -globin genes [117]. Although homozygous knockout mice are not viable, heterozygotes survive with features of severe BThal intermedia, including reduced RBC and Hb concentrations, microcytosis, reduced hematocrit and elevated reticulocytes, IE, splenomegaly, bone malformation, and IO in multiple tissues. The studied mouse models for SCD include the transgenic SAD, Berkley, and Townes strains [116]. They were generated by co-expression of the human  $\alpha 2$ -globin gene and a modified  $\beta S$ -globin gene, both linked to the  $\beta$ -globin locus regulatory region. The SAD mouse incorporates the  $\beta S$

variant with additional mutations known to enhance the severity of the sickle phenotype into a BThal background [118], whereas the Berkley and Townes transgenic strains carry the genes for human  $\alpha$ - and  $\beta$ S-globin on a genetic background deficient for the murine  $\beta$ -globin genes and incorporate a YAC containing one or both  $\gamma$ -globin gene sequences to avert the gestational lethality [119,120]. These models reproduce in vivo sickling of RBCs, hypoxia, and severe anemia with reduced hematocrit and increased reticulocytes, systemic microvascular occlusions, hemolytic and renal complications, splenomegaly, and IE of human SCD. Patient-derived samples were studied for the immunophenotypic characterization of HSCs and BM microenvironment to validate findings obtained in mice and to model in vitro the discovered alterations.

Here, we review the state of the art about the alterations of HSCs and BM niche populations in BThal and SCD.

#### 4.1. HSCs

**BThal.** A recent study by Aprile et al. has provided the first demonstration of impaired HSC function caused by an altered BM niche in BThal [114]. The authors demonstrated that th3 mice have a decreased number of HSCs, as compared to wild-type (wt) controls. Cell cycle analysis revealed a loss of quiescence with a lower frequency of HSCs in the G0 phase and an increased cycling rate with a higher fraction of cells accumulated in the S phase. These data were corroborated by RNA-seq experiments performed on sorted th3 HSCs, revealing a positive enrichment of cell-cycle-associated categories, a upregulation of genes involved in DNA damage, cellular responses to stress, and a downregulation of stemness genes (including *Cdkn1c*, *Runx1l1*, *Fgd5*, and *Hes1*), thus highlighting the increased replication stress and impaired self-renewal ability of HSCs in BThal. To evaluate the functional activity of BThal HSCs, they performed long-term in vivo transplant experiments and they observed a competitive disadvantage of th3 HSCs compared to wt ones when transplanted into th3 mice. Notably, transplantation into wt recipients rescued the long-term repopulating capacity of th3 HSCs, suggesting that the wt BM microenvironment had a corrective role in restoring HSC functions. Secondary transplants into wt animals showed that th3 HSCs recovered their reconstitution capacity with complete normalization of the quiescent state. On the contrary, th3 HSCs in BThal recipients underwent exhaustion over time. These results suggested that impaired HSC self-renewal and quiescence in BThal are not intrinsic defects, but their behavior is affected by prolonged residence in an altered BM microenvironment, which is progressively worsened by the disease.

In line with these findings, patients affected by TDT showed reduced quiescence of CD34<sup>+</sup>CD38<sup>-</sup> primitive HSPCs [114]. Moreover, the gene expression profile of patients' CD34<sup>+</sup> cells revealed an upregulation of genes associated with stress stimuli and DNA damage, thus indicating an impairment of HSPCs also in the human disease. Consistently, Hua and colleagues published a reduced frequency of Lin<sup>-</sup> CD10<sup>-</sup> CD34<sup>+</sup> CD38<sup>-</sup> CD45RA<sup>-</sup> CD90<sup>+</sup> HSCs in the CD34<sup>+</sup> cell compartment of BThal pediatric patients [121]. Moreover, and most importantly, RNA-seq analysis of BThal patients' HSCs showed increased proliferation and reduced stemness [122].

Overall, this evidence highlighted the importance of the BM microenvironment in preserving HSC fitness in the BThal context.

**SCD.** Studies in the murine models of SCD revealed defects in SCD hematopoiesis and HSCs. In SCD, the BM environment is highly enriched for ROS, mainly generated by SS-RBCs and the activated endothelium. By examining the effects of oxidative stress on SCD HSCs, Javazon et al. showed that SCD BM has a decreased colony forming unit potential and a reduced number of Lineage<sup>-</sup> Sca1<sup>+</sup> cKit<sup>+</sup> (LSK) HSPCs [123]. Cell cycle analyses revealed that fewer LSK cells were in the G0 phase, and a significant increase in lipid peroxidation and ROS in SCD LSKs was detected. HSPCs from SCD mice showed an impaired engraftment potential, which is partially restored by n-acetyl cysteine (NAC) antioxidant treatment of LSK cells before transplantation, thus suggesting that an altered redox environment in SCD affects HSC function.

The results of reduced clonogenic potential of SCD HSPCs are paralleled by the increased mobilization of multipotent cells in both mice and humans affected by SCD. A hematopoietic compensatory mechanism was described in SCD, consisting in the mobilization of progenitor cells from the BM to the peripheral blood and their subsequent uptake into the splenic extramedullary hematopoietic site in response to the erythropoietic stress [124]. The spleen of SCD mice indeed contains significantly increased numbers of cycling erythroid colony-forming cells, indicating the strong proliferative pressure on the erythroid lineage.

Alterations in SCD HSCs were reported by Tang et al., who showed a decrease in HSC frequency, increased DNA damage, and an accumulation of ROS in HSCs from SCD mice, associated with the reduced hematopoietic supportive ability of MSCs [115].

Recently, Hua et al. showed a lower proportion of  $\text{Lin}^- \text{CD10}^- \text{CD34}^+ \text{CD38}^{\text{low}} \text{CD45RA}^- \text{CD90}^+$  HSCs in the  $\text{CD34}^+$  cell compartment of SCD pediatric patients, along with an increased frequency of  $\text{CD34}^+ \text{CD10}^+$  lymphoid progenitor cells [121], suggesting hematopoietic defects also in the human disease. Moreover, the characterization of circulating hematopoietic populations from adult and pediatric SCD patients confirmed an increase in  $\text{CD34}^{\text{bright}}$  HSPCs and the mobilization of primitive HSCs in the peripheral blood as compared to healthy controls [125].

#### 4.2. The Stromal Niche

**BThal.** To explain the defects in the transplantation outcome of th3 HSCs into a BThal BM niche, Aprile et al. focused their attention on the interactions between HSCs and stromal cells, such as osteolineage cells and MSCs in the BM of BThal mice [114]. Bone disease is a common and severe complication of BThal, resulting from hormonal deficiency, BM expansion, and iron toxicity. Consistent with the common finding of osteoporosis and hypoparathyroidism in BThal patients [27], data in th3 mice confirmed a reduced BMD [126] caused by decreased OB activity and low levels of circulating PTH [114]. Moreover, the authors showed reduced levels of key niche molecules, such as OPN and JAG1 in the BM of th3 mice. Interestingly, these molecules are directly regulated by PTH in OBs and MSCs [49], and their reduction leads to a loss of HSCs quiescence [50]. PTH is a key player of calcium and phosphate homeostasis, regulating bone remodeling and HSC maintenance via its specific receptor on BM stromal cells [49]. Aprile and colleagues demonstrated that the downregulation of PTH- JAG1-Notch1 axis and OPN in BThal leads to defective stromal BM niche with impaired bone deposition and defective crosstalk between osteolineage cells and HSCs [114]. These findings were also validated in patients' samples.

Since MSCs also produce JAG1, the authors analyzed this population in th3 mice. MSCs are characterized by decreased frequency and lower expression of Jag1 as compared to wt controls [114]. Consistently, MSCs from BThal patients showed reduced frequency and clonogenic potential, lower proliferation rate, impaired differentiation potential, and a reduced capacity to support HSPCs [127].

**SCD.** Individuals suffering from SCD experience acute and chronic bone pain caused by occlusive events within the tissue vasculature that result in ischemia, necrosis, and organ degeneration [34]. However, the pathophysiology of bone defects is still under investigated. Recent studies have suggested that environmental stimuli, such as inflammation, may influence the osteoporotic-like phenotype observed in SCD bone [128,129]. Because of the interactions between SS-RBCs and vascular endothelium, SCD patients display abnormally high concentrations of inflammatory molecules, especially IL-6, IL-8, and TNF- $\alpha$ . In healthy conditions, inflammation plays a crucial role in regulating bone remodeling; however, the chronic inflammation localized within the bone microcirculation may prolong OC activity via the upregulation of RANKL [130,131]. Micro-CT image analysis of transgenic SCD mice showed altered bone microarchitecture with fewer trabeculae and deteriorated structure, indicating progressive damage of SCD bone tissue [132]. Dalle Carbonare et al. reported that recurrent hypoxia/reperfusion events, mimicking acute VOCs, activate osteoclastogenesis and bone turnover in SCD mice, with upregulation of the pro-resorptive

cytokine IL-6 and suppression of osteogenic lineage markers, such as *Runx2* and *Sparc* [133]. The administration of zoledronic acid, a potent inhibitor of osteoclastogenesis and OC activity, ameliorated bone impairment and promoted osteogenic lineage. These data supported the view that bone disease in SCD is related to the biased coordination of remodeling signals towards bone absorption. In addition, the reduced OB recruitment and the increased OC activity are induced by local hypoxia, oxidative stress, and the release of IL-6. Furthermore, IO due to chronic transfusions was reported to increase bone resorption and impair the trabecular microarchitecture in SCD [134].

Human MSCs derived from SCD BM were found to have altered expression of SCF and CXCL12, but showed normal in vitro functionality [135]. However, recent work by Tang et al. reported a reduced frequency of MSCs in the BM of SCD mice, ROS accumulation, and a decreased adipogenic and osteogenic differentiation potential, also suggesting impaired MSC functional properties [115]. Gene expression profiling revealed a decreased transcription of key niche molecules, such as *Opn*, as well as vascular cell adhesion to protein 1 (*Vcam1*), *Angpt1*, *Scf*, and *Cxcl12*, associated with an impaired ability to maintain HSCs in vitro and in vivo. These data are in line with increased HSC mobilization and reduced engraftment upon transplantation. Treatment with NAC and transfusions reduced MSC oxidative stress and improved the crosstalk between SCD MSCs and HSCs. Activation of TLR4 by hemolysis contributed to SCD MSC dysfunction.

Alterations in the BM vasculature were reported to be critical for SCD hematopoiesis too. Park et al. demonstrated that SCD mice have a disorganized BM vascular network with increased numbers of highly tortuous arterioles and fragmented sinusoidal vessels [136]. In SCD, slow RBC flow and vaso-occlusions diminish local oxygen availability in the BM cavity and increase ROS production. Elevated levels of HIF-1 $\alpha$  were found, triggering an enhanced neovascularization. Transplantation of BM cells from SCD mice into wt recipients recapitulated the SCD vascular phenotype by increasing HIF-1 $\alpha$  signaling in normal mice. Conversely, blood transfusions completely reversed the altered vascular network, highlighting the plasticity of the BM vascular niche.

#### 4.3. Hematopoietic and Soluble Niche Factors

**BThal.** Data on BThal mice indicate that multi-factorial alterations in the BM niche can impair HSC self-renewal and repopulating capacity. During the analysis of stromal components and soluble factors of the BM microenvironment, high systemic and BM local levels of FGF23 were detected [137]. FGF23 is a negative regulator of bone metabolism and PTH secretion [138], mainly produced by bone and erythroid cells in response to the anemia-related factor EPO [139]. The enhanced activation of FGF23 signaling has been proposed as the mechanism underlying bone disease and low PTH levels in th3 mice, negatively impacting the functional crosstalk between HSCs and the stromal niche [137].

In addition to the BM stroma, altered levels of multiple local and systemic factors were found, including SCF, ANGPT1, and CXCL12 [114], as well as a reduction in serum TPO [140]. Since TPO is a key regulator of both HSCs [53,141] and MKs [73,142], the TPO defect can have a dual role on BThal HSCs and BM microenvironments, thus contributing to the impaired HSC–niche crosstalk. Moreover, the condition of chronically reduced TPO stimulation in BThal is consistent with reported results of higher cycling activity of HSCs in the absence of TPO [141], and effectively correlates with data of low HSC quiescence in th3 mice [114]. Low TPO also impacts MK maturation and their downregulated expression of niche molecules in th3 mice [140].

By focusing on other hematopoietic populations of the BM niche, different BM resident M $\phi$ s have been reported to indirectly regulate HSC retention by acting on niche stromal cells [143]. Thus, the dissection of different populations of BM M $\phi$ s in BThal can contribute to the enhanced proliferation, increased mobilization, and reduced repopulating potential of th3 HSCs. Since BThal is characterized by IE with reduced erythroid terminal differentiation and expansion of the BM erythroid precursors, as expected, the frequency of erythroblastic island M $\phi$ s, essential for erythroblast survival and maturation, was significantly increased

(unpublished data). BThal neutrophils were reported to display aberrant maturation and defective effector functions [144]. Reduced BM M $\phi$ –neutrophil interactions can play a role in BThal HSC mobilization, through the indirect effect on the production of CXCL12 retention molecule by the BM stromal niche [82]. Preliminary data from the th3 mouse model showed an imbalanced polarization towards the M1 phenotype and a reduced neutrophil clearance by BThal BM M $\phi$ s, suggesting a potentially negative effect on HSCs (unpublished data).

**SCD.** In the complexity of SCD pathophysiology, many hematopoietic populations and soluble factors potentially involved in the regulation of the BM microenvironment homeostasis are altered [145]. However, their direct contribution to the HSC niche is still completely unexplored.

Among the more studied populations, neutrophils of SCD patients and mice were activated by the increased production of ROS [146]. They contribute to SCD pathogenesis by capturing circulating SS-RBCs, inducing VOCs, and secreting inflammatory cytokines [147]. Free heme induces neutrophil extracellular trap (NET) formation by activated neutrophils, significantly contributing to SCD pathogenesis [148]. In SCD mice, the aged neutrophil population is expanded and positively correlates with adhesion and interactions with RBCs. Neutrophil ageing is regulated by the microbiome [149] and neutrophil clearance by BM was reported to modulate the HSC niche [82]. Thus, the involvement of SCD neutrophils can be hypothesized in the regulation of the BM microenvironment.

Furthermore, platelets and monocytes in SCD were reported to have an activated phenotype with an active role in VOC pathogenesis, promoting the inflammation state associated with the disease [150,151]. SCD indeed have long been recognized as a chronic inflammatory disease, and, during infection or systemic inflammation, HSCs were reported to respond directly to inflammatory triggers [152], leading to their activation, expansion, and enhanced myeloid differentiation [153]. Furthermore, increased circulating heme and iron, i.e., hallmarks of SCD, were shown to induce M $\phi$  phenotypic switching toward an M1 proinflammatory phenotype [154], which has been reported to negatively regulate HSC maintenance [81]. Whether BM cell populations and HSC function are altered in SCD in response to pro-inflammatory stimuli still needs to be explored.

#### 4.4. The Role of IO in the BThal BM Niche

IO, associated with IE and therapeutic blood transfusions, is a key element of BThal pathophysiology. Despite improvements in chelation therapies over the past few years, the BThal BM niche accumulates a high content of iron. The direct impact of IO on BThal HSCs remains poorly characterized [155]. Data on BThal th3 mice showed a positive enrichment of genes involved in iron homeostasis and significantly high levels of free reactive iron in HSCs, which correlate with increased ROS content (unpublished data).

Recently, Crippa et al. demonstrated that IO negatively affects BM MSCs in TDT patients [127]. The in vitro exposure of BThal MSCs to increasing doses of iron revealed an upregulation of iron transporters, such as *ZIP14*, *ZIP18*, transferrin receptor 1 (*TFR1*), and ferritin, thus suggesting that BThal MSCs can uptake and store iron. These findings are corroborated by the direct assessment of iron content in BThal MSCs using Perl's staining. BThal MSCs display high ROS levels, as a result of the impaired antioxidant response, which correlates with a significant pauperization of the most primitive CD146<sup>+</sup> CD271<sup>+</sup> MSC pool. BThal MSCs showed reduced clonogenic capacity, lower proliferation rate, early cell cycle arrest, and impaired differentiation potential into adipocytes and bone. In addition, they express lower levels of hematopoietic supportive factors, such as SCF, CXCL12, cadherin 2 (*CDH2*), VCAM, *ANGPT1*, vascular endothelial growth factor A (*VEGFA*), *IL-6*, and *FGF2*. Therefore, they fail to attract and expand HSCs in transwell migration assays and 2D co-culture experiments. Consistently, the in vivo transplantation of CD34<sup>+</sup> HSPCs, along with BThal MSCs, revealed a reduced hematopoietic engraftment upon xenotransplantation in NSG mice. Finally, the authors developed a humanized ossicle model, consisting of gelatin scaffold pre-seeded with MSCs, ECs, and CD34<sup>+</sup> HSPCs, to



test the ability of BThal MSCs to form a proper BM niche *in vivo*. Transplantation of the humanized ossicle into NSG mice showed a delay in the formation of bone and vessels, as well as a reduced number of human CD45<sup>+</sup> hematopoietic cells ossicles derived from BThal MSCs.

Strikingly, treatment with the iron chelator deferoxamine (DFO) in the presence of iron decreased the expression of iron transporters, potentiated the antioxidant defense system in BThal MSCs, and rescued the expression of the hematopoietic supportive factors [127]. Therefore, treatment with chelating agents or antioxidants can represent a therapeutic strategy to ameliorate BThal MSC supportive capacity, thus potentially improving the transplantation outcome.

Overall, these findings highlight previously unexplored multifactorial alterations of BM components in the biocomplexity of BThal and SCD (Table 1 and Figure 1). Elucidating the overriding players and the functional interconnections between stromal and hematopoietic alterations of the BM HSC niche will pave the way towards potential combined therapies, not only targeting the genetic defect, but also HSC and the BM microenvironment, in order to improve HSC transplantation and gene therapy approaches.

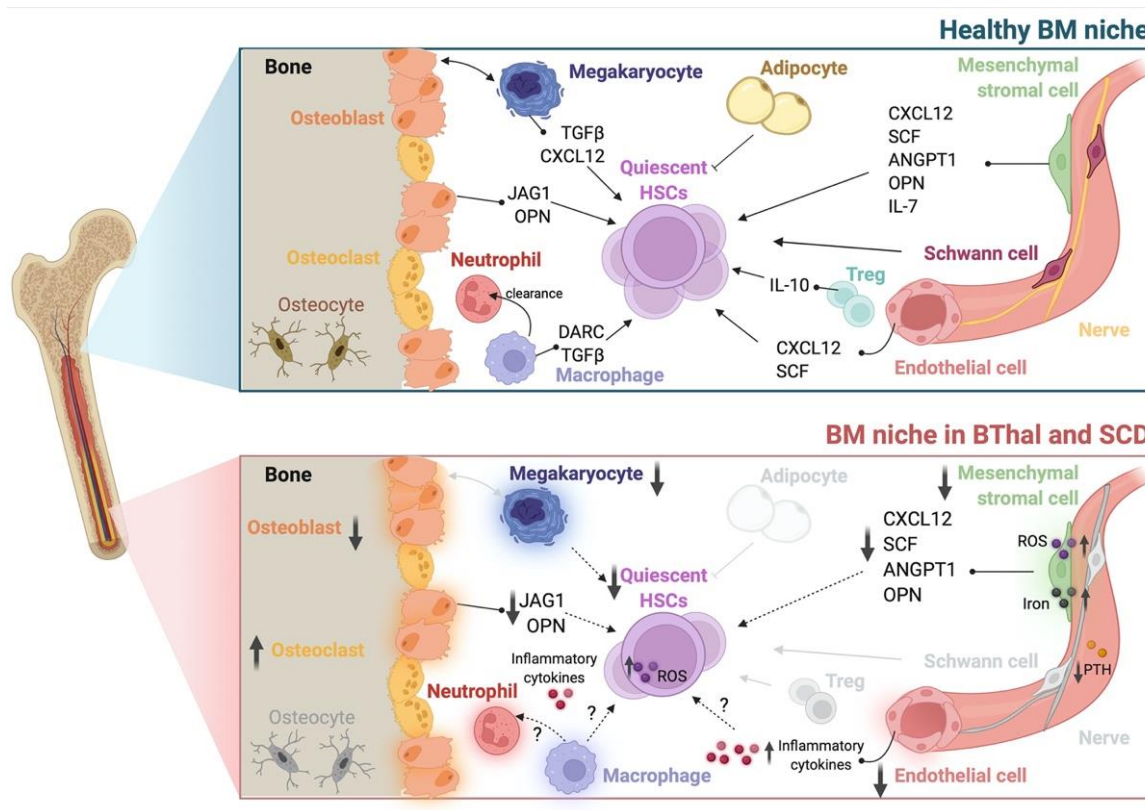


**Figure 1.** The BM HSC niche in healthy conditions and in BThal and SCD. Schematic representation of the adult BM niche in homeostasis, showing different stromal (osteoblasts, mesenchymal stromal cells, endothelial cells, Schwann cells, nerve fibers, and adipocytes) and hematopoietic (megakaryocytes, osteoclasts, macrophages, neutrophils, and Tregs) cell types and niche factors that regulate HSC quiescence and function (**upper panel**). The BM niche in BThal and SCD shows alterations in BM osteolineage cells, mesenchymal stromal cells, endothelial cells, and megakaryocytes, causing the reduced production of niche molecules supporting HSC activity. The accumulation of ROS, iron, and inflammatory cytokines contributes to the impairment of HSC maintenance (**bottom panel**). Created with BioRender.com.

**Table 1.** Altered BM niche populations in BThal and SCD. Alterations are shown as increased (↑) or decreased (↓) levels of specific features in BM niche populations.

Cell Population	Disease	Species	Alterations	References
HSC	BThal	mouse	↓ number ↓ quiescence ↓ stemness ↓ reconstitution capacity ↑ response to stress	[114]
		human	↓ frequency ↓ quiescence ↓ stemness ↑ response to stress (HSPC)	[114,121,122]
	SCD	mouse	↓ frequency ↑ ROS ↑ DNA damage ↓ quiescence (HSPC) ↑ mobilization (HSPC)	[115,123,124]
		human	↓ frequency ↑ mobilization	[121,125]
Osteolineage cell	BThal	mouse	↓ BMD ↓ systemic PTH ↓ OB activity ↓ niche molecules ↑ FGF23	[114,126,137]
		human	↓ niche molecules	[114]
	SCD	mouse	↓ bone microarchitecture ↑ osteoclastogenesis ↓ osteogenic factors	[132] [133]
		mouse	↓ frequency ↓ niche molecules	[114]
MSC	BThal	human	↓ frequency ↓ osteogenic and adipogenic potential ↑ ROS ↑ iron content ↓ niche molecules ↓ HSPC maintenance	[127]
		mouse	↓ frequency ↑ ROS ↓ osteogenic and adipogenic potential ↓ niche molecules ↓ HSC maintenance	[115]
	SCD	human	↓ niche molecules	[135]
		mouse	altered BM vasculature ↑ inflammatory cytokines	[136]
EC	SCD	mouse	altered BM vasculature ↑ inflammatory cytokines	[136]
MK	BThal	mouse	↓ systemic TPO ↓ maturation ↓ niche molecules	[140]
Neutrophil	BThal	mouse	altered maturation	[144]

### 5. Targeting the HSC Niche in BThal and SCD

The correction of genetic defects in BThal and SCD is achieved by HSCT from normal donors or by experimental gene therapy with the transplantation of autologous genetically modified cells. In both settings, the transplanted HSCs and the recipient BM niche are central elements.

In comparison to other indications for allogeneic HSCT, there is an unexplained increased risk of graft failure, including cases of late rejection and mixed chimerism [156,157]. Especially in the autologous gene therapy HSCT, where both the donor HSCs and the recipient BM niche are diseased, the additive effect of an impaired HSC function and a defective supporting activity by the BM niche components, worsened by age and disease progression, can hamper the engraftment of genetically modified HSCs. The clinical benefits of gene therapy are dependent on several factors, including the patient's clinical condition, the extent of genetic modification, the dose and quality of the engineered engrafting cells, and the status of the recipient BM niche [37,44]. It is reasonable to expect a negative effect of the BM microenvironment on HSC function, leading to potentially impaired reconstitution and premature exhaustion. In recent gene therapy trials for hemoglobinopathies, some cases of absence of clinical benefit, despite the occurrence of early hematopoietic engraftment, have been reported [9–11]. Low levels of genetically modified HSPCs in patients with a lack of clinical benefit can lead to impaired HSC function, as well as the defective supporting activity by niche components, although the root causes have not been clarified yet. Variability in terms of HSC transduction and in vivo reconstitution poses limitations for clinical outcome, and the status of the BM microenvironment influences the quality of HSCs harvested for genetic engineering, as well as their engraftment and reconstitution capacity once transplanted. Therefore, the comprehension and targeting of key mechanisms influencing HSC potential offer new avenues to improve gene therapy and develop combined transplantation approaches.

Moreover, myeloablative conditioning is required in order to obtain high levels of donor grafts upon HSCT, also in the autologous gene therapy setting, when reduced intensity conditioning is preferred. The effects of reduction in hematopoietic BM populations and the potential damages to the BM stroma are largely unknown and can have an impact on the supportive capacity of the BM niche. Recent advances in biological conditioning strategies by antibody–drug conjugates showed better preservation in the BM architecture. In this view, more studies are needed to elucidate the influence of conditioning on HSC niche activity.

Here, we reported proof of concept studies aimed to rescue the identified alterations of HSCs and BM niche components in BThal and SCD (Figure 2). Although several works described alterations in SCD BM niche components, functional studies dissecting the defective interactions between HSC and BM microenvironments are missing. Future investigation can provide new therapeutic targets to restore the HSC–niche crosstalk.

### 5.1. Targeting the BM Stromal Niche

The pioneering work by Aprile and colleagues challenged the paradigm of BThal, as a disorder confined to erythropoiesis, demonstrating that HSCs are impaired in BThal due to a defective crosstalk with the BM microenvironment because of secondary complications to the primary genetic defect [114]. Most importantly, these data emphasized the reversibility of HSC features in stressed conditions since the authors showed that the defect can be rescued by the administration of PTH and the correction of the BM stromal niche. Indeed, in vivo PTH treatment to th3 mice normalized BMD, MSC frequency, and the expression of OPN and JAG1 by the BM stromal niche, thus resulting in the restoration of HSC function. In BThal patients, treatment with PTH before HSC harvest for gene therapy can protect HSC function and improve long-term engraftment. Therapeutic targeting of the HSC niche by PTH stimulation has provided evidence of an effective strategy to stimulate the HSC pool and increase its engraftment upon transplantation [158], although subsequent studies using PTH treatment after cord blood transplantation in a heterogenous group of patients reported disappointing results [159]. The balance between the anabolic and catabolic effects of PTH needs careful clinical evaluation. Thus, more tunable molecules targeting the BThal stromal niche alterations should be explored and, in this view, investigation of mechanisms acting upstream the bone and PTH defects could be a promising option.

Encouraging results highlighted the efficacy of the FGF23 inhibition strategy to correct bone mineralization and deposition and rescue the impaired HSC–niche crosstalk in BThal [137].

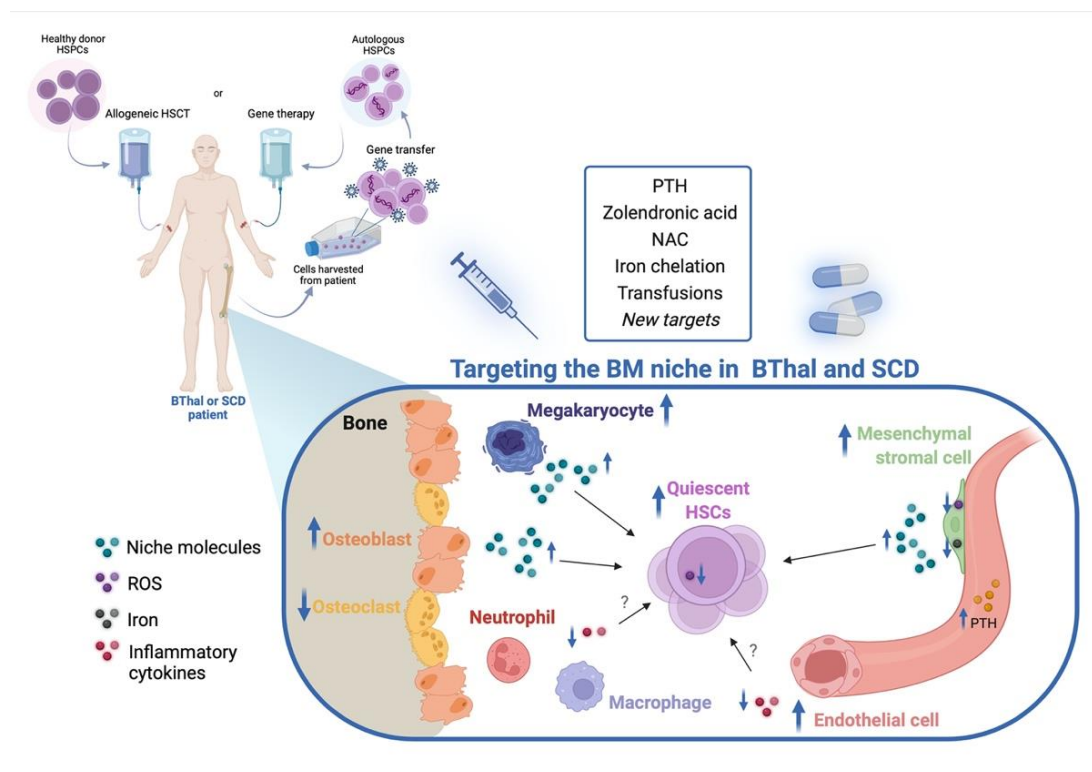


**Figure 2.** Targeting of the BM niche in BThal and SCD. Administration of treatments targeting the altered HSC niche components can be developed in combination with allogeneic or autologous gene therapy HSCT to restore the BM microenvironment. This may ameliorate the quality of patient-derived HSCs that are harvested and manipulated in gene therapy settings and, at the same time, make the BM niche more permissive for the engraftment of donor cells, both in the allogeneic and the autologous HSCT. Created with BioRender.com.

On the same line, approaches to correct secondary defects with a potential impact on the BM niche were exploited in SCD. The administration of zoledronic acid, a bisphosphonate drug acting as an inhibitor of osteoclastogenesis and OC activity, ameliorated bone defects and promoted osteogenic lineage in SCD mice [133]. However, the positive effect on the HSC niche remains unexplored.

Other potential targeting strategies are those which aim to target primary defects, i.e., anemia. Blood transfusions are the mainstay of treatment for BThal and SCD and can also ameliorate secondary complications. Park et al. demonstrated that a 6-week transfusion regimen completely reversed the abnormal SCD BM vasculature by reducing proangiogenic mediators, such as VEGF-A, ANG1, and ANG2, as well as markers of inflammatory vascular activation [71]. Transfusions were demonstrated to also alleviate SCD MSC dysfunction [115]. Upon transfusion, SCD MSCs showed decreased ROS content and enhanced expression of *Scf* and *Cxcl12*, correlating with increased HSC frequency. Similarly, NAC antioxidant treatment improved SCD MSC ability to maintain HSCs [115].

### 5.2. Targeting IO and Other Stress Signals

IO due to hemolysis and IE are common hallmarks of BThal and SCD, although damage caused by IO to the BM microenvironment is largely unknown.

IO in BThal BM was reported to have a negative impact on patient-derived MSCs, reducing their frequency, differentiation ability, and hematopoietic supportive capacity [127]. Thus, targeting the BM niche to reduce iron-induced oxidative stress can ameliorate HSCT

outcomes. Crippa et al. suggested looking for potential associations between the BM state and the risk of graft failure in BThal patients undergoing both allogeneic or gene therapy HSCT, by correlating the levels of BM IO with data of the transplant outcome. Optimizing current iron chelation therapy can ameliorate MSC status, with potential effects on other BM niche populations and HSCs.

Increased circulating heme and iron is also a hallmark of SCD pathophysiology. Heme, indeed, acts as a proinflammatory molecule that activates ECs, neutrophils, and M $\phi$ s. Hemopexin, an extracellular scavenging system that binds heme, was reported to revert heme-induced M1 switching of M $\phi$ s in SCD mice [154] and to reduce endothelial toxicity caused by heme in SCD and BThal models [160]. Whether heme and hemopexin treatment can play a role in the SCD BM microenvironment is still unknown.

Antioxidant and anti-inflammatory treatments can be effective in restoring the BM niche and HSC functions impaired by oxidative stress and inflammation, respectively. For example, NAC treatment was demonstrated to improve the engraftment capacity of HSPCs in a mouse model of SCD [123].

## 6. Conclusions and Future Perspectives

Over the last few decades, research on BThal and SCD has been mostly focused on erythropoiesis, leaving the study of the BM microenvironment and HSCs underexplored. Recent studies demonstrated that HSC and BM niche components are altered in BThal and SCD, and that targeting the identified defects can rescue the impaired HSC–BM niche crosstalk. Thus, supportive therapies which aimed to ameliorate the BM niche and preserve long-term HSC function need to be pursued and developed. In this view, the combination of autologous gene therapy with niche targeting has the potential to improve therapeutic outcomes. Treatment pre- and post-HSCT can refurbish bone and HSC niche before HSC harvest and promote early engraftment after gene therapy.

Since BThal and SCD represent the most widespread monogenic diseases worldwide, the impact of novel combined treatments also targeting the BM niche could be relevant, leading to significant advances in hematology. An investigation of the BM alteration to develop potential new pharmacological treatments can represent an effective bridge between basic research and clinical translation from genetic Hb disorders to other diseases associated with erythropoietic stress.

The works reviewed here open up new questions and point out the need for a deeper understanding of HSC biology and interactions with the BM niche in diseases. These studies on BThal and SCD mouse models and patient-derived samples pave the way towards a novel concept—the complementary investigation of hematopoiesis, not only in steady state, acute stress, and malignancies, but also in non-malignant hematological disorders, with a potential impact on HSCT, i.e., the only definitive cure for hemoglobinopathies.

Further investigation will open up new avenues in this line of research.

**Author Contributions:** S.S. and L.R. equally contributed to this work. A.A. and G.F. are corresponding authors. Conceptualization, A.A.; supervision, G.F.; writing—original draft, A.A., S.S. and L.R.; writing—review and editing A.A., S.S., L.R. and G.F. All authors have read and agreed to the published version of the manuscript.

**Funding:** This review was supported in part by Fondazione Telethon (2022 Telethon SR-TIGET Core Grant to G.F.), the European Hematology Association (2019 EHA Junior Research Grant to A.A.) and the American Society of Hematology (2021 ASH Global Research Award to A.A.).

**Institutional Review Board Statement:** Not applicable.

**Informed Consent Statement:** Not applicable.

**Data Availability Statement:** Not applicable.

**Conflicts of Interest:** The authors declare no conflict of interest.

## References

1. Modell, B.; Darlison, M. Global epidemiology of haemoglobin disorders and derived service indicators. *Bull World Health Organ* **2008**, *86*, 480–487. [[CrossRef](#)] [[PubMed](#)]
2. Taher, A.T.; Musallam, K.M.; Cappellini, M.D.  $\beta$ -Thalassemias. *N. Engl. J. Med.* **2021**, *384*, 727–743. [[CrossRef](#)] [[PubMed](#)]
3. Ware, R.E.; de Montalembert, M.; Tshilolo, L.; Abboud, M.R. Sick cell disease. *Lancet* **2017**, *390*, 311–323. [[CrossRef](#)]
4. Baronciani, D.; Angelucci, E.; Potschger, U.; Gaziev, J.; Yesilipek, A.; Zecca, M.; Orofino, M.G.; Giardini, C.; Al-Ahmari, A.; Marktel, S.; et al. Hemopoietic stem cell transplantation in thalassemia: A report from the European Society for Blood and Bone Marrow Transplantation Hemoglobinopathy Registry, 2000–2010. *Bone Marrow Transplant* **2016**, *51*, 536–541. [[CrossRef](#)]
5. Angelucci, E.; Matthes-Martin, S.; Baronciani, D.; Bernaudin, F.; Bonanomi, S.; Cappellini, M.D.; Dalle, J.H.; Di Bartolomeo, P.; de Heredia, C.D.; Dickerhoff, R.; et al. Hematopoietic stem cell transplantation in thalassemia major and sickle cell disease: Indications and management recommendations from an international expert panel. *Haematologica* **2014**, *99*, 811–820. [[CrossRef](#)]
6. Caocci, G.; Orofino, M.G.; Vacca, A.; Piroddi, A.; Piras, E.; Addari, M.C.; Caria, R.; Pilia, M.P.; Origa, R.; Moi, P.; et al. Long-term survival of beta thalassemia major patients treated with hematopoietic stem cell transplantation compared with survival with conventional treatment. *Am. J. Hematol.* **2017**, *92*, 1303–1310. [[CrossRef](#)]
7. Gluckman, E.; Cappelli, B.; Bernaudin, F.; Labopin, M.; Volt, F.; Carreras, J.; Pinto Simoes, B.; Ferster, A.; Dupont, S.; de la Fuente, J.; et al. Sick cell disease: An international survey of results of HLA-identical sibling hematopoietic stem cell transplantation. *Blood* **2017**, *129*, 1548–1556. [[CrossRef](#)]
8. Ferrari, G.; Thrasher, A.J.; Aiuti, A. Gene therapy using haematopoietic stem and progenitor cells. *Nat. Rev. Genet.* **2021**, *22*, 216–234. [[CrossRef](#)]
9. Thompson, A.A.; Walters, M.C.; Kwiatkowski, J.; Rasko, J.E.J.; Ribeil, J.A.; Hongeng, S.; Magrin, E.; Schiller, G.J.; Payen, E.; Semeraro, M.; et al. Gene Therapy in Patients with Transfusion-Dependent beta-Thalassemia. *N. Engl. J. Med.* **2018**, *378*, 1479–1493. [[CrossRef](#)]
10. Marktel, S.; Scaramuzza, S.; Cicalese, M.P.; Giglio, F.; Galimberti, S.; Lidonnici, M.R.; Calbi, V.; Assanelli, A.; Bernardo, M.E.; Rossi, C.; et al. Intrabone hematopoietic stem cell gene therapy for adult and pediatric patients affected by transfusion-dependent  $\beta$ -thalassemia. *Nat. Med.* **2019**, *25*, 234–241. [[CrossRef](#)]
11. Locatelli, F.; Thompson, A.A.; Kwiatkowski, J.L.; Porter, J.B.; Thrasher, A.J.; Hongeng, S.; Sauer, M.G.; Thuret, I.; Lal, A.; Algeri, M.; et al. Betibeglogene Autotemcel Gene Therapy for Non- $\beta(0)/\beta(0)$  Genotype  $\beta$ -Thalassemia. *N. Engl. J. Med.* **2022**, *386*, 415–427. [[CrossRef](#)] [[PubMed](#)]
12. Ribeil, J.A.; Hacein-Bey-Abina, S.; Payen, E.; Magnani, A.; Semeraro, M.; Magrin, E.; Caccavelli, L.; Neven, B.; Bourget, P.; El Nemer, W.; et al. Gene Therapy in a Patient with Sick Cell Disease. *N. Engl. J. Med.* **2017**, *376*, 848–855. [[CrossRef](#)] [[PubMed](#)]
13. Frangoul, H.; Altshuler, D.; Cappellini, M.D.; Chen, Y.S.; Domm, J.; Eustace, B.K.; Foell, J.; de la Fuente, J.; Grupp, S.; Handgretinger, R.; et al. CRISPR-Cas9 Gene Editing for Sick Cell Disease and  $\beta$ -Thalassemia. *N. Engl. J. Med.* **2021**, *384*, 252–260. [[CrossRef](#)] [[PubMed](#)]
14. Morrison, S.J.; Scadden, D.T. The bone marrow niche for haematopoietic stem cells. *Nature* **2014**, *505*, 327–334. [[CrossRef](#)] [[PubMed](#)]
15. Pinho, S.; Frenette, P.S. Haematopoietic stem cell activity and interactions with the niche. *Nat. Rev. Mol. Cell Biol.* **2019**, *20*, 303–320. [[CrossRef](#)]
16. Mendelson, A.; Frenette, P.S. Hematopoietic stem cell niche maintenance during homeostasis and regeneration. *Nat. Med.* **2014**, *20*, 833–846. [[CrossRef](#)]
17. Batsivari, A.; Haltalli, M.L.R.; Passaro, D.; Pospori, C.; Lo Celso, C.; Bonnet, D. Dynamic responses of the haematopoietic stem cell niche to diverse stresses. *Nat. Cell Biol.* **2020**, *22*, 7–17. [[CrossRef](#)]
18. Vinchi, F.; Vance, S.Z. Challenging the Erythropoiesis Paradigm in  $\beta$ -Thalassemia. *Hemasphere* **2020**, *4*, e475. [[CrossRef](#)]
19. Carlesso, N. Targeting the bone marrow niche in hemoglobinopathies. *Blood* **2020**, *136*, 529–531. [[CrossRef](#)]
20. Weatherall, D.J.; Williams, T.N.; Allen, S.J.; O'Donnell, A. The population genetics and dynamics of the thalassemias. *Hematol. Oncol. Clin. N. Am.* **2010**, *24*, 1021–1031. [[CrossRef](#)]
21. Taher, A.T.; Cappellini, M.D. How I manage medical complications of beta-thalassemia in adults. *Blood* **2018**, *132*, 1781–1791. [[CrossRef](#)] [[PubMed](#)]
22. Galanello, R.; Origa, R. Beta-thalassemia. *Orphanet J. Rare Dis.* **2010**, *5*, 11. [[CrossRef](#)] [[PubMed](#)]
23. Piel, F.B.; Weatherall, D.J. The  $\alpha$ -thalassemias. *N. Engl. J. Med.* **2014**, *371*, 1908–1916. [[CrossRef](#)] [[PubMed](#)]
24. Rund, D.; Rachmilewitz, E.  $\beta$ -thalassemia. *N. Engl. J. Med.* **2005**, *353*, 1135–1146. [[CrossRef](#)]
25. Higgs, D.R.; Engel, J.D.; Stamatoyannopoulos, G. Thalassemia. *Lancet* **2012**, *379*, 373–383. [[CrossRef](#)]
26. Voskaridou, E.; Terpos, E. New insights into the pathophysiology and management of osteoporosis in patients with beta thalassaemia. *Br. J. Haematol.* **2004**, *127*, 127–139. [[CrossRef](#)]
27. Rachmilewitz, E.A.; Giardina, P.J. How I treat thalassemia. *Blood* **2011**, *118*, 3479–3488. [[CrossRef](#)]
28. Wong, P.; Fuller, P.J.; Gillespie, M.T.; Milat, F. Bone Disease in Thalassemia: A Molecular and Clinical Overview. *Endocr. Rev.* **2016**, *37*, 320–346. [[CrossRef](#)]
29. Morabito, N.; Gaudio, A.; Lasco, A.; Atteritano, M.; Pizzoleo, M.A.; Cincotta, M.; La Rosa, M.; Guarino, R.; Meo, A.; Frisina, N. Osteoprotegerin and RANKL in the pathogenesis of thalassemia-induced osteoporosis: New pieces of the puzzle. *J. Bone Miner. Res.* **2004**, *19*, 722–727. [[CrossRef](#)]

30. Bunn, H.F. Pathogenesis and treatment of sickle cell disease. *N. Engl. J. Med.* **1997**, *337*, 762–769. [[CrossRef](#)]
31. Kato, G.J.; Piel, F.B.; Reid, C.D.; Gaston, M.H.; Ohene-Frempong, K.; Krishnamurti, L.; Smith, W.R.; Panepinto, J.A.; Weatherall, D.J.; Costa, F.F.; et al. Sickle cell disease. *Nat. Rev. Dis. Primers* **2018**, *4*, 18010. [[CrossRef](#)] [[PubMed](#)]
32. Rees, D.C.; Williams, T.N.; Gladwin, M.T. Sickle-cell disease. *Lancet* **2010**, *376*, 2018–2031. [[CrossRef](#)]
33. Manwani, D.; Frenette, P.S. Vaso-occlusion in sickle cell disease: Pathophysiology and novel targeted therapies. *Blood* **2013**, *122*, 3892–3898. [[CrossRef](#)] [[PubMed](#)]
34. Almeida, A.; Roberts, I. Bone involvement in sickle cell disease. *Br. J. Haematol.* **2005**, *129*, 482–490. [[CrossRef](#)] [[PubMed](#)]
35. McGann, P.T.; Ware, R.E. Hydroxyurea for sickle cell anemia: What have we learned and what questions still remain? *Curr. Opin. Hematol.* **2011**, *18*, 158–165. [[CrossRef](#)]
36. Li, C.; Mathews, V.; Kim, S.; George, B.; Hebert, K.; Jiang, H.; Li, C.; Zhu, Y.; Keesler, D.A.; Boelens, J.J.; et al. Related and unrelated donor transplantation for beta-thalassemia major: Results of an international survey. *Blood Adv.* **2019**, *3*, 2562–2570. [[CrossRef](#)]
37. Lidonnici, M.R.; Ferrari, G. Gene therapy and gene editing strategies for hemoglobinopathies. *Blood Cells Mol. Dis.* **2018**, *70*, 87–101. [[CrossRef](#)]
38. Magrin, E.; Semeraro, M.; Hebert, N.; Joseph, L.; Magnani, A.; Chalumeau, A.; Gabrion, A.; Roudaut, C.; Marouene, J.; Lefrere, F.; et al. Long-term outcomes of lentiviral gene therapy for the  $\beta$ -hemoglobinopathies: The HGB-205 trial. *Nat. Med.* **2022**, *28*, 81–88. [[CrossRef](#)]
39. Esrick, E.B.; Lehmann, L.E.; Biffi, A.; Achebe, M.; Brendel, C.; Ciuculescu, M.F.; Daley, H.; MacKinnon, B.; Morris, E.; Federico, A.; et al. Post-Transcriptional Genetic Silencing of BCL11A to Treat Sickle Cell Disease. *N. Engl. J. Med.* **2021**, *384*, 205–215. [[CrossRef](#)]
40. Cappellini, M.D.; Viprakasit, V.; Taher, A.T.; Georgiev, P.; Kuo, K.H.M.; Coates, T.; Voskaridou, E.; Liew, H.K.; Pazgal-Kobrowski, I.; Forni, G.L.; et al. A Phase 3 Trial of Luspatercept in Patients with Transfusion-Dependent  $\beta$ -Thalassemia. *N. Engl. J. Med.* **2020**, *382*, 1219–1231. [[CrossRef](#)]
41. Casu, C.; Oikonomidou, P.R.; Chen, H.; Nandi, V.; Ginzburg, Y.; Prasad, P.; Fleming, R.E.; Shah, Y.M.; Valore, E.V.; Nemeth, E.; et al. Minihepcidin peptides as disease modifiers in mice affected by  $\beta$ -thalassemia and polycythemia vera. *Blood* **2016**, *128*, 265–276. [[CrossRef](#)] [[PubMed](#)]
42. Nai, A.; Pagani, A.; Mandelli, G.; Lidonnici, M.R.; Silvestri, L.; Ferrari, G.; Camaschella, C. Deletion of Tmprss6 attenuates the phenotype in a mouse model of  $\beta$ -thalassemia. *Blood* **2012**, *119*, 5021–5029. [[CrossRef](#)] [[PubMed](#)]
43. Richard, F.; van Lier, J.J.; Roubert, B.; Haboubi, T.; Gohring, U.M.; Durrenberger, F. Oral ferroportin inhibitor VIT-2763: First-in-human, phase 1 study in healthy volunteers. *Am. J. Hematol.* **2020**, *95*, 68–77. [[CrossRef](#)] [[PubMed](#)]
44. Cavazzana, M.; Ribeil, J.A.; Lagresle-Peyrou, C.; Andre-Schmutz, I. Gene Therapy with Hematopoietic Stem Cells: The Diseased Bone Marrow's Point of View. *Stem Cells Dev.* **2017**, *26*, 71–76. [[CrossRef](#)]
45. Goyal, S.; Tisdale, J.; Schmidt, M.; Kanter, J.; Jaroscak, J.; Whitney, D.; Bitter, H.; Gregory, P.D.; Parsons, G.; Foos, M.; et al. Acute Myeloid Leukemia Case after Gene Therapy for Sickle Cell Disease. *N. Engl. J. Med.* **2022**, *386*, 138–147. [[CrossRef](#)]
46. Joseph, C.; Quach, J.M.; Walkley, C.R.; Lane, S.W.; Lo Celso, C.; Purton, L.E. Deciphering hematopoietic stem cells in their niches: A critical appraisal of genetic models, lineage tracing, and imaging strategies. *Cell Stem Cell* **2013**, *13*, 520–533. [[CrossRef](#)]
47. Taichman, R.S.; Emerson, S.G. Human osteoblasts support hematopoiesis through the production of granulocyte colony-stimulating factor. *J. Exp. Med.* **1994**, *179*, 1677–1682. [[CrossRef](#)]
48. El-Badri, N.S.; Wang, B.Y.; Cherry, G.; Good, R.A. Osteoblasts promote engraftment of allogeneic hematopoietic stem cells. *Exp. Hematol.* **1998**, *26*, 110–116.
49. Calvi, L.M.; Adams, G.B.; Weibrecht, K.W.; Weber, J.M.; Olson, D.P.; Knight, M.C.; Martin, R.P.; Schipani, E.; Divieti, P.; Bringhurst, F.R.; et al. Osteoblastic cells regulate the haematopoietic stem cell niche. *Nature* **2003**, *425*, 841–846. [[CrossRef](#)]
50. Nilsson, S.K.; Johnston, H.M.; Whitty, G.A.; Williams, B.; Webb, R.J.; Denhardt, D.T.; Bertonecello, I.; Bendall, L.J.; Simmons, P.J.; Haylock, D.N. Osteopontin, a key component of the hematopoietic stem cell niche and regulator of primitive hematopoietic progenitor cells. *Blood* **2005**, *106*, 1232–1239. [[CrossRef](#)]
51. Ding, L.; Saunders, T.L.; Enikolopov, G.; Morrison, S.J. Endothelial and perivascular cells maintain haematopoietic stem cells. *Nature* **2012**, *481*, 457–462. [[CrossRef](#)] [[PubMed](#)]
52. Greenbaum, A.; Hsu, Y.M.; Day, R.B.; Schuettpelz, L.G.; Christopher, M.J.; Borgerding, J.N.; Nagasawa, T.; Link, D.C. CXCL12 in early mesenchymal progenitors is required for haematopoietic stem-cell maintenance. *Nature* **2013**, *495*, 227–230. [[CrossRef](#)] [[PubMed](#)]
53. Decker, M.; Leslie, J.; Liu, Q.; Ding, L. Hepatic thrombopoietin is required for bone marrow hematopoietic stem cell maintenance. *Science* **2018**, *360*, 106–110. [[CrossRef](#)] [[PubMed](#)]
54. Zhou, B.O.; Ding, L.; Morrison, S.J. Hematopoietic stem and progenitor cells regulate the regeneration of their niche by secreting Angiopoietin-1. *eLife* **2015**, *4*, e05521. [[CrossRef](#)] [[PubMed](#)]
55. Christodoulou, C.; Spencer, J.A.; Yeh, S.A.; Turcotte, R.; Kokkaliaris, K.D.; Panero, R.; Ramos, A.; Guo, G.; Seyedhassantehrani, N.; Esipova, T.V.; et al. Live-animal imaging of native haematopoietic stem and progenitor cells. *Nature* **2020**, *578*, 278–283. [[CrossRef](#)]
56. Sacchetti, B.; Funari, A.; Michienzi, S.; Di Cesare, S.; Piersanti, S.; Saggio, I.; Tagliafico, E.; Ferrari, S.; Robey, P.G.; Riminucci, M.; et al. Self-renewing osteoprogenitors in bone marrow sinusoids can organize a hematopoietic microenvironment. *Cell* **2007**, *131*, 324–336. [[CrossRef](#)]
57. Bianco, P.; Cao, X.; Frenette, P.S.; Mao, J.J.; Robey, P.G.; Simmons, P.J.; Wang, C.Y. The meaning, the sense and the significance: Translating the science of mesenchymal stem cells into medicine. *Nat. Med.* **2013**, *19*, 35–42. [[CrossRef](#)]

58. Mendez-Ferrer, S.; Michurina, T.V.; Ferraro, F.; Mazloom, A.R.; Macarthur, B.D.; Lira, S.A.; Scadden, D.T.; Ma'ayan, A.; Enikolopov, G.N.; Frenette, P.S. Mesenchymal and haematopoietic stem cells form a unique bone marrow niche. *Nature* **2010**, *466*, 829–834. [[CrossRef](#)]
59. Sugiyama, T.; Kohara, H.; Noda, M.; Nagasawa, T. Maintenance of the hematopoietic stem cell pool by CXCL12-CXCR4 chemokine signaling in bone marrow stromal cell niches. *Immunity* **2006**, *25*, 977–988. [[CrossRef](#)]
60. Morikawa, S.; Mabuchi, Y.; Kubota, Y.; Nagai, Y.; Niibe, K.; Hiratsu, E.; Suzuki, S.; Miyauchi-Hara, C.; Nagoshi, N.; Sunabori, T.; et al. Prospective identification, isolation, and systemic transplantation of multipotent mesenchymal stem cells in murine bone marrow. *J. Exp. Med.* **2009**, *206*, 2483–2496. [[CrossRef](#)]
61. Wein, F.; Pietsch, L.; Saffrich, R.; Wuchter, P.; Walenda, T.; Bork, S.; Horn, P.; Diehlmann, A.; Eckstein, V.; Ho, A.D.; et al. N-cadherin is expressed on human hematopoietic progenitor cells and mediates interaction with human mesenchymal stromal cells. *Stem Cell Res.* **2010**, *4*, 129–139. [[CrossRef](#)] [[PubMed](#)]
62. Zhao, M.; Tao, F.; Venkatraman, A.; Li, Z.; Smith, S.E.; Unruh, J.; Chen, S.; Ward, C.; Qian, P.; Perry, J.M.; et al. N-Cadherin-Expressing Bone and Marrow Stromal Progenitor Cells Maintain Reserve Hematopoietic Stem Cells. *Cell Rep.* **2019**, *26*, 652–669.e6. [[CrossRef](#)] [[PubMed](#)]
63. Taniguchi Ishikawa, E.; Gonzalez-Nieto, D.; Ghiaur, G.; Dunn, S.K.; Ficker, A.M.; Murali, B.; Madhu, M.; Gutstein, D.E.; Fishman, G.I.; Barrio, L.C.; et al. Connexin-43 prevents hematopoietic stem cell senescence through transfer of reactive oxygen species to bone marrow stromal cells. *Proc. Natl. Acad. Sci. USA* **2012**, *109*, 9071–9076. [[CrossRef](#)] [[PubMed](#)]
64. Naveiras, O.; Nardi, V.; Wenzel, P.L.; Hauschka, P.V.; Fahey, F.; Daley, G.Q. Bone-marrow adipocytes as negative regulators of the haematopoietic microenvironment. *Nature* **2009**, *460*, 259–263. [[CrossRef](#)]
65. Zhou, B.O.; Yu, H.; Yue, R.; Zhao, Z.; Rios, J.J.; Naveiras, O.; Morrison, S.J. Bone marrow adipocytes promote the regeneration of stem cells and haematopoiesis by secreting SCF. *Nat. Cell Biol.* **2017**, *19*, 891–903. [[CrossRef](#)]
66. Itkin, T.; Gur-Cohen, S.; Spencer, J.A.; Schajnovitz, A.; Ramasamy, S.K.; Kusumbe, A.P.; Ledergor, G.; Jung, Y.; Milo, I.; Poulos, M.G.; et al. Distinct bone marrow blood vessels differentially regulate haematopoiesis. *Nature* **2016**, *532*, 323–328. [[CrossRef](#)] [[PubMed](#)]
67. Winkler, I.G.; Barbier, V.; Nowlan, B.; Jacobsen, R.N.; Forristal, C.E.; Patton, J.T.; Magnani, J.L.; Levesque, J.P. Vascular niche E-selectin regulates hematopoietic stem cell dormancy, self renewal and chemoresistance. *Nat. Med.* **2012**, *18*, 1651–1657. [[CrossRef](#)] [[PubMed](#)]
68. Doan, P.L.; Russell, J.L.; Himburg, H.A.; Helms, K.; Harris, J.R.; Lucas, J.; Holshausen, K.C.; Meadows, S.K.; Daher, P.; Jeffords, L.B.; et al. Tie2<sup>+</sup> bone marrow endothelial cells regulate hematopoietic stem cell regeneration following radiation injury. *Stem Cells* **2013**, *31*, 327–337. [[CrossRef](#)]
69. Ding, L.; Morrison, S.J. Haematopoietic stem cells and early lymphoid progenitors occupy distinct bone marrow niches. *Nature* **2013**, *495*, 231–235. [[CrossRef](#)]
70. Mendez-Ferrer, S.; Lucas, D.; Battista, M.; Frenette, P.S. Haematopoietic stem cell release is regulated by circadian oscillations. *Nature* **2008**, *452*, 442–447. [[CrossRef](#)]
71. Park, M.H.; Jin, H.K.; Min, W.K.; Lee, W.W.; Lee, J.E.; Akiyama, H.; Herzog, H.; Enikolopov, G.N.; Schuchman, E.H.; Bae, J.S. Neuropeptide Y regulates the hematopoietic stem cell microenvironment and prevents nerve injury in the bone marrow. *EMBO J.* **2015**, *34*, 1648–1660. [[CrossRef](#)] [[PubMed](#)]
72. Yamazaki, S.; Ema, H.; Karlsson, G.; Yamaguchi, T.; Miyoshi, H.; Shioda, S.; Taketo, M.M.; Karlsson, S.; Iwama, A.; Nakauchi, H. Nonmyelinating Schwann cells maintain hematopoietic stem cell hibernation in the bone marrow niche. *Cell* **2011**, *147*, 1146–1158. [[CrossRef](#)] [[PubMed](#)]
73. Bruns, I.; Lucas, D.; Pinho, S.; Ahmed, J.; Lambert, M.P.; Kunisaki, Y.; Scheiermann, C.; Schiff, L.; Poncz, M.; Bergman, A.; et al. Megakaryocytes regulate hematopoietic stem cell quiescence through CXCL4 secretion. *Nat. Med.* **2014**, *20*, 1315–1320. [[CrossRef](#)] [[PubMed](#)]
74. Zhao, M.; Perry, J.M.; Marshall, H.; Venkatraman, A.; Qian, P.; He, X.C.; Ahamed, J.; Li, L. Megakaryocytes maintain homeostatic quiescence and promote post-injury regeneration of hematopoietic stem cells. *Nat. Med.* **2014**, *20*, 1321–1326. [[CrossRef](#)]
75. Lemieux, J.M.; Horowitz, M.C.; Kacena, M.A. Involvement of integrins  $\alpha(3)\beta(1)$  and  $\alpha(5)\beta(1)$  and glycoprotein IIb in megakaryocyte-induced osteoblast proliferation. *J. Cell. Biochem.* **2010**, *109*, 927–932. [[CrossRef](#)]
76. Bord, S.; Frith, E.; Ireland, D.C.; Scott, M.A.; Craig, J.I.; Compston, J.E. Megakaryocytes modulate osteoblast synthesis of type-I collagen, osteoprotegerin, and RANKL. *Bone* **2005**, *36*, 812–819. [[CrossRef](#)]
77. Dominici, M.; Rasini, V.; Bussolari, R.; Chen, X.; Hofmann, T.J.; Spano, C.; Bernabei, D.; Veronesi, E.; Bertoni, F.; Paolucci, P.; et al. Restoration and reversible expansion of the osteoblastic hematopoietic stem cell niche after marrow radioablation. *Blood* **2009**, *114*, 2333–2343. [[CrossRef](#)]
78. Chow, A.; Lucas, D.; Hidalgo, A.; Mendez-Ferrer, S.; Hashimoto, D.; Scheiermann, C.; Battista, M.; Leboeuf, M.; Prophete, C.; van Rooijen, N.; et al. Bone marrow CD169<sup>+</sup> macrophages promote the retention of hematopoietic stem and progenitor cells in the mesenchymal stem cell niche. *J. Exp. Med.* **2011**, *208*, 261–271. [[CrossRef](#)]
79. Hur, J.; Choi, J.I.; Lee, H.; Nham, P.; Kim, T.W.; Chae, C.W.; Yun, J.Y.; Kang, J.A.; Kang, J.; Lee, S.E.; et al. CD82/KAI1 Maintains the Dormancy of Long-Term Hematopoietic Stem Cells through Interaction with DARC-Expressing Macrophages. *Cell Stem Cell* **2016**, *18*, 508–521. [[CrossRef](#)]



80. Ludin, A.; Itkin, T.; Gur-Cohen, S.; Mildner, A.; Shezen, E.; Golan, K.; Kollet, O.; Kalinkovich, A.; Porat, Z.; D'Uva, G.; et al. Monocytes-macrophages that express alpha-smooth muscle actin preserve primitive hematopoietic cells in the bone marrow. *Nat. Immunol.* **2012**, *13*, 1072–1082. [[CrossRef](#)]
81. Luo, Y.; Shao, L.; Chang, J.; Feng, W.; Liu, Y.L.; Cottler-Fox, M.H.; Emanuel, P.D.; Hauer-Jensen, M.; Bernstein, I.D.; Liu, L.; et al. M1 and M2 macrophages differentially regulate hematopoietic stem cell self-renewal and ex vivo expansion. *Blood Adv.* **2018**, *2*, 859–870. [[CrossRef](#)] [[PubMed](#)]
82. Casanova-Acebes, M.; Pitaval, C.; Weiss, L.A.; Nombela-Arrieta, C.; Chevre, R.; A-González, N.; Kunisaki, Y.; Zhang, D.; van Rooijen, N.; Silberstein, L.E.; et al. Rhythmic modulation of the hematopoietic niche through neutrophil clearance. *Cell* **2013**, *153*, 1025–1035. [[CrossRef](#)] [[PubMed](#)]
83. Kawano, Y.; Fukui, C.; Shinohara, M.; Wakahashi, K.; Ishii, S.; Suzuki, T.; Sato, M.; Asada, N.; Kawano, H.; Minagawa, K.; et al. G-CSF-induced sympathetic tone provokes fever and primes antimobilizing functions of neutrophils via PGE2. *Blood* **2017**, *129*, 587–597. [[CrossRef](#)]
84. Bowers, E.; Slaughter, A.; Frenette, P.S.; Kuick, R.; Pello, O.M.; Lucas, D. Granulocyte-derived TNFalpha promotes vascular and hematopoietic regeneration in the bone marrow. *Nat. Med.* **2018**, *24*, 95–102. [[CrossRef](#)]
85. Fujisaki, J.; Wu, J.; Carlson, A.L.; Silberstein, L.; Putheti, P.; Larocca, R.; Gao, W.; Saito, T.I.; Lo Celso, C.; Tsuyuzaki, H.; et al. In vivo imaging of Treg cells providing immune privilege to the haematopoietic stem-cell niche. *Nature* **2011**, *474*, 216–219. [[CrossRef](#)]
86. Hirata, Y.; Furuhashi, K.; Ishii, H.; Li, H.W.; Pinho, S.; Ding, L.; Robson, S.C.; Frenette, P.S.; Fujisaki, J. CD150(high) Bone Marrow Tregs Maintain Hematopoietic Stem Cell Quiescence and Immune Privilege via Adenosine. *Cell Stem Cell* **2018**, *22*, 445–453.e5. [[CrossRef](#)]
87. Tan, D.Q.; Suda, T. Reactive Oxygen Species and Mitochondrial Homeostasis as Regulators of Stem Cell Fate and Function. *Antioxid. Redox Signal.* **2018**, *29*, 149–168. [[CrossRef](#)] [[PubMed](#)]
88. Bigarella, C.L.; Liang, R.; Ghaffari, S. Stem cells and the impact of ROS signaling. *Development* **2014**, *141*, 4206–4218. [[CrossRef](#)]
89. Jang, Y.Y.; Sharkis, S.J. A low level of reactive oxygen species selects for primitive hematopoietic stem cells that may reside in the low-oxygenic niche. *Blood* **2007**, *110*, 3056–3063. [[CrossRef](#)]
90. Rimmele, P.; Liang, R.; Bigarella, C.L.; Kocabas, F.; Xie, J.; Serasinghe, M.N.; Chipuk, J.; Sadek, H.; Zhang, C.C.; Ghaffari, S. Mitochondrial metabolism in hematopoietic stem cells requires functional FOXO3. *EMBO Rep.* **2015**, *16*, 1164–1176. [[CrossRef](#)]
91. Chiabrando, D.; Vinchi, F.; Fiorito, V.; Mercurio, S.; Tolosano, E. Heme in pathophysiology: A matter of scavenging, metabolism and trafficking across cell membranes. *Front. Pharmacol.* **2014**, *5*, 61. [[CrossRef](#)] [[PubMed](#)]
92. Okabe, H.; Suzuki, T.; Uehara, E.; Ueda, M.; Nagai, T.; Ozawa, K. The bone marrow hematopoietic microenvironment is impaired in iron-overloaded mice. *Eur. J. Haematol.* **2014**, *93*, 118–128. [[CrossRef](#)] [[PubMed](#)]
93. Muto, Y.; Nishiyama, M.; Nita, A.; Moroishi, T.; Nakayama, K.I. Essential role of FBXL5-mediated cellular iron homeostasis in maintenance of hematopoietic stem cells. *Nat. Commun.* **2017**, *8*, 16114. [[CrossRef](#)] [[PubMed](#)]
94. Chai, X.; Li, D.; Cao, X.; Zhang, Y.; Mu, J.; Lu, W.; Xiao, X.; Li, C.; Meng, J.; Chen, J.; et al. ROS-mediated iron overload injures the hematopoiesis of bone marrow by damaging hematopoietic stem/progenitor cells in mice. *Sci. Rep.* **2015**, *5*, 10181. [[CrossRef](#)] [[PubMed](#)]
95. Zhang, D.; Gao, X.; Li, H.; Borger, D.K.; Wei, Q.; Yang, E.; Xu, C.; Pinho, S.; Frenette, P.S. The microbiota regulates hematopoietic stem cell fate decisions by controlling iron availability in bone marrow. *Cell Stem Cell* **2022**, *29*, 232–247.e7. [[CrossRef](#)]
96. King, K.Y.; Goodell, M.A. Inflammatory modulation of HSCs: Viewing the HSC as a foundation for the immune response. *Nat. Rev. Immunol.* **2011**, *11*, 685–692. [[CrossRef](#)] [[PubMed](#)]
97. Pietras, E.M.; Mirantes-Barbeito, C.; Fong, S.; Loeffler, D.; Kovtonyuk, L.V.; Zhang, S.; Lakshminarasimhan, R.; Chin, C.P.; Techner, J.M.; Will, B.; et al. Chronic interleukin-1 exposure drives haematopoietic stem cells towards precocious myeloid differentiation at the expense of self-renewal. *Nat. Cell Biol.* **2016**, *18*, 607–618. [[CrossRef](#)]
98. Walter, D.; Lier, A.; Geiselhart, A.; Thalheimer, F.B.; Huntscha, S.; Sobotta, M.C.; Moehrl, B.; Brocks, D.; Bayindir, I.; Kaschutnig, P.; et al. Exit from dormancy provokes DNA-damage-induced attrition in haematopoietic stem cells. *Nature* **2015**, *520*, 549–552. [[CrossRef](#)]
99. Baldrige, M.T.; King, K.Y.; Boles, N.C.; Weksberg, D.C.; Goodell, M.A. Quiescent haematopoietic stem cells are activated by IFN-gamma in response to chronic infection. *Nature* **2010**, *465*, 793–797. [[CrossRef](#)]
100. Boettcher, S.; Gerosa, R.C.; Radpour, R.; Bauer, J.; Ampenberger, F.; Heikenwalder, M.; Kopf, M.; Manz, M.G. Endothelial cells translate pathogen signals into G-CSF-driven emergency granulopoiesis. *Blood* **2014**, *124*, 1393–1403. [[CrossRef](#)]
101. Schurch, C.M.; Riether, C.; Ochsenbein, A.F. Cytotoxic CD8<sup>+</sup> T cells stimulate hematopoietic progenitors by promoting cytokine release from bone marrow mesenchymal stromal cells. *Cell Stem Cell* **2014**, *14*, 460–472. [[CrossRef](#)] [[PubMed](#)]
102. Terashima, A.; Okamoto, K.; Nakashima, T.; Akira, S.; Ikuta, K.; Takayanagi, H. Sepsis-Induced Osteoblast Ablation Causes Immunodeficiency. *Immunity* **2016**, *44*, 1434–1443. [[CrossRef](#)] [[PubMed](#)]
103. Geiger, H.; de Haan, G.; Florian, M.C. The ageing haematopoietic stem cell compartment. *Nat. Rev. Immunol.* **2013**, *13*, 376–389. [[CrossRef](#)] [[PubMed](#)]
104. Sacma, M.; Pospiech, J.; Bogeska, R.; de Back, W.; Mallm, J.P.; Sakk, V.; Soller, K.; Marka, G.; Vollmer, A.; Karns, R.; et al. Haematopoietic stem cells in perisinusoidal niches are protected from ageing. *Nat. Cell Biol.* **2019**, *21*, 1309–1320. [[CrossRef](#)]

105. Maryanovich, M.; Zahalka, A.H.; Pierce, H.; Pinho, S.; Nakahara, F.; Asada, N.; Wei, Q.; Wang, X.; Ciero, P.; Xu, J.; et al. Adrenergic nerve degeneration in bone marrow drives aging of the hematopoietic stem cell niche. *Nat. Med.* **2018**, *24*, 782–791. [[CrossRef](#)]
106. Mendez-Ferrer, S.; Bonnet, D.; Steensma, D.P.; Hasserjian, R.P.; Ghobrial, I.M.; Gribben, J.G.; Andreeff, M.; Krause, D.S. Bone marrow niches in haematological malignancies. *Nat. Rev. Cancer* **2020**, *20*, 285–298. [[CrossRef](#)]
107. Duarte, D.; Hawkins, E.D.; Akinduro, O.; Ang, H.; De Filippo, K.; Kong, I.Y.; Haltalli, M.; Ruivo, N.; Straszkowski, L.; Vervoort, S.J.; et al. Inhibition of Endosteal Vascular Niche Remodeling Rescues Hematopoietic Stem Cell Loss in AML. *Cell Stem Cell* **2018**, *22*, 64–77.e6. [[CrossRef](#)]
108. Pitt, L.A.; Tikhonova, A.N.; Hu, H.; Trimarchi, T.; King, B.; Gong, Y.; Sanchez-Martin, M.; Tsigos, A.; Littman, D.R.; Ferrando, A.A.; et al. CXCL12-Producing Vascular Endothelial Niches Control Acute T Cell Leukemia Maintenance. *Cancer Cell* **2015**, *27*, 755–768. [[CrossRef](#)]
109. Baryawno, N.; Przybylski, D.; Kowalczyk, M.S.; Kfoury, Y.; Severe, N.; Gustafsson, K.; Kokkaliaris, K.D.; Mercier, F.; Tabaka, M.; Hofree, M.; et al. A Cellular Taxonomy of the Bone Marrow Stroma in Homeostasis and Leukemia. *Cell* **2019**, *177*, 1915–1932.e16. [[CrossRef](#)]
110. Sokolic, R.; Maric, I.; Kesserwan, C.; Garabedian, E.; Hanson, I.C.; Dodds, M.; Buckley, R.; Issekutz, A.C.; Kamani, N.; Shaw, K.; et al. Myeloid dysplasia and bone marrow hypocellularity in adenosine deaminase-deficient severe combined immune deficiency. *Blood* **2011**, *118*, 2688–2694. [[CrossRef](#)]
111. Sauer, A.V.; Mrak, E.; Hernandez, R.J.; Zacchi, E.; Cavani, F.; Casiraghi, M.; Grunebaum, E.; Roifman, C.M.; Cervi, M.C.; Ambrosi, A.; et al. ADA-deficient SCID is associated with a specific microenvironment and bone phenotype characterized by RANKL/OPG imbalance and osteoblast insufficiency. *Blood* **2009**, *114*, 3216–3226. [[CrossRef](#)] [[PubMed](#)]
112. Weisser, M.; Demel, U.M.; Stein, S.; Chen-Wichmann, L.; Touzot, F.; Santilli, G.; Sujer, S.; Brendel, C.; Siler, U.; Cavazzana, M.; et al. Hyperinflammation in patients with chronic granulomatous disease leads to impairment of hematopoietic stem cell functions. *J. Allergy Clin. Immunol.* **2016**, *138*, 219–228.e9. [[CrossRef](#)]
113. Lacout, C.; Haddad, E.; Sabri, S.; Svinarchouk, F.; Garcon, L.; Capron, C.; Foudi, A.; Mzali, R.; Snapper, S.B.; Louache, F.; et al. A defect in hematopoietic stem cell migration explains the nonrandom X-chromosome inactivation in carriers of Wiskott-Aldrich syndrome. *Blood* **2003**, *102*, 1282–1289. [[CrossRef](#)] [[PubMed](#)]
114. Aprile, A.; Gulino, A.; Storto, M.; Villa, I.; Beretta, S.; Merelli, I.; Rubinacci, A.; Ponzoni, M.; Markt, S.; Tripodo, C.; et al. Hematopoietic stem cell function in beta-thalassemia is impaired and is rescued by targeting the bone marrow niche. *Blood* **2020**, *136*, 610–622. [[CrossRef](#)] [[PubMed](#)]
115. Tang, A.; Strat, A.N.; Rahman, M.; Zhang, H.; Bao, W.; Liu, Y.; Shi, D.; An, X.; Manwani, D.; Shi, P.; et al. Murine bone marrow mesenchymal stromal cells have reduced hematopoietic maintenance ability in sickle cell disease. *Blood* **2021**, *138*, 2570–2582. [[CrossRef](#)]
116. McColl, B.; Vadolas, J. Animal models of beta-hemoglobinopathies: Utility and limitations. *J. Blood Med.* **2016**, *7*, 263–274. [[CrossRef](#)]
117. Yang, B.; Kirby, S.; Lewis, J.; Detloff, P.J.; Maeda, N.; Smithies, O. A mouse model for beta 0-thalassemia. *Proc. Natl. Acad. Sci. USA* **1995**, *92*, 11608–11612. [[CrossRef](#)]
118. Trudel, M.; Saadane, N.; Garel, M.C.; Bardakdjian-Michau, J.; Blouquit, Y.; Guerquin-Kern, J.L.; Rouyer-Fessard, P.; Vidaud, D.; Pachnis, A.; Romeo, P.H.; et al. Towards a transgenic mouse model of sickle cell disease: Hemoglobin SAD. *EMBO J.* **1991**, *10*, 3157–3165. [[CrossRef](#)]
119. Paszty, C.; Brion, C.M.; Mancini, E.; Witkowska, H.E.; Stevens, M.E.; Mohandas, N.; Rubin, E.M. Transgenic knockout mice with exclusively human sickle hemoglobin and sickle cell disease. *Science* **1997**, *278*, 876–878. [[CrossRef](#)]
120. Ryan, T.M.; Ciavatta, D.J.; Townes, T.M. Knockout-transgenic mouse model of sickle cell disease. *Science* **1997**, *278*, 873–876. [[CrossRef](#)]
121. Hua, P.; Roy, N.; de la Fuente, J.; Wang, G.; Thongjuea, S.; Clark, K.; Roy, A.; Psaila, B.; Ashley, N.; Harrington, Y.; et al. Single-cell analysis of bone marrow-derived CD34<sup>+</sup> cells from children with sickle cell disease and thalassemia. *Blood* **2019**, *134*, 2111–2115. [[CrossRef](#)] [[PubMed](#)]
122. Lidonnici, M.R.; Chianella, G.; Tiboni, F.; Barcella, M.; Merelli, I.; Scaramuzza, S.; Rossi, C.; Crippa, S.; Storto, M.; Bernardo, M.E.; et al. S269 TGF-beta signaling controls the lineage cell fate of hematopoietic stem cells towards erythroid branching in beta-thalassemia. EHA2021 Virtual Congress Abstract Book. *HemaSphere* **2021**, *5*, e566. [[CrossRef](#)]
123. Javazon, E.H.; Radhi, M.; Gangadharan, B.; Perry, J.; Archer, D.R. Hematopoietic stem cell function in a murine model of sickle cell disease. *Anemia* **2012**, *2012*, 387385. [[CrossRef](#)] [[PubMed](#)]
124. Blouin, M.J.; De Paeppe, M.E.; Trudel, M. Altered hematopoiesis in murine sickle cell disease. *Blood* **1999**, *94*, 1451–1459. [[CrossRef](#)]
125. Tolu, S.S.; Wang, K.; Yan, Z.; Zhang, S.; Roberts, K.; Crouch, A.S.; Sebastian, G.; Chaitowitz, M.; Fornari, E.D.; Schwechter, E.M.; et al. Characterization of Hematopoiesis in Sickle Cell Disease by Prospective Isolation of Stem and Progenitor Cells. *Cells* **2020**, *9*, 2159. [[CrossRef](#)]
126. Vogiatzi, M.G.; Tsay, J.; Verdellis, K.; Rivella, S.; Grady, R.W.; Doty, S.; Giardina, P.J.; Boskey, A.L. Changes in bone microarchitecture and biomechanical properties in the th3 thalassemia mouse are associated with decreased bone turnover and occur during the period of bone accrual. *Calcif. Tissue Int.* **2010**, *86*, 484–494. [[CrossRef](#)]

127. Crippa, S.; Rossella, V.; Aprile, A.; Silvestri, L.; Rivis, S.; Scaramuzza, S.; Pirroni, S.; Avanzini, M.A.; Basso-Ricci, L.; Hernandez, R.J.; et al. Bone marrow stromal cells from  $\beta$ -thalassemia patients have impaired hematopoietic supportive capacity. *J. Clin. Investig.* **2019**, *129*, 1566–1580. [CrossRef]
128. Baldwin, C.; Nolan, V.G.; Wyszynski, D.F.; Ma, Q.L.; Sebastiani, P.; Embury, S.H.; Bisbee, A.; Farrell, J.; Farrer, L.; Steinberg, M.H. Association of klotho, bone morphogenetic protein 6, and annexin A2 polymorphisms with sickle cell osteonecrosis. *Blood* **2005**, *106*, 372–375. [CrossRef]
129. Seguin, C.; Kassis, J.; Busque, L.; Bestawros, A.; Theodoropoulos, J.; Alonso, M.L.; Harvey, E.J. Non-traumatic necrosis of bone (osteonecrosis) is associated with endothelial cell activation but not thrombophilia. *Rheumatology* **2008**, *47*, 1151–1155. [CrossRef]
130. Nouraie, M.; Cheng, K.; Niu, X.; Moore-King, E.; Fadojutimi-Akinsi, M.F.; Minniti, C.P.; Sable, C.; Rana, S.; Dham, N.; Campbell, A.; et al. Predictors of osteoclast activity in patients with sickle cell disease. *Haematologica* **2011**, *96*, 1092–1098. [CrossRef]
131. Kobayashi, K.; Takahashi, N.; Jimi, E.; Udagawa, N.; Takami, M.; Kotake, S.; Nakagawa, N.; Kinosaki, M.; Yamaguchi, K.; Shima, N.; et al. Tumor necrosis factor alpha stimulates osteoclast differentiation by a mechanism independent of the ODF/RANKL-RANK interaction. *J. Exp. Med.* **2000**, *191*, 275–286. [CrossRef] [PubMed]
132. Green, M.; Akinsami, I.; Lin, A.; Banton, S.; Ghosh, S.; Chen, B.; Platt, M.; Osunkwo, I.; Ofori-Acquah, S.; Guldberg, R.; et al. Microarchitectural and mechanical characterization of the sickle bone. *J. Mech. Behav. Biomed. Mater.* **2015**, *48*, 220–228. [CrossRef] [PubMed]
133. Dalle Carbonare, L.; Matte, A.; Valenti, M.T.; Siciliano, A.; Mori, A.; Schweiger, V.; Zampieri, G.; Perbellini, L.; De Franceschi, L. Hypoxia-reperfusion affects osteogenic lineage and promotes sickle cell bone disease. *Blood* **2015**, *126*, 2320–2328. [CrossRef] [PubMed]
134. Tsay, J.; Yang, Z.; Ross, F.P.; Cunningham-Rundles, S.; Lin, H.; Coleman, R.; Mayer-Kuckuk, P.; Doty, S.B.; Grady, R.W.; Giardina, P.J.; et al. Bone loss caused by iron overload in a murine model: Importance of oxidative stress. *Blood* **2010**, *116*, 2582–2589. [CrossRef]
135. Stenger, E.O.; Chinnadurai, R.; Yuan, S.; Garcia, M.; Arafat, D.; Gibson, G.; Krishnamurti, L.; Galipeau, J. Bone Marrow-Derived Mesenchymal Stromal Cells from Patients with Sickle Cell Disease Display Intact Functionality. *Biol. Blood Marrow Transplant.* **2017**, *23*, 736–745. [CrossRef]
136. Park, S.Y.; Matte, A.; Jung, Y.; Ryu, J.; Anand, W.B.; Han, E.Y.; Liu, M.; Carbone, C.; Melisi, D.; Nagasawa, T.; et al. Pathologic angiogenesis in the bone marrow of humanized sickle cell mice is reversed by blood transfusion. *Blood* **2020**, *135*, 2071–2084. [CrossRef]
137. Aprile, A.; Raggi, L.; Storto, M.; Villa, I.; Bolamperti, S.; Markt, S.; Motta, I.; Cappellini, M.D.; Rubinacci, A.; Ferrari, G. Inhibition of Fibroblast Growth Factor-23 (FGF-23) Rescues Bone and Hematopoietic Stem Cell Niche Defects in Beta-Thalassemia, Uncovering the Missing Link Between Hematopoiesis and Bone. *Blood* **2021**, *138* (Suppl. 1), 572. [CrossRef]
138. Edmonston, D.; Wolf, M. FGF23 at the crossroads of phosphate, iron economy and erythropoiesis. *Nat. Rev. Nephrol.* **2020**, *16*, 7–19. [CrossRef]
139. Clinkenbeard, E.L.; Hanudel, M.R.; Stayrook, K.R.; Appaiah, H.N.; Farrow, E.G.; Cass, T.A.; Summers, L.J.; Ip, C.S.; Hum, J.M.; Thomas, J.C.; et al. Erythropoietin stimulates murine and human fibroblast growth factor-23, revealing novel roles for bone and bone marrow. *Haematologica* **2017**, *102*, e427–e430. [CrossRef]
140. Aprile, A.; Storto, M.; Malara, A.; Gulino, A.; Raggi, L.; Sighinolfi, S.; Beretta, S.; Merelli, I.; Markt, S.; Ponzoni, M.; et al. S249 Reduced Levels of thrombopoietin Contribute to Impaired Hematopoietic stem Cell Function and Defective Megakaryopoiesis in Beta-Thalassemia. Available online: [https://library.ehaeb.org/eha/2021/eha2021-virtual-congress/324657/annamaria.aprile.reduced.levels.of.thrombopoietin.contribute.to.impaired.html?f=menu%3D6%2Abrowseby%3D8%2Asortby%3D2%2Amedia%3D3%2Ace\\_id%3D2035%2Aot\\_id%3D25563](https://library.ehaeb.org/eha/2021/eha2021-virtual-congress/324657/annamaria.aprile.reduced.levels.of.thrombopoietin.contribute.to.impaired.html?f=menu%3D6%2Abrowseby%3D8%2Asortby%3D2%2Amedia%3D3%2Ace_id%3D2035%2Aot_id%3D25563) (accessed on 4 May 2022).
141. Yoshihara, H.; Arai, F.; Hosokawa, K.; Hagiwara, T.; Takubo, K.; Nakamura, Y.; Gomei, Y.; Iwasaki, H.; Matsuoka, S.; Miyamoto, K.; et al. Thrombopoietin/MPL signaling regulates hematopoietic stem cell quiescence and interaction with the osteoblastic niche. *Cell Stem Cell* **2007**, *1*, 685–697. [CrossRef]
142. Nakamura-Ishizu, A.; Takubo, K.; Kobayashi, H.; Suzuki-Inoue, K.; Suda, T. CLEC-2 in megakaryocytes is critical for maintenance of hematopoietic stem cells in the bone marrow. *J. Exp. Med.* **2015**, *212*, 2133–2146. [CrossRef] [PubMed]
143. Seyfried, A.N.; Maloney, J.M.; MacNamara, K.C. Macrophages Orchestrate Hematopoietic Programs and Regulate HSC Function During Inflammatory Stress. *Front. Immunol.* **2020**, *11*, 1499. [CrossRef] [PubMed]
144. Siwaponanan, P.; Siegers, J.Y.; Ghazali, R.; Ng, T.; McColl, B.; Ng, G.Z.; Sutton, P.; Wang, N.; Ooi, I.; Thiengtavor, C.; et al. Reduced PU.1 expression underlies aberrant neutrophil maturation and function in beta-thalassemia mice and patients. *Blood* **2017**, *129*, 3087–3099. [CrossRef] [PubMed]
145. Zhang, D.; Xu, C.; Manwani, D.; Frenette, P.S. Neutrophils, platelets, and inflammatory pathways at the nexus of sickle cell disease pathophysiology. *Blood* **2016**, *127*, 801–809. [CrossRef]
146. Canalli, A.A.; Franco-Penteado, C.F.; Saad, S.T.; Conran, N.; Costa, F.F. Increased adhesive properties of neutrophils in sickle cell disease may be reversed by pharmacological nitric oxide donation. *Haematologica* **2008**, *93*, 605–609. [CrossRef]
147. Lum, A.F.; Wun, T.; Staunton, D.; Simon, S.I. Inflammatory potential of neutrophils detected in sickle cell disease. *Am. J. Hematol.* **2004**, *76*, 126–133. [CrossRef]
148. Chen, G.; Zhang, D.; Fuchs, T.A.; Manwani, D.; Wagner, D.D.; Frenette, P.S. Heme-induced neutrophil extracellular traps contribute to the pathogenesis of sickle cell disease. *Blood* **2014**, *123*, 3818–3827. [CrossRef]

149. Zhang, D.; Chen, G.; Manwani, D.; Mortha, A.; Xu, C.; Faith, J.J.; Burk, R.D.; Kunisaki, Y.; Jang, J.E.; Scheiermann, C.; et al. Neutrophil ageing is regulated by the microbiome. *Nature* **2015**, *525*, 528–532. [[CrossRef](#)]
150. Villagra, J.; Shiva, S.; Hunter, L.A.; Machado, R.F.; Gladwin, M.T.; Kato, G.J. Platelet activation in patients with sickle disease, hemolysis-associated pulmonary hypertension, and nitric oxide scavenging by cell-free hemoglobin. *Blood* **2007**, *110*, 2166–2172. [[CrossRef](#)]
151. Belcher, J.D.; Marker, P.H.; Weber, J.P.; Hebbel, R.P.; Vercellotti, G.M. Activated monocytes in sickle cell disease: Potential role in the activation of vascular endothelium and vaso-occlusion. *Blood* **2000**, *96*, 2451–2459. [[CrossRef](#)]
152. Mitroulis, I.; Kalafati, L.; Bornhauser, M.; Hajishengallis, G.; Chavakis, T. Regulation of the Bone Marrow Niche by Inflammation. *Front. Immunol* **2020**, *11*, 1540. [[CrossRef](#)] [[PubMed](#)]
153. Essers, M.A.; Offner, S.; Blanco-Bose, W.E.; Waibler, Z.; Kalinke, U.; Duchosal, M.A.; Trumpp, A. IFN $\alpha$  activates dormant haematopoietic stem cells in vivo. *Nature* **2009**, *458*, 904–908. [[CrossRef](#)] [[PubMed](#)]
154. Vinchi, F.; Costa da Silva, M.; Ingoglia, G.; Petrillo, S.; Brinkman, N.; Zuercher, A.; Cerwenka, A.; Tolosano, E.; Muckenthaler, M.U. Hemopexin therapy reverts heme-induced proinflammatory phenotypic switching of macrophages in a mouse model of sickle cell disease. *Blood* **2016**, *127*, 473–486. [[CrossRef](#)] [[PubMed](#)]
155. Zhou, X.; Huang, L.; Wu, J.; Qu, Y.; Jiang, H.; Zhang, J.; Qiu, S.; Liao, C.; Xu, X.; Xia, J.; et al. Impaired bone marrow microenvironment and stem cells in transfusion-dependent beta-thalassemia. *Biomed. Pharmacother.* **2022**, *146*, 112548. [[CrossRef](#)]
156. Fouzia, N.A.; Edison, E.S.; Lakshmi, K.M.; Korula, A.; Velayudhan, S.R.; Balasubramanian, P.; Abraham, A.; Viswabandya, A.; George, B.; Mathews, V.; et al. Long-term outcome of mixed chimerism after stem cell transplantation for thalassemia major conditioned with busulfan and cyclophosphamide. *Bone Marrow Transplant* **2018**, *53*, 169–174. [[CrossRef](#)]
157. Angelucci, E. Complication free survival long-term after hemopoietic cell transplantation in thalassemia. *Haematologica* **2018**, *103*, 1094–1096. [[CrossRef](#)]
158. Adams, G.B.; Martin, R.P.; Alley, I.R.; Chabner, K.T.; Cohen, K.S.; Calvi, L.M.; Kronenberg, H.M.; Scadden, D.T. Therapeutic targeting of a stem cell niche. *Nat. Biotechnol.* **2007**, *25*, 238–243. [[CrossRef](#)]
159. Ballen, K.; Mendizabal, A.M.; Cutler, C.; Politikos, I.; Jamieson, K.; Shpall, E.J.; Dey, B.R.; Attar, E.; McAfee, S.; Delaney, C.; et al. Phase II trial of parathyroid hormone after double umbilical cord blood transplantation. *Biol. Blood Marrow Transplant* **2012**, *18*, 1851–1858. [[CrossRef](#)]
160. Vinchi, F.; De Franceschi, L.; Ghigo, A.; Townes, T.; Cimino, J.; Silengo, L.; Hirsch, E.; Altruda, F.; Tolosano, E. Hemopexin therapy improves cardiovascular function by preventing heme-induced endothelial toxicity in mouse models of hemolytic diseases. *Circulation* **2013**, *127*, 1317–1329. [[CrossRef](#)]

## CHAPTER III

### NEW RESULTS

We decided to conduct a more comprehensive investigation of the molecular mechanism underlying the increased cFGF23 levels in BThal, focusing on the GALNT3 enzyme, which preserves the intact form of FGF23 and protects it from cleavage. Concurrently, we wanted to strengthen the translational relevance of FGF23 inhibition. We set up several experiments to establish the proper dose regimen with withdrawal periods for a prolonged cFGF23 treatment of thalassemic mice.

#### **1. High EPO downregulates GALNT3 through Erk1/2 and Stat5 signaling in bone and BM erythroid cells**

We have demonstrated that EPO is a primary driver of FGF23 transcription and production in BThal mice by both bone and erythroid cells. This occurs through its action on the Erk1/2 and Stat5 pathways, respectively <sup>131</sup>. To unveil the signaling pathways involved in the induction of the cleaved form of FGF23 by EPO, we modeled *in vitro* EPO stimulation of wt bone-derived and BM Ter119<sup>+</sup> erythroid cells. Upon *in vitro* exposure to rhEPO for 4 hours we showed a downregulation of *Galnt3* expression in both bone and BM erythroid cells (Fig 1A-B). Inhibition of Erk1/2 signaling by U0126 (Fig 1C) and Stat5 pathways by Pimozide (Fig 1D) increased *Galnt3* in EPO-stimulated bone and BM erythroid cells, respectively. Preliminary *in silico* bioinformatic analysis identified consensus sequences for transcription factors associated with Erk1/2 and Stat5 signaling within the promoter region of the *Galnt3* gene (Fig. 1E), suggesting a transcriptional regulation mechanism.

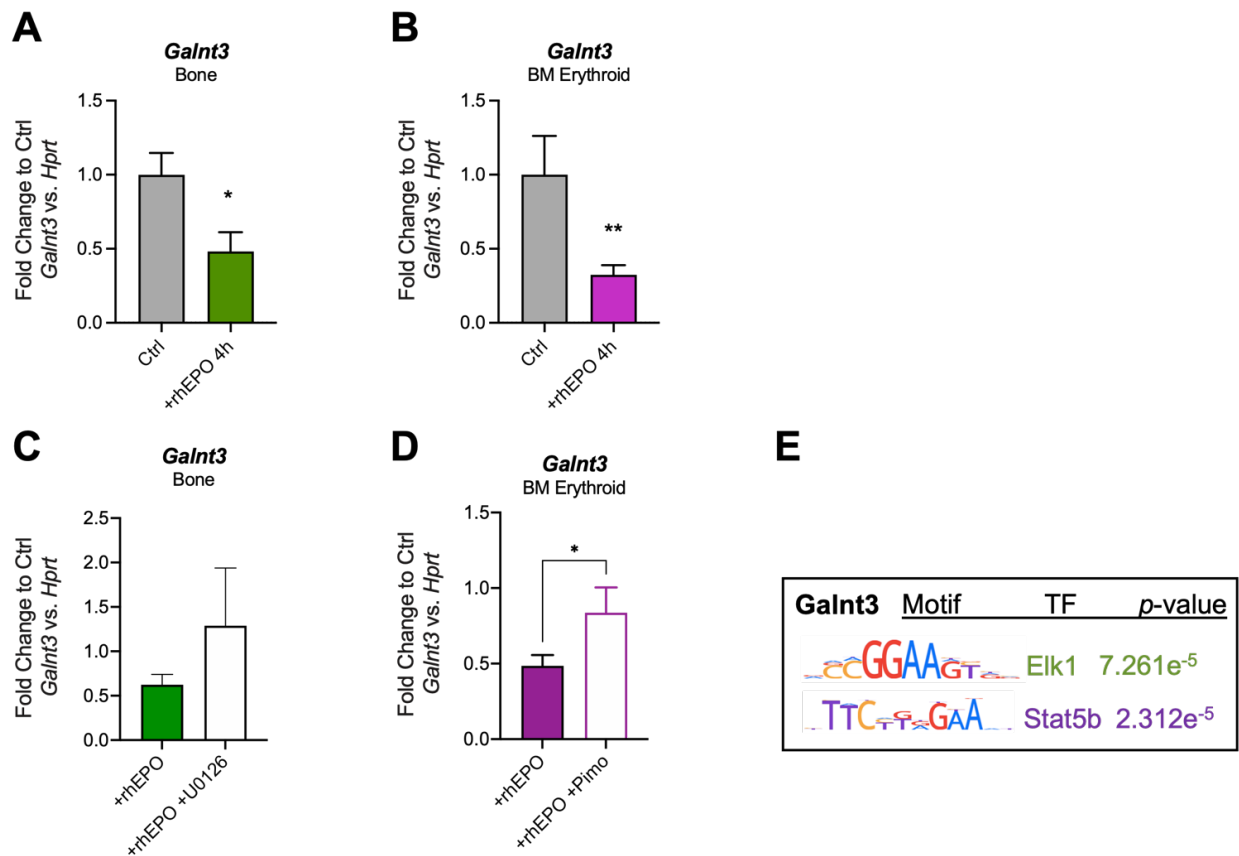


**Fig 1. High EPO levels downregulate GALNT3 through Erk1/2 and Stat5 signaling in bone and BM erythroid cells.** (A) *Galnt3* expression relative to *Hprt* by bone cells upon rhEPO treatment at 4 hours, reported as ratio to unstimulated control ( $n \geq 8$  mice/group). (B) *Galnt3* expression relative to *Hprt* by BM erythroid cells upon rhEPO treatment at 4 hours, reported as ratio to unstimulated control ( $n \geq 13$  mice/group). (C) *Galnt3* expression in bone cells upon rhEPO stimulation and Erk1/2 inhibition by U0126, reported as fold to wt relative to *Hprt* ( $n = 3$ ). (D) *Galnt3* expression in BM erythroid cells upon rhEPO stimulation and Stat5 inhibition by pimoizide (Pimo), reported as fold to wt relative to *Hprt* ( $n = 6$ ). (E) Motif enrichment analysis showing top-ranking transcription factors (TF) identified on *GALNT3* promoter by JASPAR and HOCOMOCO databases. Putative TF and associated p values are shown. Values represent means  $\pm$  SEM. One-tailed Mann-Whitney test (A-B) and Wilcoxon test (C-D) were used to evaluate statistical significance (\*  $p < 0.05$ , \*\*  $p < 0.01$ ).

## 2. Increased BMD and HSC cell cycle was maintained after the discontinuation of cFGF23 treatment.

To establish the proper dose regimen with withdrawal periods for prolonged cFGF23 treatment, we administered six doses of cFGF23 (10 mg/kg) to 6-week-old *th3* mice. We then assessed BMD and HSC cell cycle upon 14h, 1 and 2 weeks following the discontinuation of FGF23 inhibition (Fig. 2A). Our results showed that increased BMD was maintained after the discontinuation of treatment up to 2 weeks (Fig. 2B). Additionally, we

observed an increased proportion of HSC in quiescence (G0/G1-phase) which was maintained up to 2 weeks from cFGF23 treatment discontinuation. Accordingly, the frequency of cycling cells in the S-phase was decreased (Fig. 2C).

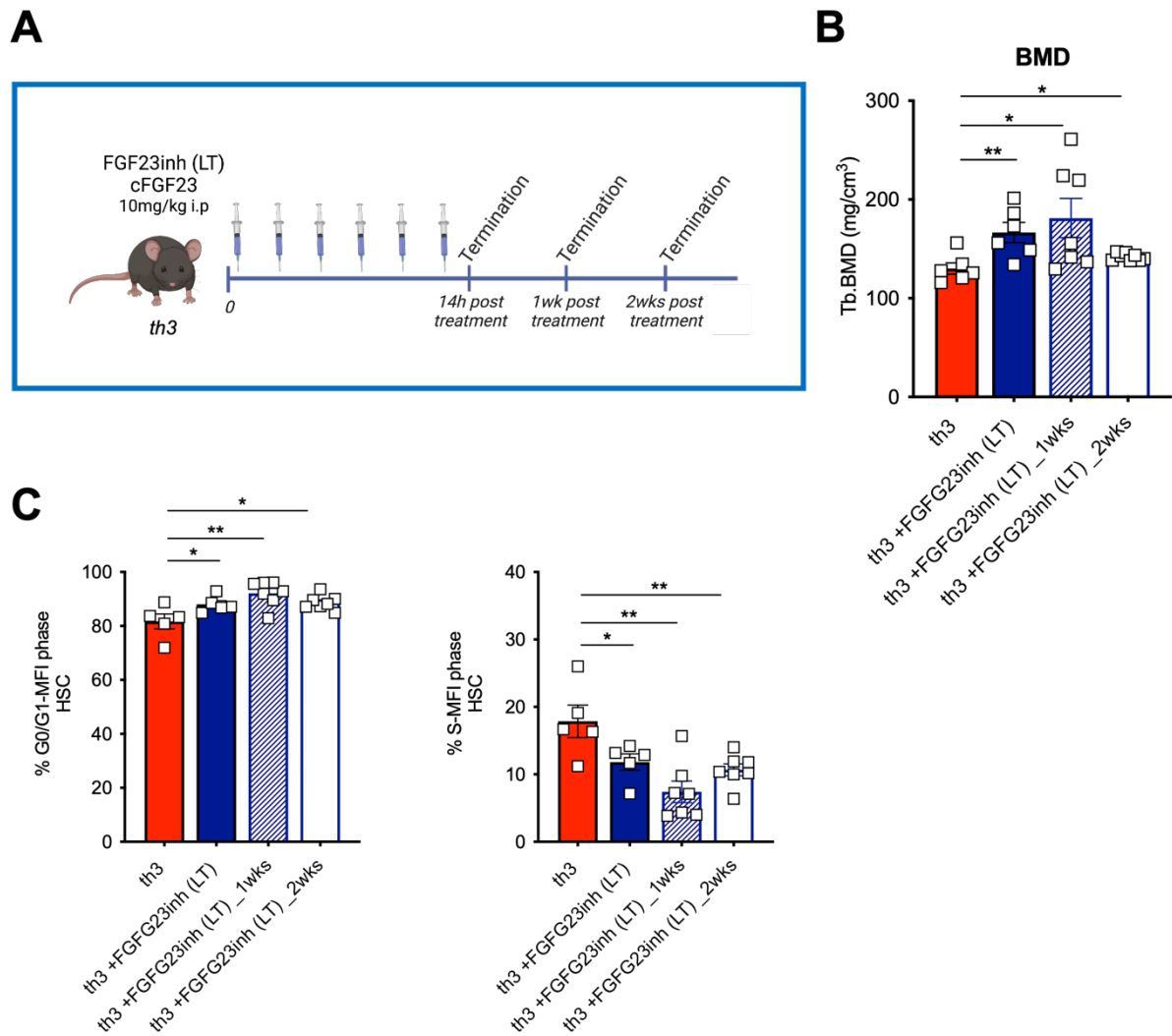


**Fig 2. Increased BMD and HSC cell cycle was maintained after the discontinuation of cFGF23 treatment.** (A) *In vivo* long-term FGF23 inhibition (FGF23inh (LT)) in *th3* mice by injection of six doses of cFGF23 (10 mg/kg i.p.); analyses were performed at termination upon 13 days, 1 and 2 wks. (B) Volumetric Tb.BMD of the proximal tibiae by pQCT of *th3* ( $n = 6$ ), *th3*+FGF23inh (LT) ( $n = 6$ ), *th3* +FGF23inh (LT)\_1wk ( $n = 7$ ) and *th3* +FGF23inh (LT)\_2wk ( $n = 7$ ). (C) Frequency of HSC in G0/G1 and S-phase of the cell cycle from *th3* ( $n = 6$ ), *th3*+FGF23inh (LT) ( $n = 6$ ), *th3* +FGF23inh (LT)\_1wk ( $n = 7$ ) and *th3* +FGF23inh (LT)\_2wk ( $n = 7$ ). Values represent means  $\pm$  SEM. One or two-tailed Mann-Whitney test was used to evaluate statistical significance (\*  $p < 0.05$ , \*\*  $p < 0.01$ ), followed by Bonferroni correction for comparison among more than 2 groups.

## DISCUSSION OF NEW RESULTS:

Our analysis in BThal *th3* mice revealed significant differences in the balance between iFGF23 and cFGF23 forms when compared to wt mice. In *th3* mice, both bioactive iFGF23 and cleaved cFGF23 were elevated in the serum, prompting us to investigate the molecular mechanisms underlying these changes.

Analysis of molecules involved in FGF23 regulation revealed increased *Fgf23* and decreased *Galnt3* expression by bone and BM erythroid cells. GALNT3 stabilizes FGF23 through glycosylation, protecting it from cleavage, thus explaining enhanced FGF23 production and cleavage in the context of chronic EPO stimulation. This was in line with a study where mice overexpressing human EPO (Tg6 mice) showed reduced *Galnt3* expression in bone and BM, thus leading to increased FGF23 cleavage<sup>167</sup>. Additionally, acute blood loss in mice, serving as a model for high endogenous EPO, significantly raises cFGF23 levels without affecting iFGF23, with a concomitant decrease of *Galnt3* mRNA expression in BM cells<sup>131,165</sup>. Overall, these findings indicate that high EPO levels enhance the total amount of circulating FGF23 (both iFGF23 and cFGF23) by shifting the iFGF23/cFGF23 ratio in favor of cFGF23<sup>164,167,199-201</sup>.

Looking at other *Fgf23*-related genes, we found downregulation of the PCSK5 protease, involved in FGF23 cleavage, in both bone and BM erythroid cells. We can speculate that the decreased *Pcsk5* mRNA expression in bone and BM acts as a mechanism to counterbalance the increased cFGF23. Conversely, Fam20c protein kinase marking FGF23 for proteolytic cleavage and Furin protease remained unchanged, as confirmed also in studies on Tg6 mice<sup>167</sup>.

To unveil the signaling pathways involved in the induction of the cleaved form of FGF23 by EPO, we modeled *in vitro* EPO stimulation of wt bone-derived and BM Ter119<sup>+</sup> erythroid cells. *In vitro* EPO stimulation and signaling inhibition strategies showed that Erk1/2 and Stat5 pathways are active in enhancing *Fgf23* and decreasing *Galnt3* transcription in bone and BM erythroid cells, respectively. Thus, EPO-induced FGF23 production can be attributed to the downregulation of the *Galnt3* expression, resulting in reduced glycosylation of the FGF23 peptide and making it susceptible to cleavage. To further elucidate the role of specific transcription factors and consensus binding sites on FGF23 and GALNT3 promoters, we will perform chromatin immunoprecipitation (ChIP) analysis.

The study of *Galnt3* has some limitations since we investigated its expression in bone and erythroid cells and not in other stromal cell populations within the BM, such as ECs and MSCs.



Furthermore, we plan to investigate FGF23 production and FGF23-related genes in other organs in the context of BThal. There is evidence to suggest that these molecules may also be produced by several organs such as the liver, brain, heart, kidney, and spleen<sup>202-204</sup>. Focusing on the FGF23 targeting strategy to improve HSC engraftment, the observation of a partial enhancement in engraftment through competitive transplantation in cFGF23-treated mice led us to hypothesize that prolonged cFGF23 administration to recipient mice post-transplantation could further restore the BM niche and boost the graft. The long-term effect of the FGF23 inhibition strategy in improving BMD and HSC cell cycle in BThal was shown to persist for up to 2 weeks by the treatment end. Ongoing histomorphometric analysis will provide a better characterization of bone quality. In the future, we plan to conduct competitive transplantation experiments by treating recipient mice with a maintenance regimen of 2 doses of cFGF23 every 2 weeks for prolonged treatment, aimed at a potential application to ameliorate clinical outcomes.

## OVERALL DISCUSSION:

The thesis presents a comprehensive investigation of the intricate interplay between anemia, bone homeostasis, and BM niche, using BThal as a paradigm to study this connection. Clinical evidence links hematological disorders to bone defects, paving the way for a detailed exploration of the molecular mechanisms underlying this association.

In the present study, we investigated the pivotal role of FGF23 in maintaining bone and BM niche homeostasis in the context of BThal. Elevated FGF23 production in serum and BMEF, attributed to increased FGF23 synthesis by chronic high EPO levels, emerges as a key factor in the bone alterations observed in this congenital hemolytic anemia.

The thesis further explores the broader implications of the FGF23-anemia-bone axis by demonstrating a positive correlation between EPO and FGF23 in BThal. This association is linked to bone quality and ineffective erythropoiesis, establishing FGF23 as a central molecule at the crossroads of erythropoiesis and bone metabolism in BThal patients.

Mechanistically, we showed EPO as a causative factor in up-regulating FGF23 production. Indeed, EPO stimulation and signaling inhibition strategies showed that Erk1/2 and Stat5 pathways are active in enhancing *Fgf23* and decreasing *Galnt3* transcription in bone and BM erythroid cells, respectively. EPO-induced FGF23 production can be attributed to the downregulation of the *Galnt3* expression, resulting in reduced glycosylation of the FGF23 peptide and making it susceptible to cleavage.

Furthermore, we plan to investigate FGF23 production and FGF23-related genes in other organs in the context of BThal. There is evidence to suggest that these molecules may also be produced by several organs such as the liver, brain, heart, kidney, and spleen<sup>202-204</sup>.

Clinical evidence showed that congenital hemolytic anemia has a detrimental impact on bone health and is often associated with osteoporosis and bone defects. This insight into the extra hematopoietic effects of erythropoietic stress has implications not only for BThal but also for conditions like CKD<sup>205</sup>, MDS<sup>206</sup>, and cancer<sup>207</sup> where EPO is clinically used. Understanding the increase in FGF23 and the impact on the bone in EPO-treated patients will be relevant.

While the homodimer EPOR mediates canonical erythropoiesis, the tissue-protective effects of EPO operate through a heteromeric receptor composed of EPOR and CD131<sup>208</sup>. The study conducted by Z. Awida et al. is the first to address the *in vitro* and *in vivo* beneficial effects of Cibinetide on bone metabolism, which specifically binds heteromeric receptors, either alone or in combination with EPO<sup>209</sup>. We showed that cFGF23 administration rescued

bone defects without interference with the erythropoietic activity of EPO. However, further studies are needed to explore if cFGF23 binds heteromeric EPOR.

Interestingly, a new generation of erythropoiesis-stimulating agents, such as Luspatercept, recently approved for the treatment of TDT patients<sup>210</sup> with improvements in IE and anemia, was initially developed as exploratory therapies for osteopenia and osteoporosis. Our future experiments will explore the correlation of FGF23 with anemia and bone parameters in BThal patients before and during the treatment with Luspatercept.

From the translational point of view, our study validates the efficacy of the FGF23 inhibition strategy, employing the naturally produced blocking peptide cFGF23, in correcting bone mineralization and deposition, and rescuing impaired crosstalk between HSCs and the BM niche with potential translational relevance in improving HSC transplantation and gene therapy for BThal. We observed to some extent enhanced engraftment of transplanted cells in the cFGF23-treated recipient mice indicating that FGF23 inhibition might improve the supportive capacity of the damaged niche, although the short-term treatment of recipient mice before transplantation is not sufficient to maintain the restoration of bone compartment for a long period. We reasoned that prolonged cFGF23 administration to recipient mice after transplantation could further restore the BM niche and boost the graft, thus achieving therapeutic outcomes.

Moreover, in a translational context, we are exploring a promising strategy that combines autologous gene therapy with FGF23 inhibition. We will transduce *th3* Lin<sup>neg</sup> BM cells with a lentiviral vector carrying the  $\beta$ -globin gene (GLOBE LV). Although the use of cFGF23 peptide alone is insufficient to recover the decreased Hb production and RBCs count caused by genetic defects in congenital anemia, our research has shown that inhibition of FGF23 improves erythropoiesis by preventing the apoptosis in erythroid populations. We will plan to use cFGF23 treatment pre-transplantation to refurbish bone and HSC niche before HSC harvest to better increase the quality of donor HSC and use cFGF23 to treat recipient mice post-transplantation to promote the early engraftment of donor cells.

The role of FGF23 in the BM niche has also become a topic of increasing interest due to its involvement in the regulation of HSC mobilization. It remains to be determined whether high circulating levels of FGF23 in CKD and other congenital anemia including BThal may impair HSPC retention in the BM. In this line, we will analyze the expression of FGF23 and stemness-related genes in sorted HSCs at steady state and upon stressed conditions induced *in vivo* and *in vitro* culture systems to evaluate any intrinsic or microenvironment-mediated defect in BThal mice compared to controls. We will test our FGF23 inhibition

strategy by cFGF23 blocking peptide injection in *th3* mice alone and in combination with G-CSF or Plerixafor to monitor HSC mobilization.

Our work provides the first evidence of the efficacy of cFGF23 blocking peptide in correcting bone mineralization and deposition. The potential translation of our findings to clinical application might include the use of cFGF23 as a promising anti-osteoporotic therapy to preserve a healthy bone in BThal, addressing a current medical gap despite the available treatments. The potential advantage of using a physiological regulatory pathway of FGF23 versus a current treatment (i.e. anti-FGF23 antibody administration) is worth to be investigated.

## **PERSONAL CONTRIBUTION:**

During the 3 yrs PhD program, I have actively designed, performed, and analyzed several experiments, contributing to various topics covered in this thesis. I assembled and created most of figures and panels included in the thesis, except for those showing results obtained with specific techniques attributed to other co-authors or collaborators. The collaborators' contribution is relative to the collection of samples from BThal patients reported in Figure 1, as well as the histomorphology and pQCT analysis on bone, as shown in Figure 3 (panels A to C, G to J) and Supplementary Figures S6 (panels A, B, F), S7 (panels A, B), and S8. Additionally, the histopathological analysis illustrated in Figure 4 (panels A to C) and Supplementary Figures S9 A and S10 also benefited from contributions by other team members. I provide this clarification to ensure transparency regarding the authorship of data represented in individual figures, providing a general understanding of my specific contribution to this thesis work.

## REFERENCES

### REFERENCES

- 1 Rund, D. & Rachmilewitz, E. Beta-thalassemia. *N Engl J Med* **353**, 1135-1146 (2005). <https://doi.org/10.1056/NEJMra050436>
- 2 Piel, F. B. & Weatherall, D. J. The alpha-thalassaemias. *N Engl J Med* **371**, 1908-1916 (2014). <https://doi.org/10.1056/NEJMra1404415>
- 3 Origa, R. beta-Thalassemia. *Genet Med* **19**, 609-619 (2017). <https://doi.org/10.1038/gim.2016.173>
- 4 Taher, A. T., Weatherall, D. J. & Cappellini, M. D. Thalassaemia. *Lancet* **391**, 155-167 (2018). [https://doi.org/10.1016/S0140-6736\(17\)31822-6](https://doi.org/10.1016/S0140-6736(17)31822-6)
- 5 Kattamis, A., Kwiatkowski, J. L. & Aydinok, Y. Thalassaemia. *Lancet* **399**, 2310-2324 (2022). [https://doi.org/10.1016/S0140-6736\(22\)00536-0](https://doi.org/10.1016/S0140-6736(22)00536-0)
- 6 Cappellini, M. D., Porter, J. B., Viprakasit, V. & Taher, A. T. A paradigm shift on beta-thalassaemia treatment: How will we manage this old disease with new therapies? *Blood Rev* **32**, 300-311 (2018). <https://doi.org/10.1016/j.blre.2018.02.001>
- 7 Higgs, D. R., Engel, J. D. & Stamatoyannopoulos, G. Thalassaemia. *Lancet* **379**, 373-383 (2012). [https://doi.org/10.1016/S0140-6736\(11\)60283-3](https://doi.org/10.1016/S0140-6736(11)60283-3)
- 8 Taher, A. T., Musallam, K. M. & Cappellini, M. D. beta-Thalassaemias. *N Engl J Med* **384**, 727-743 (2021). <https://doi.org/10.1056/NEJMra2021838>
- 9 Centis, F. *et al.* The importance of erythroid expansion in determining the extent of apoptosis in erythroid precursors in patients with beta-thalassemia major. *Blood* **96**, 3624-3629 (2000).
- 10 Orkin, S. H. Diversification of haematopoietic stem cells to specific lineages. *Nat Rev Genet* **1**, 57-64 (2000). <https://doi.org/10.1038/35049577>
- 11 Dulmovits, B. M., Hom, J., Narla, A., Mohandas, N. & Blanc, L. Characterization, regulation, and targeting of erythroid progenitors in normal and disordered human erythropoiesis. *Curr Opin Hematol* **24**, 159-166 (2017). <https://doi.org/10.1097/MOH.0000000000000328>
- 12 Thiagarajan, P., Parker, C. J. & Prchal, J. T. How Do Red Blood Cells Die? *Front Physiol* **12**, 655393 (2021). <https://doi.org/10.3389/fphys.2021.655393>
- 13 Elliott, S., Sinclair, A., Collins, H., Rice, L. & Jelkmann, W. Progress in detecting cell-surface protein receptors: the erythropoietin receptor example. *Ann Hematol* **93**, 181-192 (2014). <https://doi.org/10.1007/s00277-013-1947-2>
- 14 Rankin, E. B. *et al.* The HIF signaling pathway in osteoblasts directly modulates erythropoiesis through the production of EPO. *Cell* **149**, 63-74 (2012). <https://doi.org/10.1016/j.cell.2012.01.051>
- 15 Kapitsinou, P. P. *et al.* Hepatic HIF-2 regulates erythropoietic responses to hypoxia in renal anemia. *Blood* **116**, 3039-3048 (2010). <https://doi.org/10.1182/blood-2010-02-270322>
- 16 Saad, H. K. M. *et al.* Activation of STAT and SMAD Signaling Induces Hcpidin Re-Expression as a Therapeutic Target for beta-Thalassemia Patients. *Biomedicines* **10** (2022). <https://doi.org/10.3390/biomedicines10010189>
- 17 Willimann, R., Chougar, C., Wolfe, L. C., Blanc, L. & Lipton, J. M. Defects in Bone and Bone Marrow in Inherited Anemias: the Chicken or the Egg. *Curr Osteoporos Rep* (2023). <https://doi.org/10.1007/s11914-023-00809-3>
- 18 Voskaridou, E. & Terpos, E. New insights into the pathophysiology and management of osteoporosis in patients with beta thalassaemia. *Br J Haematol* **127**, 127-139 (2004). <https://doi.org/10.1111/j.1365-2141.2004.05143.x>
- 19 Rachmilewitz, E. A. & Giardina, P. J. How I treat thalassemia. *Blood* **118**, 3479-3488 (2011). <https://doi.org/10.1182/blood-2010-08-300335> [pii]

- 20 Rossi, F. *et al.* Iron overload causes osteoporosis in thalassemia major patients through interaction with transient receptor potential vanilloid type 1 (TRPV1) channels. *Haematologica* **99**, 1876-1884 (2014). <https://doi.org:10.3324/haematol.2014.104463>
- 21 Piga, A. Impact of bone disease and pain in thalassemia. *Hematology Am Soc Hematol Educ Program* **2017**, 272-277 (2017). <https://doi.org:10.1182/asheducation-2017.1.272>
- 22 Morabito, N. *et al.* Osteoprotegerin and RANKL in the pathogenesis of thalassemia-induced osteoporosis: new pieces of the puzzle. *J Bone Miner Res* **19**, 722-727 (2004). <https://doi.org:10.1359/JBMR.040113>
- 23 Haidar, R., Musallam, K. M. & Taher, A. T. Bone disease and skeletal complications in patients with beta thalassemia major. *Bone* **48**, 425-432 (2011). <https://doi.org:10.1016/j.bone.2010.10.173>
- 24 Zaidi, M. *et al.* Bone circuitry and interorgan skeletal crosstalk. *Elife* **12** (2023). <https://doi.org:10.7554/eLife.83142>
- 25 Wong, P., Fuller, P. J., Gillespie, M. T. & Milat, F. Bone Disease in Thalassemia: A Molecular and Clinical Overview. *Endocr Rev* **37**, 320-346 (2016). <https://doi.org:10.1210/er.2015-1105>
- 26 Angelopoulos, N. G. *et al.* Hypoparathyroidism in transfusion-dependent patients with beta-thalassemia. *J Bone Miner Metab* **24**, 138-145 (2006). <https://doi.org:10.1007/s00774-005-0660-1>
- 27 McColl, B. & Vadolas, J. Animal models of beta-hemoglobinopathies: utility and limitations. *J Blood Med* **7**, 263-274 (2016). <https://doi.org:10.2147/JBM.S87955>
- 28 Shehee, W. R., Oliver, P. & Smithies, O. Lethal thalassemia after insertional disruption of the mouse major adult beta-globin gene. *Proc Natl Acad Sci U S A* **90**, 3177-3181 (1993). <https://doi.org:10.1073/pnas.90.8.3177>
- 29 Skow, L. C. *et al.* A mouse model for beta-thalassemia. *Cell* **34**, 1043-1052 (1983). [https://doi.org:10.1016/0092-8674\(83\)90562-7](https://doi.org:10.1016/0092-8674(83)90562-7)
- 30 Yang, B. *et al.* A mouse model for beta 0-thalassemia. *Proc Natl Acad Sci U S A* **92**, 11608-11612 (1995).
- 31 Vogiatzi, M. G. *et al.* Changes in bone microarchitecture and biomechanical properties in the th3 thalassemia mouse are associated with decreased bone turnover and occur during the period of bone accrual. *Calcif Tissue Int* **86**, 484-494 (2010). <https://doi.org:10.1007/s00223-010-9365-0>
- 32 Weizer-Stern, O. *et al.* mRNA expression of iron regulatory genes in beta-thalassemia intermedia and beta-thalassemia major mouse models. *Am J Hematol* **81**, 479-483 (2006). <https://doi.org:10.1002/ajh.20549>
- 33 Rivella, S. Iron metabolism under conditions of ineffective erythropoiesis in beta-thalassemia. *Blood* **133**, 51-58 (2019). <https://doi.org:10.1182/blood-2018-07-815928>
- 34 Cappellini, M. D., Musallam, K. M. & Taher, A. T. Iron deficiency anaemia revisited. *J Intern Med* **287**, 153-170 (2020). <https://doi.org:10.1111/joim.13004>
- 35 Musallam, K. M., Bou-Fakhredin, R., Cappellini, M. D. & Taher, A. T. 2021 update on clinical trials in beta-thalassemia. *Am J Hematol* **96**, 1518-1531 (2021). <https://doi.org:10.1002/ajh.26316>
- 36 Dussiot, M. *et al.* An activin receptor IIA ligand trap corrects ineffective erythropoiesis in beta-thalassemia. *Nat Med* **20**, 398-407 (2014). <https://doi.org:10.1038/nm.3468>
- 37 Longo, F. *et al.* Treating Thalassemia Patients with Luspatercept: An Expert Opinion Based on Current Evidence. *J Clin Med* **12** (2023). <https://doi.org:10.3390/jcm12072584>
- 38 Cappellini, M. D. *et al.* Sotatercept, a novel transforming growth factor beta ligand trap, improves anemia in beta-thalassemia: a phase II, open-label, dose-finding study. *Haematologica* **104**, 477-484 (2019). <https://doi.org:10.3324/haematol.2018.198887>
- 39 Carrancio, S. *et al.* An activin receptor IIA ligand trap promotes erythropoiesis resulting in a rapid induction of red blood cells and haemoglobin. *Br J Haematol* **165**, 870-882 (2014). <https://doi.org:10.1111/bjh.12838>

- 40 Suragani, R. N. *et al.* Transforming growth factor-beta superfamily ligand trap ACE-536 corrects anemia by promoting late-stage erythropoiesis. *Nat Med* **20**, 408-414 (2014). <https://doi.org:10.1038/nm.3512>
- 41 Matte, A. *et al.* The pyruvate kinase activator mitapivat reduces hemolysis and improves anemia in a beta-thalassemia mouse model. *J Clin Invest* **131** (2021). <https://doi.org:10.1172/JCI144206>
- 42 Kuo, K. H. M. *et al.* Safety and efficacy of mitapivat, an oral pyruvate kinase activator, in adults with non-transfusion dependent alpha-thalassaemia or beta-thalassaemia: an open-label, multicentre, phase 2 study. *Lancet* **400**, 493-501 (2022). [https://doi.org:10.1016/S0140-6736\(22\)01337-X](https://doi.org:10.1016/S0140-6736(22)01337-X)
- 43 Casu, C. *et al.* Minihepcidin peptides as disease modifiers in mice affected by beta-thalassemia and polycythemia vera. *Blood* **128**, 265-276 (2016). <https://doi.org:10.1182/blood-2015-10-676742>
- 44 Nai, A. *et al.* Deletion of TMPRSS6 attenuates the phenotype in a mouse model of beta-thalassemia. *Blood* **119**, 5021-5029 (2012). <https://doi.org:10.1182/blood-2012-01-401885>
- 45 Nyffenegger, N., Flace, A., Doucerain, C., Durrenberger, F. & Manolova, V. The Oral Ferroportin Inhibitor VIT-2763 Improves Erythropoiesis without Interfering with Iron Chelation Therapy in a Mouse Model of beta-Thalassemia. *Int J Mol Sci* **22** (2021). <https://doi.org:10.3390/ijms22020873>
- 46 Porter, J. *et al.* Oral ferroportin inhibitor vamifeport for improving iron homeostasis and erythropoiesis in beta-thalassemia: current evidence and future clinical development. *Expert Rev Hematol* **14**, 633-644 (2021). <https://doi.org:10.1080/17474086.2021.1935854>
- 47 Perrotta, S. *et al.* Osteoporosis in beta-thalassaemia major patients: analysis of the genetic background. *Br J Haematol* **111**, 461-466 (2000). <https://doi.org:10.1046/j.1365-2141.2000.02382.x>
- 48 Russell, R. G., Watts, N. B., Ebetino, F. H. & Rogers, M. J. Mechanisms of action of bisphosphonates: similarities and differences and their potential influence on clinical efficacy. *Osteoporos Int* **19**, 733-759 (2008). <https://doi.org:10.1007/s00198-007-0540-8>
- 49 Jobke, B., Milovanovic, P., Amling, M. & Busse, B. Bisphosphonate-osteoclasts: changes in osteoclast morphology and function induced by antiresorptive nitrogen-containing bisphosphonate treatment in osteoporosis patients. *Bone* **59**, 37-43 (2014). <https://doi.org:10.1016/j.bone.2013.10.024>
- 50 Adler, R. A. Bisphosphonates and atypical femoral fractures. *Curr Opin Endocrinol Diabetes Obes* **23**, 430-434 (2016). <https://doi.org:10.1097/MED.0000000000000287>
- 51 Cummings, S. R. *et al.* Denosumab for prevention of fractures in postmenopausal women with osteoporosis. *N Engl J Med* **361**, 756-765 (2009). <https://doi.org:10.1056/NEJMoa0809493>
- 52 Sugimoto, T. *et al.* Three-year denosumab treatment in postmenopausal Japanese women and men with osteoporosis: results from a 1-year open-label extension of the Denosumab Fracture Intervention Randomized Placebo Controlled Trial (DIRECT). *Osteoporos Int* **26**, 765-774 (2015). <https://doi.org:10.1007/s00198-014-2964-2>
- 53 Yassin, M. A. *et al.* Effects of the anti-receptor activator of nuclear factor kappa B ligand denosumab on beta thalassemia major-induced osteoporosis. *Indian J Endocrinol Metab* **18**, 546-551 (2014). <https://doi.org:10.4103/2230-8210.137516>
- 54 Voskaridou, E. *et al.* Denosumab in transfusion-dependent thalassemia osteoporosis: a randomized, placebo-controlled, double-blind phase 2b clinical trial. *Blood Adv* **2**, 2837-2847 (2018). <https://doi.org:10.1182/bloodadvances.2018023085>
- 55 Bolamperti, S., Villa, I. & Rubinacci, A. Bone remodeling: an operational process ensuring survival and bone mechanical competence. *Bone Res* **10**, 48 (2022). <https://doi.org:10.1038/s41413-022-00219-8>



- 56 McDonald, M. M. *et al.* Osteoclasts recycle via osteomorphs during RANKL-stimulated bone resorption. *Cell* **184**, 1330-1347 e1313 (2021). <https://doi.org:10.1016/j.cell.2021.02.002>
- 57 Zanchetta, M. B. *et al.* Significant bone loss after stopping long-term denosumab treatment: a post FREEDOM study. *Osteoporos Int* **29**, 41-47 (2018). <https://doi.org:10.1007/s00198-017-4242-6>
- 58 Niimi, R. *et al.* Analysis of daily teriparatide treatment for osteoporosis in men. *Osteoporos Int* **26**, 1303-1309 (2015). <https://doi.org:10.1007/s00198-014-3001-1>
- 59 Neer, R. M. *et al.* Effect of parathyroid hormone (1-34) on fractures and bone mineral density in postmenopausal women with osteoporosis. *N Engl J Med* **344**, 1434-1441 (2001). <https://doi.org:10.1056/NEJM200105103441904>
- 60 Gagliardi, I. *et al.* Efficacy and Safety of Teriparatide in Beta-Thalassemia Major Associated Osteoporosis: A Real-Life Experience. *Calcif Tissue Int* **111**, 56-65 (2022). <https://doi.org:10.1007/s00223-022-00963-3>
- 61 Pazianas, M. Anabolic effects of PTH and the 'anabolic window'. *Trends Endocrinol Metab* **26**, 111-113 (2015). <https://doi.org:10.1016/j.tem.2015.01.004>
- 62 Makino, A. *et al.* Frequent administration of abaloparatide shows greater gains in bone anabolic window and bone mineral density in mice: A comparison with teriparatide. *Bone* **142**, 115651 (2021). <https://doi.org:10.1016/j.bone.2020.115651>
- 63 Cosman, F. *et al.* FRAME Study: The Foundation Effect of Building Bone With 1 Year of Romosozumab Leads to Continued Lower Fracture Risk After Transition to Denosumab. *J Bone Miner Res* **33**, 1219-1226 (2018). <https://doi.org:10.1002/jbmr.3427>
- 64 Angelucci, E. *et al.* Hematopoietic stem cell transplantation in thalassemia major and sickle cell disease: indications and management recommendations from an international expert panel. *Haematologica* **99**, 811-820 (2014). <https://doi.org:10.3324/haematol.2013.099747>
- 65 Ferrari, G., Thrasher, A. J. & Aiuti, A. Gene therapy using haematopoietic stem and progenitor cells. *Nat Rev Genet* **22**, 216-234 (2021). <https://doi.org:10.1038/s41576-020-00298-5>
- 66 Lidonnici, M. R. & Ferrari, G. Gene therapy and gene editing strategies for hemoglobinopathies. *Blood Cells Mol Dis* **70**, 87-101 (2018). <https://doi.org:10.1016/j.bcmd.2017.12.001>
- 67 Ferrari, S. *et al.* Genetic engineering meets hematopoietic stem cell biology for next-generation gene therapy. *Cell Stem Cell* **30**, 549-570 (2023). <https://doi.org:10.1016/j.stem.2023.04.014>
- 68 Thompson, A. A. *et al.* Gene Therapy in Patients with Transfusion-Dependent beta-Thalassemia. *N Engl J Med* **378**, 1479-1493 (2018). <https://doi.org:10.1056/NEJMoa1705342>
- 69 Locatelli, F. *et al.* Betibeglogene Autotemcel Gene Therapy for Non-beta(0)/beta(0) Genotype beta-Thalassemia. *N Engl J Med* **386**, 415-427 (2022). <https://doi.org:10.1056/NEJMoa2113206>
- 70 Markt, S. *et al.* Intrabone hematopoietic stem cell gene therapy for adult and pediatric patients affected by transfusion-dependent  $\beta$ -thalassemia. *Nature Medicine* **25**, 234-241 (2019). <https://doi.org:10.1038/s41591-018-0301-6>
- 71 Frangoul, H. *et al.* CRISPR-Cas9 Gene Editing for Sickle Cell Disease and beta-Thalassemia. *N Engl J Med* **384**, 252-260 (2021). <https://doi.org:10.1056/NEJMoa2031054>
- 72 Laurenti, E. & Gottgens, B. From haematopoietic stem cells to complex differentiation landscapes. *Nature* **553**, 418-426 (2018). <https://doi.org:10.1038/nature25022>
- 73 Notta, F. *et al.* Isolation of single human hematopoietic stem cells capable of long-term multilineage engraftment. *Science* **333**, 218-221 (2011). <https://doi.org:10.1126/science.1201219>
- 74 Akashi, K., Traver, D., Miyamoto, T. & Weissman, I. L. A clonogenic common myeloid progenitor that gives rise to all myeloid lineages. *Nature* **404**, 193-197 (2000). <https://doi.org:10.1038/35004599>

- 75 Rodrigues, C. P., Shvedunova, M. & Akhtar, A. Epigenetic Regulators as the Gatekeepers of Hematopoiesis. *Trends Genet* (2020). <https://doi.org:10.1016/j.tig.2020.09.015>
- 76 Haas, S. *et al.* Inflammation-Induced Emergency Megakaryopoiesis Driven by Hematopoietic Stem Cell-like Megakaryocyte Progenitors. *Cell Stem Cell* **17**, 422-434 (2015). <https://doi.org:10.1016/j.stem.2015.07.007>
- 77 Velten, L. *et al.* Human haematopoietic stem cell lineage commitment is a continuous process. *Nat Cell Biol* **19**, 271-281 (2017). <https://doi.org:10.1038/ncb3493>
- 78 Carrelha, J. *et al.* Hierarchically related lineage-restricted fates of multipotent haematopoietic stem cells. *Nature* **554**, 106-111 (2018). <https://doi.org:10.1038/nature25455>
- 79 Rodriguez-Fraticelli, A. E. *et al.* Clonal analysis of lineage fate in native haematopoiesis. *Nature* **553**, 212-216 (2018). <https://doi.org:10.1038/nature25168>
- 80 Weinreb, C., Rodriguez-Fraticelli, A., Camargo, F. D. & Klein, A. M. Lineage tracing on transcriptional landscapes links state to fate during differentiation. *Science* **367** (2020). <https://doi.org:10.1126/science.aaw3381>
- 81 Oguro, H., Ding, L. & Morrison, S. J. SLAM family markers resolve functionally distinct subpopulations of hematopoietic stem cells and multipotent progenitors. *Cell Stem Cell* **13**, 102-116 (2013). <https://doi.org:10.1016/j.stem.2013.05.014>
- 82 Pinho, S. & Frenette, P. S. Haematopoietic stem cell activity and interactions with the niche. *Nat Rev Mol Cell Biol* **20**, 303-320 (2019). <https://doi.org:10.1038/s41580-019-0103-9>
- 83 Adams, G. B. & Scadden, D. T. The hematopoietic stem cell in its place. *Nat Immunol* **7**, 333-337 (2006). <https://doi.org:10.1038/ni1331>
- 84 Christodoulou, C. *et al.* Live-animal imaging of native haematopoietic stem and progenitor cells. *Nature* **578**, 278-283 (2020). <https://doi.org:10.1038/s41586-020-1971-z>
- 85 Kohler, A. *et al.* Altered cellular dynamics and endosteal location of aged early hematopoietic progenitor cells revealed by time-lapse intravital imaging in long bones. *Blood* **114**, 290-298 (2009). <https://doi.org:10.1182/blood-2008-12-195644>
- 86 Batsivari, A. *et al.* Dynamic responses of the haematopoietic stem cell niche to diverse stresses. *Nat Cell Biol* **22**, 7-17 (2020). <https://doi.org:10.1038/s41556-019-0444-9>
- 87 Aprile, A., Sighinolfi, S., Raggi, L. & Ferrari, G. Targeting the Hematopoietic Stem Cell Niche in beta-Thalassemia and Sickle Cell Disease. *Pharmaceuticals (Basel)* **15** (2022). <https://doi.org:10.3390/ph15050592>
- 88 Asada, N. & Katayama, Y. Regulation of hematopoiesis in endosteal microenvironments. *Int J Hematol* **99**, 679-684 (2014). <https://doi.org:10.1007/s12185-014-1583-1>
- 89 Calvi, L. M. *et al.* Osteoblastic cells regulate the haematopoietic stem cell niche. *Nature* **425**, 841-846 (2003). <https://doi.org:10.1038/nature02040>
- 90 Lo Celso, C. *et al.* Live-animal tracking of individual haematopoietic stem/progenitor cells in their niche. *Nature* **457**, 92-96 (2009). <https://doi.org:10.1038/nature07434>
- 91 Bowers, M. *et al.* Osteoblast ablation reduces normal long-term hematopoietic stem cell self-renewal but accelerates leukemia development. *Blood* **125**, 2678-2688 (2015). <https://doi.org:10.1182/blood-2014-06-582924>
- 92 Taichman, R. S. & Emerson, S. G. Human osteoblasts support hematopoiesis through the production of granulocyte colony-stimulating factor. *J Exp Med* **179**, 1677-1682 (1994). <https://doi.org:10.1084/jem.179.5.1677>
- 93 El-Badri, N. S., Wang, B. Y., Cherry & Good, R. A. Osteoblasts promote engraftment of allogeneic hematopoietic stem cells. *Exp Hematol* **26**, 110-116 (1998).
- 94 Ding, L. & Morrison, S. J. Haematopoietic stem cells and early lymphoid progenitors occupy distinct bone marrow niches. *Nature* **495**, 231-235 (2013). <https://doi.org:10.1038/nature11885>
- 95 Greenbaum, A. *et al.* CXCL12 in early mesenchymal progenitors is required for haematopoietic stem-cell maintenance. *Nature* **495**, 227-230 (2013). <https://doi.org:10.1038/nature11926>

- 96 Nilsson, S. K. *et al.* Osteopontin, a key component of the hematopoietic stem cell niche and regulator of primitive hematopoietic progenitor cells. *Blood* **106**, 1232-1239 (2005). <https://doi.org:10.1182/blood-2004-11-4422>
- 97 Decker, M., Leslie, J., Liu, Q. & Ding, L. Hepatic thrombopoietin is required for bone marrow hematopoietic stem cell maintenance. *Science* **360**, 106-110 (2018). <https://doi.org:10.1126/science.aap8861>
- 98 Zhou, B. O., Ding, L. & Morrison, S. J. Hematopoietic stem and progenitor cells regulate the regeneration of their niche by secreting Angiopoietin-1. *Elife* **4**, e05521 (2015). <https://doi.org:10.7554/eLife.05521>
- 99 Bianco, P. Reply to MSCs: science and trials. *Nat Med* **19**, 813-814 (2013). <https://doi.org:10.1038/nm.3255>
- 100 Sacchetti, B. *et al.* Self-renewing osteoprogenitors in bone marrow sinusoids can organize a hematopoietic microenvironment. *Cell* **131**, 324-336 (2007). <https://doi.org:10.1016/j.cell.2007.08.025>
- 101 Mendez-Ferrer, S. *et al.* Mesenchymal and haematopoietic stem cells form a unique bone marrow niche. *Nature* **466**, 829-834 (2010). <https://doi.org:10.1038/nature09262>
- 102 Sugiyama, T., Kohara, H., Noda, M. & Nagasawa, T. Maintenance of the hematopoietic stem cell pool by CXCL12-CXCR4 chemokine signaling in bone marrow stromal cell niches. *Immunity* **25**, 977-988 (2006). <https://doi.org:10.1016/j.immuni.2006.10.016>
- 103 Wein, F. *et al.* N-cadherin is expressed on human hematopoietic progenitor cells and mediates interaction with human mesenchymal stromal cells. *Stem Cell Res* **4**, 129-139 (2010). <https://doi.org:10.1016/j.scr.2009.12.004>
- 104 Taniguchi Ishikawa, E. *et al.* Connexin-43 prevents hematopoietic stem cell senescence through transfer of reactive oxygen species to bone marrow stromal cells. *Proc Natl Acad Sci U S A* **109**, 9071-9076 (2012). <https://doi.org:10.1073/pnas.1120358109>
- 105 Meacham, C. E. *et al.* Adiponectin receptors sustain haematopoietic stem cells throughout adulthood by protecting them from inflammation. *Nat Cell Biol* **24**, 697-707 (2022). <https://doi.org:10.1038/s41556-022-00909-9>
- 106 Naveiras, O. *et al.* Bone-marrow adipocytes as negative regulators of the haematopoietic microenvironment. *Nature* **460**, 259-263 (2009). <https://doi.org:10.1038/nature08099>
- 107 Itkin, T. *et al.* Distinct bone marrow blood vessels differentially regulate haematopoiesis. *Nature* **532**, 323-328 (2016). <https://doi.org:10.1038/nature17624>
- 108 Winkler, I. G. *et al.* Vascular niche E-selectin regulates hematopoietic stem cell dormancy, self renewal and chemoresistance. *Nat Med* **18**, 1651-1657 (2012). <https://doi.org:10.1038/nm.2969>
- 109 Doan, P. L. *et al.* Epidermal growth factor regulates hematopoietic regeneration after radiation injury. *Nat Med* **19**, 295-304 (2013). <https://doi.org:10.1038/nm.3070>
- 110 Mendez-Ferrer, S., Lucas, D., Battista, M. & Frenette, P. S. Haematopoietic stem cell release is regulated by circadian oscillations. *Nature* **452**, 442-447 (2008). <https://doi.org:10.1038/nature06685>
- 111 Park, M. H. *et al.* Neuropeptide Y regulates the hematopoietic stem cell microenvironment and prevents nerve injury in the bone marrow. *EMBO J* **34**, 1648-1660 (2015). <https://doi.org:10.15252/embj.201490174>
- 112 Yamazaki, S. *et al.* Nonmyelinating Schwann cells maintain hematopoietic stem cell hibernation in the bone marrow niche. *Cell* **147**, 1146-1158 (2011). <https://doi.org:10.1016/j.cell.2011.09.053>
- 113 Hur, J. *et al.* CD82/KAI1 Maintains the Dormancy of Long-Term Hematopoietic Stem Cells through Interaction with DARC-Expressing Macrophages. *Cell Stem Cell* **18**, 508-521 (2016). <https://doi.org:10.1016/j.stem.2016.01.013>

- 114 Ludin, A. *et al.* Monocytes-macrophages that express alpha-smooth muscle actin preserve primitive hematopoietic cells in the bone marrow. *Nat Immunol* **13**, 1072-1082 (2012). <https://doi.org:10.1038/ni.2408>
- 115 Luo, Y. *et al.* M1 and M2 macrophages differentially regulate hematopoietic stem cell self-renewal and ex vivo expansion. *Blood Adv* **2**, 859-870 (2018). <https://doi.org:10.1182/bloodadvances.2018015685>
- 116 Casanova-Acebes, M. *et al.* Rhythmic modulation of the hematopoietic niche through neutrophil clearance. *Cell* **153**, 1025-1035 (2013). <https://doi.org:10.1016/j.cell.2013.04.040>
- 117 Chow, A. *et al.* Bone marrow CD169<sup>+</sup> macrophages promote the retention of hematopoietic stem and progenitor cells in the mesenchymal stem cell niche. *J Exp Med* **208**, 261-271 (2011). <https://doi.org:10.1084/jem.20101688>
- 118 Fujisaki, J. *et al.* In vivo imaging of Treg cells providing immune privilege to the haematopoietic stem-cell niche. *Nature* **474**, 216-219 (2011). <https://doi.org:10.1038/nature10160>
- 119 Hirata, Y. *et al.* CD150(high) Bone Marrow Tregs Maintain Hematopoietic Stem Cell Quiescence and Immune Privilege via Adenosine. *Cell Stem Cell* **22**, 445-453 e445 (2018). <https://doi.org:10.1016/j.stem.2018.01.017>
- 120 Kawano, Y. *et al.* G-CSF-induced sympathetic tone provokes fever and primes antimobilizing functions of neutrophils via PGE2. *Blood* **129**, 587-597 (2017). <https://doi.org:10.1182/blood-2016-07-725754>
- 121 Heino, T. J., Hentunen, T. A. & Vaananen, H. K. Osteocytes inhibit osteoclastic bone resorption through transforming growth factor-beta: enhancement by estrogen. *J Cell Biochem* **85**, 185-197 (2002). <https://doi.org:10.1002/jcb.10109>
- 122 Miyamoto, K. *et al.* Osteoclasts are dispensable for hematopoietic stem cell maintenance and mobilization. *J Exp Med* **208**, 2175-2181 (2011). <https://doi.org:10.1084/jem.20101890>
- 123 Juarez, J. G. *et al.* Sphingosine-1-phosphate facilitates trafficking of hematopoietic stem cells and their mobilization by CXCR4 antagonists in mice. *Blood* **119**, 707-716 (2012). <https://doi.org:10.1182/blood-2011-04-348904>
- 124 Bruns, I. *et al.* Megakaryocytes regulate hematopoietic stem cell quiescence through CXCL4 secretion. *Nat Med* **20**, 1315-1320 (2014). <https://doi.org:10.1038/nm.3707>
- 125 Zhao, M. *et al.* Megakaryocytes maintain homeostatic quiescence and promote post-injury regeneration of hematopoietic stem cells. *Nat Med* **20**, 1321-1326 (2014). <https://doi.org:10.1038/nm.3706>
- 126 Dominici, M. *et al.* Restoration and reversible expansion of the osteoblastic hematopoietic stem cell niche after marrow radioablation. *Blood* **114**, 2333-2343 (2009). <https://doi.org:10.1182/blood-2008-10-183459>
- 127 Mendelson, A. & Frenette, P. S. Hematopoietic stem cell niche maintenance during homeostasis and regeneration. *Nat Med* **20**, 833-846 (2014). <https://doi.org:10.1038/nm.3647>
- 128 Aprile, A. *et al.* Hematopoietic stem cell function in beta-thalassemia is impaired and is rescued by targeting the bone marrow niche. *Blood* **136**, 610-622 (2020). <https://doi.org:10.1182/blood.2019002721>
- 129 Crippa, S. *et al.* Bone marrow stromal cells from  $\beta$ -thalassemia patients have impaired hematopoietic supportive capacity. *Journal of Clinical Investigation* **130** (2019). <https://doi.org:10.1172/JCI123191>
- 130 Fan, Y. *et al.* Parathyroid Hormone Directs Bone Marrow Mesenchymal Cell Fate. *Cell Metab* **25**, 661-672 (2017). <https://doi.org:10.1016/j.cmet.2017.01.001>
- 131 Aprile, A. *et al.* Inhibition of FGF23 is a therapeutic strategy to target hematopoietic stem cell niche defects in beta-thalassemia. *Sci Transl Med* **15**, eabq3679 (2023). <https://doi.org:10.1126/scitranslmed.abq3679>

- 132 Seyfried, A. N., Maloney, J. M. & MacNamara, K. C. Macrophages Orchestrate Hematopoietic Programs and Regulate HSC Function During Inflammatory Stress. *Front Immunol* **11**, 1499 (2020). <https://doi.org:10.3389/fimmu.2020.01499>
- 133 Vinchi, F. *et al.* Hemopexin therapy reverts heme-induced proinflammatory phenotypic switching of macrophages in a mouse model of sickle cell disease. *Blood* **127**, 473-486 (2016). <https://doi.org:10.1182/blood-2015-08-663245>
- 134 Richter, B. & Faul, C. FGF23 Actions on Target Tissues-With and Without Klotho. *Front Endocrinol (Lausanne)* **9**, 189 (2018). <https://doi.org:10.3389/fendo.2018.00189>
- 135 Itoh, N. & Ornitz, D. M. Evolution of the Fgf and Fgfr gene families. *Trends Genet* **20**, 563-569 (2004). <https://doi.org:10.1016/j.tig.2004.08.007>
- 136 Mohammadi, M., Olsen, S. K. & Goetz, R. A protein canyon in the FGF-FGF receptor dimer selects from an a la carte menu of heparan sulfate motifs. *Curr Opin Struct Biol* **15**, 506-516 (2005). <https://doi.org:10.1016/j.sbi.2005.09.002>
- 137 Dailey, L., Ambrosetti, D., Mansukhani, A. & Basilico, C. Mechanisms underlying differential responses to FGF signaling. *Cytokine Growth Factor Rev* **16**, 233-247 (2005). <https://doi.org:10.1016/j.cytogfr.2005.01.007>
- 138 Kurosu, H. *et al.* Regulation of fibroblast growth factor-23 signaling by klotho. *J Biol Chem* **281**, 6120-6123 (2006). <https://doi.org:10.1074/jbc.C500457200>
- 139 Urakawa, I. *et al.* Klotho converts canonical FGF receptor into a specific receptor for FGF23. *Nature* **444**, 770-774 (2006). <https://doi.org:10.1038/nature05315>
- 140 White, K. E. *et al.* Molecular cloning of a novel human UDP-GalNAc:polypeptide N-acetylgalactosaminyltransferase, GalNAc-T8, and analysis as a candidate autosomal dominant hypophosphatemic rickets (ADHR) gene. *Gene* **246**, 347-356 (2000). [https://doi.org:10.1016/s0378-1119\(00\)00050-0](https://doi.org:10.1016/s0378-1119(00)00050-0)
- 141 Edmonston, D. & Wolf, M. FGF23 at the crossroads of phosphate, iron economy and erythropoiesis. *Nat Rev Nephrol* **16**, 7-19 (2020). <https://doi.org:10.1038/s41581-019-0189-5>
- 142 Ben-Dov, I. Z. *et al.* The parathyroid is a target organ for FGF23 in rats. *J Clin Invest* **117**, 4003-4008 (2007). <https://doi.org:10.1172/JCI32409>
- 143 Musgrove, J. & Wolf, M. Regulation and Effects of FGF23 in Chronic Kidney Disease. *Annu Rev Physiol* **82**, 365-390 (2020). <https://doi.org:10.1146/annurev-physiol-021119-034650>
- 144 Vervloet, M. G. *et al.* Effects of dietary phosphate and calcium intake on fibroblast growth factor-23. *Clin J Am Soc Nephrol* **6**, 383-389 (2011). <https://doi.org:10.2215/CJN.04730510>
- 145 Takashi, Y. *et al.* Activation of unliganded FGF receptor by extracellular phosphate potentiates proteolytic protection of FGF23 by its O-glycosylation. *Proc Natl Acad Sci U S A* **116**, 11418-11427 (2019). <https://doi.org:10.1073/pnas.1815166116>
- 146 Kolek, O. I. *et al.* 1alpha,25-Dihydroxyvitamin D3 upregulates FGF23 gene expression in bone: the final link in a renal-gastrointestinal-skeletal axis that controls phosphate transport. *Am J Physiol Gastrointest Liver Physiol* **289**, G1036-1042 (2005). <https://doi.org:10.1152/ajpgi.00243.2005>
- 147 David, V. *et al.* Calcium regulates FGF-23 expression in bone. *Endocrinology* **154**, 4469-4482 (2013). <https://doi.org:10.1210/en.2013-1627>
- 148 Lavi-Moshayoff, V., Wasserman, G., Meir, T., Silver, J. & Naveh-Many, T. PTH increases FGF23 gene expression and mediates the high-FGF23 levels of experimental kidney failure: a bone parathyroid feedback loop. *Am J Physiol Renal Physiol* **299**, F882-889 (2010). <https://doi.org:10.1152/ajprenal.00360.2010>
- 149 Wein, M. N. *et al.* SIKs control osteocyte responses to parathyroid hormone. *Nat Commun* **7**, 13176 (2016). <https://doi.org:10.1038/ncomms13176>
- 150 Nagata, Y. *et al.* Parathyroid Hormone Regulates Circulating Levels of Sclerostin and FGF23 in a Primary Hyperparathyroidism Model. *J Endocr Soc* **6**, bvac027 (2022). <https://doi.org:10.1210/jendso/bvac027>

- 151 Qin, C., D'Souza, R. & Feng, J. Q. Dentin matrix protein 1 (DMP1): new and important roles for biomineralization and phosphate homeostasis. *J Dent Res* **86**, 1134-1141 (2007). <https://doi.org:10.1177/154405910708601202>
- 152 Murali, S. K. *et al.* FGF23 Regulates Bone Mineralization in a 1,25(OH)<sub>2</sub> D<sub>3</sub> and Klotho-Independent Manner. *J Bone Miner Res* **31**, 129-142 (2016). <https://doi.org:10.1002/jbmr.2606>
- 153 Meyer, R. A., Jr., Conway, W. F. & Chan, J. C. X-linked hypophosphatemia. *Semin Nephrol* **9**, 56-61 (1989).
- 154 Moe, S. M. Vascular calcification and renal osteodystrophy relationship in chronic kidney disease. *Eur J Clin Invest* **36 Suppl 2**, 51-62 (2006). <https://doi.org:10.1111/j.1365-2362.2006.01665.x>
- 155 Gutierrez, O. *et al.* Fibroblast growth factor-23 mitigates hyperphosphatemia but accentuates calcitriol deficiency in chronic kidney disease. *J Am Soc Nephrol* **16**, 2205-2215 (2005). <https://doi.org:10.1681/ASN.2005010052>
- 156 Portale, A. A. *et al.* Disordered FGF23 and mineral metabolism in children with CKD. *Clin J Am Soc Nephrol* **9**, 344-353 (2014). <https://doi.org:10.2215/CJN.05840513>
- 157 Haring, R. *et al.* Plasma Fibroblast Growth Factor 23: Clinical Correlates and Association With Cardiovascular Disease and Mortality in the Framingham Heart Study. *J Am Heart Assoc* **5** (2016). <https://doi.org:10.1161/JAHA.116.003486>
- 158 Kurpas, A., Supel, K., Idzikowska, K. & Zielinska, M. FGF23: A Review of Its Role in Mineral Metabolism and Renal and Cardiovascular Disease. *Dis Markers* **2021**, 8821292 (2021). <https://doi.org:10.1155/2021/8821292>
- 159 Yoshiko, Y. *et al.* Mineralized tissue cells are a principal source of FGF23. *Bone* **40**, 1565-1573 (2007). <https://doi.org:10.1016/j.bone.2007.01.017>
- 160 Coe, L. M. *et al.* FGF-23 is a negative regulator of prenatal and postnatal erythropoiesis. *J Biol Chem* **289**, 9795-9810 (2014). <https://doi.org:10.1074/jbc.M113.527150>
- 161 Goetz, R. *et al.* Isolated C-terminal tail of FGF23 alleviates hypophosphatemia by inhibiting FGF23-FGFR-Klotho complex formation. *Proc Natl Acad Sci U S A* **107**, 407-412 (2010). <https://doi.org:10.1073/pnas.0902006107>
- 162 Tagliabracci, V. S. *et al.* Dynamic regulation of FGF23 by Fam20C phosphorylation, GalNAc-T3 glycosylation, and furin proteolysis. *Proc Natl Acad Sci U S A* **111**, 5520-5525 (2014). <https://doi.org:10.1073/pnas.1402218111>
- 163 van Vuren, A. J. *et al.* Interplay of erythropoietin, fibroblast growth factor 23, and erythroferrone in patients with hereditary hemolytic anemia. *Blood Adv* **4**, 1678-1682 (2020). <https://doi.org:10.1182/bloodadvances.2020001595>
- 164 Clinkenbeard, E. L. *et al.* Erythropoietin stimulates murine and human fibroblast growth factor-23, revealing novel roles for bone and bone marrow. *Haematologica* **102**, e427-e430 (2017). <https://doi.org:10.3324/haematol.2017.167882>
- 165 Rabadi, S., Udo, I., Leaf, D. E., Waikar, S. S. & Christov, M. Acute blood loss stimulates fibroblast growth factor 23 production. *Am J Physiol Renal Physiol* **314**, F132-F139 (2018). <https://doi.org:10.1152/ajprenal.00081.2017>
- 166 Agoro, R. *et al.* Inhibition of fibroblast growth factor 23 (FGF23) signaling rescues renal anemia. *FASEB J* **32**, 3752-3764 (2018). <https://doi.org:10.1096/fj.201700667R>
- 167 Hanudel, M. R. *et al.* Effects of erythropoietin on fibroblast growth factor 23 in mice and humans. *Nephrol Dial Transplant* **34**, 2057-2065 (2019). <https://doi.org:10.1093/ndt/gfy189>
- 168 Imel, E. A., Hui, S. L. & Econs, M. J. FGF23 concentrations vary with disease status in autosomal dominant hypophosphatemic rickets. *J Bone Miner Res* **22**, 520-526 (2007). <https://doi.org:10.1359/jbmr.070107>
- 169 Imel, E. A. *et al.* Serum fibroblast growth factor 23, serum iron and bone mineral density in premenopausal women. *Bone* **86**, 98-105 (2016). <https://doi.org:10.1016/j.bone.2016.03.005>

- 170 Bozentowicz-Wikarek, M. *et al.* Plasma fibroblast growth factor 23 concentration and iron status. Does the relationship exist in the elderly population? *Clin Biochem* **48**, 431-436 (2015). <https://doi.org:10.1016/j.clinbiochem.2014.12.027>
- 171 David, V., Francis, C. & Babitt, J. L. Ironing out the cross talk between FGF23 and inflammation. *Am J Physiol Renal Physiol* **312**, F1-F8 (2017). <https://doi.org:10.1152/ajprenal.00359.2016>
- 172 Nicolas, G. *et al.* The gene encoding the iron regulatory peptide hepcidin is regulated by anemia, hypoxia, and inflammation. *J Clin Invest* **110**, 1037-1044 (2002). <https://doi.org:10.1172/JCI15686>
- 173 Courbon, G. *et al.* Bone-derived C-terminal FGF23 cleaved peptides increase iron availability in acute inflammation. *Blood* **142**, 106-118 (2023). <https://doi.org:10.1182/blood.2022018475>
- 174 Finberg, K. E. *et al.* Mutations in TMPRSS6 cause iron-refractory iron deficiency anemia (IRIDA). *Nat Genet* **40**, 569-571 (2008). <https://doi.org:10.1038/ng.130>
- 175 Li, X., Lozovatsky, L., Tommasini, S. M., Fretz, J. & Finberg, K. E. Bone marrow sinusoidal endothelial cells are a site of Fgf23 upregulation in a mouse model of iron deficiency anemia. *Blood Adv* **7**, 5156-5171 (2023). <https://doi.org:10.1182/bloodadvances.2022009524>
- 176 Czaya, B. & Faul, C. FGF23 and inflammation-a vicious coalition in CKD. *Kidney Int* **96**, 813-815 (2019). <https://doi.org:10.1016/j.kint.2019.05.018>
- 177 Aono, Y. *et al.* Therapeutic effects of anti-FGF23 antibodies in hypophosphatemic rickets/osteomalacia. *J Bone Miner Res* **24**, 1879-1888 (2009). <https://doi.org:10.1359/jbmr.090509>
- 178 Carpenter, T. O. *et al.* Burosumab Therapy in Children with X-Linked Hypophosphatemia. *N Engl J Med* **378**, 1987-1998 (2018). <https://doi.org:10.1056/NEJMoal714641>
- 179 Xiao, L., Homer-Bouthiette, C. & Hurley, M. M. FGF23 Neutralizing Antibody Partially Improves Bone Mineralization Defect of HMWFGF2 Isoforms in Transgenic Female Mice. *J Bone Miner Res* **33**, 1347-1361 (2018). <https://doi.org:10.1002/jbmr.3417>
- 180 Weidner, H. *et al.* Increased FGF-23 levels are linked to ineffective erythropoiesis and impaired bone mineralization in myelodysplastic syndromes. *JCI Insight* **5** (2020). <https://doi.org:10.1172/jci.insight.137062>
- 181 Florenzano, P. *et al.* Approach to patients with hypophosphataemia. *Lancet Diabetes Endocrinol* **8**, 163-174 (2020). [https://doi.org:10.1016/S2213-8587\(19\)30426-7](https://doi.org:10.1016/S2213-8587(19)30426-7)
- 182 Johnson, K. *et al.* Therapeutic Effects of FGF23 c-tail Fc in a Murine Preclinical Model of X-Linked Hypophosphatemia Via the Selective Modulation of Phosphate Reabsorption. *J Bone Miner Res* **32**, 2062-2073 (2017). <https://doi.org:10.1002/jbmr.3197>
- 183 Fuente, R. *et al.* Blocking FGF23 signaling improves the growth plate of mice with X-linked hypophosphatemia. *J Endocrinol* **259** (2023). <https://doi.org:10.1530/JOE-23-0025>
- 184 Wöhrle, S. *et al.* FGF receptors control vitamin D and phosphate homeostasis by mediating renal FGF-23 signaling and regulating FGF-23 expression in bone. *J Bone Miner Res* **26**, 2486-2497 (2011). <https://doi.org:10.1002/jbmr.478>
- 185 Wöhrle, S. *et al.* Pharmacological inhibition of fibroblast growth factor (FGF) receptor signaling ameliorates FGF23-mediated hypophosphatemic rickets. *J Bone Miner Res* **28**, 899-911 (2013). <https://doi.org:10.1002/jbmr.1810>
- 186 Quarles, L. D. Role of FGF23 in vitamin D and phosphate metabolism: implications in chronic kidney disease. *Exp Cell Res* **318**, 1040-1048 (2012). <https://doi.org:10.1016/j.yexcr.2012.02.027>
- 187 Erben, R. G. & Andrukhova, O. FGF23-Klotho signaling axis in the kidney. *Bone* **100**, 62-68 (2017). <https://doi.org:10.1016/j.bone.2016.09.010>
- 188 Shimada, T. *et al.* Cloning and characterization of FGF23 as a causative factor of tumor-induced osteomalacia. *Proc Natl Acad Sci U S A* **98**, 6500-6505 (2001). <https://doi.org:10.1073/pnas.101545198>

- 189 Gattineni, J. *et al.* FGF23 decreases renal NaPi-2a and NaPi-2c expression and induces hypophosphatemia in vivo predominantly via FGF receptor 1. *Am J Physiol Renal Physiol* **297**, F282-291 (2009). <https://doi.org/10.1152/ajprenal.90742.2008>
- 190 Fukumoto, S. Physiological regulation and disorders of phosphate metabolism--pivotal role of fibroblast growth factor 23. *Intern Med* **47**, 337-343 (2008). <https://doi.org/10.2169/internalmedicine.47.0730>
- 191 Vervloet, M. Renal and extrarenal effects of fibroblast growth factor 23. *Nat Rev Nephrol* **15**, 109-120 (2019). <https://doi.org/10.1038/s41581-018-0087-2>
- 192 Ishii, S. *et al.* FGF-23 from erythroblasts promotes hematopoietic progenitor mobilization. *Blood* **137**, 1457-1467 (2021). <https://doi.org/10.1182/blood.2020007172>
- 193 Comazzetto, S., Shen, B. & Morrison, S. J. Niches that regulate stem cells and hematopoiesis in adult bone marrow. *Dev Cell* **56**, 1848-1860 (2021). <https://doi.org/10.1016/j.devcel.2021.05.018>
- 194 Rafii, S., Butler, J. M. & Ding, B. S. Angiocrine functions of organ-specific endothelial cells. *Nature* **529**, 316-325 (2016). <https://doi.org/10.1038/nature17040>
- 195 Heil, J. *et al.* Bone marrow sinusoidal endothelium controls terminal erythroid differentiation and reticulocyte maturation. *Nat Commun* **12**, 6963 (2021). <https://doi.org/10.1038/s41467-021-27161-3>
- 196 Mattinzoli, D. *et al.* FGF23 and Fetuin-A Interaction and Mesenchymal Osteogenic Transformation. *Int J Mol Sci* **20** (2019). <https://doi.org/10.3390/ijms20040915>
- 197 Shalhoub, V. *et al.* Fibroblast growth factor 23 (FGF23) and alpha-klotho stimulate osteoblastic MC3T3.E1 cell proliferation and inhibit mineralization. *Calcif Tissue Int* **89**, 140-150 (2011). <https://doi.org/10.1007/s00223-011-9501-5>
- 198 Li, Y., He, X., Olauson, H., Larsson, T. E. & Lindgren, U. FGF23 affects the lineage fate determination of mesenchymal stem cells. *Calcif Tissue Int* **93**, 556-564 (2013). <https://doi.org/10.1007/s00223-013-9795-6>
- 199 Flamme, I., Ellinghaus, P., Urrego, D. & Kruger, T. FGF23 expression in rodents is directly induced via erythropoietin after inhibition of hypoxia inducible factor proline hydroxylase. *PLoS One* **12**, e0186979 (2017). <https://doi.org/10.1371/journal.pone.0186979>
- 200 Daryadel, A. *et al.* Erythropoietin stimulates fibroblast growth factor 23 (FGF23) in mice and men. *Pflugers Arch* **470**, 1569-1582 (2018). <https://doi.org/10.1007/s00424-018-2171-7>
- 201 Toro, L. *et al.* Erythropoietin induces bone marrow and plasma fibroblast growth factor 23 during acute kidney injury. *Kidney Int* **93**, 1131-1141 (2018). <https://doi.org/10.1016/j.kint.2017.11.018>
- 202 Li, D. J., Fu, H., Zhao, T., Ni, M. & Shen, F. M. Exercise-stimulated FGF23 promotes exercise performance via controlling the excess reactive oxygen species production and enhancing mitochondrial function in skeletal muscle. *Metabolism* **65**, 747-756 (2016). <https://doi.org/10.1016/j.metabol.2016.02.009>
- 203 Radhakrishnan, K. *et al.* Orphan nuclear receptor ERR-gamma regulates hepatic FGF23 production in acute kidney injury. *Proc Natl Acad Sci U S A* **118** (2021). <https://doi.org/10.1073/pnas.2022841118>
- 204 Yamashita, T., Yoshioka, M. & Itoh, N. Identification of a novel fibroblast growth factor, FGF-23, preferentially expressed in the ventrolateral thalamic nucleus of the brain. *Biochem Biophys Res Commun* **277**, 494-498 (2000). <https://doi.org/10.1006/bbrc.2000.3696>
- 205 Cowper, B. *et al.* Comprehensive glycan analysis of twelve recombinant human erythropoietin preparations from manufacturers in China and Japan. *J Pharm Biomed Anal* **153**, 214-220 (2018). <https://doi.org/10.1016/j.jpba.2018.02.043>
- 206 Hellstrom-Lindberg, E. *et al.* Treatment of anemia in myelodysplastic syndromes with granulocyte colony-stimulating factor plus erythropoietin: results from a randomized phase II study and long-term follow-up of 71 patients. *Blood* **92**, 68-75 (1998).



- 207 Bohlius, J. *et al.* Management of cancer-associated anemia with erythropoiesis-stimulating agents: ASCO/ASH clinical practice guideline update. *Blood Adv* **3**, 1197-1210 (2019). <https://doi.org:10.1182/bloodadvances.2018030387>
- 208 Brines, M. & Cerami, A. The receptor that tames the innate immune response. *Mol Med* **18**, 486-496 (2012). <https://doi.org:10.2119/molmed.2011.00414>
- 209 Awida, Z. *et al.* The Non-Erythropoietic EPO Analogue Cibinetide Inhibits Osteoclastogenesis In Vitro and Increases Bone Mineral Density in Mice. *Int J Mol Sci* **23** (2021). <https://doi.org:10.3390/ijms23010055>
- 210 Cappellini, M. D. *et al.* A Phase 3 Trial of Luspatercept in Patients with Transfusion-Dependent beta-Thalassemia. *N Engl J Med* **382**, 1219-1231 (2020). <https://doi.org:10.1056/NEJMoa1910182>